ISSN 1408-7073

RMZ

MATERIALS AND GEOENVIRONMENT

MATERIALI IN GEOOKOLJE

Volume 53
Letnik

Ljubljana, September 2006

No. 1
Št.

RMZ - Materials and Geoenvironment
RMZ - Materiali in geokolje

Old title: Rudarsko-metalurški zbornik (Mining and Metallurgy Quarterly),
ISSN 0035-9645, 1952-1997.

Is issued quarterly by the *Faculty of Natural Science and Engineering, Ljubljana*, the *Institute for Mining, Geotechnology and Environment Ljubljana* and *Premogovnik Velenje, Velenje*.
Izdaja *Naravoslovnotehniška fakulteta Univerze v Ljubljani, Inštitut za rudarstvo, geotehnologijo in okolje Ljubljana in Premogovnik Velenje,* štirikrat letno.
Financially supported also by Ministry of Education, Science and Sport of Republic of Slovenia.
Pri financiranju revije sodeluje *Ministrstvo za šolstvo, znanost in šport Republike Slovenije.*

Indexation bases of RMZ-M&G: CA SEARCH-Chemical Abstracts, METADEX, GeoRef, Energy Science and Technology, PASCAL. Main of 23 bases registrated
Baze v katerih je RMZ-M&G indeksiran: CA SEARCH-Chemical Abstracts, METADEX, GeoRef, Energy Science and Technology, PASCAL. Najpomembnejši med 23 registriranimi

---

Naklada 300 izvodov. Printed in 300 copies.
Online Journal/Elektronska revija: http://www.rmz-mg.com
Letna naroč za posameznike: 4.000,00 SIT, za inštitucije: 8.000,00 SIT
Yearly subscribtion 20 EUR, institutions 40 EUR

Tekoči račun pri Novi Ljubljanski banki, d.d. Ljubljana:
UJP 01100-6030708186
Davčna številka: 24405388

ISSN 1408-7073

RMZ - MATERIALS AND GEOENVIRONMENT

PERIODICAL FOR MINING, METALLURGY AND GEOLOGY

RMZ - MATERIALI IN GEOKOLJE

REVIJA ZA RUDARSTVO, METALURGIJO IN GEOLOGIJO

RMZ-M&G, Vol. 53, No. 1 pp. 1-153 (2006)

Ljubljana, September 2006

Historical Review

More than 80 years have passed since in 1919 the University Ljubljana in Slovenia was founded. Technical fields were joint in the School of Engineering that included the Geologic and Mining Division while the Metallurgy Division was established in 1939 only. Today the Departments of Geology, Mining and Geotechnology, Materials and Metallurgy are part of the Faculty of Natural Sciences and Engineering, University of Ljubljana.

Before War II the members of the Mining Section together with the Association of Yugoslav Mining and Metallurgy Engineers began to publish the summaries of their research and studies in their technical periodical Rudarski zbornik (Mining Proceedings). Three volumes of Rudarski zbornik (1937, 1938 and 1939) were published. The War interrupted the publication and not untill 1952 the first number of the new journal Rudarsko-metalurški zbornik - RMZ (Mining and Metallurgy Quarterly) has been published by the Division of Mining and Metallurgy, University of Ljubljana. Later the journal has been regularly published quarterly by the Departments of Geology, Mining and Geotechnology, Materials and Metallurgy, and the Institute for Mining, Geotechnology and Environment.

On the meeting of the Advisory and the Editorial Board on May 22nd 1998 Rudarsko-metalurški zbornik has been renamed into “RMZ - Materials and Geoenvironment (RMZ - Materiali in Geookolje)” or shortly RMZ - M&G.

RMZ - M&G is managed by an international advisory and editorial board and is exchanged with other world-known periodicals. All the papers are reviewed by the corresponding professionals and experts.

RMZ - M&G is the only scientific and professional periodical in Slovenia, which is published in the same form nearly 50 years. It incorporates the scientific and professional topics in geology, mining, and geotechnology, in materials and in metallurgy.

The wide range of topics inside the geosciences are wellcome to be published in the RMZ - Materials and Geoenvironment. Research results in geology, hydrogeology, mining, geotechnology, materials, metallurgy, natural and antropogenic pollution of environment, biogeochemistry are proposed fields of work which the journal will handle. RMZ - M&G is co-issued and co-financed by the Faculty of Natural Sciences and Engineering Ljubljana, and the Institute for Mining, Geotechnology and Environment Ljubljana. In addition it is financially suported also by the Ministry of Education Science and Sport of Slovenian Government.

Editor in chief

Table of Contents - Kazalo

δ^{15}N of particulate organic matter and *Anemonia sulcata* as a tracer of sewage effluent transport in the marine coastal ecosystem of Pirovac Bay and the Murter Sea (Central Adriatic)

δ^{15}N v partikulatni organski snovi in *Anemoni sulcati* kot sledilo transporta odpadnih voda v priobalnem delu Pirovaškega zaliva in Murterskega morja (srednji Jadran)

Tadej Dolenec[1,2*], Sonja Lojen[2], Goran Kniewald[3], Matej Dolenec[1] and Nastja Rogan[1]

[1]Faculty of Natural Sciences and Engineering, University of Ljubljana,
Department of Geology, Aškerčeva 12, 1000 Ljubljana, Slovenia;
E-mail: tadej.dolenec@ntfgeo.uni-lj.si
[2]Jožef Stefan Institute, Jamova 39, 1000 Ljubljana, Slovenia;
E-mail: sonja.lojen@ijs.si
[3]Ruđer Bošković Institute, Bijenička 54, Zagreb, Croatia;
E-mail: kniewald@irb.hr

Received: January 6, 2006 **Accepted**: July 20, 2006

Abstract: The present study shows that the stable isotopic composition of nitrogen in particulate organic matter (POM) and in selected marine organisms, such as the sea anemone *Anemonia sulcata,* may be excellent parameters for detecting and monitoring human sewage inputs into the marine coastal ecosystems of Pirovac Bay and the Murter Sea. The δ^{15}N values of POM and *A. sulcata* tissue were significantly higher at sites in the semi-enclosed Pirovac Bay and in the coastal part of the Murter Sea (Central Adriatic) affected by sewage, compared to the off-shore reef flats of the Murter Sea, the coastal parts of the Kornati Islands and at a pristine reference location at the Lumbarda Reef Flat. ^{15}N enrichment was as high as 7.0 ‰ in POM and 7.7 ‰ in *A. sulcata* tissue and is significantly larger than the natural δ^{15}N variability of the same species at unaffected locations. Geochemical maps of δ^{15}N values were created, which could be useful in monitoring the influence of human sewage impacts in marine coastal ecosystems. Maps of sewage nitrogen distribution could also be used for planning municipal and industrial waste management in the region and to assist in monitoring the efficiency of environmental protection measures after the construction of a new wastewater treatment plant in Murter.

Scientific paper

Izvleček: Rezultati pričujoče raziskave kažejo, da je izotopska sestava dušika v partikulatni organski snovi (POM) in v nekaterih morskih organizmih, kot je naprimer anemona *Anemonia sulcata* odličen parameter za sledenje in monitoring komunalnih in drugih odplak v morskih priobalnih ekosistemih Pirovaškega zaliva in Murterskega morja (srednji Jadran). Vrednosti $\delta^{15}N$ v partikulatni organski snovi in v tkivu *A. sulcate* na območju Pirovaškega zaliva in v priobalju Murterskega morja, ki sta onesnažena predvsem z odplakami iz septičnih sistemov so bistveno večje v primerjavi z referenčno neonesnaženo lokacijo - plitvino Lumbarda na odprtem delu Kornatskega arhipelaga. Partikulatna organska snov iz onesnaženih območij vsebuje za 7,0 ‰, tkiva *A. sulcate* pa za 7,7 ‰ večji $\delta^{15}N$ v primerjavi s POM in tkivom anemon iz referenčne, neonesnažene lokacije. Omenjena obogatitev je znatno večja v primerjavi z variabilnostjo $\delta^{15}N$ v primerkih iste vrste na neonesnaženih lokacijah. Na podlagi dobljenih podatkov so bile napravljene tudi geokemične karte porazdelitve parametra $\delta^{15}N$, ki so uporabne za monitoring vpliva odpadnih voda iz septičnih sistemov na priobalne ekosisteme na tem območju. Omenjene geokemične karte bodo koristile tudi pri načrtovanju izpusta nove čistilne naprave na otoku Murter in v kasnejši fazi tudi za ugotavljanje njene efikastnosti, glede na zmanjšanje onesnaženja obalnih ekosistemov na tem območju z odpadnimi vodami.

Key words: sewage, pollution monitoring, nitrogen, stable isotope, particulate organic matter, *Anemonia sulcata*, Pirovac Bay, Murter Sea- Central Adriatic
Ključne besede: odpadne vode, monitoring onesnaženosti, dušik, stabilni izotop, partikulatna organska snov, *Anemonia sulcata*, Pirovaški zaliv, Murtersko morje, srednji Jadran

*Corresponding author. Tel.: +00386-1-4704-620;
e-mail address: tadej.dolenec@ntfgeo.uni-lj.si

INTRODUCTION

Increased nitrogen loading in particulate organic matter (POM) and sediments is commonly related to the eutrophication of coastal seas worldwide. A significant component of marine eutrophication in many near-shore environments can be attributed to inputs of anthropogenic nitrogen from untreated domestic sewage and municipal and industrial effluents (LEE AND OLSEN, 1985; NIXON ET AL., 1986; BACHTIAR ET AL., 1996; COSTANZO ET AL., 2001). Managing the effects of sewage entering marine ecosystems has become one of the major environmental challenges of today. Septic systems for household waste disposal and the tourist infrastructure (hotels, camps, marinas) are the predominant point sources of contaminants in the semi-enclosed Pirovac Bay and in the coastal part of the Murter Sea, Dalmatia. The expansion of the human population during the tourist season not serviced by an adequate municipal infrastructure represents an additional impact of human sewage on the marine coastal ecosystems of Murter Island, creating an increasing demand for on-site sewage treatment system on Murter Island.

The results presented are a part of a comprehensive study employing different tools such as geochemistry, hydrology, microbiology, etc., to investigate the impact of sewage effluents and their possible transport pattern in the investigated area of Pirovac Bay and the Murter Sea. The distribution of sewage effluents in marine ecosystems can be mapped using various parameters, such as salinity, nutrient concentrations, bacteria, organic matter composition, radioisotopic tracers, dye fluorescence, water current measurements and nitrogen isotope composition in water and sediments (Sweeney et al., 1980; Lindau et al., 1989; Smith-Evans and Dawes, 1996). The nitrogen stable isotopic composition of marine plants (Costanzo et al., 2001; Dolenec et al., 2005) and higher organisms (Moore et al., 1996; Hansson et al., 1997; Tucker et al., 1999; Costanzo et al., 2001) or POM (Heikoop et al., 2000) has also been used as a tracer of anthropogenic pollution. Here we present an approach that shows the extent and fate of bio-available sewage nitrogen in coastal marine ecosystems, also enabling identification of the location of the pollution source. It is based on the assumption that (1) the nitrogen isotope composition ($\delta^{15}N$) of POM (representing a mixture of phytoplankton, bacteria, micro-zooplankton and detritus) is affected by sewage-derived nitrogen enriched in ^{15}N, and (2) tissues of organisms of the same species or groups of organisms with a similar position in the food web, in our case *A. sulcata* individuals, reflect the $\delta^{15}N$ of their N source (Wada et al., 1991).

Stable nitrogen isotopes have been widely used to trace dissolved and particulate nutrients derived from animal wastes, septic systems and waste water treatment plants, as they physically and biologically move through ecosystems (Risk and Erdmann, 2000; Heikoop et al., 2000). Benthic and benthic feeding animals, as well as other organisms from sewage-impacted areas have shown $\delta^{15}N$ values distinct from those collected at unaffected reference sites (Van Dover et al., 1992; Spies et al., 1989; Moore et al., 1996; Hansson et al., 1997; Tucker et al., 1999; Costanzo et al., 2001). Stable isotopes of nitrogen can thus be used to distinguish between natural and anthropogenic nitrogen sources in the environment or ecosystems (Mariotti et al., 1984; Tucker et al., 1999; Sigleo and Macko, 2002). For illustration, $\delta^{15}N$ values of nitrate of commercial fertiliser typically range from – 2.5 to + 2.0 ‰, organic soil nitrate ranges from – 2 to + 9 ‰, and human and animal wastes range from + 10 to + 22 ‰ (Kreitler and Jones, 1975; Kreitler and Browning, 1983; Heaton, 1986; Barrett et al., 1999). Generally, $\delta^{15}N$ values of $NO_3 > +10$ ‰ are regarded as being indicative of the presence of faecal N (Barrett et al., 1999). Treated sewage shows $\delta^{15}N$ values around + 10 ‰ (Heaton, 1986). Marine POM in pristine oligotrophic environments exhibits $\delta^{15}N$ values distinctly lower than that collected in areas impacted by fin-fish aquaculture (Sara et al., 2004). Increased $\delta^{15}N$ values of about + 8 ‰ were measured in POM near the inflows from septic systems in the port of Murter (Dolenec et al., 2005); similar values were reported for POM dominated by untreated faecal matter of Jepara Bay (+ 7.9 ‰, Heikoop et al., 2000).

Stable nitrogen isotopes are also useful in tracing organic matter through food webs. Animals raised on diets with a known nitrogen composition preferentially incorporated ^{15}N rather than ^{14}N, producing proteins enriched in ^{15}N relative to the food (Minagawa and Wada, 1984; DeNiro and Epstein, 1981). In the trophic network among animals, $\delta^{15}N$ values of their tissues systematically increase by 1.3 to 5.3‰ per trophic level (Minagawa and Wada 1984; Wada et al. 1991, 1993; Lajtha and Michener 1994).

This study was designed with the following aims:

1) to test the hypothesis that the ^{15}N content of POM and *A. sulcata* tissue collected near-shore and off-shore along the coastal part of the semi-enclosed Pirovac Bay and Murter Sea (Central Adriatic) is a reliable indicator of anthropogenic nitrogen impact arising from mostly untreated domestic and industrial wastes discharged into the coastal marine environment;

2) to create maps of $\delta^{15}N$ values, which would enable determination of the geographical extent of anthropogenic impact on the adjacent area of the Murter Sea arising from transport by currents.

MATERIALS AND METHODS

POM considered as a potential food source for *A. sulcata* was sampled at 1m depth at 57 localities of the Murter Sea and semi-enclosed Pirovac Bay in August 2005 (Fig. 1). 5 l samples were filtered through glass fibre filters (GF/F, Whatman).

Individuals of *A. sulcata* were collected by scuba diving from the sea at depths of approximately 2 - 5 m at 31 localities in the same area (Fig. 2). All sampled individuals were size-matched (basal diameter 3 - 4 cm; tentacles extending 10 - 15 cm) and weighed (fresh weight: 40 - 50 g, dry weight after freeze-drying 8 - 10 g) to avoid possible isotope effects caused by ontogenetic dietary

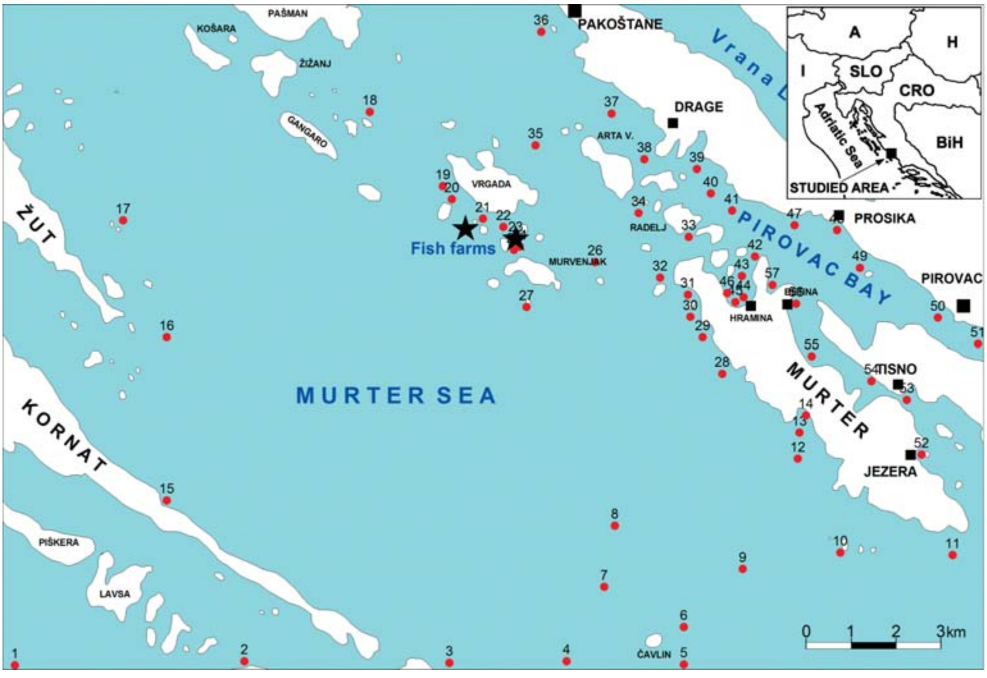

Figure 1. Map of the study area in the Murter Sea and Pirovac Bay (Central Adriatic) showing sites of POM sampling
Slika 1. Geografska karta vzorčnih točk partikulatne organske snovi (POM) v Murterskem morju in Pirovaškem zalivu (srednji Jadran)

shifts (DeNiro and Epstein, 1981; Muscatine and Kaplan, 1994) or age (Owens, 1987). Only pale green- coloured individuals with purple tentacle tips were chosen. To avoid the small seasonal differences in $\delta^{15}N$ values of anemone tissue observed during a preliminary study (Dolenec and Vokal, unpublished), we limited our analyses in this study to *A. sulcata* individuals collected during August 2002 (Dolenec et al., 2005). Fresh *A. sulcata* samples were placed in plastic bags and stored at - 20°C till further processing. Each sample was weighed prior to use in subsequent experiments. Samples of POM and A. *sulcata* were freeze-dried for >72 h and stored in a dessicator at room temperature. *A. sulcata* samples were crushed and homogenised by grinding in an agate mortar prior to analyses.

Nitrogen isotope composition of all samples was measured using a Europa 20-20 mass spectrometer with an ANCA SL preparation module (PDZ Europa Ltd., U.K.).The results were expressed in the standard $\delta^{15}N$ notation in permil (‰) relative to atmospheric nitrogen. The analytical precision (1 standard deviation) of triplicate analyses of IAEA N-1 and N-2 standards was better than ± 0.16 ‰. Precision (1 standard deviation) of duplicate isotope analyses of samples was within ± 0.2 ‰.

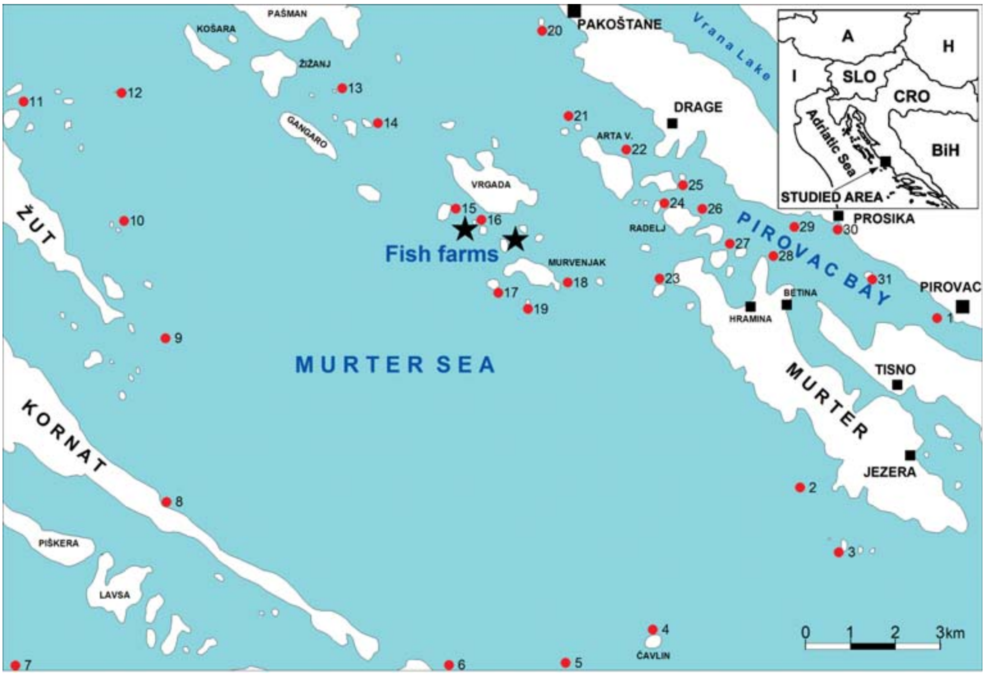

Figure 2. Map of the study area in the Murter Sea and Pirovac Bay (Central Adriatic) showing sites of *Anemonia sulcata* sampling

Slika 2. Geografska karta vzorčnih točk *Anemonie sulcate* v Murterskem morju in Pirovaškem zalivu (srednji Jadran)

RESULTS

The results of $\delta^{15}N$ determination in POM are listed in Table 1, while Table 2 shows the nitrogen isotope composition of *A. sulcata* (whole single animal). $\delta^{15}N$ of POM ranged from + 2.7 to + 9.7 ‰. Similar $\delta^{15}N$ values in the range from + 4.0 to + 11.9 ‰ were measured in *A. sulcata.*

The regional distribution pattern of POM $\delta^{15}N$ values in August 2005 is shown on Fig. 3, while the regional distribution pattern of $\delta^{15}N$ values of Anemonia sulcata individuals collected in the year 2002 is presented in Fig. 4.

Table 1. $\delta^{15}N$ values of particulate organic matter (POM) collected in the Murter Sea and Pirovac Bay - Central Adriatic in August 2005 (* reference site)
Tabela 1. Vrednosti $\delta^{15}N$ v partikulatni organski snovi (POM) v avgustu 2005 na območju Murterskega morja in Pirovaškega zaliva - srednji Jadran (* referenčna lokacija)

Sample No.	Sampling site	$\delta^{15}N$ (‰)	Sample No.	Sampling site	$\delta^{15}N$ (‰)
1	Reef Flat Lumbarda*	2.7	30	Podvrške - Bakarela	6.8
2	Sedlo Island	2.8	31	Podvrške - Port	4.9
3	Reef Flat Bačvica	3.0	32	Prišnjak V. Island	4.0
4	Samograd Island	3.6	33	Radelj Island	5.1
5	Reef Flat Kablinac	3.6	34	Prišnjak M. Island	4.3
6	Čavlin Island	3.8	35	Vrgada / Arta	4.6
7	Reef Flat Čavlin	3.5	36	Žavinac Island	4.6
8	Murter Sea I	3.8	37	Drage	4.6
9	Murter Sea II	4.2	38	Reef Flat Kušija	6.4
10	Kukuljari Island	4.0	39	Reef Flat Arta	5.1
11	Cap of Murter S	3.9	40	Pirovac Bay I	7.2
12	Tužbina Island	4.4	41	Pirovac Bay II	8
13	Kosirina Bay I	4.5	42	Cap of Gradina	7.2
14	Kosirina Bay II	5.7	43	Port of Murter	5.9
15	Bikarijca (coast)	2.8	44	Hramina (Marina)	7.5
16	Reef Flat Kamenjar	3.0	45	Luke	8.5
17	Dinariči Islands	3.5	46	Luke / Vinici	7.3
18	Runjava Kotula	-	47	Reef Flat Spličak	6.8
19	Špinata Island	4.5	48	Prosika (coast)	8.8
20	Obrovanj Island	4.6	49	Sustipanac Island	9.7
21	Reef Flat Kamičić	4.5	50	Port of Pirovac	6.2
22	Fish farms I	5.1	51	Makirina Bay	5.1
23	Fish farms II	4.5	52	Port of Jezera	6.3
24	Fish farms III	3.4	53	Tisno I	4.8
25	Fish farms IV	5.5	54	Tisno II	5.4
26	Visovac Island	4.5	55	Plitka Vala	5.4
27	Vrtlič Island	3.6	56	Port of Betina	5.0
28	Pod Raduč	4.8	57	Betina (Marina)	6.1
29	Slanica Bay	4.9			

Table 2. δ^{15}N values of *Anemonia sulcata* individuals (whole animal; Dolenec et al., 2005) collected in the Murter Sea and Pirovac Bay - Central Adriatic in August 2002 (* reference site)
Tabela 2. Vrednosti δ^{15}N v *Anemonii sulcati* v avgustu 2002 (celotni primerek; Dolenec et al., 2005) na območju Murterskega morja in Pirovaškega zaliva - srednji Jadran (* referenčna lokacija)

Sample No.	Sampling site	δ^{15}N (‰)	Sample No.	Sampling site	δ^{15}N (‰)
1	Pirovac (coast)	11.9	17	Gira Island	6.1
2	Murter Island SE	6.4	18	Murvenjak Island	5.8
3	Kukuljari Islands	6.1	19	Vrtlič Island	5.4
4	Reef Flat Čavlin	5.8	20	Žavinac Island	7.3
5	Nozdra Island	5.0	21	Sestrice Islands	7.1
6	Reef Flat Puh	4.7	22	Arta V. Island	7.1
7	Reef Flat Lumbarda*	4.2	23	Prišnjak V. Island	6.3
8	Bikarijca (coast)	5.1	24	Prišnjak M. Island	7.8
9	Reef Flat Kamenjar	5.4	25	Arta M. Island	7.6
10	Dinariči Islands	5.6	26	Radelj Island	7.3
11	Gustac Island	5.1	27	Vinik Island	9.8
12	Reef Flat Galijolica	5.8	28	Cap of Gradina	9.5
13	Ošljak Island	5.2	29	Reef Flat Spličak	10.1
14	R. Kotula Island	5.3	30	Prosika (coast)	10.8
15	Špinata Island	6.7	31	Sustipanac Island	11.8
16	Rakita Island	6.3			

From Tables 1 and 2, as well as from Fig. 3 and 4, it is evident that:

1) The variations in ^{15}N content of both POM and of *A. sulcata* appear to be influenced primarily by the environment in which they were collected.
2) δ^{5}N values of POM and *A. sulcata* tissue were significantly higher at the anthropogenically affected sites in the semi-enclosed Pirovac Bay, along the coast of the Murter Sea and the rocky shores of islands close to Murter Island, compared to POM and *A. sulcata* from an unaffected reference site on the shallow Lumbarda reef flat in the open sea (approx. 3 m deep) and those from small uninhabited offshore islands (Dolenec et al., 2005).
3) δ^{15}N values of POM showed significant differences between ^{15}N depleted sampling sites (1-8, 15-17 and 27) from the reference location (Reef Flat of Lumbarda) as well as the relatively unaffected offshore part of the Murter Sea and the sampling sites (12-14 and 28-57) from Pirovac Bay and the coastal part of the Murter Island affected due to dissolved faecal organic matter. Samples of POM from the reference site (1) and offshore locations (2-8, 15-17 and 27) had δ^{15}N values in the range between + 2.7 and + 3.3 ‰, while those dominated by untreated faecal matter (12-14 and 28-57) typically had values within the range from + 4.6 to + 9.7 ‰. The δ^{15}N values of POM

collected in the area around the fish farms at the Vrgada Island (sampling sites 19-26) have been determined to vary from + 4.5 to 5.1 ‰. A gradient towards lower $\delta^{15}N$ values was observed from the impacted sites around fish cages toward locations further away, as also observed in previous studies (DOLENEC ET AL., 2005).

4) *Anemonia sulcata* individuals living on the offshore reef flats or on rocky shores of small isolated islands of the Murter Sea, as well as along the coastal part of the Kornati Islands and small uninhabited islands around the Island of Žut (sample sites 4 to 12) had consistently lower $\delta^{15}N$ values (average: + 5.2 ‰; range: + 4.2 to + 5.8 ‰) than individuals living on rocky surfaces of the coastal parts of the islands closer to the coast (sample sites 13 to 19). These latter had $\delta^{15}N$ values with an average of + 5.8 ‰, ranging from + 5.2 to + 6.7 ‰ (Table 2). Slightly enriched $\delta^{15}N$ values (up to 2.5 ‰ relative to the reference site) in this region were found in anemones from small islands around fish farms (sample points 15, 16 and 17). Considerably higher $d^{15}N$ values (average + 6.9 ‰; range + 6.1 to + 7.8 ‰) were measured along the islands separating Pirovac Bay from the Murter Sea (sampling sites 21, 22, 24 and 25), as well as along the coastal part of Murter Island (sampling sites 2 and 23) and the Islands of Kukuljari (sampling site 3). However, the highest $\delta^{15}N$ values (+7.3 to +11.9 ‰, averaging +10.2 ‰) were found in *A. sulcata* tissues from the inner part of Pirovac Bay (sampling sites 1 and 26-31), (DOLENEC ET AL., 2005).

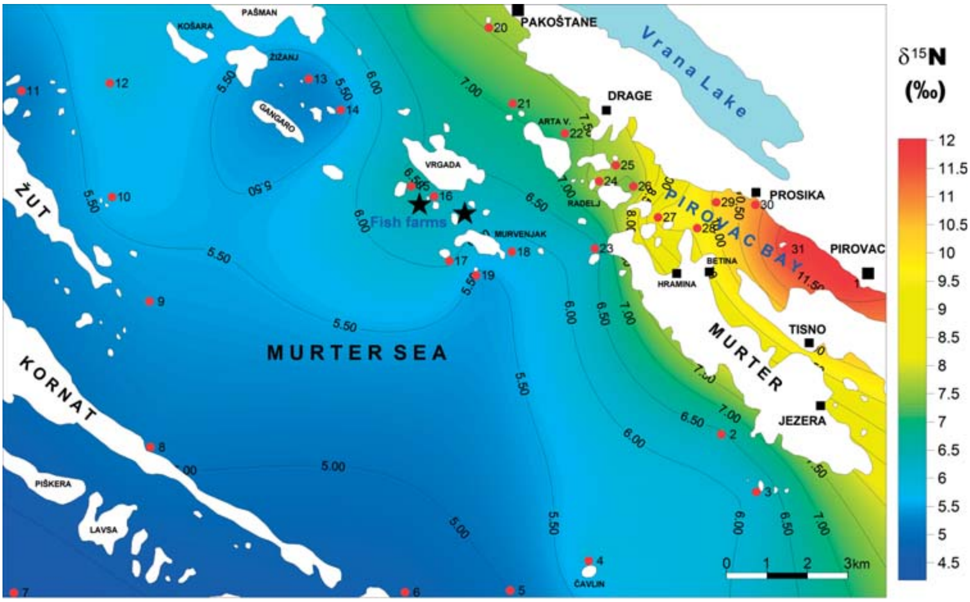

Figure 3. Spatial distribution pattern of $\delta^{15}N$ values of POM throughout the Murter Sea and Pirovac Bay (Central Adriatic)

Slika 3. Prostorska porazdelitev vrednosti $\delta^{15}N$ v partikulatni organske snovi (POM) v Murterskem morju in Pirovaškem zalivu (srednji Jadran)

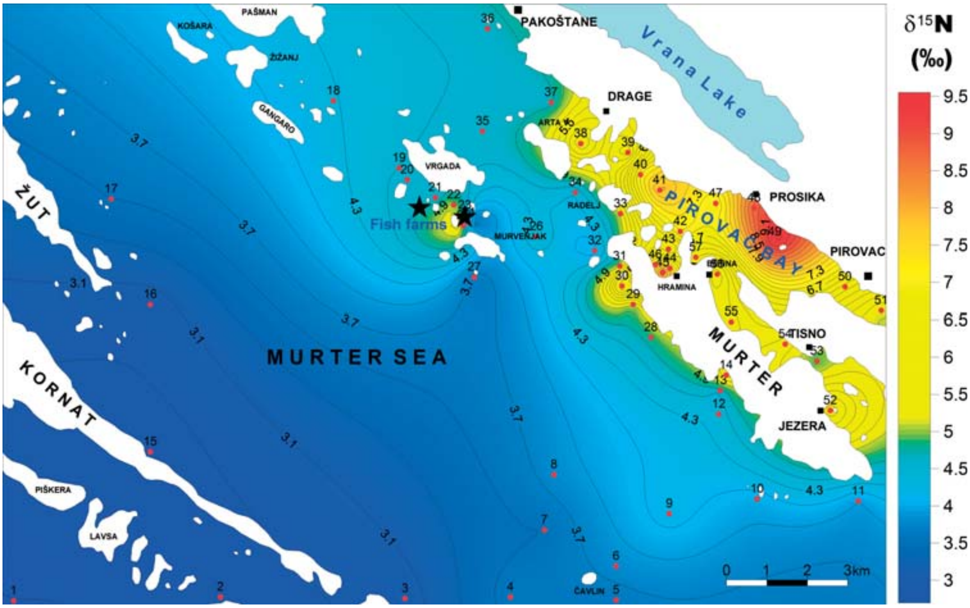

Figure 4. Spatial distribution pattern of δ^{15}N values of *Anemonia sulcata* throughout Pirovac Bay and the Murter Sea - Central Adriatic (Dolenec et al., 2005)

Slika 4. Prostorska porazdelitev vrednosti δ^{15}N v *Anemonii sulcati* v Murterskem morju in Pirovaškem zalivu - srednji Jadran (Dolenec et al., 2005)

Discussion

The ^{15}N enrichment of POM and anemones from the semi-enclosed Pirovac Bay, coastal parts of Murter Island, as well as from the inshore islands that separate Pirovac Bay from the Murter Sea, indicates that their primary food source is affected by heavy nitrogen due to local inputs of untreated sewage effluents into the coastal marine environment. Since sewage-derived wastewater DIN (dissolved inorganic nitrogen) is typically enriched in ^{15}N and exhibits δ^{15}N values mostly in the range between + 10 and + 22 ‰ (Heaton, 1986), this source term may also be responsible for the ^{15}N enrichment in phytoplankton. Such enrichment in ^{15}N due to ground water DIN was found in both primary producers and consumers in estuarine settings of Cape Cod, Massachusetts (McClelland et al., 1997; McClelland and Valiela, 1998). ^{15}N enrichment has also been found in reef molluscs, stomatopods, fishes and corals in settings exposed to anthropogenic nutrient pollution (Risk and Heikoop, 1997; Mendes et al., 1997, Heikoop et al., 2000; Risk and Erdman, 2000, Weiss et al., 2002). Zooplankton and reef particulate organic matter may have higher δ^{15}N values at sewage-polluted sites if ^{15}N-enriched wastewater is utilised by phytoplankton at the base of the food chain (Hansson et al., 1997). Elevated δ^{15}N values have also been measured in marine plants exposed to ground water contaminated by septic systems (McClelland et al., 1997) and sewage effluents (Grice et al., 1996; Udy and Dennison, 1997; Costanzo et al., 2001).

The spatial distributions of the sewage source indicators such as the $\delta^{15}N$ signal in POM and *A. sulcata* tissues allow us to draw conclusions on the impact pattern of sewage effluents and their transport in the coastal part of the Murter Island and Pirovac Bay. In line with the $\delta^{15}N$ values of *A. sulcata,* a similar spatial distribution of $\delta^{15}N$ was found also in other marine organisms such as *Aplysina aerophoba, Balanus perforatus, Mytilus galloprovincialis, Arca noae, Ostrea edulis* and marine plants (*Posidonia oceanica)* from the same sampling sites collected during the years 2004 and 2005 (DOLENEC ET AL., IN PREPARATION). A small difference in the sewage plumes delineated by $\delta^{15}N$ values of POM and *A. sulcata* was observed, but the overall trends are the same. POM shows the clearest plume resolution, extending up to several km from the major sources. This undoubtedly suggests that the isotope techniques used in this study are useful not only for showing the actual uptake and assimilation of sewage nutrients by marine organisms and plants, but also in tracing sewage effluent transport in the sampling area under consideration.

From Figures 3 and 4 it is evident that the enrichment decreases with distance from the coast toward open sea ecosystems. Such on-shore to offshore $\delta^{15}N$ variations most probably indicate that the sewage-induced ^{15}N enrichment signal is rapidly attenuated with distance from the sewage sources (within some kilometres for sewage from the inhabited areas of Pirovac Bay and Murter Island). Similar inshore-offshore $\delta^{15}N$ variations have also been observed in stomatopods from southwest Sulawesi (Risk and Erdman, 2000) and corals from Indonesia, Zanzibar and the Maldives (HEIKOOP ET AL., 2000; RISK AND ERDMAN, 2000).

The most important characteristic of the Adriatic Sea is the general counter-clockwise water circulation pattern, which is reflected in the spatial distribution of $\delta^{15}N$ values of POM and sea anemones (Fig. 2). The strongest $\delta^{15}N$ signal is typical of polluted coastal ecosystems, especially those of the semi-enclosed Pirovac Bay. Here ^{15}N enrichment undoubtedly resulted from wastewater nutrients derived mostly from septic systems in the surrounding villages, tourist centres in Pirovac Bay (Murter, Betina, Tisno, Jezera and Pirovac), marinas (Hramina, Betina and Jezera), and seasonally open auto camps. The ^{15}N sewage signal of Pirovac Bay was evident up to 6 km NW of the Bay, though it decreases with distance from the shore. It is supposed that mixing of sewage affected seawater from Pirovac Bay with less polluted south-east to north-west sea currents may have diluted the signal from the Bay.

The elevated $\delta^{15}N$ signal in the SW coastal part of Murter Island also suggests that pollutants may reach the coastal ecosystems of the Murter Sea from local septic systems in the settlement of Podraduč, the Colentum hotel, as well as by prevalently current-derived mass transport from the south-east where such pollution sources are located (i. e. the cities of Split and Šibenik releasing urban and industrial waste, and the tourist centres of Vodice and Tribunj). It is noteworthy that a similar regional distribution pattern influenced by the counter-clockwise system of the Adriatic Sea currents, showing an onshore to offshore attenuation, was also observed in heavy metal concentrations in the Central Adriatic (DOLENEC ET AL., 1998).

The net transport pattern inferred from the previous isotope tracer indicators such as the $\delta^{15}N$ signal in POM (Fig. 3) seem to be compatible with models of two dimensional circulation of a buoyant effluent plume, under the influence of the prevailing tidal and wind-driven current regime. The overall transport direction of sewage-derived effluents with a predominant component of faecal matter is shown to be toward the NW, more or less parallel to the shore. The secondary trend is directed toward the west and southwest and could be explained by wind driven circulation of the surface water and local tidal currents. Preliminary observations during summer 2005 indicated that during SW-NE and NW-SE winds (bura, tramontana), south-westward and north-eastward currents are developed in the coastal area of Pirovac Bay and the Murter Sea, which are capable of redistribution of sewage effluents enriched by ^{15}N in the above mentioned prevalent directions.

Conclusions

Stable nitrogen isotopes enabled us to identify a sewage signal in POM and *A. sulcata* in Pirovac Bay and the Murter Sea and suggested a higher fraction of faecal sewage-derived N in the whole food web in coastal ecosystems. The results of this study further indicate that *A. sulcata* from the most polluted sites are most probably consuming food with a significant sewage component. This is also confirmed by ^{15}N enrichment in POM from more polluted sampling sites of Pirovac Bay and the Murter Sea, which represent the base of the food web. The observed variations in POM and *A. sulcata* $\delta^{15}N$ values appear to be primarily explained by variation in the extent of domestic and industrial wastes, which have been discharged into the coastal ecosystems of the investigated area. By using $\delta^{15}N$ values of POM and *A. sulcata* the anthropogenic nitrogen inputs in many other marine coastal ecosystems could be also easily detected and mapped.

This technique also provides some insight into sewage effluent plume transport, which can be effectively traced by analyses of the spatial distribution of $\delta^{15}N$ values of POM. The distribution-transport patterns identified by this study provide a useful preliminary survey of the possible transport/deposition cycles involving domestic and other sewage wastes associated with the proposed construction of a new sewage treatment plant (STP) in Murter.

Acknowledgements

This research was financially supported by the Ministry of Higher Education, Science and Technology, Republic of Slovenia (research programmes P1-0195-1555 and P1-0143-0106, and a Bilateral Project between Croatia and Slovenia for the years 2005-2006), and Geoexp, d. o. o., Tržič, Slovenia. Thanks also to Dr. Anthony Byrne for the linguistic corrections.

REFERENCES

BACHTIAR, T., COAKLEY, J. P., RISK, M. J. (1996). Tracing sewage contaminant sediments in Hamilton Harbour using selected geochemical indicators. *The Science of the Total environment* **179**, 3-16.

BARRETT, M. H., HISCOCK, K. M., PEDLEY, S., LERNER, D. N., TELLAM, J. H. AND FRENCH, M. J. (1999). Marker species for identifying urban groundwater recharge sources: a review and case study in Nottingham, UK. *Water Research* **33**, 3083-3097.

CABANA, G. AND RASMUSEN, I. B. (1994). Modelling food chain structure and contaminant bioaccumulation using stable nitrogen isotopes. *Nature* **372**, 255-257.

COSTANZO, S. D., O´DONOHUE, M. J., DENNISON, W. C., LONERAGAN, N. R., AND THOMAS, M. (2001). A new approach for detecting and mapping sewage impacts. *Marine Pollution Bulletin* **42**, 149 - 156.

DENIRO, M. I. AND EPSTEIN, S. (1981). Influence of diet on the distribution of carbon isotopes in animals. *Geochimica et Cosmochimica Acta* **45**, 341-351.

DOLENEC, T., VOKAL, B. AND DOLENEC, M. (2005). Nitrogen - 15 signals of anthropogenic nutrient loading in *Anemonia sulcata* as a possible indicator of human sewage impacts on marine coastal ecosystems: a case study of Pirovac Bay and the Murter Sea (Central Adriatic). *Croatica Chemica Acta* **78/4**, 593'600.

GRICE, A. M., LONERAGAN, N. R. AND DENNISON, W. C. (1996). Light intensity and the interactions between physiology, morphology and stable isotope ratios in five species of seagrass. *Journal of Experimental Marine Biology and Ecology* **195**, 91-110.

HANSSON, S., HOBBIE, J. E., ELMGREN, R., LARSSON, U., FRY, B. AND JOHANSSON, S. (1997). The stable nitrogen isotope ratio as a marker of food-web interactions and fish migration. *Ecology* **78**, 2249-2257.

HEATON, T. H. E. (1986). Isotopic studies of nitrogen pollution in the hydrosphere and atmosphere: a review. *Chemical Geology (Isotype Geoscience Section)* **59**, 87-102.

Heikoop, J. M., Risk, M. J., Lazier, A. V., Edinger, E. N., Jompa, J., Limmon, G. V., Dunn, J. J., Browne, D. R. and Schwarcz, H. P. (2000). Nitrogen-15 signals of anthropogenic nutrient loading in reef corals. *Marine Pollution Bulletin* **40**, 628-636.

KREITLER, C. W. AND JONES, D. C. (1975). Natural soil nitrate: the cause of the nitrate contamination of ground water in Runnels County, Texas. *Ground Water* **13**, 53-61.

KREITLER, C. W. AND BROWNING, L. A. (1983). Nitrogen-isotope analysis of groundwater nitrate in carbonate aquifers: natural sources versus human pollution. *Jorunal of Hydrology* **61**, 285-301.

LAJTHA, K. AND MICHENER, R.M. (EDS) (1994) Stable Isotopes in Ecology and Environmental Sciences. Blackwell Science, New York.

LEE, V. AND OLSEN, S. (1985). Eutrophication and management initiatives for the control of nutrients input to Rhode Island coastal lagoons. *Estuaries* **8**, 191-202.

LINDAU, C. W., DELAUNE R. D., PATRICK W. H. JR. AND LAMBREMONT, E. N. (1989) Assessment of stable nitrogen isotopes in fingerprinting surface water inorganic nitrogen sources. *Water, Air and Soil Pollution* **48**, 489-496.

MARIOTTI, A., LANCELOT, C. AND BILLEN, G. (1984). Natural isotopic composition of nitrogen as a tracer of origin for suspended organic matter in the Scheldt estuary. *Geochimica et Cosmochimica Acta* **48**, 549-555.

MCCLELLAND, J. W., VALIELA, I. AND MICHENER, R. H. (1997). Nitrogen stable isotope signatures in estuarine foodwebs: A record of increasing urbanization in coastal watersheds. *Limnology and Oceanography* **42**, 930-937.

MCCLELLAND, J. W. AND VALIELA, I. (1998). Linking nitrogen in estuarine producers to land-derived sources. *Limnology and Oceanography* **43**, 577-585.

MENDES, J. M., RISK, M. J., SCHWARCZ, H. P. AND WOODLEY, J. D. (1997). Stable isotope of nitrogen as measures of marine pollution: a preliminary assay of coral tissue from Jamaica, *Proceeding of the Eight International Coral Reef Symposium* **2**, 1869-1872.

MINAGAWA, M., AND WADA, E. (1984) Stepwise enrichment of ^{15}N along food chains: Further evidence and the relation between δ^{15}N and animal age. Geochim Cosmochim Acta **48** 1135-1140.

Moore, M. J., Shea, D., Hillman, R. and Stegeman, J. J. (1996). Trends in hepatic tumours and hydropic vacuolation, fin erosion, organic chemicals and stable isotope ratios in winter flounder from Massachusetts, USA. *Marine Pollution Bulletin* **32**, 458-470.

Muscatine, L. and Kaplan, I. R. (1994). Resource partitioning by reef corals as determined from stable isotope composition: II. δ^{15}N of zooxanthellae and animal tissue versus depth. *Pacific Science* **48**, 304-312.

Nixon, S. W., Oviatt, C. A., Frithsen, J. and Sullivan, B. (1986). Nutrients and the productivity of estuarine and coastal marine ecosystems. *Journal of the Limnology Society of South Africa* **12**, 43-71.

Owens, N. J. P. (1987). δ^{15}N in the marine environment. *Advances in Marine Biology* **24**, 389-451.

Risk, M. J. and Heikoop, J. M. (1997). Stable isotope ratios of nitrogen (δ^{15}N) as a measure of sewage stress on tropical coal reefs. *Abstracts of Papers of the American chemical Society* **214**, 68.

Risk, M. I. and Erdman, M. V. (2000). Isotopic composition of nitrogen in stomatopod (Crustacea) tissues as an indicator of human sewage impacts on Indonesian coral reefs. *Marine Pollution Bulletin* **40**, 50-58.

Sarŕ, G., Scilipoti, D., Mazzola, A. and Modica, A. (2004). Effects of fish farming waste to sedimentary and particulate organic matter in a southern Mediterranean area (Gulf of Castellammare, Sicily): a multiple stable isotope study (δ^{13}C and δ^{15}N). *Aquaculture,* 2004 (online).

Sigleo, A. C. and Macko, S. A. (2002). Carbon and nitrogen isotopes in suspended particles and colloids, Chesapeake and San Francisco Estuaries, U.S.A. *Estuarine, Coastal and Shelf Science* **54**, 701-711.

Smith-Evans, M. and Dawes, A. (1996). Early experiences in monitoring the effect of Hong Kong's new generation of sewage outfalls on the environment. *Marine Pollution Bulletin* **121**, 317-321.

Spies, R. B., Kruger, H., Ireland, R. and Rice, D. W. (1989). Stable isotope ratios and contaminant concentrations in a sewage-distorted food web. *Marine Ecological Programming Series* **54**, 157-170.

Sweeney, R. E., Kalil, E. K. and Kaplan, I. R. (1980). Characterisation of domestic and industrial sewage in southern California coastal sediments using nitrogen, carbon, sulphur and uranium tracers. *Marine Environmental Research* **3**, 225-243.

Tucker, J., Sheats, N., Giblin, A. E., Hopkinson, C. S. and Montoya, J. P. (1999). Using stable isotopes to trace sewage-derived material through Boston Harbor and Massachusetts Bay. *Marine Environmental Research* **48**, 353-375.

Udy, J. W. and Dennison, W. C. (1997). Physiological responses of seagrasses used to identify anthropogenic nutrient inputs. *Marine Freshwater Research* **48**, 605 - 614.

Van Dover, C. L., Grassle, J. F., Fry, B., Garritt, R. H. and Starczak, V. R. (1992). Stable isotope evidence for entry of sewage-derived organic material into a deep-sea food web. *Nature* **360**, 153-155.

Wada, E., Mizutani, H. and Minagawa, M. (1991). The use of stable isotopes for food web analysis. *Critical Reviews in Food Science and Nutrition* **30**, 361-371.

Wada, E., Kabaya, Y. and Kurihara, Y. (1993) Stable isotopic structure of aquatic ecosystems. Journal of Biosciences **18**, 483-499.

Weiss, E. T., Carmichael, R. H. and Valiela, I. (2002). The effect of nitrogen loading on the growth rates of quahogs (*Mercenaria mercenaria*) and soft-shell clams (*Mya arenaria*) through changes in food supply. *Aquaculture* **211**, 175-189.

Importance of detailed measurements in assessment of safe levels of radon

Janja Vaupotič, Ivan Kobal

Jožef Stefan Institute, POB 3000, SI-1001 Ljubljana, Slovenia;
E-mail: janja.vaupotic@ijs.si

Received: March 9, 2006 **Accepted**: July 20, 2006

Abstract: In a school in the Žirovski vrh area, a classroom with an indoor radon concentration of more than 3000 Bq m^{-3} was found. The floor in the room was the major radon source. After a new floor was built with a concrete slab and perforated tubes underneath, the indoor radon concentration was reduced to 250 Bq m^{-3}.

Key words: radon, indoor air, schools, elevated concentrations, mitigation

Introduction

The Slovene indoor radon programme was introduced in 1990 by the Slovenian Radiation Protection Administration at the Ministry of Health and was executed in three stages. In the first stage, instantaneous indoor radon concentrations under 'closed conditions', and gamma dose rates were measured in all 730 kindergartens and play schools (Vaupotič et al., 1994; 1998). In the second stage similar measurements were carried out in all 890 elementary and high schools (Bilban and Vaupotič, 2001; Vaupotič et al., 2000; Vaupotič, 2001: Popit and Vaupotič, 2002), and in the third stage three month average indoor radon concentrations were obtained in 1000 randomly-selected dwellings by exposing etched track detectors (Ilić et al., 1995).

In the second stage, the indoor radon concentration in 25 schools was found to exceed 1000 Bq m^{-3}. Some of these schools are located in the area of the Žirovski vrh uranium ore deposits. The uranium mine was in operation from 1984 to 1990. The Slovene Nuclear Safety Administration initiated an additional radon survey in all 19 schools in the broader Žirovski vrh area (Vaupotič, 2001). Among them was the Ret-OS elementary school in which a fast radon screening in the second stage showed a value of only 79 ± 13 Bq m^{-3}. During the additional radon survey in this school, all the ground floor classrooms were examined. Everywhere radon levels were low, less than 400 Bq m^{-3}, with the only exception of classroom-1 in which it exceeded 3000 Bq m^{-3}. A thorough inspection of the whole school confirmed that the enhanced concentration was limited to this classroom. The Slovenian Radiation Protection Administration issued a decree to the management of the school requiring radon mitigation accompanied by radon monitoring.

This paper discusses radon monitoring in the Ret-OS elementary school, with special emphasis to measurements before, during and after mitigation of the high radon level classroom-1.

Scientific paper

Experimental

Alpha scintillation cells were used to measure instantaneous indoor radon concentration (Vaupotič et al., 1992) while to obtain long-term averages, KfK etched track detectors were exposed for 2 to 3 months (Urban and Schmitz, 1993). For continuous radon monitoring AlphaGuard (Genitron, Germany) and for continuous radon and radon decay products monitoring EQF 3010 and EQF 3020 (Sarad, Germany) instruments were used. Gamma dose rates were measured by a portable ASP-1 scintillation counter (Eberline, USA) and by exposing thermoluminescent dosimeters (Mihelič et al., 1985). Samples of the building material were analysed for radioactivity by gamma spectrometry at the Department of Low and Medium Energy Physics at the Jožef Stefan Institute.

All measuring devices have been regularly checked at the intercomparison experiments organised annually by the Nuclear Safety Administration at the Slovene Ministry of the Environment (Križman, 1997; 2000; 2001).

Results and discussion

The Ret-OS elementary school was built of stone in 1938. It is a two-story building with a basement under only part of it. The building was renovated two years before our radon survey and in each of the classrooms on the first floor a slab of poured concrete was built, except in classroom-1, in which the elevated radon level was found. Thus, from the very beginning, the floor was suspected as the major source of high radon concentration in the room.

During the second stage of radon survey, the Ret-OS elementary school was found to show low radon concentration and the *hot spot* was discovered by subsequent, more detailed measurements in all the schools in the Žirovski vrh uranium ore deposit area. Alpha scintillation cells were used to measure radon in all the classrooms and at potential radon sources (Vaupotič, 2002a; 2002b), and additionally etched track detectors were exposed in some of them. Gamma dose rates measured in five classrooms ranged from 70 to 172 mSv per

Table 1. Radon concentrations in the Ret-OS elementary school prior to mitigation. Instantaneous values were obtained using alpha scintillation cells, and 3-month average values by etched track detectors

Room	Instantaneous Bq m^{-3} *21.12.1995*	3-month average Bq m^{-3} *13.09.1995 – 11.12.1995*	3-month average Bq m^{-3} *11.12.1995 – 17.01.1996*
Classroom-1	3700 ± 100	600 ± 50	2100 ± 170
Classroom-2	79 ± 13	68 ± 10	130 ± 10
Gym	570 ± 50	185 ± 10	470 ± 40
Basement	845 ± 120		660 ± 60

month. A selection of the obtained radon concentrations are collected in Table 1. It was confirmed that the radon level is high only in the classroom-1, in which the floor slab was not rebuilt during the renovation of the school. Therefore, we focused our investigations only on this classroom.

An etched track detector was exposed for the period February 10 to May 10, 1995. During the period March 16–26, 1995 radon concentration was recorded continuously by the AlphaGuard instrument. The curve in Figure 1 shows the expected diurnal run with a high maximum every morning and during the weekends. From these data, different averages of radon concentration were calculated and are collected in Figure 2. Daily averages during teaching hours only (black squares) are usually higher than 24-hour daily averages (empty squares). The 11-day (duration of continuous measurement) average (thin line) is 2490 Bq m^{-3}. Considering the broken line (overall average during teaching hours, 2850 Bq m^{-3}) and the thick line (3-month average concentration, 1600 Bq m^{-3}), we see that the etched track detectors underestimated the exposure of teachers and pupils during the occupancy hours by a factor of two for this particular week. Hence, the results from etched track detectors should be interpreted with a caution.

Week long continuous monitoring of radon and radon decay products in classroom-1 were later repeated several times under different meteorological conditions. An example of such a measurement in the winter period December 11–20, 1995, is presented in Figure 3. The shape of the radon curve is similar to that in Figure 1, with a 9-day average radon concentration of 2386 Bq m^{-3} and average radon decay products concentration of 1320 Bq m^{-3}, giving an equilibrium factor of 0.55.

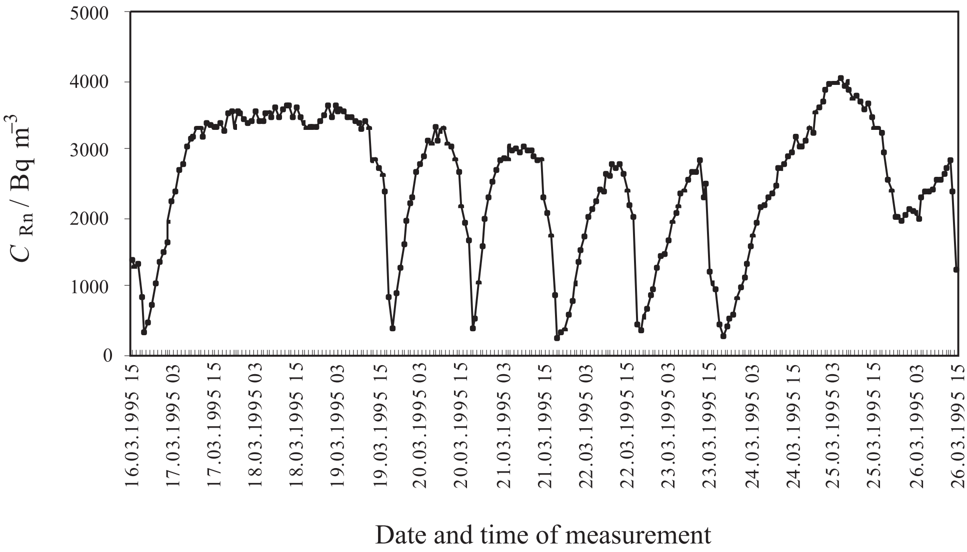

Figure 1. Diurnal variation of radon concentration in classroom-1 obtained by using the AlphaGuard device in the period of March 16–26, 1995, prior to mitigation

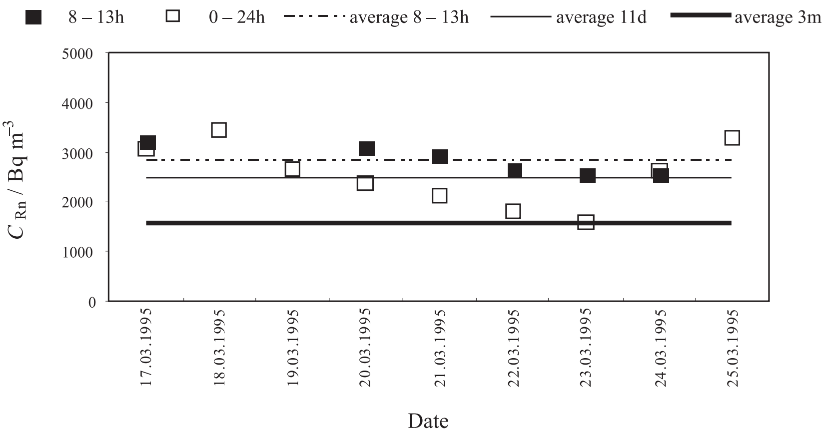

Figure 2. Average radon concentrations calculated from the data in Figure 1, and compared with the average value obtained by etched track detector: full squares: (8–13h)-daily average, during teaching hours only; broken line: (8–13h)-daily averages averaged over all working days; open squares: (0–24h) daily average, the whole day; thin line: (0–24h) daily averages averaged over the entire period of measurement, 11 days; thick line: average obtained by etched track detector in the period from February 10 to May 10, 1995

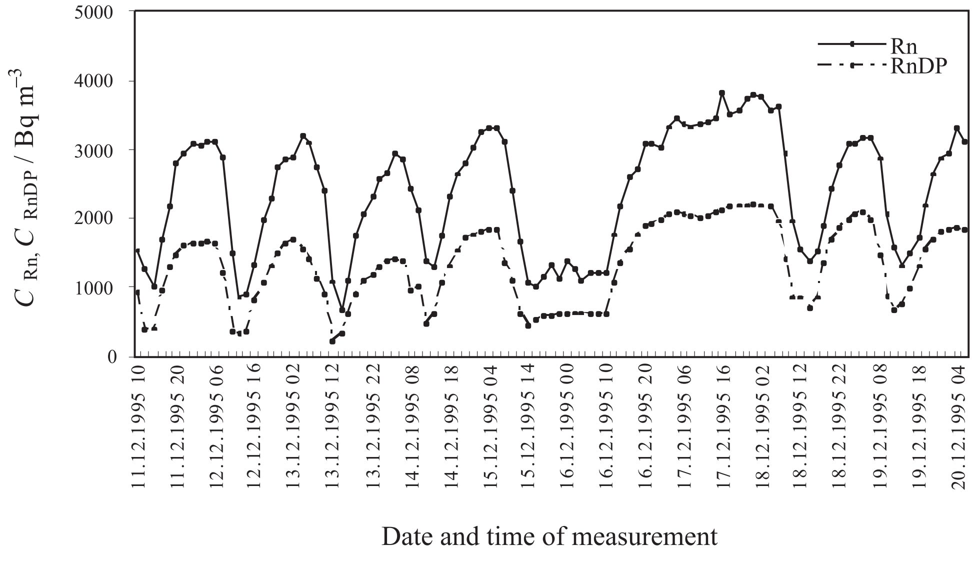

Figure 3. Diurnal variation of radon concentration in classroom-1 obtained by using EQF 3020 device in the period of December 11–20, 1995, prior to mitigation

Based on these results, in May 1996 the Slovenian Radiation Protection Administration required from the management of the school to undertake mitigation measures in classroom-1 during summer vacations.

According to our experience with radon mitigation in kindergartens (VAUPOTIČ ET AL., 1994), the floor, not properly constructed initially and then not renovated, was suspected to be the major source of the enhanced radon

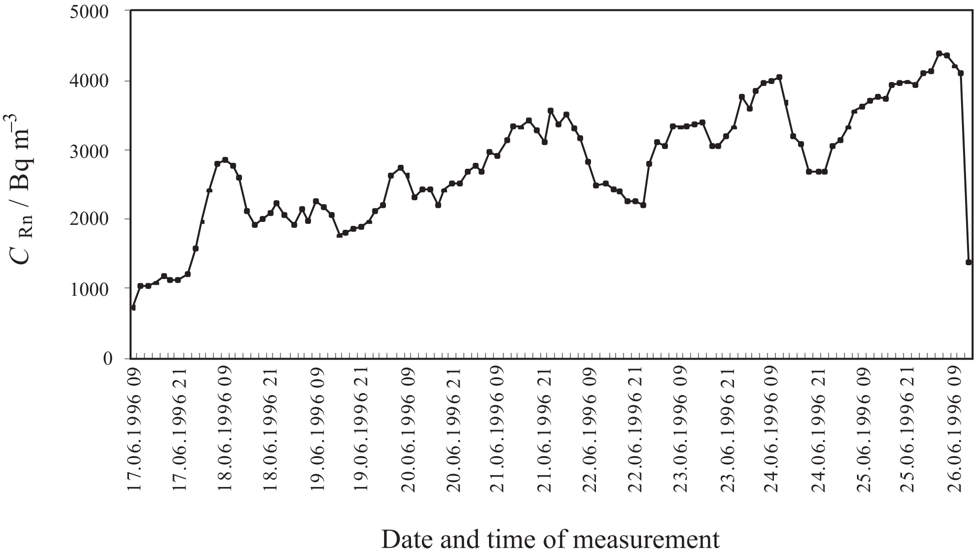

Figure 4. Diurnal variation of radon concentration in classroom-1 obtained by using the AlphaGuard device in the period of June 17–26, 1996, after removing the floor

concentration in classroom-1. In order to obtain more information, samples of the building material and surrounding soils were analysed by gamma spectrometry (Table 2). In no sample a ^{226}Ra content higher than somewhere else in Slovenia (Andjelov and Brajnik, 1996; Brajnik et al., 1992; Kobal et al., 1990) was found. Building material was thus ruled out as a significant radon source.

Reconstruction of the floor started in June 1996. First, the wooden parquet and a thin concrete layer were removed. The concrete layer was found to have been made very badly, showing numerous cracks and faults. Radon and radon decay products were monitored again in the period of June 17–26, 1996 (Figure 4). This time, the door and windows were kept closed during

Table 2. Results of high-resolution gamma spectrometric analyses of building material and surrounding soil

Sample	^{238}U Bq kg^{-1}	^{226}Ra Bq kg^{-1}	^{210}Pb Bq kg^{-1}	^{228}Ra Bq kg^{-1}	^{228}Th Bq kg^{-1}	^{40}K Bq kg^{-1}
Wall, plaster	33 ± 5	24 ± 6	< 76	16 ± 8	19 ± 4	240 ± 5
Wall, brick	48 ± 8	48 ± 1		45 ± 2	50 ± 1	640 ± 15
Concrete-1	25 ± 4	24 ± 6		13 ± 1	14 ± 1	180 ± 4
Concrete-2	22 ± 4	23 ± 1	< 38	12 ± 1	12 ± 1	160 ± 4
Soil-1	28 ± 5	25 ± 1		14 ± 1	14 ± 1	180 ± 4
Soil-2	20 ± 4	25 ± 1	< 27	16 ± 1	15 ± 1	220 ± 4
Soil-3	22 ± 2	23 ± 1	< 20	12 ± 1	12 ± 1	160 ± 3
Gravel	20 ± 3	17 ± 1		6 ± 1	7 ± 1	77 ± 3

measurements. No drastic increase in radon concentration was observed. A 9-day average radon concentration of 3000 Bq m^{-3} was again obtained. This meant that the floor had offered practically no barrier to radon exhalation from the ground.

The complete floor was removed. The foundation of the room was filled with gravel into which perforated plastic tubes 150 mm in diameter were buried, running from the inner wall toward the openings in the outer front wall. For the time being these tubes only enable natural air ventilation of the sub-floor space, but if necessary, fans can be installed. Over the gravel a poured concrete slab of high quality cement was constructed, covered first with a hydro insulator and then with a skim of cement onto which a wooden parquet was laid.

All stages of renovation were accompanied by measuring radon and radon decay products in the air. The last continuous measurement, carried out during the period September 20–30, 1996, under the normal working regime of the school, with regular classes in classroom-1, is shown in Figure 5. After remediation, radon measurements were performed several times using etched track detectors. Results are summarized in Table 3. These values and Figure 5 show a reduction of radon concentration by a factor of about 10 from the values before mitigation. Now, radon concentration never exceeds the national limit for homes (kindergartens and schools) of 400 Bq m^{-3} (ULRS, 2002; 2004).

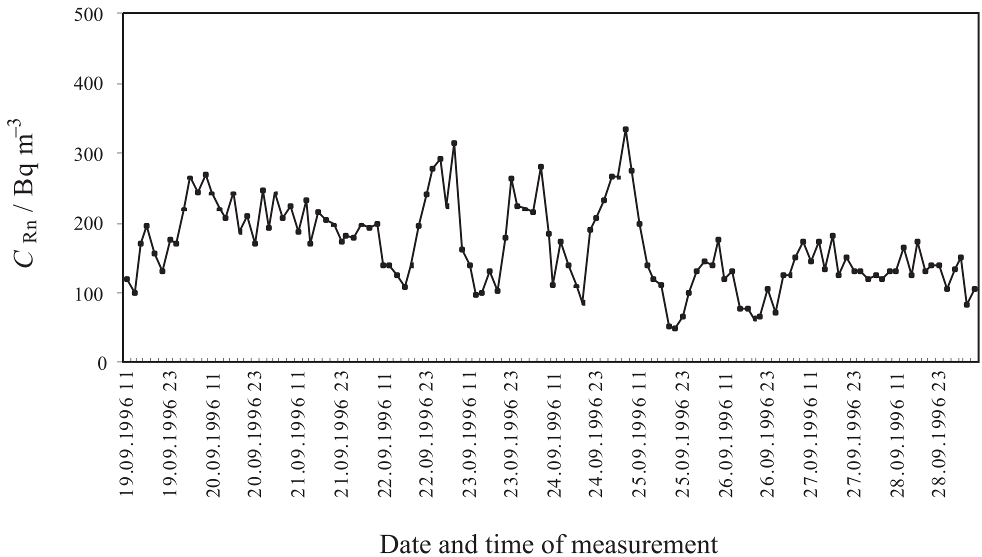

Figure 5. Diurnal variation of radon concentration in classroom-1 obtained by using the AlphaGuard device during a normal working regime in the period of September 19–28, 1996, after mitigation was completed

Table 3. Average radon concentrations obtained by etched track detectors in classroom-1 following mitigation

Period of measurement	Radon concentration Bq m^{-3}
07.04. – 16.06.1997	211 ± 15
16.06. – 17.09.1997	251 ± 15
15.12.1997 – 17.06.1998	223 ± 11
21.09.1999 – 15.06.2000	230 ± 15

Conclusions

In the radon survey in schools in the Žirovski vrh uranium ore deposit area, the highest indoor radon concentration was found only in one classrooms of the Ret-OS elementary school. After thorough monitoring of indoor air radon and radon decay products, and gamma spectrometric analyses of building materials and surrounding soil, the floor was suspected and then proved to be the major source of the elevated radon levels. The floor was rebuilt: a new concrete slab was made of a high quality cement under which perforated tubes were set to enable natural ventilation of the air in the sub-floor space. The renovation reduced the indoor radon concentration from about 3000 Bq m^{-3} down to below the national limit of 400 Bq m^{-3}.

It should be emphasised that after the results of measurements carried out according to the fast radon screening protocol in which only one room in every building was considered, the Ret-OS elementary school had been classified as a low radon level building with no additional radon monitoring planned. The high radon level classroom-1 was found subsequently, when all rooms in the school were systematically surveyed. This example clearly shows that the fast radon screening protocol is not adequate in old buildings, which are not uniformly constructed or have been partly remodelled in steps. In these cases radon should be checked in all rooms, or at least in all those with different construction characteristics, otherwise a high radon level room can easily be missed.

Acknowledgements

Financing by the Škofja Loka Municipality is appreciated. The authors want to thank Mr. I. Draksler, the Mayor of Škofja Loka, for his co-ordination and technical advice. They are also grateful to the Ret-OS elementary school personnel for their general kindness and assistance. The authors also thank Ms Petra Dujmović for her technical assistance and Dr. Matjaž Korun for his gamma spectrometric analyses.

REFERENCES

ANDJELOV, M., BRAJNIK, D. (1996): Map of natural radioactivity and radon emanation in Slovenia. *Environ. Int.*; 22, S799–S804.

BILBAN, M., VAUPOTIČ, J. (2001): Chromosome aberrations study of pupils in high radon level elementary school. *Health Phys.*; 80, 157–163.

BRAJNIK D., MIKLAVŽIČ U., TOMŠIČ J. (1992): Map of natural radioactivity in Slovenia and its correlation to emanation of radon. *Radiat. Prot. Dosim.*; 45, 273–276.

KOBAL, I., BRAJNIK, D., KALUŽA, F., VENGUST, M. (1990): Radionuclides in effluent from coal mines, a coal-fired power plant, and a phosphate processing plant in Zasavje, Slovenia (Yugoslavia). *Health Phys.*; 58, 81–85.

KRIŽMAN, M., ILIĆ, R., SKVARČ, J., JERAN, Z. (1995): A national survey of indoor radon concentrations in dwellings in Slovena. In Proceedings of the *Symposium on Radiation Protection in Neighbouring Countries in Central Europe*, Portorož, Slovenia, p.p. 66.

KRIŽMAN, M. (1997): Report on the Inter-comparison Experiment for Radon and Progeny in Air, *URSJV Report RP 026*, Nuclear Safety Administration, Ljubljana.

KRIŽMAN, M. (2000): Report on the Inter-comparison Experiment for Radon and Progeny in Air, *URSJV Report RP 46/2000*, Nuclear Safety Administration, Ljubljana.

KRIŽMAN, M. (2001): Report on the Inter-comparison Experiment for Radon and Progeny in Air, *URSJV Report RP 47/2001*, Nuclear Safety Administration, Ljubljana.

MIHELIČ, M., RUPNIK, Z., SATALIĆ, P., MIKLAVŽIČ, U. (1985): Microcomputer TL analyser IJS MR-200 as a routine dose reader. In Proceedings of *13th Yugoslav Radiation Protection Symposium*, Pula, Croatia, p.p. 641.

POPIT, A., VAUPOTIČ, J. (2002): The influence of geology on elevated radon concentrations in Slovenian schools and kindergartens. *Geologija*; 45, 499–504.

URBAN, M., SCHMITZ, J. (1993): Radon and radon daughter metrology: Basic aspects. In Proceedings of *Fifth International Symposium on the Natural Radiation Environment*, Commission of the European Communities, *CEC, Report EUR 14411 EN*, p.p. 150.

ULRS (Uradni list RS, *Gazette of the Republic of Slovenia*), (2002) Regulations for ventilation and air-conditioning of buildings. (42), 4139–4161.

ULRS (Uradni list RS, *Gazette of the Republic of Slovenia*), (2004) Guidelines for dose limitations, radioactive contamination and intervention levels.

VAUPOTIČ, J., ANČIK, M., ŠKOFLJANEC, M., KOBAL, I. (1992): Alpha scintillation cell for direct measurement of indoor radon. *J. Environ. Sci. Health*; A27, 1535–1540.

VAUPOTIČ, J., KRIŽMAN, M., PLANINIĆ, J., PEZDIČ, J., ADAMIČ, K., STEGNAR, P., KOBAL, I. (1994): Systematic indoor radon and gamma measurements in kindergartens and play schools in Slovenia. *Health Phys.*; 66, 550–556.

VAUPOTIČ, J., KRIŽMAN, M., PLANINIĆ, J., KOBAL, I. (1994): Radon level reduction in two kindergartens in Slovenia. *Health Phys.*; 66, 568–572.

VAUPOTIČ, J., KOBAL, I., PLANINIĆ, J. (1998): Long-term radon investigation in four selected kindergartens in different geological and climate regions of Slovenia. *J. Radioanal. Nucl. Chem.*; 238, 61–66.

VAUPOTIČ, J., ŠIKOVEC, M., KOBAL, I. (2000): Systematic indoor radon and gamma-ray measurements in Slovenian schools. *Health Phys.*; 78, 559–562.

VAUPOTIČ, J. (2001): Radon and gamma-radiation measurements in schools on the territory of the abandoned uranium mine "Žirovski vrh". *J. Radioanal. Nucl. Chem.*; 247, 291–295.

VAUPOTIČ, J., ANDJELOV, M., KOBAL, I. (2002): Relationship between radon concentrations in indoor air and soil gas. *Environ. Geol.*; 42, 583–587.

VAUPOTIČ, J. (2002a): Search for radon sources in buildings – kindergartens. *J. Environ. Radioact.*; 61, 365–372.

VAUPOTIČ, J. (2002b): Identification of sources of high radon levels in Slovenian schools. *Radiat. Prot. Dosim.*; 102, 75–80.

Deterioration of the granodiorite façade – case example Maximarket, Ljubljana

Propadanje granodioritne fasade – študijski primer Maximarket, Ljubljana

Alenka Mauko[1], Breda Mirtič[2], Ana Mladenovič[1], Bent Grelk[3]

[1] Slovenian National Building and Civil Engineering Institute, Dimičeva 12, SI-1000 Ljubljana, Slovenia; E-mail: alenka.mauko@zag.si
[2]Faculty of Natural Sciences and Engineering, University of Ljubljana, Aškerčeva 12, SI-1000 Ljubljana, Slovenia
[3] Rambøll, Hanneman & Højlund A/S, Bredevej 2, DK-2830 Virum, Denmark

Received: February 15, 2006 **Accepted**: July 20, 2006

Abstract: Problems related to natural stone panels bowing have been often reported in the past decades. Most of the reported examples are related to marble and limestone panels, rarely to other natural stones. In the following article deterioration features of granodiorite façade of Maximarket in Ljubljana are described. Special attention is given to the bowing of panels, since this is the first reported case of bowing granodiorite facade panels so far. The causes of bowing are discussed, especially thermal and hydric expansion of quartz and other minerals in granodiorite. Some other deterioration features are discussed like different type of stains, cracks and break-downs of the panels.

Izvleček: Problemi, povezani z ukrivljanjem fasadnih plošč iz naravnega kamna, so v preteklih desetletjih v nekaterih primerih imeli velik negativen vpliv na kamnarsko industrijo in na sloves naravnega kamna kot trajnega gradbenega materiala. Poročila o problemih zaradi ukrivljanja so vezana predvsem na nekatere marmorje in apnence, v redkih primerih je ukrivljanje bilo opaženo na granitnih nagrobnikih. Konkavno ukrivljanje granodioritnih plošč na fasadi objekta Maximarket v Ljubljani je tako prvi tovrsten pojav, opažen na nekarbonatnih fasadah. Avtorji v članku na podlagi laboratorijskih in terenskih opažanj podajajo posamezne značilnosti pojava. Poleg ukrivljanja so podane še nekatere druge karakteristične oblike staranja granodioritne fasade na objektu Maximarketa.

Key words: bowing, granodiorite, "pohorje tonalite", stone façade cladding, weathering
Ključne besede: ukrivljanje, granodiorit, "pohorski tonalit", ventilirana fasada, preperevanje

Introduction

Natural stone façade cladding has been used extensively in Slovenia in the past century. A number of prestigious buildings were clad with natural stones that originated mostly from localities in Slovenia, but also from other parts of the former Yugoslavia. Although bowing of natural stone panels has been known among scientists for almost a century (Kessler, 1919, Bain, 1940, Grimšičar, 1974), public interest of this

Scientific paper

phenomena has increased substantially over the last couples of decades, because of deterioration of some marble claddings on buildings such as Lincoln tower in Rochester - USA, the Amoco building in Chicago – USA (COHEN & MOINTEIRO, 1991), the Finlandia hall in Helsinki – Finlandia (ROYER-CARFAGNI, 1999), and others. Since bowing was accompanied by substantial strength loss (LOGAN ET AL, 1993) questions on the claddings' safety become more frequent. Many hypotheses about bowing development have been drawn (e.g. WINKLER, 1994, ERLIN, 1999, TSCHEGG 1999), most of them explain bowing of marble panels as effect of anisotropic expansion of calcite grains. Importance of moisture present is also recognized by many authors (KOCH & SIEGESMUND, 2004).

Since most of the reported bowing problems are related to marble cladding and because a good correlation between observed problems and laboratory examinations of the respective marble types has been established (ROYER-CARFAGNI, 1999, GRELK ET AL, 2004), a general feeling among scientists has prevailed that bowing is prone only to marbles. Furthermore, some authors conclude that other minerals such as quartz and feldspars do not posses the unique thermal characteristics of calcite, and rocks consisting of such minerals are thus not prone to such strength loss. In contrary, WINKLER (1994) reports about bowing granite tombstones at the Greenwood cemetery in subtropical humid climate of New Orleans. WINKLER (1996) also reports of tent-like spalling of thin slabs of granite on urban buildings. It is in his opinion that the bowing of granite panels shares some of the complex factors with marble panels such as the action of moisture dilatation, stress relief and temperature action causing microcracking by excessive contraction of the quartz grains during cooling.

This article features a case study of a 34 years old building at the Maximarket in Ljubljana, Slovenia, which is covered by façade panels of granodiorite exhibiting severe bowing. Field studies were supplemented with laboratory test of bowing potential of the rock type, flexural strength measurements and microscopic analyses in order to clarify some of the reasons for the bowing granodiorite panels.

Thermal-Hydric Deformation Of Granitoid Stones

Stone as all other solid materials changes the dimension due to cooling and heating. The change in dimension of the stone depends on mineral composition (the amount and type of minerals), porosity and fabric - the grain size and the orientation of grains (BILBIJA, 1984). The maximum temperature on the surface of the panels and in the stone due to solar radiation are indirectly related to the colour of stone surface. WINKLER (1994) showed that the surface temperature of some granodiorites could be more than ten degrees higher than the air temperature. It was reported by MAUKO (2004) that some natural stones in the climate of central Slovenia can exhibit temperatures higher than 55 ^{o}C. In such circumstances the stone panel can suffer from severe damage due to the cyclic thermal expansion in the range of 60 ^{o}C and more. The linear dilatation coefficient of the most common minerals in granodiorite (e.c. quartz: linear dilatation in interval of 20-100 ^{o}C is 0.14 % perpendicular to c axis and 0.08 % parallel to c axis, K-feldspar: 0.049 % parallel to a-axis (Clark, 1966)) show the importance of mineral composition on the expansion caused by the temperature changing. An average linear dilatation coefficient of granite type of stone is 37 x 10^{-7}/ ^{o}C up to 60 x 10^{-7}/ ^{o}C (Bilbija, 1984), which means an average of 0.296 % up to 0.48 % of linear dilatation in interval of 20-100 ^{o}C. That means that granite is the rock of the highest dilatation coefficient and is as high as the quartz sandstones and quartzite. By other words granite stone of 1 meter length can expand during sunny winter day up to 0.36 mm/m in the temperature interval of 60 degrees. Repeated cooling and heating cause about 20 % of irreversible deformation and is finally expresses as mechanical damage of stone.

The porosity and presence of microcracks also influence on the amount of water absorbed after the raining. Porosity is one of the main controlling factors of the expansion of the stone slabs (see also Malaga-Starzec et al, 2002; Koch & Siegesmund, 2004). Although the hydric dilatation of granite is only 0.004 up to 0.009 % after the repeated wetting and drying the presence of water is also important for thermal degradation of granitoid panels. For the example, the expansion of granite at the temperature of 60 ^{o}C is 0.15 % and water has the expansion of 1.5 % at the same temperature. The difference results as the stress on pore walls of about 39.5 MPa (Bilbija,1984). If stone slabs are anchoraged the strain would be promoted and it would lead to bowing of slabs.

Building Characteristics

“Maximarket”, which is situated at Trg republike 1, is one of the first department stores built in Ljubljana. It was designed by the architect Edo Ravnikar and his associates in the 1960s. The building was completed in November 1971.

The building’s facades of approximately 1000 m^2 are covered by one of Slovenia’s most widely used types of architectural stone: “tonalite” or “pohorje granite” from the quarry Cezlake I. The quarry is situated on the southern part of this magmatic massive of Miocene age (Dolenec, 1995), which borders on the south to the metamorphic complex. Petrographic name of stone is granodiorite (Zupančič, 1994). It consists mostly of white feldspars (55-70 %) with 50-60 % plagioclase and 5-10 % orthoclase, light grey quartz (20-30 %) and almost black biotite in amount of 10 – 15 % and 1 % of hornblende. Other minerals are: apatite, zircon, pyrite, chlorite, titanite, calcite and epidote (Mirtič et al, 1999). The rock is fine to medium grained, grey in colour with a hypidiomorphic texture.

The preferred grain boundary orientation of quartz and biotite defines the foliation, which is intersected by veins of pegmatite and aplite, up to 10 and more centimetres thick. Cohesion between the veins and ground mass is very good. Mafic minerals (mostly biotite and chlorite) are sometimes condensed in mafic nests or in lenses having a size measured in centimetres. The basic mechanical and physical properties of granodiorite from Cezlak I are presented in Table 1.

Table 1. Mechanical characteristic of granodiorite from Cezlak I according to MIRTIČ ET AL (1999)

REAL DENSITY (kg/m^3)	2687		
APPARENT DENSITY (kg/m^3)	2726		
DENSITY COEFFICIENT	0.986		
POROSITY (%)	1.4		
WATER ABSORPTION (%m/m)	0.3		
ABRASION RESISTANCE (cm^3/50 cm^2)	5.9		
TENSILE STRENGTH (MPa)	max.	min.	medium
dry	241	200	225
water saturated	199	165	185
after 25 freeze/thaw cycles	202	160	182
FLEXURAL STRENGTH (MPa)	max.	min.	medium
dry	24	20	23
water saturated	22	18	20
after 25 freeze/thaw cycles	21	18	19
LINEAR COEFFICIENT OF THERMAL EXPANSION (mm/m $^{\circ}$C)			
(-20)$^{\circ}$C TO +70°C	0,0084		
THERMAL CONDUCTIVITY (W/mK)	1		
MODULUS OF ELASTICITY (MPa)			
static modulus	41437		
dynamic longitudinal modulus	45204		
dynamic transversal modulus	19684		
dynamic Poisson's number	0.13		
SLIP RESISTANCE			
Polished surface	13.6		
Honed surface	78.8		
FROST RESISTANCE AFTER 25 FREEZE/THAW CYCLES (%m/m)	0.08		

Due to its good mechanical properties, as well as to the possibility of quarrying blocks of large dimensions, both structural and ornamental functions have been historically attributed to "Pohorje granite". This stone has been frequently used for external and internal paving, for stone façade cladding, for monuments and others.

The façade cladding consists rectangular panels of granodiorite, of different sizes. The most frequently used type of panels is 1700 mm high and 375 mm wide. Smaller panels with a height of 1385 mm are situated in the bottom row. The measured thickness of panels varies between 16.2 mm and 24.7 mm, though most of them are less than 20 mm thick. The texture of stone was not considered by the manufacturer, when the panels were cut and the preferred orientation of the mineral grains in panels varies. The top and bottom edges of the slabs are clipped (Fig. 1), and their surface is coarse textured. The panels were cut with Fe-particles, which were later washed with HCl.

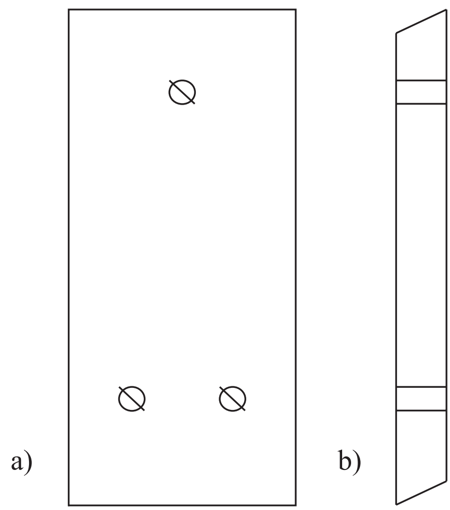

Figure 1. Illustration of the panel from the front (a) and lateral view (b)

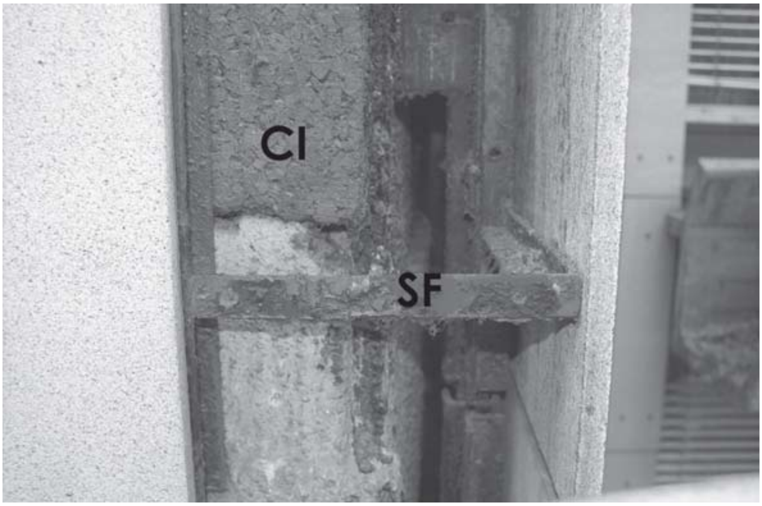

Figure 2. Construction of the façade. The slabs are fixed onto a steel frame (SF). The concrete structure is covered by cork isolation (CI)

The stone cladding is ventilated from the rear side. The clearance between the cladding and the cork isolation on the top of the reinforced-concrete walls is approximately 150 mm. Three steel dowels, up to one cm in diameter, anchor the rectangular panels onto the supporting steel frame (Fig.1, 2). Two of them pass through dowel holes drilled a few centimetres from the bottom edge of the panel and one passes through a hole, which is located a few centimetres from the panel's upper edge. Such a method of anchorage allows a certain clearance between the holes and the anchors. The expansion joints between adjoining slabs are suitable large, approximately 10 to 15 mm and are sufficient for their expansion.

Climatic Conditions

The city of Ljubljana, Slovenia's capital, is situated at about 300 m above sea level. Ljubljana has a continental inland climate, with relativelycold winters with frost and hot dry summers. The average annual temperature is 9.8 ^{o}C. Average annual precipitation amounts to 1393 mm, and average annual insulation to 1712 hours per year.

The local climate of the building is not the same in all directions of the compass. The north façade and almost the entire west façade is open to the square, whereas the south and the east façades, as well as part of the west façade, are in the shade caused by surrounding buildings. This is the reason for the exposing time of the parts of façade to the sun and to the rain is different and also the intensity of heating, cooling, wetting and drying is distinctly different.

Experimental

The field investigations were carried out according to Nordtest Method NT Build 500 - Cladding panels: Field method for measurement of bowing. Two deteriorated panels were dismounted from the façade and subsequently tested in the laboratory. The flexural strength test according to SIST EN

12372: 2000 and petrographic examination according to SIST EN 12407: 2002 were performed in order to correlate the observed deterioration of the panels with a loss of flexural strength and mineralogical-structural alteration at the microscopic level. Laboratory measurements of bowing potential on fresh stone samples and samples used on the façade were conducted at Rambřll in Denmark according to improved Nordtest method NT Build 499. Three sets of rectangular panels of 400x100 mm, partly immersed in water, were heated to 80 °C in three hours. After 4 hours of exposure at 80 °C specimens were cooled down to ambient temperature. Bowing was measured and calculated after every fifth cycle according to following formulas (TEAM WP6.1-RMB-041112):

$$B = H_N / L_N \quad (1)$$

and

$$H_N \approx H \cdot \left(\frac{1\,\mathrm{m}}{L} \right)^2 \quad (2)$$

where:

B is the bowing expressed in mm/m,
H_N is the normalized height difference expressed in mm,
H is the measured height difference expressed in mm and
L is the distance between the supports under the specimens (0.35 m).

For the field measurements of bowing a *bow-meter* with total length of 2000 mm was used, which was made according to NT Build 500. The bow meter is an aluminium measuring bridge with two supporting mounts, one with two legs and the other with one, which is insuring the stability. The measuring bridge is equipped with a ruler so the distance between two supporting points is adjustable and measurable. The measuring mount also includes a vernier calliper, with precision of 0.01 mm.

Six locations were selected for the measurement of bowing, this selection being made basically with regard to accessibility by lift

Figure 3. Bowing measurements of panels, which had been detached from the west façade

and the amount of observed bowing. Bowing was measured at the mid-point of the vertical mid-line due to the panel's small width (Fig. 3). The distance (L) between the supporting points depended upon the size of the panel.

The measured results have been presented in the form (NT Build 500):

$$B = \frac{d}{L} \cdot 1000 \quad (3)$$

where:
B is the bowing expressed in mm/m to the second decimal,
d is the measured value of bowing in mm to the second decimal,
L is the measuring distance in mm to the nearest mm.

Results And Discussion

Bowing

Results of onsite bowing measurements are listed in Table 2-3. All of the examined panels demonstrated concave bowing (i.e. the edges of the panels protruded outwards, away from the building). Because of remote edges water penetration behind the stone facade increased and speeded up the deterioration of the steel structure behind it. The development of concave bowing (Fig. 4) was not restricted by lateral fixing, since panels are anchored frontally.

The largest amount of bowing (B = 12.8 mm/m) was measured on the west façade on the bottom row of panels. In general, the panels on the west façade are more bowed than those on the east, although this assumption cannot be statistically proved due to the scarcity of measurement results. Lateral bowing was not observed. A visual inspection of the entire façade revealed that bowing is most pronounced on the south

Table 2. Results of measurements carried out on the east façade

Stone mark	Height (mm)	Width (mm)	Thickness (mm)	L (mm)	d (mm)	Type of bowing	B (mm/m)
M2-5.1	1385	375	194	1285	2.96	concave	2.30
M2-4.1	1385	373	177	1285	2.93	concave	2.28
M2-1.1	1695	375	194	1595	1.62	concave	1.02
M2-1.4	1685	375	187	1585	3.81	concave	2.40
M2-2.4	1372	375	192	1272	3.30	concave	2.59
M1-2.6	1385	223	162	1285	4.70	concave	3.66
M1-1.6	1700	223	194	1600	5.90	concave	3.69
M1-5.6	1385	225	188	1285	5.26	concave	4.09
M1-1.4	1700	375	230	1600	5.06	concave	3.16
M1-1.3	1700	373	247	1600	2.64	concave	1.65
M1-1.2	1700	224	190	1600	3.24	concave	2.03
M1-1.1	1700	375	192	1600	3.03	concave	1.89

Table 3. Results of measurements carried out on the west façade

Stone mark	Height (mm)	Width (mm)	L (mm)	d (mm)	Type of bowing	B (mm/m)
M3-1.8	1700	375	1600	20.35	concave	12.72
M3-5.7	1700	375	1600	15.81	concave	9.88
M3-4.5	1380	375	1280	11.33	concave	8.85
M4-5.3	1380	375	1280	7.45	concave	5.82
M6-1.2	1380	375	1280	11.52	concave	9.00
M3-6.8	1375	375	1275	10.11	concave	7.93
M3-1.6	1700	223	1600	12.55	concave	7.84
M3-5.1	1375	375	1275	4.11	concave	3.22
M3-2.1	1375	370	1275	5.17	concave	4.05
M3-1.1	1700	375	1600	8.29	concave	5.18

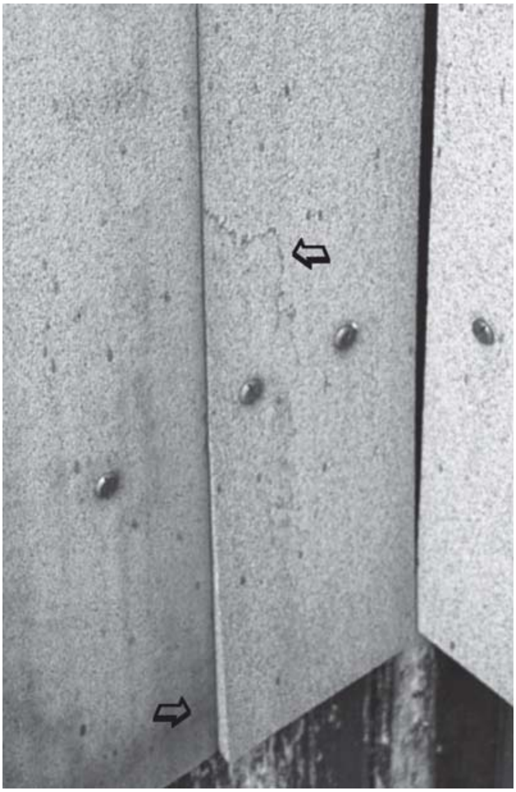

Figure 4. Concave bowing of granodiorite panel on the west façade (left arrow) and crack in chlorite vein (right arrow)

façade. Pronounced bowing was also observed on south facade of the neighbouring building, which was built in the beginning of 1980ies and is covered with the same granodiorite panels (Fig. 5).

Figure 5. Bowing on the south facade of neighbouring building

Table 4. Results of measurements carried out in the laboratory on the panels which were detached from the east façade

Stone mark	Height (mm)	Width (mm)	Thickness (mm)	L (mm)	d (mm)	Type of bowing	B (mm/m)
M6-1.3*	1700	320	160	1600	9.04	concave	5.65
M7-1.1	1320	224	140	1220	5.60	concave	4.59
M7-3.1	1220	223	180	1120	4.78	concave	4.27

*Laboratory tests (optical microscopic analyse and a flexural strength test) were performed on this slab

Other Deterioration Features

Ljubljana is a mostly residential city, and there is hardly any heavy industry. Severe stone deterioration due to pollutants therefore does not occur to a significant degree. Chemical deterioration of the panels is characterized by the appearance of stains on the surface of the panels, which have an influence mainly on the aesthetic appearance of the façade. Four types of stains were distinguished:

- stains formed due to mineral alteration (especially minerals, which contain iron, such as pyrite),
- corrosion stains formed mainly by chemical attack of the supporting steel frame,
- stains formed by oxidation of remaining iron particles from the cutting process,
- stains due to bird excrements.

The stains formed by the alteration of iron minerals and solubility of minerals which contain iron (e.c. biotite) due to weathering conditions are yellowish-brown in colour. They appear in the groundmass as well as in the veins of pegmatite and aplite, where they are more obvious due to the white colour of the substratum. Such stains can form very quickly after installation in unfavourable weathering conditions (this phenomenon has been observed on several buildings with granodiorite cladding in Ljubljana). The staining of stone by iron hidroxides as the result of pyrite and biotite alteration were proved on different stones, such as limestone (Bilbija, 1984) and other igneous stones (Winkler, 1994; Bilbija 1984; Matias & Alves, 2002) and also in concretes (Bilbija, 1984).

During the inspection, state of the supporting steel structure was also evaluated. It was concluded that steel framework was in poor shape, and that repair works are urgently needed. Rainwater had penetrated into and under the stone façade through the joints between the panels and through other

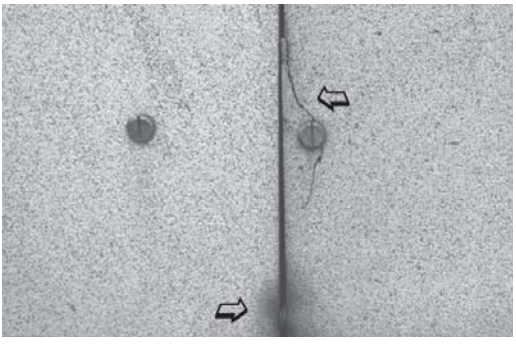

Figure 6: Corrosion stains (left arrow) formed due to oxidation of metal subframe and crack near the dowel (right arrow)

openings like cracks and breakouts, and had attacked the steel structure (BORTZ ET AL, 1988). As a result stains begin to appear on the edges of the panels, around the anchors and along cracks. Such corrosion stains (see Fig. 6, 7) are more obvious on the west façade, where variations in temperature and moisture are greater. The corrosion of the steel framework due to temperature and moisture variations was studied also by BILBIJA (1984).

Many birds' nests were observed under the edge of the roof. Bird excrements accelerate the deterioration processes of the stone. Organic acids from excrements cause the dissolution and other changes of the stone minerals in the presence of the rain water. Reactions of this type has previously been studied by (WINKLER, 1975; 1994).

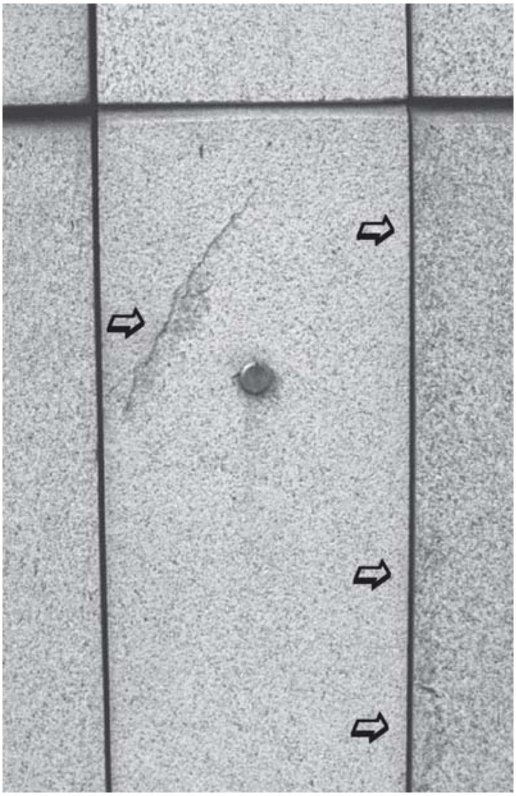

Figure 7. A crack formed on the boundary between the matrix and the lens of mafic minerals (left arrow) and corrosion stain on the edge of the panel (right arrows)

Apart from aesthetic façade colour changes, a certain amount of mechanical damages was observed. This can be attributed to:

- some degree of poor workmanship,
- deterioration due to physical and mechanical changes in the rock.

Signs of poor workmanship are damages due to the incorrect treatment and installation of stone panels. Such damages are rare, but can sometimes be visible as double-drilled anchor holes and broken edges. Double-drilled holes are areas with a high potential for failure and water leakage in façade system. Installation of panels with different thickness panels and chlorite veins are also a sign of poor workmanship, although scarce standardisation and recommendation existed at the time of construction.

Several different types of mechanical deterioration were also observed:

- cracks near the dowels (Fig. 6),
- cracks on the boundaries with the mafic lenses (Fig. 7) ,
- cracks in the aplite veins (fig. 8),
- cracks in chlorite veins (Fig. 4),
- broken slabs.

Thin chlorite veins can be observed in the fresh rock (ZUPANČIČ, 1994). Blocks with chlorite veins are usually rejected in the extraction process due to their low mechanical resistance.

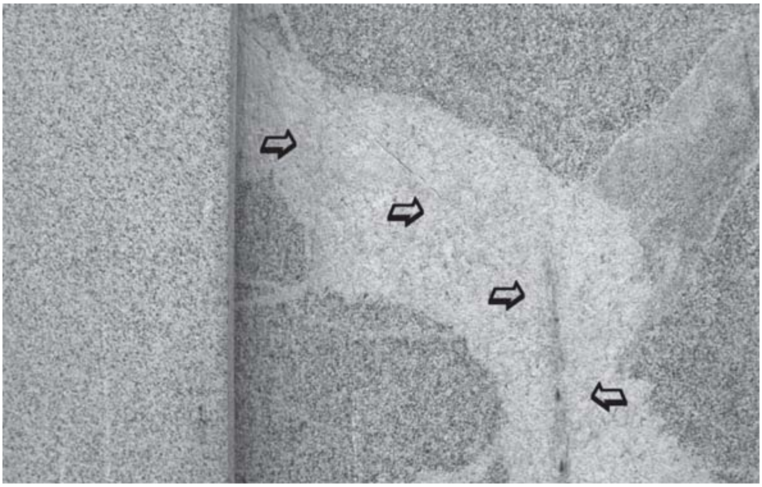

Figure 8. Cracks in an aplite vein (left arrows) and a vertical stain formed by bird excrement (right arrow)

Laboratory Research

Microscopic inspection was carried out on one of the demounted panels, but no major alteration of minerals in comparison with fresh rock, except kaolinization of the feldspars, was observed (Mladenovič et al, 2003). Comparison of samples taken from one of the removed panel and from fresh rock shows higher frequency of transgranular and intragranular cracks in the case of deteriorated panel (Fig. 9). From the same

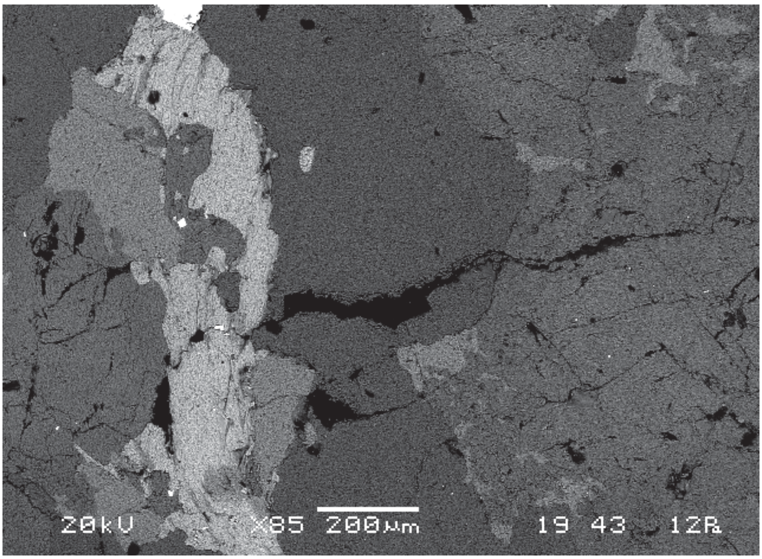

Figure 9. Formation of transgranular cracks in specimen taken from the exposed panel. SEM, BSE

panel six test specimens were cut for flexural strength test. The average flexural strength of the six specimens was 16MPa (MLADENOVIČ ET AL., 2003).

A comparison with the results for fresh rock (which shows a flexural strength of between 15 and 20 MPa) showed, somewhat surprisingly, no difference. Prediction was made that granodiorite stone is more stable because of lack of soluble minerals. The most common minerals, which compose granodiorite, are very inert.

Laboratory determination of bowing potential was conducted on two sets of granodiorite panels of different thickness and on one set of specimens taken from removed panel. Almost no bowing was observed on 30 mm (Fig. 10) or 10 mm (Fig. 11) thick panels although slight difference in curvature of average bowing curve was observed between two sets of specimens (Fig. 12). Clear bowing tendency was observed on specimens taken from removed panel (Fig. 12). After 15 cycles of heating and cooling a bowing of approximate 2 mm/m was determined.

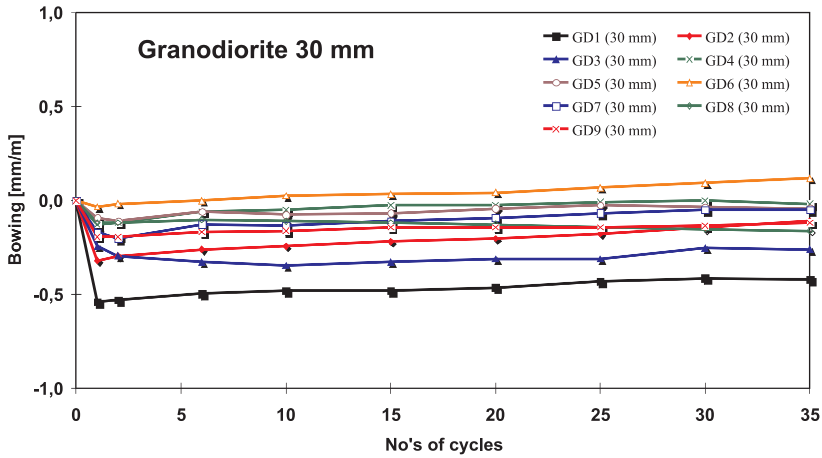

Figure 10. Bowing of 30 mm thick panels during 35 cycles

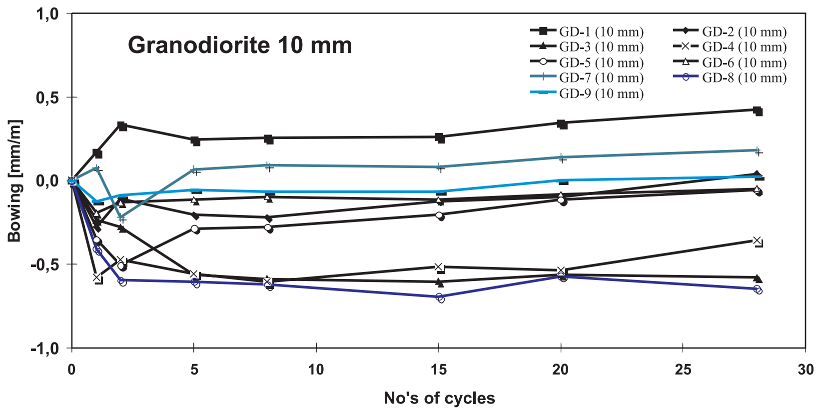

Figure 11. Bowing of 10 mm thick panels after 28 cycles of heating and cooling of partly immersed specimens from 20 to 80 °C

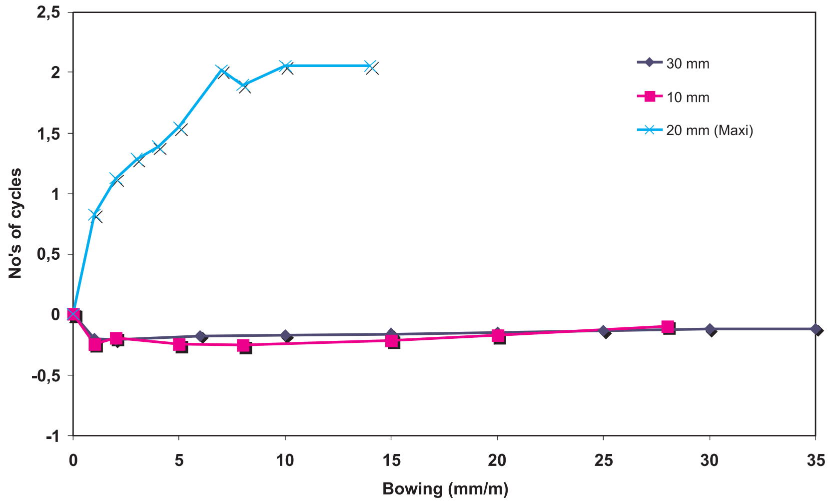

Figure 12. Comparision of average values of three sample sets

The pattern that the fresh granodiorite panels show less bowing than weathered panels was also determined for fresh and weathered marble panels (Grelk et al, 2004). Because of different mechanical characteristics more brittle deformations (transgranular, intragranular cracks) are observed in the case of granodiorite bowing than in the case of marble bowing, which is characterised by granular decohesion on the microscopic level (Alnaes et al, 2004). Additional factor of bowing development is small thickness of façade panels, since no bowing was observed on thicker panels in the case of other granodiorite façades in Ljubljana (Mauko et al, 2005) and which was also proved in laboratory. The influence of thickness on development of bowing is also visible on some marble façades in Ljubljana (Mauko, 2004).

Conclusions

In the case of granodiorite façade of Maximarket, a significant shape and dimension changes of the granodiorite panels has been observed. Observed bowing is probably produced by a number of factors, which can act in a complementary or even catalytic manner, but it most likely is governed by the same factors as it seen in the bowing of marble panels. This is supported by the fact, that the façade panels, which were removed from the building after 33 years, bowed significantly during the accelerated weathering test - bow test developed for marble panels. This indicates that moisture and temperature variations are very important parameters for granodiorite bowing. Due to thermal expansion of quartz crystals, which is followed by formation of transgranular and intergranular cracks and due to hydric expansion, dimensional change of granodiorite panels occur. Since accelerated aging of fresh panels in the controlled conditions shows almost no bowing or very slow increase of panels deformation, we can assume that smaller residual deformation due thermal cycling is formed than in the case of some calcitic rocks. Because of this deformation of facade panels in the form of bowing develops slower and less distinctive than in the case of some marble panels. Further investigation within the scope of this and other similar projects should reveal the role of texture orientation due to panel's orientation. Also the influence of surface treatment and production processes should be included, such as increase of porosity due to surface treatment with chloric acid. Besides bowing other types of deteriorations were observed, such as stains on the surfaces, cracks, breakouts, and signs of poor workmanship. Some of these deteriorations are unfavourable only from the aesthetic point of view, while others are more critical. The most critical areas on the stone cladding are those with cracks and cracks initiations, and for these restoration and replacement of the affected slabs are necessary and urgent. It is expected that this should take place in the near future, when the steel frame, which carries the stone façade, will be repaired.

Acknowledgments

The authors would like to thank the authorities responsible for Maximarket, for permitting surveying and sampling works. We would also like to thank partners of TEAM project (Contract No.: G5RD-CT-2000-00233) for their comments, especially Claes Christiansen for his reviews.

LITERATURE:

ALNÆ, L., KOCH, A. SCHOUENBORG, B., ÅKESSON, U. AND MOEN, K. (2004): Influence of rock and mineral properties on the durability of marble panels. *Proceedings Dimension Stone 2004, Prague.*

BAIN, G. W. (1940): Geological, Chemical and Physical Problems in the Marble Industry. *American Institute of Mininig and Metallurgical Engineers, Technical Publication No. 1261*.

BILBIJA, N. (1984): Tehnička petrografija, svojstva i primene kamena. *Naučna knjiga, Beograd.*

BORTZ, S.A., ERLIN, B. and MONK, C.B. (1988): Some field problems with thin veneer building stones new stone technology, design, and construction for exterior wall systems. *In.: B. Donaldson (Ed.) ASTM STP 996. 11-31, ASTM, Philadelphia*.

CLARK, S.P. (ED.) (1966): Handbook of physical constants. *The Geological Society of America.*

COHEN, J. M. and MONTEIRO, P. J. M. (1991): Durability and Integrity of Marble Cladding: A State-of-the-Art Review. *Journal od Performance of Constructed Facilities, 5,* pp. 113-124.

DOLENEC, T. (1995): Novi izotopski in radiometrični podatki o pohorskih magmatskih kamninah. *RMZ 41, 3-4, Ljubljana*, pp. 147-152.

ERLIN, B. (1999): Contribution on a better understanding of the mechanism causing dishing failures of the carrara marble when used for outside building facades. *Dimension stone cladding*.

GRELK, B., GOLTERMANN, P., SCHOUENBORG, B., KOCH, A. AND ALN?S, L. (2004): The laboratory testing of potential bowing and expansion of marble. *Proceedings Dimension Stone 2004, Prague.*

GRIMŠIČAR, A. (1974): Odpornost marmorja izpostavljenega temperaturnim spremembam pri laboratorijskih preiskavah z aplikacijo na objektih. *Simpozijum ukrasni i tehnički kamen, Beograd,* pp. 1-8.

KESSLER, D.W. (1919): Physical and chemical tests on the commercial marbles of the United States. *Technological papers of the bureau of standards, 123, Washington*, 54 p.

Koch, A. and Siegesmund, S. (2004): The combined effect of moisture and temperature on the anomalous behaviour of marbles. *Environmental Geology46/3-4,* pp. 350-363.

Logan, J. M., Hatedt, M., Lehbrt, D. and Denton, M. (1993): A case study of the properties pf marble as building veneer. *Int. J. Rock Mech. Min. Sci. & Geomech. Abstr., 33,* pp. 1531-1537.

Malaga-Starzec, K., Lindquest, J. E. and Schournborg, B. (2002): Experimental study on the variation in porosity of marble as a function of temperature. *In Siegesmund, S., Weiss,T & Vollbrecht (Ed.): Natural Stone, Weathering Phenomena, Conservation Strategies and Case Studies. 81-88. The Geological Society, London,* pp. 81-88.

Matias, J.M.S. and Alves, C.A.S. (2002): The influence of petrographic, architectural and environmental factors in decay patterns and durability of granite stones in Braga monuments (NW Portugal). *In Siegesmund, S., Weiss,T & Vollbrecht (Ed.): Natural Stone, Weathering Phenomena, Conservation Strategies and Case Studies. 273 - 283. The Geological Society, London.*

Mauko, A. (2004): Ukrivljanje fasadnih plošč iz slovenskega naravnega kamna: Diplomsko delo. *Naravoslovnotehniška fakulteta, Ljubljana*. 94 p.

Mauko, A., Mladenovič. A. and Mirtič, B. (2005): Mechanical and chemical deterioration of granodiorite facades - case examples from Ljubljana, Slovenia. *In Srdič, V.V. & Ranogajec, J. (Ed,): School of ceramics. The Sixth Students' meeting. December 1-2, 2005, Novi Sad. Faculty of Technology, University of Novi Sad.*

Mirtič, B., Mladenovič. A., Ramovš, A., Senegačnik, A., Vesel, J. and Vižintin, N. (1999): Slovenski naravni kamen. *Geološki zavod Slovenije, Zavod za gradbeništvo Slovenije, Oddelek za geologijo NTF, Univerza v Ljubljani, Ljubljana.*

Mladenovič, A., Mauko, A., Golež, M. and Drnovšek, S. (2003): Poročilo o pregledu in oceni stanja kamnite fasade na objektu Maximarket. Zavod za gradbeništvo Slovenije, 12 str.

Nordtest Method Nt Build 500, Cladding Panels: Field method for measurement of bowing. *Nordtest, Finland.*

Royer-Carfagni, G. (1999): Some considerations on the warping of marble facades: the example of Alvar Aalto's Finland Hall in Helsinki. *Construction and Building Materials, 13,* pp. 449-457.

Sist en 12372: 2000 Preskušanje naravnega kamna - Ugotavljanje upogibne trdnosti s koncentrirano obremenitvijo na sredini razpona - Natural stone test methods - Determination of flexural strength under concentrated load.

Sist en 12407: 2002 Preskušanje naravnega kamna – Petrografska preiskava - Natural stone test methods - Petrographic examination.

Team wp6.1-rmb-041112 (2004): Natural Stone Test Methods: Determination bowing potential of marble.

Tschegg, E. K., Widhalm, C. and Eppensteiner, W. (1999): Ursachen mangelnder Formbeständigkeit von Marmorplatten. Zeitschrift der Deutschen Geologischen Gesellschaft, 150/ 2 ., pp. 283-297.

Winkler, E.M. (1975): Stone: properties, durability in mans's environment. *Springer – Verlag,* pp. 193.

Winkler, E.M. (1994): Stone in architecture. Properties, durability. *Springer–Verlag.* 313 p.

Winkler, E.M. (1996): Buttressed expansion in granitic rocks in the filed and on the buildings. *4. Internationales Kolloquium, Technische Akademie Esslingen,* pp. 537-542.

Zupančič, N. (1994): Petrološke in geokemične značilnosti pohorskih magmatskih kamnin: doktorska disertacija. *Naravoslovnotehniška fakultea. Ljubljana*, 178 p.

Budurovignathus mungoensis (Conodonta) iz ladinijskega dela "Psevdoziljske formacije" pri Blagovici (Posavske gube, Slovenija)

Budurovignathus mungoensis (Conodonta) from the Ladinian part of the "Pseudogailtal Formation" near Blagovica (Sava Folds, Slovenia)

TEA KOLAR-JURKOVŠEK[1] , IGOR RIŽNAR[2]

[1]Geološki zavod Slovenije, Dimičeva 14, 1000 Ljubljana, Slovenija;
E-mail: tea.kolar@geo-zs.si
[2]Ulica bratov Martinec 40, 1000 Ljubljana, Slovenija;
E-mail: igor.riznar@s5.net

Received: July 12, 2006 **Accepted**: July 20, 2006

Izvleček: "Psevdoziljska formacija" je razdeljena na štiri člene, od katerih najvišji in najnižji vsebujeta klastite. V raziskanem južnem delu Trojanske antiklinale med Blagovico in Trojanami je bila v najnižjem delu karbonatno-klastičnega člena ugotovljena prisotnost konodontnega elementa *Budurovignathus mungoensis* (Diebel), ki potrjuje ladinijsko starost spodnjega dela "Psevdoziljske formacije".

Abstract: "Pseudogailtal Formation" (="Pseudozilian Formation") is divided into four members. The oldest and the youngest ones include clastites. The Trojane Anticline was mapped between Blagovica and Trojane, where conodont element of *Budurovignathus mungoensis* (Diebel) was collected in the lowest part of the carbonate-clastic member of the "Pseudogailtal Formation" confirming its Ladinian age.

Ključne besede: konodonti, trias, ladinij, Posavske gube, Slovenija
Key words: conodonts, Triassic, Ladinian, Sava Folds, Slovenia

UVOD

V letih 2004 in 2005 je bil v okviru geološke spremljave avtocestnega odseka med Blagovico in Trojanami skartiran približno 3,5 km širok pas ozemlja, ki sovpada z osjo Trojanske antiklinale. V južnem krilu Trojanske antiklinale JV od Blagovice izdanjajo plasti "Psevdoziljske formacije", ki so zanimive predvsem zaradi svoje paleontološke vsebine. Mikropaleontološka analiza dveh vzorcev je namreč potrdila prisotnost elementov skupine *Budurovignathus mungoensis*.

Plasti spodnjega dela "Psevdoziljske formacije" južnega krila Trojanske antiklinale je podrobneje opisal KUŠČER (1967), ki je izdelal geološko karto zagorskega terciarja in njegove podlage.

Scientific paper

Prikazal jih je kot normalno odložene na t.i. mendolski in schlernski dolomit ter enako sinklinalno upognjene kot kenozojske plasti, ki leže nad njimi.

Med leti 1969 in 1978 je za potrebe OGK SFRJ 1 : 100.000 potekalo geološko kartiranje lista Ljubljana (PREMRU, 1983), kjer so plasti "Psevdoziljske formacije" v okolici Borij označene kot skitijske (werfenske plasti), ki so z normalno mejo ločene od srednjetriasnega dolomita. Geološka zgradba južnega krila Trojanske antiklinale je predstavljena kot kompleksna, vendar enosmerna sukcesija pokrovne tektonike, gubanja, narivanja in neotektonskega razkosanja na posamezne bloke, kjer so deformacije posledica napetosti v smeri S - J (PREMRU, 1974).

Med leti 1982 in 1984 je Placer kartiral zahodni del Laške sinklinale. KOLAR-JURKOVŠEK IN PLACER (1987) sta opisala profil "Psevdoziljske formacije" južno od Borij, kjer se v spodnjem delu pojavlja intermediarni do kisli tuf, na katerem leži več kot 100 m temno sivega ploščastega apnenca z vložki glinovca in peščenjaka. Kasneje sta ista avtorja objavila še sintetični profil "Psevdoziljske formacije" v južnem krilu Trojanske antiklinale (PLACER & KOLAR-JURKOVŠEK, 1990), kjer sta razkrila pomembno dejstvo, da sta na območju Posavskih gub razvita dva horizonta psevdoziljskih plasti.

GEOLOŠKE RAZMERE

Raziskane plasti "Psevdoziljske formacije" izdanjajo ob cesti skozi vas Borje pri Mlinšah (slika 1).

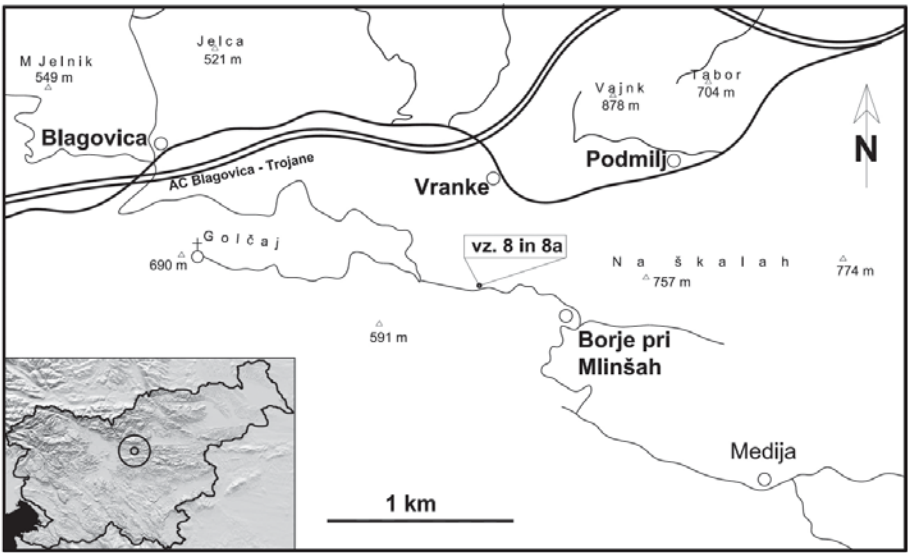

Slika 1. Geografska skica osrednjega dela Posavskih gub z označeno lego raziskanih vzorcev
Figure 1. Geographic sketch map of the central part of the Sava Folds with marked position of the studied samples

Gre za južno krilo Trojanske antiklinale, kjer so triasne plasti v zadnji fazi narinjene proti severu na klastite zgornjega paleozoika. Plasti debeloplastnatega zrnatega dolomita severno od Borij (Golčaj, Vranke, Podmilj) namreč vpadajo strmo proti severu. Južno od Golčaja in grebena Na škalah so razmere drugačne, saj vse vodilne strukture slemenijo v smeri SZ-JV. V useku ceste približno 500 m zahodno od Borij so na svetlosiv zrnat dolomit narinjene plasti "psevdoziljske formacije". Narivna ploskev vpada proti VSV z elementi vpada 70/50. Prevladuje tanko do srednjeplastnat temno siv do črn mikritni apnenec (mudstone). Nekatere plasti apnenca vsebujejo redke gastropode, med plastmi apnenca pa je tudi apnenčeva breča s klasti sivega in črnega mikritnega apnenca ter odlomki krinoidov, koral, školjk in polžev. Osnova breče je temno siv do črn mikritni apnenec, zelo ostrorobi klasti pa merijo do 5 cm (slika 2).

Plasti opisanega apnenčevega zaporedja so nagubane v dve sinklinalni z vmesno antiklinalno gubo v smeri SZ-JV. Meja s talnino in krovnino, ki jo prav tako predstavlja zrnat dolomit, je tektonska, vendar ni jasno, kolikšen je premik vzdolž struktur. Vzorca, iz katerih izvira raziskana konodontna favna, sta odvzeta v zahodnejši sinklinalni gubi v useku ceste 500 m zahodno od cerkve v Borjah. V vasi Borje je v useku ob cesti nad cerkvijo še en večji izdanek "Psevdoziljske formacije". V zahodnem delu useka so plasti močno nagubane, proti vzhodu pa prehajajo v dolomit in vpadajo proti JV. V tem izdanku so plasti temno sivega mikritnega apnenca debele do 10 cm in se menjavajo s plastmi črnega glinovca in laminiranega laporastega apnenca z redkimi školjkami. Talnina plasti sicer ni razkrita, vendar glede na položaj ustreza zgornjemu delu profila, ki sta ga opisala Kolar-Jurkovšek in Placer (1987).

Slika 2. Apnenčeva breča s koralami. Povečava 6,3X
Figure 2. Limestone breccia with corals. Magnification 6,3X

KONODOTNA ZDRUŽBA

Preiskani konodontni material vsebuje Pa-elemente enega samega rodu *Budurovignathus* iz skupine *mungoensis (B.* ex gr. *mungoensis*) (tabla 1, sl. 1-7).

Vsi primerki imajo značilno spodnjo stran z nekoliko ukrivljenim gredljem ter zgornjo stran, ki jo označuje prisotnost vozlov, omejeno le na prednjo stran robov platforme. Med temi primerki se nahaja tudi tipična vrsta rodu *Budurovignathus mungoensis* (Diebel). Dva primerka imata zaokrožen zadnji rob platforme, vendar so na robovih platforme že oblikovani vozli značilni za omenjeno skupino. Preostali primerki niso popolnoma ohranjeni, večinoma jim manjka prosti list.
Barva konodontnih elementov je črna in njihova CAI vrednost ustreza 5 (CAI=5) (EPSTEIN ET AL., 1977; REJEBIAN ET AL., 1987).

Razmeroma maloštevilna konodontna združba kaže precejšno morfološko raznolikost rodu *Budurovignathus*. Stratigrafski razpon tega rodu je zelo kratek in omejen predvsem na ladinijsko stopnjo (KOZUR, 1980; KOZUR & KOVACS, 1980). V tem času je rod doživel hiter razvoj in razvile so se številne oblike. Mnogi predstavniki rodu so poznani iz večine provinc Tetidinega prostora. Glede izvora rodu *Budurovignathus* obstajajo različna mnenja, kar je razvidno iz taksnomije. Ta rod v Sloveniji in na sosednjih območjih še ni bil predmet podrobnejšega študija. Zaradi ugotovljene prisotnosti rodu pri prejšnjih raziskavah na širšem področju Posavskih gub (KOLAR-JURKOVŠEK & PLACER, 1987; PLACER & KOLAR-JURKOVŠEK, 1990) in glede na pojavljanje raznovrstnih elementov je tudi pri bodočih raziskavah pričakovati dobre rezultate. Predvidevamo, da bi z dodatnimi paleontološkimi podatki uspeli rešiti vsaj nekatere podrobnosti pomembne za morfologijo rodu *Budurovignathus* ter tako razrešili tudi del taksonomske problematike, pri čemer bi bilo potrebno upoštevali tudi dosedanje podatke o najdbah v osrednji Sloveniji. Na osnovi novih spoznanj je mogoče pričakovati odgovor pri razreševanju problematike plasti "Psevdoziljske formacije", ki je zaradi tektonskih odnosov na tem delu Posavskih gub dokaj zapletena. Konodonti so pomembni parakronostratigrafski fosili in so marskije v Sloveniji že dokazali svojo uporabnost predvsem zato, ker amoniti (ortokronostratigrafski fosili) marsikje niso prisotni ali so preslabo ohranjeni za določevanje. Smiselnost nadaljevanja konodontnih raziskav v teh plasteh potrjuje tudi ugotovitev, da vsebujejo le malo določljivih makrofosilov.

STAROST PREISKANIH VZORCEV NA OSNOVI KONODONTOV TER BIOSTRATIGRAFSKA IN KRONOSTRATIGRAFSKA DISKUSIJA

Konodontna združba obeh preiskanih vzorcev je enaka in jo sestavljajo podobni element iz skupine *Budurovignathus mungoensis* (Diebel) (tabla 1, sl. 1-7). Pomembna je najdba elementov vrste *B. mungoensis*, ki označuje ladinijsko starost preiskanih plasti (cona *mungoensis*). *B. mungoensis* je zgornjeladinijska kozmopolitska vrsta (MOSHER, 1968). Po KRYSTYNU (1983) je njen razpon znotraj langobarda (od zgornjega dela cone gredleri do zgornjega dela cone regoledanus) in je vodilna vrsta konodontne cone *mungoensis*

Tabla 1: Konodonti iz "Psevdoziljske formacije" (ladinij, *mungoensis* A.Z.) pri Blagovici
Plate 1: Conodonts from the "Pseudogailtal Formation" (Ladinian, *mungoensis* A.Z.) near Blagovica

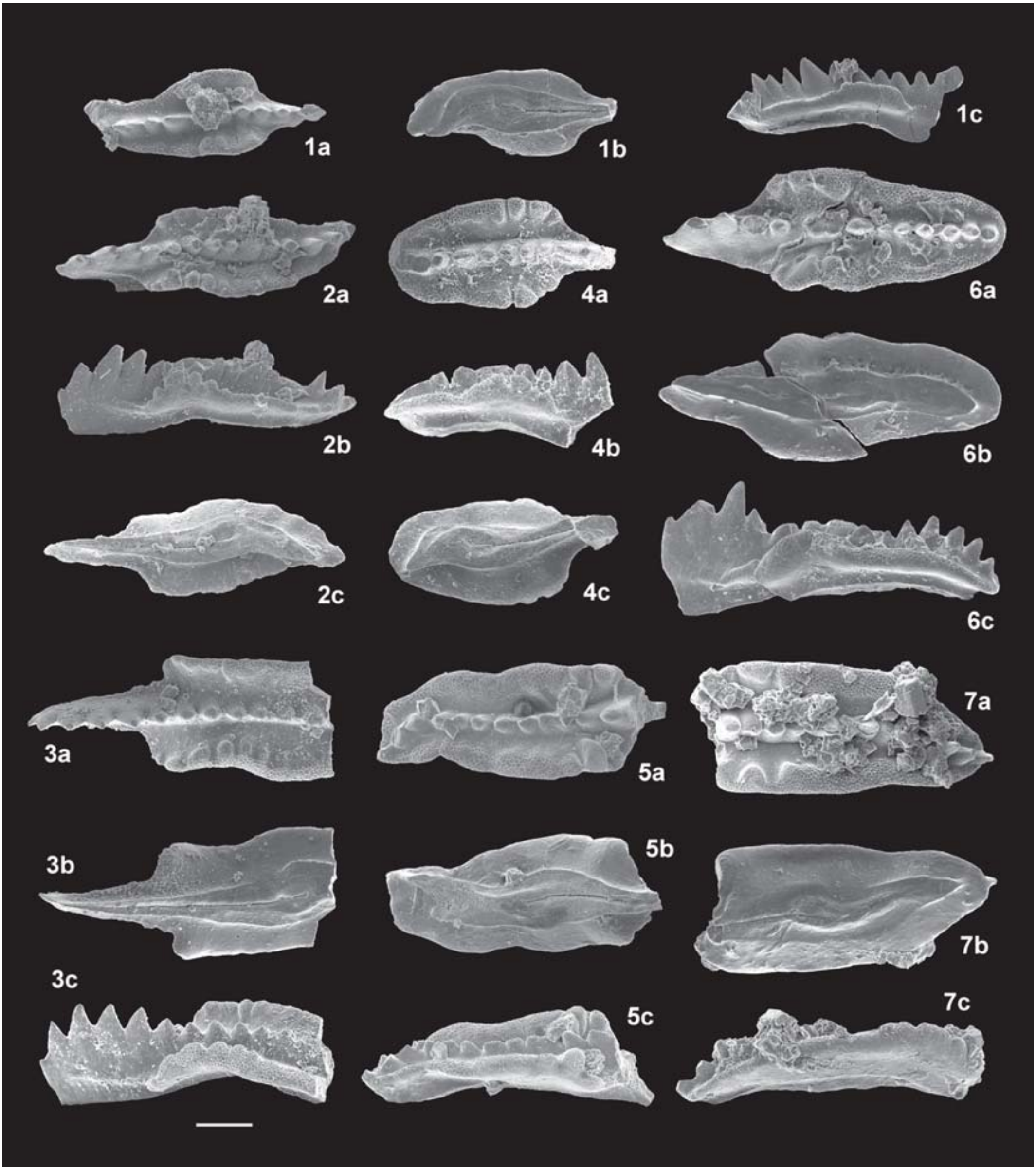

1. *Budurovignathus mungoensis* (Diebel), vzorec/sample 8A (GeoZS 3751),
2. *Budurovignathus mungoensis* (Diebel), vzorec/sample 8 (GeoZS 3750),
3. *Budurovignathus* cf. *mungoensis* (Diebel), vzorec/sample 8A (GeoZS 3751),
4-7. *Budurovignathus* ex gr. *mungoensis* (Diebel), 4, 5, 7 - vzorec/sample 8 (GeoZS 3750),
6 - vzorec/sample 8A (GeoZS 3751).

a - pogled od zgoraj, b - pogled od strani, c - pogled od spodaj / a - upper, b - lateral, c - lower views.
Merilo ustreza 100 mikronov / Scale bar 100 microns.

Tabela 1. Primerjava conacije na osnovi amonitov in konodotov v zgornjem ladiniju in spodnjem karniju (prirejeno po KOZUR, 1980, 2003; KRYSTYN, 1983)
Table 1. Comparison of the Upper Ladinian and Lower Carnian zones based on ammonoids and conodonts (modified after KOZUR, 1980, 2003; KRYSTYN, 1983)

LADINIJ			KARNIJ	stopnja	
LANGOBARD			JUL	podstopnja	
gredleri	archelaus	regoledanus	aonoides	amonitne cone	(Krystyn, 1983)
hungaricus	mungoensis	diebeli	tadpole	konodontne cone	

LADINIJ		KARNIJ			stopnja	
LANGOBARD		CORDEVOL			podstopnja	
poseidon	megine / maclearni	sutherlandi	aon	aonoides	amonitne cone	(Kozur, 1980)
hungaricus	mungoensis	diebeli			konodontne cone	

LADINIJ			KARNIJ			stopnja	
FASS. ali LANGOB.	LANGOBARD		CORDEVOL		JUL	podstopnja	
margaritosum - gredleri	archelaus	regoledanus	canadensis - sutherlandi	aon	aonoides	amonitne cone	(Kozur, 2003)
hungaricus	mungoensis	supralongobardica	diebeli - polygnathiformis		tethydis - polygnathiformis	konodontne cone	

A. Z. (zgornji del cone gredleri do zgornji del cone archelaus). Po nekaterih podatkih se vrsta pojavlja nekoliko kasneje in sicer od cone archelaus do cone aon (langobard do karnij) (KOZUR, 1980, 2003; KOVACS & KOZUR, 1980). Tabela 1 prikazuje primerjavo amonitnih in konodotnih con v zgornjem ladiniju in spodnjem karniju (po KOZURJU, 1980, 2003 in KRYSTYNU, 1983).

Iz tabele 1 je razviden različen položaj ladinijsko-karnijske meje. Ob tem je potrebno opozoriti, da je definiranje večine mej znotraj triasnega sistema, bodisi med stopnjami kot tudi med podstopnjami, vključno z omenjeno ladinijsko-karnijsko mejo, še v fazi raziskav (OGG, 2004). Karnijska starost preiskanih vzorcev je izključena ne le zaradi spremljevalnih konodontnih elementov, marveč zaradi odsotnosti nekaterih vrst tipičnih za mlajšo konodontno združbo, kot sta *B. diebeli* in/ali *Metapolygnathus polygnathiformis* (BUDUROV & STEFANOV).

Konodontna vrsta *B. mungoensis* je bila v Sloveniji doslej ugotovljena v številnih lokalitetah osrednje in zahodne Slovenije, njen razpon pa ustreza intervalu od amonitne cone Meginoceras meginae do amonitne cone Trachyceras aon (KOLAR-JURKOVŠEK, 1991). Na planini Svilaja, v sosednji Hrvaški, ta element označuje konodontno cono *mungoensis* A. Z. Njena spodnja meja je definirana s prvim pojavom te vrste, medtem ko njena zgornja meja s prvim pojavom vrste *Pseudofurnishius murchianus*, ki označuje naslednjo konodontno cono, *murchianus* A. Z. (JELASKA ET AL., 2003; BALINI ET AL., 2006).

Material in metode: Za mikropaleontološke analize smo preiskali dva vzorca kamnin s težo približno 1 kg. Vzorca smo preparirali po standardnem postopku za pripravo konodontnih vzorcev z uporabo ocetne kisline. V kislini netopni ostanek je bil nato ločen z bromoformom. Mikrofosilno vsebino vzorcev sestavljajo le konodontni elementi. Fosilni inventar je shranjen na Geološkem zavodu Slovenije in je zaveden pod številkama GeoZS 3750 in 3751. Upodobljeni konodontni elementi so bili posneti na vrstičnem mikroskopu JEOL JSM-330 na Paleontološkem inštitutu Ivana Rakovca ZRC SAZU.

Zaključek

“Psevdoziljska formacija” Posavskih gub sestoji iz štirih členov, od katerih najnižji in najvišji del vsebujeta klastite (Placer & Kolar-Jurkovšek, 1990), med njima pa ležita dva člena karbonatnih kamnin (slika 3).

Zgornji karbonatno-klastični člen za razliko od spodnjega vsebuje tudi roženec, ki iz raziskanega južnega dela Trojanske antiklinale ni poznan. Sklepamo, da vzorčevane karbonatno-klastične plasti med Blagovico in Trojanami pripadajo najnižjemu delu t. j. prvemu členu “Psevdoziljske

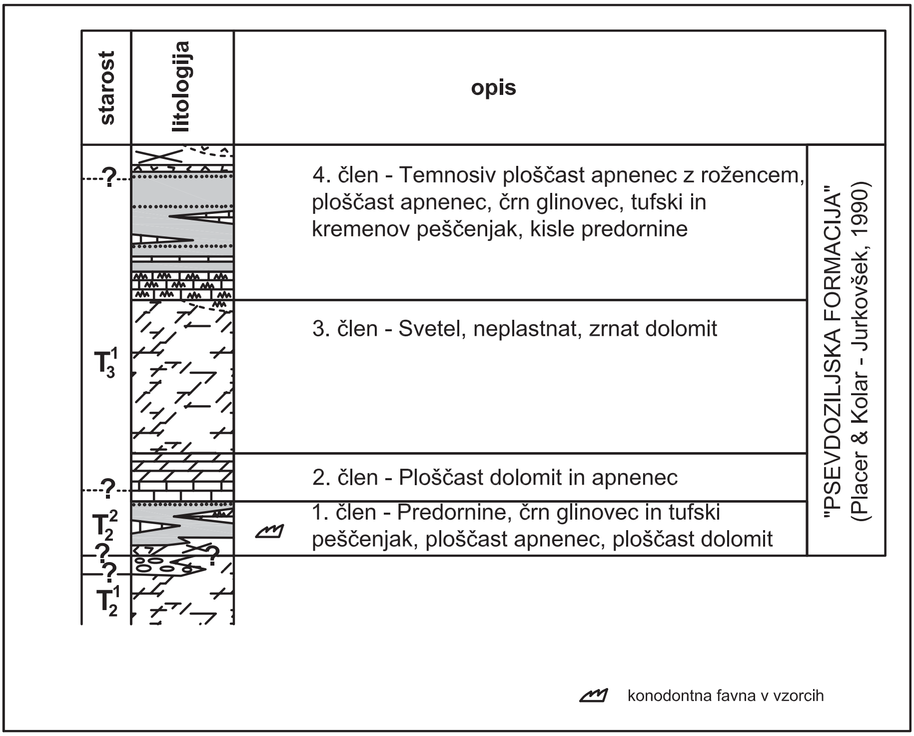

Slika 3. Profil “Psevdoziljske formacije” v južnem krilu Trojanske sinklinale z označeno lego raziskanih vzorcev (prirejeno po Placer & Kolar-Jurkovšek, 1990)
Figure 3. Section of the “Pseudogailtal Formation” in the southern limb of the Trojane Anticline with marked position of the studied samples (modified after Placer & Kolar-Jurkovšek, 1990)

formacije". To ugotovitev potrjujejo tudi ladinijski konodontni elementi rodu *Budurovignathus* z značilno vrsto *B. mungoensis* (Diebel) v prvem členu. V konodontni združbi višje ležečega drugega člena se pojavlja karnijska vrsta *Metapolygnathus polygnathiformis* (BUDUROV & STEFANOV) (KOLAR-JURKOVŠEK & PLACER, 1987).

CONCLUSION

Budurovignathus mungoensis (Conodonta) from the Ladinian part of the "Pseudogailtal Formation" near Blagovica (Sava Folds, Slovenia)

"Pseudogailtal Formation" ("Pseudozilian Formation") in the Sava Folds consists of four members. The lowest and the youngest members include clastites (PLACER & KOLAR-JURKOVŠEK, 1990), but the two in-between members consist of carbonate rocks (Figure 3). The upper carbonate-clastic member comprises also chert. It can be concluded that the sampled carbonate-clastic strata exposed between Blagovica and Trojane belong to the lowermost part, that is to the first member of the "Pseudogailtal Formation". This statement can be confirmed by the presence of the Ladininan conodont element *Budurovignathus mungoensis* (DIEBEL) in the studied strata of the first member. Moreover, the Carnian species *Metapolygnathus polygnathiformis* (BUDUROV & STEFANOV) is present in the second member of the "Pseudogailtal Formation" (KOLAR-JURKOVŠEK & PLACER, 1987).

Zahvale

Geološke raziskave avtocestnega odseka med Blagovico in Trojanami je omogočila DDC svetovanje in inženiring. Avtorja se zahvaljujeva B. Jurkovšku za branje rokopisa in L. Placerju, D. Skabernetu ter U. Premruju za številne diskusije pri razumevanju "Psevdoziljske formacije" in H. Kozurju za koristne nasvete. Del raziskave je bil opravljen v okviru programske skupine "Regionalna geologija" (P1-0011), ki jo finančno omogoča Agencija za raziskovalno dejavnost Republike Slovenije.

LITERATURA

BALINI, M., JURKOVŠEK, B.. & KOLAR-JURKOVŠEK, T. (2006): New Ladinian ammonoids from Mt. Svilaja (External Dinarides, Croatia). *Riv. It. Paleont. Strat.*, Milano (v tisku).

EPSTEIN, A.G., EPSTEIN, J.B. & HARRIS, L.D. (1977): Conodont Alteration Index - and Index to Organic Metamorphism. - *Geol. Surv. Prof. Pap.* 995, 1-27, Washington.

JELASKA, V., KOLAR-JURKOVŠEK, T., JURKOVŠEK, B. & GUŠIĆ, I. (2003): Triassic beds in the basement of the AdriaticDinaric carbonate platform of Mt. Svilaja (Croatia). *Geologija* 46/2, 225-230, Ljubljana.

KOLAR-JURKOVŠEK, T. (1990): Mikrofavna srednjega in zgornjega triasa Slovenije in njen biostratigrafski pomen. *Geologija* 33, 21-170, Ljubljana.

KOLAR-JURKOVŠEK, T. & PLACER, L. (1987): Ladinijsko-karnijska mikrofavna iz psevdoziljskih plasti Posavskih gub. *Geol vjesnik* 40, 53-64, Zagreb.

KOVACS, S. & KOZUR, H. (1980): Stratigraphische Reichweite der wichsten Conodonten (ohne Zahnreihenconodonten) der Mittel- und Obertrias. *Geol. Paläont. Mitt. Innsbruck* 10/2, 47-78, Innsbruck.

Kozur, H. (1980): Revision of der Conodontenzonierung der Mittel- und Obertrias des Tethyalen Faunenreich. *Geol. Paläont. Mitt. Innsbruck* 10/3-4, 79-172, Innsbruck.

Kozur, H. W. (2003): Integrated ammonoid-, conodont and radiolarian zonation of the Triassic. Hallesches Jahrb. *Geowiss. B 25,* 49-79, Halle (Salle).

Krystyn, L. (1983): Das Epidaurus-Profil (Griechenland) – ein Beitrag zur Conodonten-Standardzonierung des tethyalen Ladin und Unterkarn. *Schrift. Erdwiss. Kom*. 5, 231-258, Wien.

Kuščer, D. (1967): Zagorski terciar. *Geologija* 10, 5-58, Ljubljana.

OGG, J. G. (2004): The Triassic Period. V: GRADSTEIN, F. M., OGG, J. G. & SMITH, A. G. (Ur.): A Geologic Time Scale 2004. *Cambridge University Press*, 271-306.

Placer, L. & Kolar-Jurkovšek, T. (1990): O starosti psevdoziljskih skladov v Posavskih gubah. *Rudar.-metal. zb.* 37/4, 529-534, Ljubljana.

Premru, U., (1983): Osnovna geološka karta SFRJ 1 : 100.000, list Ljubljana. *Zvezni geološki zavod*, Beograd.

Premru, U. (1974): Triadni skladi v zgradbi osrednjega dela Posavskih gub. *Geologija* 17, 261-297, Ljubljana.

Rejebian, V.A., Harris, A.G. & Huebner, J.S. (1987): Conodont color and textural alteration: An index to regional metamorphism, contact metamorphism and hydrothermal alteration. *Geol. Soc. Am. Bull*. 99, 471-497, Washington.

Izvorna surovina in način žganja neolitske keramike iz Srmina

Nina Zupančič[1], Metka Munda[2]

[1]Oddelek za geologijo, Naravoslovnotehniška fakulteta, Univerza v Ljubljani, Aškerčeva 12, 1000 Ljubljana, Slovenija; E-mail: nina.zupancic@ntfgeo.uni-lj.si
[2]Geoinženiring d.o.o., Enota Maribor, Gorkega 1, 2000 Maribor, Slovenija; E-mail: metka.munda@email.si

Recived: July 7, 2006 **Accepted**: July 20, 2006

Izvleček: Na območju Srmina pri Kopru so ob arheoloških izkopavanjih našli ostanke neolitske in rimske keramike. Raziskali smo 16 vzorcev neolitske keramike, da bi ugotovili kakšna je bila izvorna surovina keramike ter kakšna je bila tehnologijah žganja. Rezultate smo primerjali z analizami rimske keramike. Kemijsko sestavo smo določili z metodo ICP, mineralno z metodo rentgenske difrakcije. Keramika je bila izdelana iz dveh nekoliko različnih glin, ene bolj karbonatne in druge z več glinenimi minerali in glinenci. Glina je nastala s preperevanjem fliša, ki je bil prav tako bolj ali manj karbonaten in je vseboval amfibole, piroksene, glinene minerale, glinence, sljude, kremen, kalcit. Mineralna sestava je pokazala, da je bila neolitska keramika žgana v dveh temperaturnih območjih med 600 in 700 °C ter 700 in 800 °C. Neolitska in rimska keramika se razlikujeta tako po temperaturi žganja kot po kemični sestavi. Rimska keramika je bil žgana pri višjih temperaturah in izdelana iz drugačne gline kot neolitska keramika.

Abstract: During archaeological excavations in Srmin near Koper Neolithic and Roman pottery was found. 16 samples of Neolithic pottery were investigated to establish the source material and firing conditions. The results were compared with analyses of Roman pottery. Chemical composition was determined by ICP, mineral by X-ray diffraction. Pottery was made from two different clays, of which one contained more carbonate, the other more clay minerals and feldspars. Clays originated from weathering of flysch which comprised also more or less carbonate and had contained amphiboles, pyroxenes, clay minerals, feldspars, micas, quartz and calcite. From mineralogical compositions of the samples it is clear that pottery was fired at two different temperature ranges. At approximate 600 to 700 °C and 700 to 800 °C. Neolithic and Roman pottery show different firing temperatures and chemical composition. Roman pottery was fired at higher temperatures and produced from different clay in comparison to Neolithic ceramics.

Ključne besede: arheološka keramika, izvorna surovina, provenienca, temperatura žganja, neolitik, Srmin

Keywords: archaeological ceramics, raw material, provenance, firing temperature, Neolithic, Srmin

Scientific paper

UVOD

Na območju Srmina pri Kopru so se leta 1987 pričela arheološka izkopavanja, ki so, s prekinitvami, trajala do leta 1991. Našli so precej kosov rimske keramike, ki sta jo mineraloško in kemično analizirali ZUPANČIČ IN BOLE (1997). Pri delih, ki so potekala leta 1991 in jih je vodil arheolog Damijan Snoj, pa je bilo najdenih tudi več kosov neolitske keramike.

Poznavanje kemične sestave keramike omogoča določitev izvorne surovine, iz katere je bila keramika izdelana (WILSON, 1978; ADAN-BAYEWITZ IN PERLMAN, 1985; KING, 1987; MOMMSEN ET AL., 1988). Kemična sestava izvornega materiala je namreč enaka kemični sestavi keramike in se torej po žganju ne spremeni (WILSON, 1978; KING ET AL., 1986). Vsebnosti in zlasti razmerja med kemičnimi prvinami so značilna za določen tip gline oz. nahajališče (WILSON, 1978; ADAN-BAYEWITZ IN PERLMAN, 1985; VITALI IN FRANKLIN, 1986). Običajno je surovina, ki so jo uporabljali za manj zahtevno keramko lokalnega izvora. Glino, iz katere so izdelovali keramiko, so pridobivali blizu kraja oblikovanja in žganja keramike (KING ET AL., 1986). Težje je sestavo izvorne surovine določiti, kadar je bilo materialu dodano pustilo, ki vsebuje visoke koncentracije določenih prvin (drobci keramike, vulkanski pepel), ki povzročijo, da se porušijo razmerja med elementi (WILSON, 1978; RICE IN SAFFER, 1982; KING ET AL., 1986; NEFF ET AL., 1989; ZUPANČIČ IN BOLE, 1997).

Medtem ko ostane kemična sestava po žganju enaka, se tekom žganja spremeni mineralna sestava (SCHUBERT, 1986; MOMMSEN ET AL., 1988; NEFF ET AL., 1989). V odvisnosti od temperature in atmosfere med žganjem se iz mineralov, ki sestavljajo surovino, formirajo drugi minerali, ki so pri določeni temperaturi obstojni. Mineraloška analiza tako omogoča, da določimo temperaturo žganja (MANIATIS IN TITE, 1981; MAGGETTI, 1986; MANDOUR ET AL., 1989; WANSARD, 1990). Prvotni minerali, ki sestavljajo izvorni material, pri žganju razpadejo in nastanejo novi minerali. Temperature teh sprememb so eksperimentalno določene. Tako lahko, na podlagi pojava nekega višjetemperaturnega minerala, sklepamo, do katere temperature je bila keramika žgana. Na nastanek novih mineralov vplivata tudi zrnavost ter homogenost materiala. Pri temperaturah nižjih od 110 °C odpari najprej fizikalno vezana voda, sledi izguba kemično vezane vode pri temperaturah nad 200 °C (DEER ET AL., 1992). V oksidacijski atmosferi se prične pri okrog 300 °C zgorevanje organskih snovi, če je atmosfera redukcijska lahko nastanejo črna jedra. Illit pri žganju popolnoma razpade pri temperaturah višjih od 950 °C (MAGGETTI IN GALETTI, 1986; WANSARD, 1990; SCHOMBURG, 1991), razpad se prične že pri 850 °C (SCHOMBURG, 1991). Iz njega nastajata špinel in mullit (WANSARD, 1990; SCHOMBURG, 1991). Pri 700 °C razpade klorit (WANSARD, 1990). Termična stabilnost klorita je odvisna od razmerja Fe/(Fe + Mg). Razpad klorita se prične že pri 500 °C, Mg-klorit, ki je temperaturno najbolj obstojen, pa razpade pri temperaturah 650–850 °C. Pri 850 °C se prične dekarbonatizacija kalcita (MAGGETTI IN GALETTI, 1986). Nekateri menijo, da je dekarbonatizacija kalcita končana že pri 850–900 °C tudi v reduk-cijskem okolju (GANCEDO ET AL., 1985). Sekundarni kalcit nastane pri razpadu gehlenita ali kakega drugega Ca-silikatnega minerala, nastalega pri žganju (MAGGETTI, 1986).

Barva črepinje po žganju je odvisna od kemične in mineralne sestave gline, od temperature žganja, atmosfere med žganjem in od zrnavosti ter homogenosti materiala. S karbonatom bogata keramika, žgana v oksidacijski atmosferi, dobi rdečkasto do rumenkasto barvo, tista, žgana pri redukcijskih pogojih, je po žganju sive do črne barve. Obarvanost je odvisna od prisotnosti železa. Rdečo barvo povzroča hematit, črno oz. sivo barvo pa Fe–špinel (Maggetti in Galetti, 1986). Keramika, ki je prvotno žgana v oksidacijski atmosferi, pri ponovnem žganju v redukcijski atmosferi, pri temperaturi 850 °C, spremeni barvo iz prej rdeče in sive v črno (Gancedo et al., 1985). Pri 680 °C kristali hematit. Pojavil naj bi se že pri 600 °C, vendar je v amorfni obliki in zato ni njegovih uklonov na rentgenogramu. Železo izhaja iz klorita, muskovita in illita. Od 700 °C do 1000 °C se povečuje količina hematita (Wansard, 1990). Iz železa, ki izhaja iz illita lahko, v odvisnosti od atmosfere, nastajata hematit ali magnetit (Mandour et al., 1989). Hematit lahko nastane tudi v fazi ohlajanja pri reoksidaciji Fe^{2+} (Maggetti in Galetti, 1986). Med žganjem v oksidacijskem okolju nastaja hematit tudi iz železovih mineralov kot so goethit, siderit in pirit (Kreimeyer, 1987).

Namen raziskave je bil, s pomočjo mineraloške analize določiti, temperaturo žganja 16 vzorcev neolitske keramike iz arheološkega najdišča Srmin ter ugotoviti ali je bilo okolje žganja oksidacijsko ali redukcijsko. Na podlagi kemične analize smo poskušali določiti izvorni material. Ugotovitve smo želeli primerjali s karakteristikami rimske keramike iz istega najdišča, da bi tako ugotovili morebitne razlike v kemični in mineralni sestavi kot tudi v tehnologiji žganja.

Materiali in metode

Preiskali smo 16 vzorcev neolitske keramike (oznake vzorcev: A204, A251, A252, A255, A255-4, A298, A308, A318, A321a, A337, A340, A353, A358, A359, A416, A417) ki so se med seboj razlikovali po barvi ter vzorec tal (A001), vzet blizu mesta najdbe keramike. Opis vzorcev je podan v tabeli 1.

Mineralno sestavo smo določili z metodo rentgenske difrakcije. Difraktogrami so bili posneti na Naravoslovnotehniški fakulteti, na Oddelku za geologijo, na rentgenskem difraktometru Philips. Pogoji snemanja so bili: $Cu_k a$, Ni filter, moč 40 kV, napetost 20 mA, hitrost snemanja 2°/min, območje snemanja 2q 70-2°, občutljivost $1x10^3$, $2x10^3$ in $4x10^2$ cps. Hitrost papirja je bila 20 mm/min, detektor je bil proporcionalni števec, uporabljen je bil monokromator. Prisotnost kalcita smo dodatno preverjali z 10% HCl.

Okside glavnih prvin (SiO_2, Al_2O_3, Fe_2O_3, MgO, CaO, Na_2O, K_2O, TiO_2, P_2O_5, MnO, Cr_2O_3) ter sledne prvine (Ba, Be, Co, Cs, Ga, Hf, Nb, Rb, Sc, Sn, Sr, Ta, Th, U, V, W, Zr) so določili v kemijskem laboratoriju ACME v Kanadi. 0,2 g vzorca so spojili s $LiBO_2$ in analizirali z metodo ICP–ES (induktivno vezana plazma – emisijska spektroskopija). Na tak način so določili tudi elemente redkih zemelj (REE), le da so uporabili metodo ICP–MS (induktivno vezana plazma – masna spektroskopija). Za analizo Ag, As, Au, Bi, Cd, Cu, Hg, Mo, Ni, Pb, Sb, Se, Tl in Zn so 0,5 g vzorca izluževali s 3 ml 2-2-2 HCl–HNO_3–H_2O pri 95 °C eno uro, razredčili na 10 ml in analizirali z ICP–MS metodo. Določili so tudi žaroizgubo (LOI) in količino ogljika (TOT/C). Količina vzorca A337 je bila premajhna, da bi lahko v laboratoriju

Tabela 1. Opis vzorcev
Table 1. Sample description

	Opis Description	Barva Colour	Opombe Remarks
A204		črna black	
A251		temnorjava dark brown	črna sredina, oranžni rob black core, orange rim
A252		oranžna orange	črna sredina, oranžni rob + vključki kalcita black core, orange rim + calcite inclusions
A255		črna black	beli vključki white inclusions
A255-4		črna black	črna sredina, oranžni rob + beli vključki black core, orange rim + white inclusions
A298		svetlorjava light brown	črna sredina, oranžni rob black core, orange rim
A308		oranžna orange	
A318		oranžna orange	vključki kalcita calcite inclusions
A321a		oranžna orange	beli vključki white inclusions
A337	ni posoda not pottery	črna black	
A340	ni posoda not pottery	oranžna orange	
A353		temnorjava dark brown	beli vključki white inclusions
A358		rjava brown	oranžna sredina, črni rob + beli vključki black core, orange rim + white inclusions
A359	hišni lep adobe	črna black	
A416	ni posoda not pottery	oranžna orange	
A417	ni posoda not pottery	oranžna orange	
A001	tla soil	rjava brown	glinasto-laporasta preperina clay-marly weathered material

naredili popolno analizo. Vzorca zato pri obdelavi kemičnih značilnosti keramike ne obravnavamo. Glede na dodane standarde in ponovitve je bila kakovost analitike zadovoljiva.

REZULTATI IN RAZPRAVA

Izvorna surovina

Rezultati mineraloške analize so zbrani v tabeli 2, kemijske v tabeli 3. Rezultati obeh analiz se dobro ujemajo. Bistvena razlike med vzorci je zlasti v vsebnosti kalcita in CaO. Mineraloška analiza je pokazala, da vsebujejo vzorci z veliko kalcita, manj glinenih mineralov in glinencev in obratno.

Vzorci z veliko CaO vsebujejo manj ostalih oksidov glavnih prvin, slednih prvin in elementov redkih zemelj kot vzorci z manj CaO. Vzorci, pri katerih je kemična analiza pokazala večjo vsebnost CaO, mineraloška analiza pa večjo količino kalcita, imajo tudi višjo žaroizgubo (LOI) in več ogljika (TOT/C). Žaroizguba je merilo količine hlapnih snovi v vzorcih, ki jih je zaradi sproščenega CO_2, več v bolj karbonatnih vzorcih.

Tabela 2. Mineralna sestava in relativna količina mineralov, znotraj posameznih vzorcev, v 16-ih vzorcih neolitske keramike in enem vzorcu tal iz Srmina. (količina mineralov v vzorcu upada od 1 naprej, ? - prisotnost minerala je vprašljiva). Q – kremen, CC – kalcit, Pl – plagioklazi, M/I – muskovit/illit, Mont – montmorillonit, H – hematit, K-gl – K-glinenci, L – lizardit

Table 2. Mineral composition and relative mineral content inside the sample, of 16 Neolithic ceramics and one soil sample from Srmin (the mineral content in sample is decreasing from 1 onwards, ? – mineral presence is questionable). Q – quartz, CC – calcite, Pl – plagioclases, M/I – muscovite/illite, Mont – montmorillonite, H – hematite, K-gl – K-feldspars, L – lizardit

	Q	CC	Pl	M/I	Mont	H	K-gl	L
A204	1	2	3	4	5			
A251	1		2	3	4			
A252	2	1		3	?	4		
A255	1	2	3	4				
A255-4	1	2	3	4	5			
A298	1		2	3	4	5		
A308	1	2	4	3	5			
A318	2	1	4	3	5			
A321a	1	2	3	4			?	
A337	1		3	4	2			
A340	1		2	3	5	4	6	
A353	1	2	4	3	5		?	
A358	1	2	4	3	5		?	
A359	1	5	2	3	4			
A416	1		3	2	4			
A417	1	2	3	4	6	5		
A001	1	2	3	4	5			?

Matrika korelacijskih koeficientov kaže, da so med seboj močno povezani oksidi glavnih prvin: SiO_2-Al_2O_3-Fe_2O_3–MgO–Na_2O–K_2O–TiO_2, medtem ko je povezava med zgoraj omenjenimi oksidi in CaO obratno sorazmerna. CaO izkazuje visoko pozitivno korelacijo le s Sr, kar naj bi kazalo na vsebnost kalcita v vzorcih (Zupančič in Bole, 1997). Navedeni prvini nista izrazito povezani z MgO, zato lahko izključimo prisotnost dolomita, vendar se kaže dokaj visoka pozitivna korelacija med Ba in Sr, ki je značilna za glinence (Deer et al., 1992; Rollinson, 1993). Močno so korelirani tudi SiO_2–Al_2O_3–Fe_2O_3–MgO–K_2O–TiO_2–Rb kar lahko kaže na prisotnost biotita in muskovita (Deer et al., 1992; Rollinson, 1993). Povezave med SiO_2–Al_2O_3–Fe_2O_3–K_2O–TiO_2–La–Co–Sc in SiO_2–Al_2O_3–Fe_2O_3–MgO–Na_2O–TiO_2–Ce kažejo na piroksene in amfibole (Deer et al., 1992; Rollinson, 1993). Na amfibole in piroksene kažejo tudi povezave oksidov glavnih prvin (razen CaO) z elementi redkih zemelj, predvsem z Y, Yb in Lu, medtem ko bi se naj Eu vključeval predvsem v glinence (Rollinson, 1993). Pri preperevanju izvorne kamnine v glino so iz amfibolov in piroksenov nastali glineni minerali, v katerih so se ohranile enake koncentracije in razmerja slednih prvin in elementov redkih zemelj. V času nastajanja gline je preperel tudi del glinencev in biotit, katerega prisotnosti mineraloška analiza ne potrjuje. Glino, iz katere je bila izdelana neolitska keramika, so sestavljali glineni minerali, glinenci, muskovit, kalcit in kremen, kar po sestavi ustreza flišnim kamninam, ki so lahko razvite bolj ali manj karbonatno in ki so značilne za območje ob Jadranu. Večja količina amfibolov in piroksenov v izvorni kamnini kaže na magmatsko ali metamorfno zaledje od koder

Tabela 3. Vsebnost glavnih prvin, žaroizgube (LOI) in celotnega ogljika (C) v % ter slednih prvin v ppm, v 16-ih vzorcih neolitske keramike iz Srmina. – količine prvine v vzorcu ni bilo mogoče izmerit, ker je bila količina vzorca premajhna

Table 3. Major element, loss of ignition (LOI) and total carbon (TOT/C) content in %, and trace element content in ppm, in 16 samples from Srmin. – Element content in sample was immeasurable due to small sample size

vzorec	A204	A251	A252	A255	A255-4	A298	A308	A318	A321a	A340	A353	A358	A359	A416	A417
SiO_2	58,25	57,12	43,97	56,46	49,88	62,23	54,23	39,51	55,24	66,02	37,34	44,11	62,87	62,84	62,93
Al_2O_3	15	15,31	13,28	15,44	12,27	15,31	13,83	9,88	13,43	14,2	13,6	11,69	14,74	16,25	16,27
Fe_2O_3	6,66	6,93	5,65	6,96	5,78	7,18	7,37	4,93	6,57	6,42	5,08	5,57	6,01	6,96	7,47
MgO	1,37	1,42	1,18	1,88	1,46	1,96	1,26	1,02	0,9	1,52	0,87	1	1,78	1,68	2,35
CaO	4,54	2,91	15,54	7,84	12,35	1,95	6,96	21,06	5,65	1,26	17,31	15,05	2,39	1,57	2,87
Na_2O	0,6	0,91	0,47	0,54	0,79	1,25	0,55	0,56	0,71	1,1	0,36	0,53	0,93	0,7	1,34
K_2O	2,21	2	1,62	2,33	1,79	2,16	1,87	1,41	1,45	2,04	1,42	1,34	2,1	2,35	2,33
TiO_2	0,8	0,84	0,67	0,81	0,66	0,85	0,76	0,53	0,76	0,85	0,58	0,67	0,81	0,8	0,87
P_2O_5	1,24	2,42	0,63	0,41	0,4	0,48	1,21	1,22	1,01	0,33	0,79	1,25	0,59	0,5	0,31
LOI	8,8	9,8	16,6	6,8	14,2	6,2	11,4	19,6	14	6	22,4	18,4	7,5	6,1	3
C	1,57	1,09	3,96	1,97	4,16	0,63	0,94	4,84	-	1,71	4,84	4,04	1,04	0,41	-
Ba	1159,5	1236,1	757	1042,4	606,4	708,1	685,1	771,4	622,2	565,8	846,9	997,5	618,8	631	377,2
Co	37,8	24,9	17,3	25,6	20,3	27,9	28	17,8	26,7	28,2	20,9	20	23,2	22,5	24,3
Cr	0,02	0,02	0,01	0,02	0,02	0,02	0,02	0,02	0,02	0,02	0,03	0,02	0,02	0,02	0,02
Cs	6	4,4	5,2	6,6	4,6	6,2	5,9	2,5	3,6	5,2	23,5	3,9	5,8	7,1	7,6
Cu	70,7	49,3	28,7	23	37,4	40,1	39,2	21,8	40,2	20,5	47,2	27,3	34,6	32,3	22,1
Ga	20,5	19,5	17,4	18,6	16	20,8	19,2	12,2	16,9	20,4	17,6	15,1	19,4	21,1	21,9
Hf	4,6	5	4,2	4,4	4	5,3	4,7	3,2	5,4	5,8	3	4,1	4,8	4,8	4,9
Hg	0,22	0,77	0,21	0,07	0,12	0,09	0,24	0,1	0,3	0,02	0,74	0,24	0,09	0,18	0,05
Mn	0,24	0,08	0,1	0,16	0,12	0,12	0,21	0,11	0,11	0,11	0,05	0,12	0,1	0,1	0,11
Mo	0,7	0,5	1,1	0,4	0,3	0,7	0,4	0,4	0,5	0,6	3,4	0,4	0,2	0,6	1,5
Nb	14	14	12,1	13,6	11,1	14,4	13,9	9,2	14,1	16,1	10,5	11,7	14,6	13,9	14,3
Ni	157,7	151,7	89,3	89,9	86,6	134,5	169,9	111,7	122,5	99,9	137,9	98,9	117,1	140,4	96,7
Pb	22,5	21,8	18,1	19	15,2	18	22,5	12,9	24	19,7	17,6	18,5	17	16,7	4,7
Rb	130,1	105,8	108,2	133,4	97,8	125,3	122,3	71,7	81,4	121,4	78,9	75,8	123,8	131,2	142,1
Sc	15	17	13	16	13	16	15	11	14	14	12	11	14	16	17
Sr	277,1	256,9	223,8	264,5	310,5	164,1	235,5	382,6	251,4	131,1	180,5	396,5	198,2	126,8	138,8
Ta	0,9	0,9	0,8	0,8	0,7	0,9	0,8	0,6	0,9	1	0,7	0,8	0,9	0,9	1
Th	11,5	11,6	10,6	10,9	9	10,3	11,2	6,4	10,8	11,3	9,1	9,1	10,4	10,9	11,6
Tl	0,4	0,2	0,4	0,4	0,1	0,2	0,3	0,2	0,2	0,3	0,2	0,2	0,2	0,2	0,1
U	2,5	2,8	2,4	2,4	1,9	2,3	2,3	1,6	2,3	2,5	2,3	1,9	2,3	2,3	2,2
V	168	143	146	154	122	153	140	82	129	147	244	117	145	153	145
W	2,1	1,9	1,8	1,9	1,5	1,8	1,8	1,1	2	1,9	1,4	1,6	1,6	1,9	1,9
Zn	154	132	108	100	92	113	163	88	79	100	113	103	98	111	40
Zr	138,8	149,3	118,4	118	116,7	150,2	134,6	91,7	154,5	164,7	84,5	122,7	143	132,6	133,4
Y	30,2	35,9	27,4	29,4	25	29,4	27,8	21,2	25,9	31,3	21	23,1	29,2	34,8	32
La	31,5	32,8	29,4	30,5	24,5	29,3	28,1	19	28,4	32,3	23,9	22,9	28,7	33,6	30,1
Ce	74,1	73,2	61,1	69,1	55,3	70	68,6	43,4	74,4	73,7	50,9	54,4	65,9	70,1	67,1
Pr	7,88	8,52	7,25	7,59	6,25	7,57	7,22	4,87	7,3	8,01	5,72	5,64	7,4	8,42	7,68
Nd	30	33,2	26,5	27,4	23,8	28,3	27,6	18,8	27,4	30,1	21,2	21,1	28	32,1	29,5
Sm	5,9	6,6	5,4	5,4	5	5,8	5,6	3,8	5,4	6,1	4,3	4,3	5,6	6,9	6,4
Eu	1,2	1,41	1,08	1,13	0,99	1,19	1,1	0,8	1,01	1,34	0,78	0,86	1,22	1,38	1,27
Gd	4,96	5,97	4,6	4,66	4,05	4,92	4,62	3,26	4,31	5,29	3,61	3,37	4,81	5,73	5,23
Tb	0,85	0,97	0,75	0,78	0,71	0,78	0,77	0,53	0,72	0,87	0,56	0,56	0,8	0,94	0,87
Dy	4,68	5,58	4,27	4,76	3,96	5,08	4,52	3,29	4,2	4,97	3,48	3,4	4,84	5,64	5,34
Ho	0,98	1,16	0,86	0,92	0,82	1,01	0,9	0,63	0,88	1,03	0,68	0,73	0,93	1,08	1,05
Er	3,05	3,56	2,67	2,91	2,66	3,07	2,79	2	2,69	3,16	2,12	2,25	2,93	3,47	3,25
Tm	0,42	0,54	0,42	0,41	0,37	0,46	0,43	0,32	0,4	0,46	0,31	0,34	0,41	0,51	0,45
Yb	2,99	3,29	2,52	2,81	2,45	2,91	2,8	1,98	2,78	3,01	2,07	2,21	2,91	3,31	3,18
Lu	0,45	0,49	0,39	0,44	0,39	0,44	0,39	0,29	0,39	0,45	0,31	0,32	0,42	0,49	0,44

je bil prinešen material, ki se je nato sedimentiral na območju Srmina in širše (Pleničar et al., 1965). Mineraloška analiza vzorca tal, vzetega blizu mesta najdbe keramike, je pokazala, da ta vsebuje kremen, kalcit, plagioklaze, muskovit/illit, montmorillonit in lizardit, kar je zelo podobno sestavi gline, ki smo jo določili na podlagi sestave vzorcev keramike. Domnevo o uprabi flišne gline iz okolice Srmina potrjujejo tudi dejstvo, da je pri izdelavi keramike značilna uporaba lokalnega materiala (King et al., 1986).

Kemična sestava vzorcev neolitske keramike je na prvi pogled dokaj enotna, kar kaže, da je bil izvorni material generalno enak oz. da je izhajal iz istega področja. Kljub temu obstajajo določena odstopanja med posameznimi vzorci, kar je lahko posledica heterogenosti znotraj istega glinokopa, lahko so material pridobivali iz različnih glinokopov ali je na razlike v kemični sestavi med vzorci vplivalo dodajanje talil ali pustil (Zupančič in Bole, 1997).

Clusterska analiza (slika 1) je pokazala, da se 15 vzorcev neolitske keramike generalno deli v dve skupini. V prvo skupino so se uvrstili vzorci: A252, A255-4, A318, A353, A358 in v drugo: A204, A251, A255, A298, A308, A321a, A340, A359, A416, A417. Druga skupina se deli še v dve podskupini; v skupino 2.1 spadajo vzorci: A298, A340, A359, A416, A417, v skupino 2.2 spadajo vzorci: A204, A251, A255, A308, A321a.

Primerjava povprečij obeh osnovnih skupin kaže, da vzorci prve skupine vsebujejo več CaO, P_2O_5, Ba in Sr, druge skupine pa višje vsebnosti vseh oksidov glavnih in večine slednih prvin. Prvine CaO, Ba in Sr kažejo na višjo količino kalcita v tej skupini, ki jo je potrdila tudi mineraloška analiza (tabela 2) – vzorci iz prve skupine so namreč tisti, ki vsebujejo največ kalcita in v njih so že s prostim očesom vidni vključki kalcita (tabela 1). To dodatno potrjujeta žaroizguba (LOI) in količina ogljika (TOT/C) (tabela 4), ki sta v vzorcih iz skupine 1 najvišji in je posledica CO_2, ki se pri žganju sprošča iz $CaCO_3$.

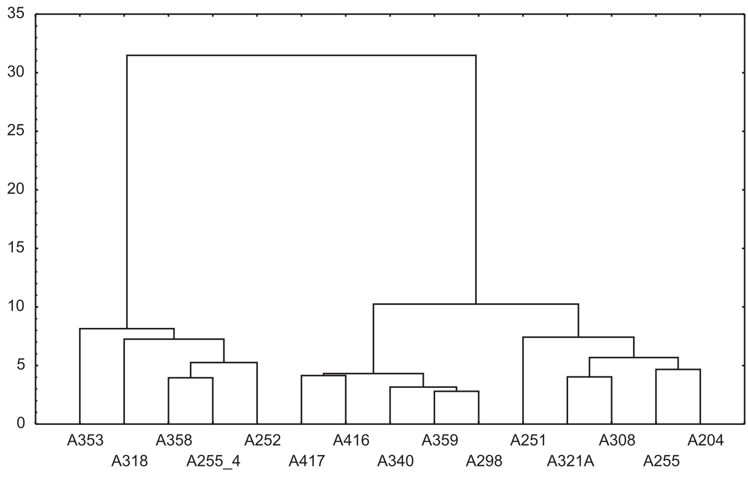

Slika 1. Drevesasti digram clusterske analize za 15 vzorcev neolitske keramike iz Srmina
Figure 1. Cluster analysis hierarchical tree for 15 samples of Neolithic ceramics from Srmin

Skupini 2.1 in 2.2 sta si precej podobni v smislu kemične sestave in se statistično ločita v manj prvinah. Več CaO, P_2O_5, Ba in Sr v skupini 2.2 kaže, da kljub vsemu vzorci iz te skupine vsebujejo več kalcita kot vzorci iz skupine 2.1, kar potrjujeta mineraloška analiza (tabela 2) in preizkus s HCl, vendar obe skupini vsebujeta bistveno manj kalcita kot skupina 1. V skupini 2.1 so višje vsebnosti SiO_2, MgO, Na_2O, TiO_2 in Cr, kar morda odraža nekoliko višje vsebnosti glinenih mineralov v vzorcih te skupine, saj tudi rezultati rentgenske difrakcije (tabela 2) kažejo, da so vzorci skupine 2.1 nekoliko bogatejši z montmorillonitom in tudi muskovit/illitom. Višje vsebnosti Ba in Sr v skupini 2.2 lahko, razen na kalcit, nakazujejo tudi na višjo vsebnost K-glinencev v tej skupini v primerjavi s skupino 2.1. Zanimivo je, da vsi vzorci iz skupine 2.1, razen A298, po arheološki interpretaciji niso deli posode.

Razdelitev vzorcev v skupine potrjujejo tudi diferenciacijski diagrami različnih parov prvin. Na sliki 2 je prikazan diagram SiO_2/CaO.

Varianca in standardni odklon sta za okside glavnih prvin, razen SiO_2 in CaO, majhna. Večjo varianco pa imajo nekatere sledne prvine, kar kaže, da material za izdelavo keramike res ni bil homogen. Oblike vzorcev REE za 15 vzorcev keramike (slika 3) kažejo, da so vzorci REE za vso keramiko podobni, razlikujejo se le po količini posameznega elementa redkih zemelj. Vzorci iz skupin 2.1 in 2.2 vsebujejo več elementov redkih zemelj, vzorci iz skupine 1 vsebujejo manj teh prvin, kar kaže na to, da je šlo generalno za isti izvorni material oz. material iz istega področja. Nižje vsebnosti REE v prvi skupini so posledica "razredčenja" vzorcev s CaO oz. višje vsebnosti kalcita, ki ni nosilec teh prvin (ROLLINSON, 1993). Verjetno je šlo za dve nekoliko različni izvorni kamnini oz različna glinokopa nastala iz iste heterogene kamnine. Ena kamnina je bil verjetno bolj karbonatni fliš, iz katerega je pri prepe-

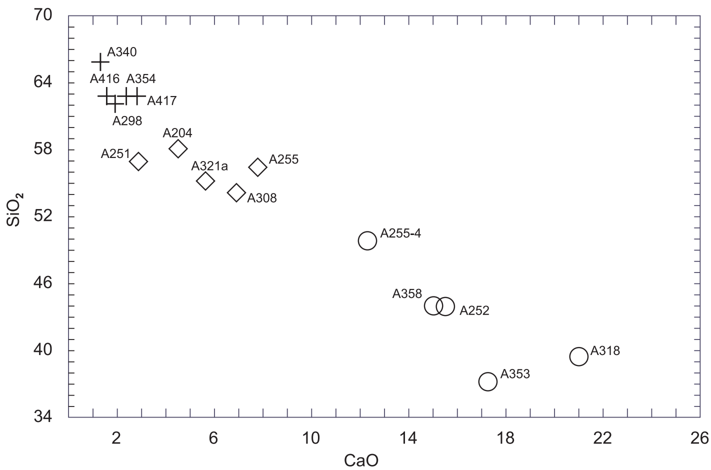

Slika 2. Diferenciacijski diagram CaO/SiO_2 (v %) za 15 vzorcev neolitske keramike iz Srmina: o skupina 1, + skupina 2.1, ◇ skupina 2.2

Figure 2. Differentiation diagram CaO/SiO_2 (in %) for 15 Neolithic ceramics samples from Srmin: o group1, + group 2.1, ◇ group 2.2

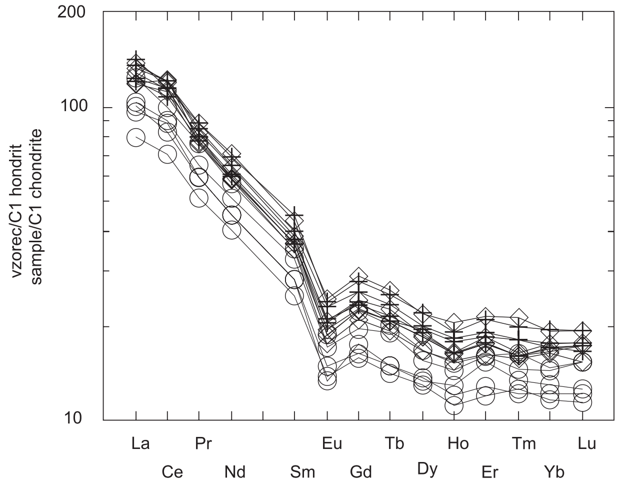

Slika 3. Oblike vzorcev REE za 15 vzorcev neolitske keramike iz Srmina: o skupina 1, + skupina 2.1, ◊ skupina 2.2
Figure 3. REE patterns for 15 samples of Neolithic ceramics from Srmin: o group 1, + group 2.1, ◊ group 2.2

revanju nastala glina z več kalcita, druga kamnina je bil fliš z manjšim deležem karbonata in z več glinene komponente, ki je dal pri preperevanju glino z manj kalcita.

Atmosfera med žganjem

Barva keramike kaže na atmosfero med žganjem. Keramika, žgana v oksidacijski atmosferi, dobi rdečkasto do rumenkasto barvo, tista žgana pri redukcijskih pogojih je po žganju sive do črne barve (Maggetti in Galetti, 1986). Vzorci A308, A318, A321a, A340, A416 in A417 so oranžne barve (tabela 1) in so bili žgani v oksidacijski atmosferi, pri čemer kaže oranžna barva na prisotnost hematita. Rdečo in rdečerjavo ter tudi oranžno barvo keramike povzroča drobnozrnat, enakomerno dispergiran hematit, ki nastaja med žganjem v oksidacijskem okolju (Kreimeyer, 1985; 1987). Na rentgenogramih so ukloni hematita prisotni le v primeru vzorcev A340 in A417, vendar je hematit verjetno prisoten tudi v ostalih vzorcih a je drobnozrnat ali celo amorfen.

Vzorci A204, A255, A337, A353 in A359 so črne oz. temne barve (tabela 1), kar kaže na žganje v redukcijskem okolju.

Nekoliko posebni so vzorci A251, A252, A255-4 in A298, ki imajo črno notranjost ter oranžen rob (tabela 1). Žgani so bili v redukcijskih razmerah, ki so se proti koncu žganja spremenile v oksidacijske. Če predvidimo, da so redukcijsko atmosfero ustvarili z izdelavo kope, je oranžni rob posledica odprtja te kope. Ugotovili so, da je keramika, ki je bila prvotno žgana v oksidacijski atmosferi, pri ponovnem žganju v redukcijsi atmosferi spremenila barvo iz prej rdeče in sive v črno (Gancedo et al., 1985). Sklepamo, da velja tudi obratno, da se pri spremembi atmosfere iz redukcijske v oksidacijsko spremeni barva iz črne v oranžno. Podobno velja za vzorec A358, ki ima oranžno notranjost in črni rob. Verjetno so se pogoji žganja spremenili iz oksidacijskih v redukcijske, zato so v zunanjih delih keramike že potekle reakcije, ki so povzročile spremembo barve.

Temperatura žganja

Rentgenske difrakcija je pokazala (tabela 2), da so v vseh vzorcih prisotni ali kalcit ali glineni minerali ali oboji, kar kaže na nizke temperature žganja (MAGGETTI IN KÜPFER, 1977; BEZECZKY, 1994). V nobenem vzorcu ni prisotnih piroksenov ali gehlenita, kar prav tako potrjuje nižje temperature žganja (BEZECZKY, 1994). Vseh 16 vzorcev neolitske keramike je bilo žganih pri temperaturah nižjih od 800 °C. Če upoštevamo pred-postavko, da kalcit in montmorillonit lahko razpadeta že pri 800 °C (MAGGETTI, 1986), je bila najvišja temperatura žganja okrog 750 °C. Med vzorci pa obstajo razlike, kar nakazuje da niso bili vsi žgani pri istih temperaturah.

Pri štirih vzorcih (A252, A298, A340, A417) so na rentgenogramih prisotni ukloni hematita. Hematit prične kristaliti pri 680 °C, njegova količina se povečuje od temperature 700 °C do temperature 1000 °C. Hematit naj bi se sicer pojavil že pri 600 °C, vendar je v amorfni obliki in zato ni njegovih uklonov na rentgenogramu (WANSARD, 1990). Omenjeni vzorci, vsebujejo tudi illit/muskovit, nekateri tudi kalcit in montmorillonit, zato je morala biti temperatura žganja približno 700–750 °C oz. največ 800 °C, saj bi pri višji temperaturi prišlo do dekarbonatizacije kalcita in razpada glinenih mineralov. Na rentgenogramu vzorca A340, so prisotni tudi ukloni K-glinencev, manj je glinenih mineralov, kar bi lahko bil dodaten dokaz, da je bila temperatura žganja višja, kot pri vzorcih brez hematita. Z višanjem temperature žganja se namreč v vzorcih povečuje količina glinencev in manjša količina glinenih mineralov. Možno pa je, da je bila večja količina glinencev prisotna že v izvornem materialu in ne gre za spremembo količine teh mineralov pri žganju.

V vzorcih A321a, A353 in A358 je prav tako prisotna nekoliko večja količina glinencev in nekoliko manjša količina glinenih mineralov, zato je možno, da so bile temperature žganja okrog 650–700 °C. Pri takšnih temperaturah je bil verjetno žgan tudi vzorec A255, kjer smo zaznali nižjo vsebnost glinenih mineralov. Vendar spet obstaja možnost, da je večja količina glinencev odraz mineralne sestave izvorne surovine in ne žganja.

Vzorci (A204, A251, A255-4, A308, A318, A337, A359, A416), katerih rentgenogrami ne kažejo uklonov hematita ali povečane količine glinencev, kažejo pa večjo količino glinenih mineralov, so bili verjetno žgani pri temperaturah 600–650 °C.

Natančno temperaturo žganja je težko določiti, saj so reakcije, ki v vzorcih potečejo, odvisne od več dejavnikov, ne samo od temperature. Tako bo recimo dekarbo-natizacija kalcita potekla prej v primeru, ko bo material drobnozrnat, kot v primeru velikih zrn karbonata. Verjetno se vsaka keramika pri žganju obnaša nekoliko drugače. Keramike, ki imajo zelo podobno ali celo enako sestavo izvornega materiala, se morda, tudi zaradi nekoliko drugačne priprave materiala, obnašajo različno, zato je težko enoznačno določiti temperaturo žganja.

V redukcijski atmosferi bi naj pri žganju keramike nastala talina prej kot v oksidacijski atmosferi (Maniatis in Tite, 1981; Edwards in Segnit, 1984), torej bi morale tudi spremembe mineralov in tvorba višjetemperaturnih mineralov, poteči hitreje v redukcijski atmosferi kot v oksidacijski atmosferi. V primeru vzorcev neolitske keramike to ni opazno, verjetno tudi zato, ker so bile temperature žganja vseh vzorcev razmeroma nizke. Verjetno bi se razlike med atmosferama odrazile na vzorcih pri višjih temperaturah žganja, pri katerih bi se že formirali visokotemperaturni minerali, še posebej pa pri takih temperaturah, ki bi že povzročale delno taljenje materiala.

Ker so razlike v mineralni sestavi oz. količini posameznih mineralov, predvsem glinenih mineralov, med vzorci, za katere menimo, da so bili žgani pri temperaturah 600–650 °C in vzorci, za katere menimo, da so bili žgani pri temperaturah 650–700 °C majhne, je možno, da so bili vzorci iz teh dveh skupin žgani tudi pri istih temperaturah, to je okrog 650 °C ali tudi nekoliko višje, do približno 700 °C. Lahko, da je večja količina glinencev v skupini vzorcev, za katere je možno, da so bili žgani pri temperaturah 650–700 °C, posledica večje vsebnosti teh v izvornem materialu in ni posledica višjih temperatur, ko bi se večala količina glinencev in manjšala količina glinenih mineralov. Če privzamemo to dejstvo, potem bi lahko vzorce razdelili na tiste, ki nedvomno vsebujejo hematit in so bili žgani pri temperaturah 700–750 °C oz. 800 °C in tiste, ki ne vsebujejo nobenega višjetemperaturnega minerala oz. lahko vsebujejo hematit, vendar je ta amorfen in so bili žgani pri temperaturah nižjih od 700 °C (verjetno 600–700 °C). Razlike v temperaturah žganja so kljub vsemu dokaj majhne in verjetno niso bile ustvarjene načrtno, ampak je šlo za običajno nihanje temperature v času žganja. Morda so pri enem žganju temperature dosegle nekoliko višje vrednosti, pri drugem nekoliko nižje, v splošnem pa so dobili približno enako trdno črepinjo.

Primerjava neolitske in rimske keramike iz Srmina

Izvorna surovina

Kemični sestavi neolitske in rimske keramike (Zupančič in Bole, 1997) sta na pogled podobni, vendar posamezne prvine kažejo odstopanja, zato smo razlike statistično preverili. Glede na t-test se neolitska in rimska keramika 95 % statistično značilno ločita po vsebnostih: Fe_2O_3, TiO_2, Co, Cr, La, Nb, Ni, Sc, Sn, Th, V, Zn, Zr, Y, ki jih je več v neolitski keramiki in po vsebnostih MgO, K_2O, Ag, Cd, Pb, Sb, Sr in W, katerih vsebnost je višja v vzorcih rimske keramike. Tudi diferenciacijski diagrami kažejo, da je v splošnem težko enačiti sestavo neolitske in rimske keramike. Rimska keramika izkazuje večjo enotnost, medtem ko se vzorci neolitske keramike grupirajo v dve skupini. Še posebej so razlike med neolitsko in rimsko keramiko opazne na diferenciacijskih diagramih slednih prvin (slika 4).

Tudi clusterska analiza vseh vzorcev (slika 5), potrjuje, da se vzorci med seboj razlikujejo in da so bili verjetno narejeni iz različnega izvornega materiala. V drevesastem diagramu so namreč ne eni strani vzorci rimske keramike (oznaka R), na drugi strani

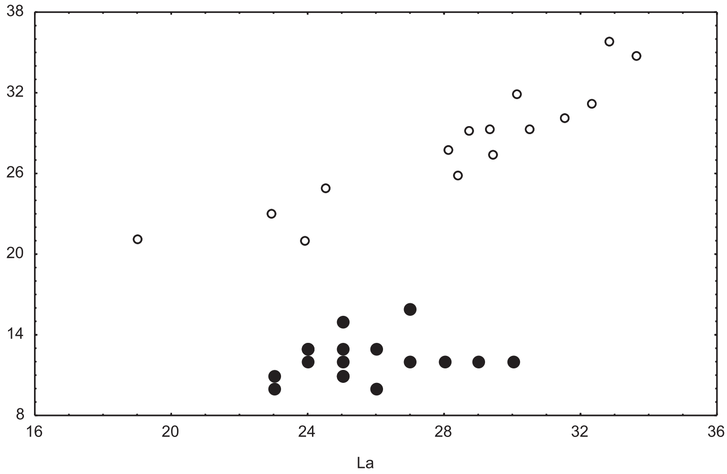

Slika 4. Diferenciacijski diagram La/Y (v ppm) za 15 vzorcev neolitske keramike in 17 vzorcev rimske keramike iz Srmina: ○ vzorci neolitske keramike, ● vzorci rimske keramike
Figure 4. Differentiation diagram La/Y (in ppm) for15 samples of Neolithic ceramics and 17 samples of Roman ceramics from Srmin: ○ Neolithic ceramics samples, ● Roman ceramics samples

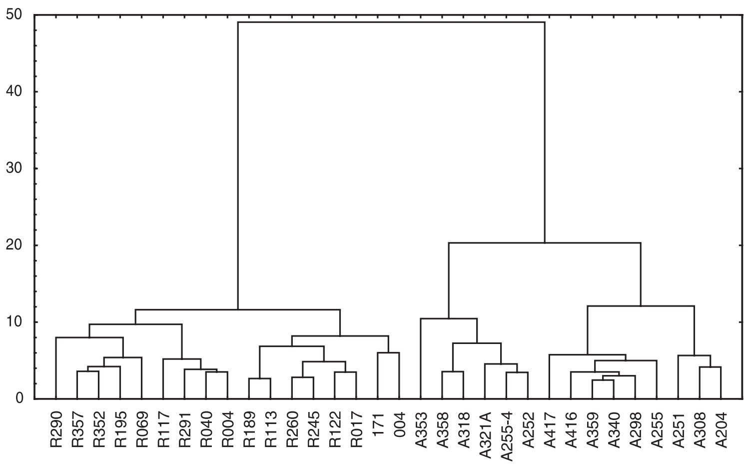

Slika 5. Drevesasti diagram clusterske analize 15 vzorcev neolitske in 17 vzorcev rimske keramike iz Srmina.
Figure 5. Cluster analysis hierarchical tree for 15 samples of Neolithic and 17 samples of Roman ceramics from Srmin.

vzorci neolitske keramike pri čemer niti dva vzorca izmed teh različnih keramik, ne izkazujeta povezovanja.

Za rimsko keramiko obstaja verjetnost, da je bila izdelana v Lokavcu, ki je eden od možnih centrov proizvodnje amfor (ZUPANČIČ IN BOLE, 1997). Razlika v kemični sestavi, v primerjavi z neolitsko keramiko, je tako posledica drugega izvornega materiala. Možno je tudi, da so bile amfore in pokrovčki za amfore izdelani iz lokalnega materiala, torej tistega iz bližine Srmina. V tem primeru kaže razlika v sestavi neolitske in rimske keramike na uporabo glin iz različnih glinokopov ali pa na dodajane talil in/ali pustil pri proizvodnji rimske keramike. Ker ni bila kemično analizirana niti glina iz okolice Srmina, niti glina iz okolice Lokavca, je težko zagotovo določiti izvorni material.

Temperatura žganja

Primerjava mineralne sestave neolitske keramike (tabela 2) in rimske keramike (Zupančič in Bole, 1997) pokaže, da so bile temperature žganja obeh keramik različne. Najnižja temperatura žganja rimske keramike je primerljiva z najvišjo temperaturo žganja neolitske keramike (700–750 °C oz. 800 °C). Tako v neolitski kot rimski keramiki je v vzorcih, žganih pri teh temperaturah, že prisoten hematit, ni pa drugih višje-temperaturnih mineralov. V vzorcih rimske keramike, ki so bili žgani pri temperaturah 750 °C do 850 °C (Zupančič in Bole, 1997), se že pojavlja diopsid, količina illita pa je ustrezno manjša. Temperatura žganja neolitske keramike je nižja kot temperatura žganja rimske keramike, kar je posledica boljše tehnologije žganja v času izdelave rimske keramike. Skozi zgodovino so se večala spoznanja tako o izbiri in pripravi materiala, iz katerega so dobili bolj kvalitetno keramiko, kot tudi o tehnologiji žganja. Pri višjih temperaturah, še posebej, če že pride do delnega taljenja materiala, se poveča tudi trdnost keramike. V keramiki, žgani pri nižjih temperaturah (pod 700 °C), je efekt sintranja slab in taka keramika ima manjšo trdnost (Schomburg, 1991). Verjetno je bila rimska keramika žgana pri višjih temperaturah tudi zaradi namena, kateremu je služila. Amfore, ki so služile shranjevanju živil, so morale biti dovolj trdne in nepropustne, kar so dosegli deloma z višjo temperaturo žganja, deloma pa tudi z izbiro kakovostne gline. Kosom preiskane neolitske keramike arheološka tipologija ni bila v celoti določena. V enem primeru je šlo za hišni lep, za nekatere vzorce se tudi ve, da niso deli posod, tako da sklepamo, da je šlo za keramiko, katere namen uporabe verjetno ni zahteval tako kvalitetne oz. trdne keramike. Zato je bilo dovolj, če je bila ta žgana pri nižjih temperaturah.

Sklepi

Kemična in mineraloška analiza 16 vzorcev neolitske keramike iz Srmina in statistične obdelave teh podatkov so pokazale, da sestava vzorcev ni enotna ampak se vzorci generalno delijo v dve skupini. Prva skupina vzorcev vsebuje več kalcita in manj glinenih mineralov in glinencev, druga skupina vzorcev je bogatejša z glinenci in glinenimi minerali in vsebuje manj kalcita. Vzorci iz druge skupine se med seboj prav tako nekoliko ločijo po vsebnostih kalcita in glinenih mineralov, poleg tega so v nekaterih vzorcih višje vsebnosti plagioklazov, v drugih višje vsebnosti K-glinencev.

Sestava vzorcev kaže, da je vseboval izvorni material, iz katerega je bila keramika izdelana, kremen, kalcit, glinene minerale, glinence in muskovit ter je nastal s preperevanjem bolj ali manj karbonatnega fliša, ki so ga sestavljali kremen, kalcit, glineni minerali (nastali s preperevanjem magmatskih in/ali metamorfnih kamnin), glinenci in sljude. Kemična sestava vzorcev predvsem pa količina elementov redkih zemelj in njihovi vzorci so pokazali, da je izhajal izvorni material za izdelavo keramike iz istega področja, vendar ni bil homogen oz. je šlo za dva različna glinokopa v bližini Srmina. Vzorci z več kalcita so bili izdelani iz bolj karbonatne gline, ki je verjetno nastala s preperevanjem karbonatnega fliša. Vzorci z višjo vsebnostjo glinenih mineralov in glinencev ter z manj kalcita so bili verjetno narejeni iz gline z manjšim deležem karbonata, ki je nastala pri preperevanju manj karbonatnega fliša.

Mineralna sestava je pokazala, da so bili vzorci neolitske keramike žgani v dveh različnih temperaturnih območjih. Štirje vzorci so bili žgani pri temperaturah 700–800 °C na kar kaže prisotnost uklonov hematita na rentgenogramih. Dvanajst vzorcev je bilo žganih pri temperaturah 600–700 °C. Ti vzorci ne vsebujejo nedvoumno dokazljivega hematita ali kakega drugega višje-temperaturnega minerala. Šest vzorcev keramike je bilo žganih v oksidacijskih razmerah, pet vzorcev v redukcijskih razmerah. En vzorec je bil žgan v oksidacijskem okolju, vendar so se razmere proti koncu žganja spremenile v redukcijske. Pri štirih vzorcih keramike so se, prvotno redukcijske razmere, kasneje spremenile v oksidacijske. Ne kaže se neposredna povezava med temperaturami žganja (razdelitvijo vzorcev v dve skupini na podlagi temperatur žganja) in razdelitvijo vzorcev v skupine na podlagi mineralne oz. kemične sestave.

Primerjava vzorcev neolitske in rimske keramike iz istega najdišča je pokazala, da so bili vzorci rimske keramike žgani pri višjih temperaturah kot vzorci neolitske keramike. Najnižja temperatura žganja rimske keramike je bila okoli 750 °C, kar približno ustreza najvišji temperaturi žganja neolitske keramike. V kemičnem smislu se vzorci neolitske in rimske keramike precej ločijo, kar kaže na uporabo gline iz različnih glinokopov v okolici Srmina oz. obstaja možnost, da so bile amfore izdelane v Lokavcu. Vzorci rimske keramike kažejo tudi večjo enotnost v smislu kemične sestave, kar kaže na načrtno izkoriščanje čim bolj kvalitetne gline, medtem ko je bila za neolitsko keramiko verjetno bolj kot kvaliteta gline pomembna bližina glinokopa.

SUMMARY

During archaeological excavations in Srmin near Koper Neolithic and Roman pottery was found. 16 samples of Neolithic ceramics (A204, A251, A252, A255, A255-4, A298, A308, A318, A321a, A337, A340, A353, A358, A359, A416, A417), which differ in color, and one soil sample (A001) from the vicinity of archaeological site, were investigated to establish the source material and firing conditions. Chemical composition was determined by ICP method by ACME Analytical Labs., Canada, and mineral composition by X-ray powder diffraction at Department of Geology. The analytics quality is established as good.

Statistical processing of chemical and mineralogical data of Neolithic pottery showed that composition of samples is not uniform and generally two groups can be distinguished. The characteristics of first group are higher calcite and lower clay

minerals and feldspars content. In second group this ratio is opposite. Samples from second group slightly differ in calcite and clay minerals content; besides in some samples feldspars are prevailingly palgioclases in other K-feldspars.

From mineral composition of samples is concluded that source material for ceramics production comprised quartz, calcite, clay minerals, feldspars and muscovite. The clay formed during more or less carbonate-rich flysh, which consisted of quartz, calcite, clay minerals (formed by weathering of igneous and/or metamorphic rocks), feldspars and micas. Chemical analysis of samples, especially REE content and pattern, indicates that source material originated from the generally same area, but it was not homogenous or there were two different clay pits, both close to Srmin. Samples with higher calcite content were made from clay, which formed during carbonate-rich flysh weathering. Samples which contained more clay minerals and feldspars and less carbonate, were produced from clay, which originated from flysh with smaller amount or no carbonate.

From mineralogical compositions of the samples it is clear that pottery was fired at two different temperature ranges. Four samples were fired at temperatures 700–800 °C, indicated from hematite peaks on the X-ray diffractogrames. Twelve samples were fired at temperatures 600–700 °C. Neither hematite nor any other high-temperature mineral was established in this material. Firing conditions were oxidising in case of six ceramics samples and reducing for five samples. One sample was at first fired in oxidising conditions, but towards the end of firing conditions changed into reducing. In the contrary for four samples conditions changed from reducind to oxidising.

We didn't establish any direct connection between firing temperature and grouping of samples in the groups due to chemical and mineralogical composition.

Neolithic and Roman pottery show different firing temperatures and chemical composition. Roman pottery was fired at higher temperatures and produced from different clay in comparison to Neolithic ceramics. The lowest temperature reached in Roman ceramics was 750 °C, which corresponds to the highest firing temperature of Neolithic samples. Chemical composition of Roman and Neolithic ceramic is quite variable, indicating the use of different clay pits in the vicinity of Srmin. Other possibility is that Roman amphorae were manufactured in Lokavec. Chemical composition of Roman pottery is also much more uniform, what speaks for more carefully planned exploration of higher-quality clay, whilst in case of Neolithic ceramics production the vicinity of the clay pit was more important than clay quality.

REFERENCE

ADAN-BAYEWITZ, D. & PERLMAN, I. (1985): Local pottery provenience studies: a role for clay analysis. *Archaeometry*; Vol. 27, No. 2, pp. 203-217.

BEZECZKY, T. (1994): Amphorenfunde vom Magdalensberg und aus Pannonien. *Kärntner Museumsschriften*, No. 74, pp. 29-166.

EDWARDS, W. I. & SEGNIT, E. R. (1984): Pottery technology at the chalcolithic site of Teleilat Ghassul (Jordan). *Archaeometry*, Vol. 26, No. 1, pp. 69-77.

DEER, W. A., HOWIE, R. A. & ZUSSMAN, J. (1992): *An introduction to the rock-forming minerals*. Edited by Longman Scientific & Technical. Essex : Longman Group,. 696 pp.

GANCEDO, J. R., GRACIA, M., HERNANDEZ-LAGUNA, A., RUIZ-GARCIA, C. & PALOMARES, J. (1985): Moessbauer scpectroscopic, chemical and mineralogical characterization of Iberian pottery. *Archaeometry*, Vol. 27, No. 1, pp. 75-82.

KING, R. H., RUPP, D. W. & SORENSON, L. W. (1986): A multivariate analysis of pottery from southwestern Cyprus using neutron activation analysis data. *Journal of Archaeological Science*, Vol. 13, pp. 361-374.

KING, R. H. (1987): Provenance of clay material used in the manufacture of archaeological pottery from Cyprus. *Applied Clay Science*, Vol. 2, pp. 199-213.

KREIMEYER, R. (1985): Zur Entstehung heller Brennfarben bei eisenhaltigen Ziegelrohstoffen. *Geologische Jahrbuch*, No. 75, pp. 89-122.

KREIMEYER, R. (1987): Some notes on the firing colour of clay bricks. *Applied Clay Science*, Vol. 2, pp. 175-183.

MAGGETTI, M. & KÜPFER, T. (1977): Composition of the terra sigillata from La Péniche (Vidy/ Lausanne, Switzerland). *Archaeometry*, Vol. 20, No. 2, pp. 183-188.

MAGGETTI, M. (1986): Majolika aus Mexiko – ein archäometrisches Fallbeispiel. *Fortschr. Miner.*, Vol. 64, No.1, pp. 87-103.

MAGGETTI, M. & GALETTI, G. (1986): Chemischer Herkunftsnachweis der "Schwarzen Sigillata" vom Magdalensberg. *Magdalensberg-Grabungsbericht*, No. 15, pp. 391-431.

MANDOUR, M. A., TAHA, A. S. & SERRY, M. A. (1989): Ceramic properties of some Egyptian clayey deposits as related to their mineralogical and chemical composition. *Applied Clay Science*, Vol. 4, pp. 83-94.

MANIATIS, Y. & TITE, M. S. (1981): Technological examination of neolithic-bronze age pottery from central and southeast Europe and from the Near East. *Journal of Archaeological Science*, Vol. 8, pp. 59-76.

MOMMSEN, H., KREUSER, A. & WEBER, J. (1988): A method for grouping pottery by chemical composition. *Archaeometry*, Vol. 30, No. 1, pp. 47-57.

NEFF, H., BISHOP, R. L. & SAYRE, E. V. (1989): More observations on the problem of tempering in compositional studies of archaeological ceramics. *Journal of Archaeological Science*, Vol. 16, pp. 57-69.

PLENIČAR, M., POLŠAK, A. & ŠIKIĆ, D. (1965): *Osnovna geološka karta SFRJ. 1:100.000. Tolmač lista Trst : L 33-88*. Beograd : Zvezni geološki zavod,. 68 pp.

RICE, P. M. & SAFFER, M. E. (1982): Cluster analysis of mixes-level data: pottery provenience as an example. *Journal of Archaeological Science*, Vol. 9, pp. 395-409.

ROLLINSON, H. R. (1993): *Using geochemical data: Evaluation, presentation, interpretation*. Edited by Longman Scientific & Technical. Essex : Longman Group, 352 pp.

SCHOMBURG, J. (1991): Thermal reactions of clay minerals: their significance as "archaeological thermometers" in ancient potteries. *Applied Clay Science*, Vol. 6, pp. 215-220.

SCHUBERT, P. (1986): Petrographic modal analysis – a necessary complement to chemical analysis of ceramic coarse ware. *Archaeometry*, Vol. 28, No. 2, pp. 163-178.

VITALI, V. & FRANKLIN, U. M. (1986): New approaches to the characterization and classification of ceramics on the basis of their elemental composition. *Journal of Archaeological Science*, Vol. 13, pp. 161-170.

WANSARD, G. (1990): Effets de la temperature sur la composition mineralogique et sur la structure de la brique de Wanlin (Belgique). *Bulletin de la Société belge de Géologie*, Vol. 99, No. 2, pp. 207-219.

WILSON, A. L. (1978): Elemental analysis of pottery in the study of its provenance: a review. *Journal of Archaeological Science*, Vol. 5, pp. 219-236.

ZUPANČIČ, N. & BOLE, M. (1997): Kemične in mineraloške raziskave keramike amfor. V *Sermin*. Uredila Jana Horvat. Ljubljana : Znanstvenoraziskovalni center SAZU, Inštitut za arheologijo, pp. 83-99.

Vpliv mineralne sestave in mikroorganizmov na propadanje peščenjaka iz kamnoloma Sedovec

Influence of mineral composition and microorganisms on sandstone degradation from Sedovec quarry

Sabina Kramar[1], Breda Mirtič[2], Nina Gunde-Cimerman[3], Polona Zalar[3], Mateja Golež[4]

[1]Zavod za varstvo kulturne dediščine Slovenije, Restavratorski center, Poljanska 40, 1000 Ljubljana; E-mail: sabina.kramar@rescen.si
[2]Univerza v Ljubljani, Naravoslovnotehniška fakulteta, Oddelek za geologijo, Aškerčeva 12, 1000 Ljubljana; E-mail: breda.mirtic@guest.arnes.si
[3]Univerza v Ljubljani, Biotehniška fakulteta, Oddelek za biologijo,Večna pot 111, 1000 Ljubljana; E-mail: nina.gunde-cimerman@uni-lj.si; polona.zalar@uni-lj.si
[4]Zavod za gradbeništvo Slovenije, Dimičeva 12, 1000 Ljubljana; E-mail: mateja.golez@zag.si

Received: July 8, 2006 **Accepted**: July 20, 2006

Abstract: The Baroque chapels of the Way of the Cross of St. Rok's church near Šmarje pri Jelšah and the farmhouse at Strtenica which are built of Middle Miocene sandstone from Sedovec quarry, have been under constant attack of combination of various environmental factors that resulted in severe damage and destruction of the monuments. Proper knowledge of sandstone properties and understanding of degradation causes is necessary for successful maintenance, protection and restoration work of buildings made of natural stone. With the intention to limit degradation, the comparison between fresh sandstone from quarry and deteriorated sandstone has been made. The present study is focused on identifying the petrographycal factors that affect the durability of the sandstone, which were determined by X-ray diffraction, optical and scanning electron microscopy analyses. The main mechanisms of sandstone deterioration are dissolution of calcite and feldspars, secondary minerals (kaolinite, gypsum) crystallization and biodegradation. Using different techniques we have isolated diverse filamentous fungi from the sandstone. The isolated fungi are primarily terrestric xerophilic and xerotolerant species, which belong to the following genera: *Cladosporium, Alternaria, Trichoderma sp., Penicillium, Trichotecium, Nigrospora, Coelomycetes* and an unidentified fungus from the classis *Basidiomycota.*

Scientific paper

Izvleček: Na objektih kompleksa sv. Roka nad Šmarjem pri Jelšah ter domačije iz Strtenice, kjer je bil pri zidavi uporabljen srednjemiocenski peščenjak iz kamnoloma Sedovec, je tekom let prišlo do znatnih poškodb. Poznavanje lastnosti peščenjaka in razumevanje procesov preperevanja nam omogoči pravilnejšo odločitev pri načinu vzdrževanja naravnega kamna, njegove zaščite in restavratorskega posega, ki bi zmanjšal in zaustavil propadanje. Z željo ugotoviti vzroke propadanja je bila narejena primerjava med svežo kamnino iz kamnoloma in preperelega peščenjaka iz posameznih objektov. Osredotočili smo se predvsem na ugotavljanje petrografskih lastnosti, ki vplivajo na obstojnost peščenjaka. Določili smo jih na podlagi uporabe rentgenske difrakcije, optičnega in elektronskega mikroskopa. Procesi razpadanja peščenjaka vključujejo raztapljanje kalcita in glinencev, oksidacijo pirita, nastanek sekundarnih mineralov (kaolinit) oziroma kristalizacijo sadre in delovanje mikroorganzimov. Z uporabo različnih tehnik smo iz peščenjaka izolirali nitaste glive. Izolirane glive so v glavnem terestrične kserofilne in kserotolerantne vrste, ki pripadajo naslednjim rodovom: Cladosporium, Alternaria, Trichoderma sp., Penicillium, Trichotecium, Nigrospora, Coelomycetes in pa neidentificirana gliva iz razreda Basidiomycota.

Key words: sandstone, stone decay, biodegradation, mineralogical transformations, soluble salts, filamentous fungi

Ključne besede: peščenjak, propadanje kamnin, biodegradacija, mineraloške spremembe, topne soli, nitaste glive

UVOD

V danes opuščenem kamnolomu Sedovec pri Šmarju pri Jelšah so že v prejšnjih stoletjih občasno pridobivali srednjemiocenski kremenovo apnenčev peščenjak (VESEL and SENEGAČNIK, 2002). Še posebej veliko ga je bilo uporabljenega pri zidavi objektov domačije iz Strtenice (19.st.) v neposredni bližini kamnoloma in kompleksa cerkve sv. Roka s križevim potom (barok) nad Šmarjem pri Jelšah, kar je bilo potrjeno tudi na podlagi petrografskih analiz (GOLEŽ, 1999, GOLEŽ ET AL., 2005). Zaradi vpliva različnih abiotskih in biotskih dejavnikov na kamnino je prišlo s časom na teh objektih do znatnih poškodb.

Preperevanje kamnine je progresiven naravni proces, ki ga je z današnjim znanjem praktično nemogoče zaustaviti. Obnašanje vgrajenega naravnega kamna v različnih razmerah je kompleksno predvsem zaradi časovno pogojenih sprememb in ponovne vzpostavitve ravnotežja v novih razmerah. V preperevanje so vključeni številni fizikalni, kemični in biološki procesi in reakcije, ki potekajo zaporedno ali sočasno. Kamnina je zato podvržena kemičnim in mineraloškim spremembam, ki vodijo do oslabitve vezi med zrni in izgube materiala (PAQUET and CLAUER, 1997).

Obstojnost kamnine je v glavnem odvisna od narave kamnine, to je njenih lastnosti kot so mineralna in kemična sestava, tekstura in struktura (FRANKLIN, 2000), od načina obdelave (AMOROSSO and FASSINA, 1983), mesta in načina vgradnje ter stika z drugimi materiali (ometi, malte) na objektu (GOSSELIN, 2005) ter od okolja, kateremu je izpostavljena (LORUSSO ET AL., 1999). Propadanje v naravi, še bolj pa na spomenikih, najpogosteje povzročajo zmrzal, kristalizacija topnih soli in mikroorganizmi (AMOROSO and FASSINA, 1983, WINKLER, 1997, WARSCHEID and BRAAMS, 2000).

Kristalizacija topnih soli v porah je pomemben povzročitelj propadanja kamnin, saj na okolna zrna deluje tako hidratacijski kot kristalizacijski pritisk (Benavente et al., 2001). Pri subflorescenci topne soli potujejo proti površini, kjer tik pod njo kristalijo. Zaradi tega se kamnina lušči. Topne soli so lahko prisotne v sami kamnini že pred vgraditvijo, so posledica razpada kamnine ali pa imajo zunanji izvor (tla, atmosfera, konservatorska sredstva, konstrukcija z ostalimi materiali) (Hueston, 1997).

Pojem biodegradacije označuje vse nezaželene in škodljive učinke na lastnosti kamnine zaradi delovanja mikroorganizmov - bakterije, alge, glive, lišaji in makro-organizmov - višje rastline in živali (Bos, 1990, Warscheid and Braams, 2000). Organizmi povzročajo tako mehansko kot kemično propadanje, poleg tega pa tudi kvarijo estetski videz kamnitega objekta (Warscheid and Braams, 2000). Vzroki za biogeofizikalno oziroma mehansko propadanje so v glavnem penetracija hif gliv in glivnih mikobiontov v lišajih in korenin višjih rastlin v mikrorazpoke in medzrnske prostore, kar pospeši drobljenje kamnine. Biogeokemično propadanje pa je posledica delovanja mikroorganizmov bodisi s privzemom elementov iz substrata v svoje metabolne procese, bodisi z izločanjem različnih hidrolitičnih ali oksidacijskih encimov in drugih metabolnih produktov. Običajni fizikalni in biogeokemični procesi, kot je biokorozija in biooksidacija, lahko torej oslabijo strukturo kamnine, sodelujejo tudi pri kopičenju soli in kristaljenju le teh (Koestler et al., 1996, Price, 1996, Cameron et al., 1997, Saiz-Jimenez, 1998, Lorusso et al., 1999, Warscheid and Braams, 2000, Viles and Gorbushina, 2003).

Peščenjak iz kamnoloma Sedovec so v zadnjem desetletju že preiskovali nekateri avtorji. Opisano je bilo nahajališče kamnine (Golež, 1999, Vesel and Senegačnik, 2002, Aničić and Oblak, 2005, Golež et al., 2005). Za obnovitvena dela na kompleksu cerkve sv. Roka je Geološki zavod Slovenije opravil analize peščenjaka v kamnolomu (Vesel and Senegačnik, 2002), prav tako pa so bili že preučeni nekateri procesi preperevanja te kamnine (Golež, 1999, Golež et al., 2004, Golež et al., 2005).

V pričujočem članku smo izpostavili predvsem mineraloške spremembe pri propadanju peščenjaka v odvisnosti od njegovih petrografskih lastnosti in biotski potencial, ki je vodil do propadanja peščenjaka tudi na račun delovanja mikroorganizmov.

Eksperimentalni del

Opis kamnine

Kamnolom peščenjaka se nahaja v severnem delu Kozjanskega, ki se razprostira vzhodno od Celjske kotline. Produktivna kamnina je srednjezrnat kremenovo apnenčev peščenjak, ki v nekaterih delih že prehaja v zelo peščen apnenec (Vesel and Senegačnik, 2002). Plasti vpadajo pod kotom približno 160°/30°. Vidna debelina plasti je različna, od nekaj cm do 30 cm, v spodnjih delih tudi 70-80 cm in največ okrog 2 m. Ritmična tekstura kamnine se kaže v menjavanju svetlejših (mehansko odpornejših) in temnejših (mehansko manj odpornih) plasti. Omenjeni pasovi se ne ločijo med seboj le po videzu, temveč tudi po sestavi. V nekaterih delih nekoliko prevladujejo karbonatna zrna nad nekarbonatnimi, predvsem kremenovimi (VESEL and SENEGAČNIK, 2002). Tenzijske razpoke, debeline 1mm do 1 cm, so v kamnini prisotne v svetlejših mehansko bolj odpornih plasteh, na prehodu v temnejše mehansko manj odporne plasti pa se razcepijo (ANIČIĆ and OBLAK, 2005). Načeloma so razvite v smeri pravokotno na smer plastnatosti. Iz njihove lege v prostoru lahko določimo smer raztezanja (e_3), ki je razvita v smeri 285°-105° (KASTELIC, USTNO, 2005). Te razpoke predstavljajo ploskve šibkosti, po katerih se bo kamnina ob izpostavljenosti novim ustrezno usmerjenim napetostim porušila, kar se je izkazalo kot problematično pri sedanjih kamnoseških delih. Prav tako te razpoke predstavljajo tudi ploskve diskontinuitete in na stikih z matično prikamnino bo tudi proces mehanskega kot tudi kemičnega ter biološkega preperevanja hitrejši in bolj intenziven (KASTELIC and KRAMAR, 2005).

Izbira vzorcev

Odvzem vzorcev je bil zaradi destruktivnosti metod številčno omejen. Vzorci so bili odvzeti na dveh različnih lokacijah, na zavetnem in izpostavljenem mestu objektov. Iz objektov kompleksa cerkve sv. Roka, ki spada v obdobje baroka, ter iz gostinskega objekta domačije v Strtenici iz 19.st., ki se nahaja v neposredni bližini kamnoloma, smo odvzeli vzorce kamnine za ugotavljanje mineraloških sprememb. Na peti kapeli križevega pota sv. Roka so bile odvzete tri vrtine s premerom 2 cm in dolžino 4 cm z dveh ločnih portalov (1ŠJ in 2ŠJ) ter oltarne mize (3ŠJ). Ta metoda vzorčenja je bila uporabljena s predpostavko, da je vsakokratnemu propadanju podvržen približno 4 do 5 cm debel zunanji del kamnine (Winkler, 1997). Globlje naj bi bila kamnina nespremenjena. Naslednje tri vrtine so bile odvzete iz stopnic gostinskega objekta domačije iz Strtenice. Vzorec je bil odvzet iz druge stopnice čelno (1S) ter iz pete stopnice s strani (2S) in čelno (3S). Iz teh šestih vrtin ter iz dekorativne krogle (4ŠJ) iz pete kapele so bili narejeni tudi zbruski za preiskave peščenjaka pod optičnim mikroskopom. Za rentgensko preiskavo smo odvzeli vzorce iz teh vrtin v enocentimetrskih intervalih: od površine do 1 cm (oznaka a), 1-2 cm (oznaka b), 2-3 cm (oznaka c) in 3-4 cm (oznaka d) v globino, da smo ugotavljali spremembe mineralne sestave. Vzorci 1ŠJ, 2ŠJ, 4ŠJ so bili odvzeti z izpostavljenih mest vgradnje, medtem ko so bili vzorci 3ŠJ, 1S, 2S, 3S iz zavetnejših predelov objektov. Za primerjavo so bili odvzeti tudi vzorci sveže kamnine iz kamnoloma (za petrografske analize), in sicer iz obeh litoloških členov; peščeni apnenec (P1) in rjav laminiran peščenjak (P2) ter iz geološke vrtine Sd-1/02 (GZS) za rentgensko difrakcijo; peščeni apnenec (P3) in rjav laminiran peščenjak (P4). Vzorci za mikrobiološko analizo so bili odvzeti samo iz preperele kamnine. Vzorčen je bil površinski sloj ter sloj na globini 1cm od površine kamnine naslednjih vzorcev: 1ŠJ, 2ŠJ, 3ŠJ, 4ŠJ, 1S, 2S in 3S. V vseh primerih so bili vzorci nanešeni na dve različni gojišči.

Uporabljene metode

Petrografske in mineraloške preiskave

Za preiskavo zbruskov v presevni svetlobi je bil uporabljen optični mikroskop AMPLIVAL, proizvajalca Carl Zeiss. Za ločevanje apnenca od dolomita so bili zbruski obarvani z organskim alizarin S-rdečim barvilom.

Vsa opazovanja pod elekronskim mikroskopom in kemične analize na površini vzorca so bile opravljene na Zavodu za Gradbeništvo, s pomočjo sekundarnih elektronov (SE) in odbitih elektronov (BSE). Uporabljen je bil vrstični elektronski mikroskop LV SEM (JEOL 5500 LV) z EDS analizatorjem.

Rentgenska difrakcija je bila opravljena na Naravoslovnotehniški fakulteti na Oddelku za geologijo z rtg-difraktometrom znamke Philips pri 1,2 kW moči, napetosti 40 kW in toku 30 mA z bakrovo cevjo in Kα žarki. Uporabljen je bil nikljev filter in grafitni monokromator v kotnem območju 2θ med 3° in 69°. Hitrost goniometra je bila 0,3 °/min. Mineralno sestavo vzorcev smo določili z računalniškim programom Philips x´Pert software.

Izolacija gliv iz kamnin

Za izolacijo gliv smo uporabili metodo direktnega nanosa peščenega drobirja na Petrijeve plošče s selekcijskim agarnim gojiščem. Za izolacijo mezofilnih gliv smo uporabili gojišče z dodanim sladnim ekstraktom (MEA) za izolacijo kserotolerantnih/halotolerantnih gliv pa MEA z dodatkom soli (MEA +5 % NaCl). Čas inkubacije je bil do 4 tedne pri sobni temperaturi in pri 30 °C. Kot so se glive pojavljale, smo jih sproti izolirali v čiste kulture na krompirdekstrozno (PDA) ali MEA gojišče. Za shranjevanje kultur v genetsko stabilni obliki v mikrobiološki zbirki EX Oddelka za biologijo BF UL, smo glive nacepili na MEA in MEA + 5 % NaCl. V vseh primerih je bil gojiščem dodan kloramfenikol v koncentraciji 100 mg/l.

Identifikacija gliv

Glive smo identificirali s pomočjo makroskopskih in mikroskopskih karakteristik. Za proučevanje makromorfologije smo jih nacepili na MEA in nativne preparate opazovali pod lupo. Za mikroskopsko opazovanje zlasti reproduktivnih struktur pa smo jih obarvali z anilinskim modrilom v mlečni kislini in pregledali pod Olympus BX -51 mikroskopom.

Rezultati in razprava

Mikroskopski opis kamnine

V kamnolomu Sedovec se menjavajo plasti kremenovega peščenjaka s kalcitnim vezivom s plastmi peščenega biosparita. Med vzorci prihaja do manjšega odklona v zrnavosti in sortiranosti kamnine. Kamnino v splošnem sestavlja približno 70 % zrn in 30 % veziva, neupoštevaje por.

V kremenovem peščenjaku (slika 1a) je med zrni približno 40 % nekarbonatnih, pretežno terigenih zrn, in 30% kalcitnih drobcev fosilov. Zrna so velika od 0,07 do 0,9 mm, povprečno okoli 0,3 mm in so slabo do srednje sortirana. Preseki zrn so izometrični do podolgovati, prevladujejo pa vmesne oblike. Zrna se dotikajo s točkastimi, ravnimi in konkavno-konveksnimi stiki. Med terigenimi zrni močno prevladuje kremen, medtem ko so glinenci, litična zrna (drobci metamorfnih, magmatskih kamnin in rožencev) in filosilikati (predvsem muskovit) količinsko podrejeni. Nekateri glinenci so sericitizirani. Od alokemičnih komponent prevladujejo fosili (predvsem ploščice

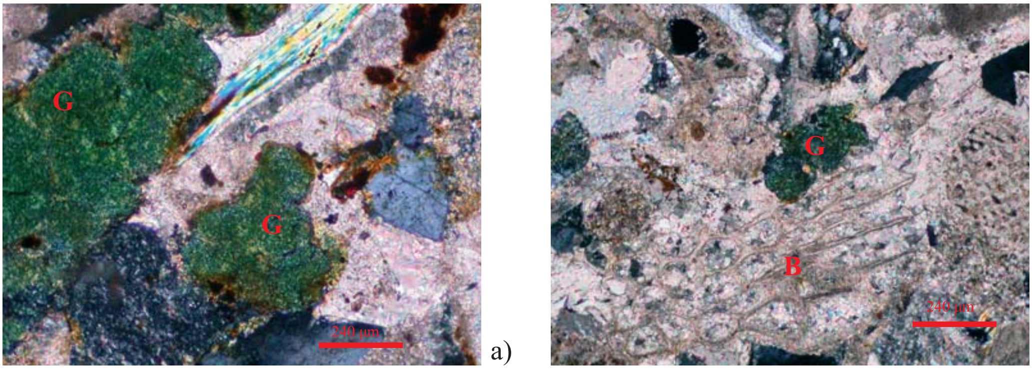

a) b)

Slika 1. Primerjava strukture in sestave obeh litoloških členov kamnine. Pres. sv., +N.a) Kremenov peščenjak s kalcitnim vezivom. Zrni glavkonita (G), ki pa sta že limonitizirani, kar nakazuje rjav rob. Pres. sv., +N. b) Peščen biosparit. Limonitizirano zrno glavkonita (G) in delec briozoja (B) z znotrajzrnskim kalcitnim cementom. Pres. sv., +N
Figure 1. Texture and composition comparison of both lithological sequences of the rock. Trans. light, +N. a) siliceous sandstone with calcite cement. Braun rim around glauconite grains (G) shows process of limonitisation. Trans. light, +N. b) Sandy biosparite. Limonitisation of glauconite grains (G) and briozoi particle (B) with intergrain calcite cement. Trans. light, +N

ehinodermov, foraminifere, drobci školjčnih lupin, rdečih alg in briozojev), pojavlja se tudi glavkonit. Slednji je ponekod že limonitiziran.

Peščen biosparit (slika 1b) sestavlja več karbonatnih drobcev fosilov, približno 40 % in manj nekarbonatnih zrn, približno 25 %, sestava pa je podobna kot pri prej opisanem vzorcu.

Vezivo je v glavnem kalcitni cement, ki nastopa kot sintaksialni obrobni cement, medzrnski in znotrajzrnski cement. Kemična analiza površine vzorca 4ŠJ je pokazala, da peščenjak vsebuje kalcitni cement, zrna kremena in alumosilikatno zrno (slika 2 in 3). Piritni cement je prisoten v sledovih in je povečini že limonitiziran. Ponekod se glavkonit pojavlja tudi kot medzrnski in znotrajzrnski cement.

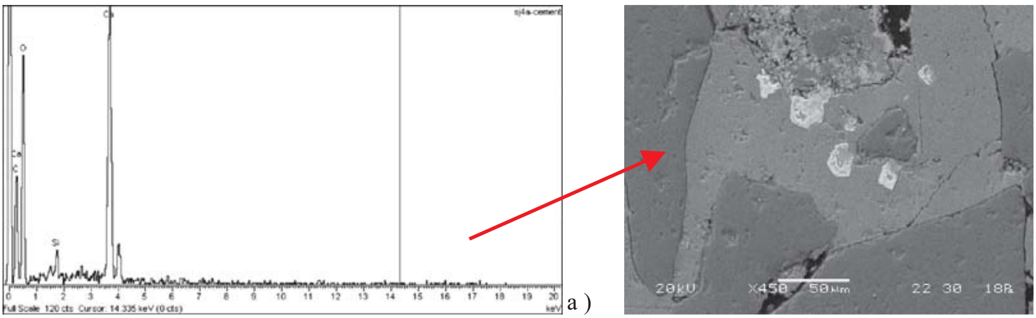

a) b)

Slika 2. Točkovna analiza cementa na vzorcu 4ŠJ prikazuje, da ga sestavlja kalcijev karbonat, ki povezuje zrna kremena. SEM, EDS (a), BSE (b)
Figure 2. Point analysis of pore cement on sample 4ŠJ shows calcium carbonate binding quartz grains. SEM, EDS (a), BSE (b)

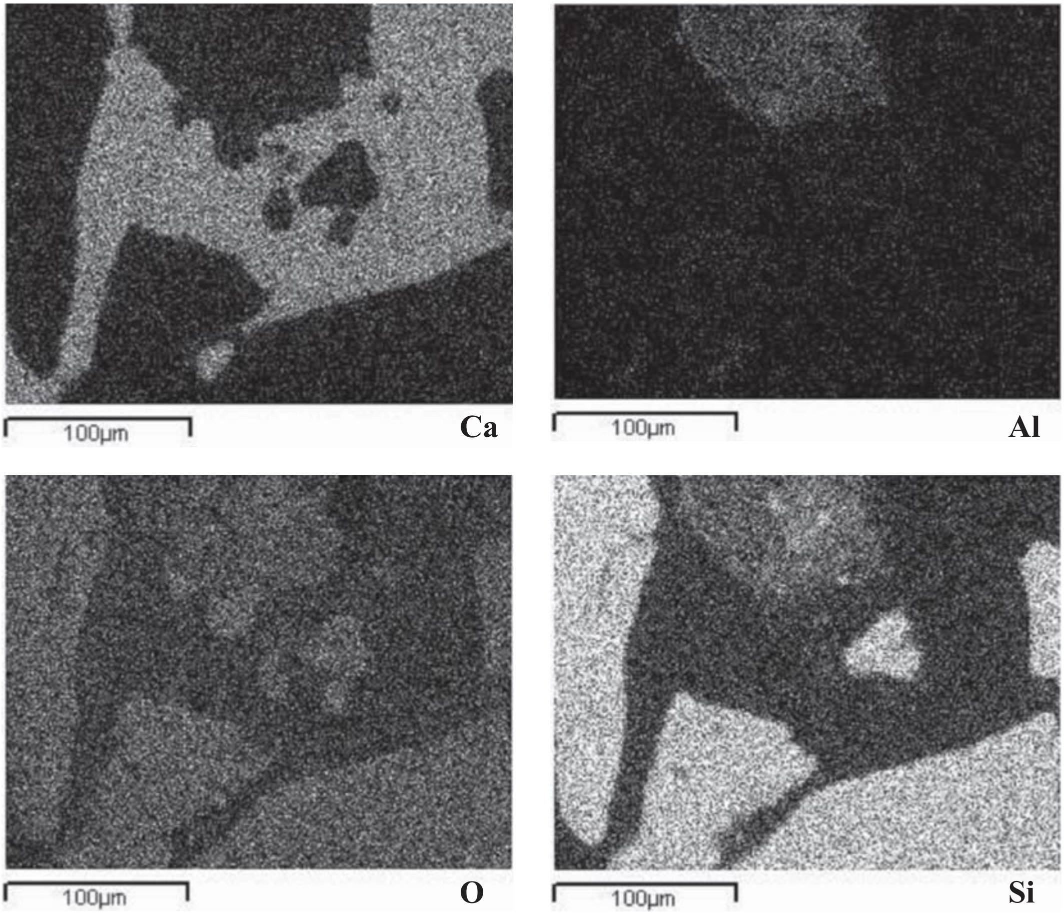

Slika 3. EDS posnetek polirane površine vzorca 4ŠJ
Figure 3. EDS shot of polished surface of sample 4ŠJ

Preperevanje kamnine in nastanek sekundarnih mineralov

Procese preperevanja kamine povzročajo različni dejavniki, ki pa se med seboj prepletajo. Tudi reakcije preperevanja so različne, zato je nemogoče izdelati preprost linearni model propadanja. Nekatere spremembe v kamnini nastanejo že v kamnolomu. Zato marsikdaj med vzorci kamnine iz kamnoloma in kamnine, vgrajene v objektih, ni opaziti razlike v mineralnih spremembah, saj so že v sveži kamnini iz kamnoloma prisotne sericitizacija, limonitizacija in kloritizacija mineralov. V nekaterih vzorcih lahko vzporedno z laminacijo pod optičnim mikroskopom opazujemo razpoke in oslabitev vezi med zrni. Razpoke sledimo v notranjost vzorca, kjer pa postopoma izginejo. Verjetno gre za delaminacijo.

V mineralni sestavi vzorcev sveže kamnine, ugotovljeni z rentgensko difrakcijo, ni opazne bistvene razlike med vzorcema. Rezultati sovpadajo s tistimi, ki jih je dobila tudi Goleževa (Golež, 1999). V sveži kamnini iz svetlejšega litološkega člena (P3) so prisotni kalcit, kremen, muskovit, plagioklazi, kalijevi glinenci, pirit, glavkonit, amfibol in kaolinit, v temnejšem litološkem členu (P4) pa kalcit, kremen, muskovit, plagioklazi, kalijevi glinenci, glavkonit in kaolinit. Pri vzorcih preperele kamnine z rentgensko difrakcijo nismo ugotovili pirita, niti Fe oksidov ali hidroksidov, ki pa so lepo vidni pod optičnim mikroskopom. Vzrok je verjetno v slabi stopnji kristaličnosti in majhni količini hidroksidov, pirit pa je povečini že oksidiran. Prav tako z rentgensko difrakcijo nismo ugotovili morebitnih kalcijevih oksalat hidratov, produktov lišajev.

V prepereli kamnini nastajajo razlike v mineralni sestavi glede na globino odvzetega vzorca. V vseh vzorcih preperele kamnine so prisotni kalcit, kremen, muskovit in plagioklazi, kalijevi glinenci so v manjšini. Sadra je bila potrjena v vzorcih 1aŠJ, 2aŠJ, 2bŠJ, 2cŠJ, 4dŠJ, 1aS, 2aS, 3aS, 3bS (tabela 1). V nekaterih vzorcih je sadra prisotna do globine 3 cm. Izjemo predstavlja vzorec 3ŠJ, kjer sadre nismo določili na nobeni globini. Sadra se pojavlja v gnezdih in pa v medzrnskih prostorih, posamezni kristali so veliki od 5 do 20 μm v ploščasti obliki (slika 4a).

Pri peščenjakih je znatno predvsem preperevanje kalcitnega cementa, kar vodi do zrnatega razpadanja. Obravnavani peščenjak vsebuje okrog 60 % kalcita, kot smo lahko videli pri mikroskopskem opazovanju. Podatke lahko podpremo z rezultati kompleksometrične analize karbonatov, ki so jo napravili na GZS (VESEL and SENEGAČNIK, 2002), ki je pokazala vsebnost karbonata v peščenjaku 56-70 %. Kalcit raztaplja žveplova kislina, katere vir so lahko produkti, nastali pri oksidaciji pirita, kisli dež ali pa organske kisline, katerih nastanek povzročajo mikroorganizmi. Kot možen vzrok preperevanja smo tako opazovali prisotnost pirita v peščenjaku in pojavljanje sadre. Pri oksidaciji pirita namreč nastaja tudi žveplova kislina, ki raztaplja kalcitno vezivo, kar vodi do nastanka sadre, ki kvarno vpliva na obstojnost kamnine. Pirit se večinoma pojavlja kot framboidalni pirit (slika 4b), lahko pa tudi v obliki euhedralnih zrn. Mono in poliframboidalni pirit nastopata ob forameniferah ali zapolnjujeta kamrice


a)

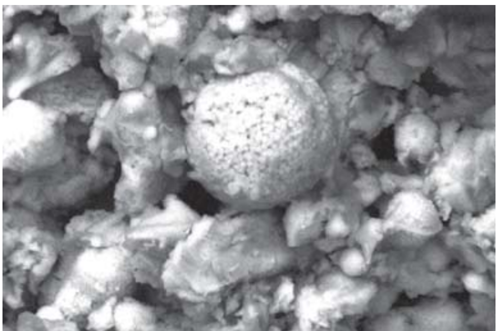
b)

Slika 4. a) Ploščasta sadra v vzorcu 1S. SEM. b) Framboidalni pirit v vzorcu 1ŠJ. SEM
Figure 4. a) Flatty gypsum crystals in sample 1S. SEM. b) Framboidal pyrite in sample 1ŠJ. SEM

Tabela 1. Kaolinit in sadra v preiskovanih vzorcih, določena z rentgensko difrakcijo (pogoji snemanja 0,3 °/min)
Table 1. Kaolinite and gypsum in samples, determined by X-ray diffraction

vzorec	globina	sadra	kaolinit
1ŠJ	a	x	x
	b		
	c		
	d		
2ŠJ	a	x	
	b	x	
	c	x	x
	d		x
3ŠJ	a		
	b		
	c		
	d		x
4ŠJ	a		
	b		
	c		
	d	x	x
1S	a	x	
	b		
	c		
	d		
2S	a	x	
	b	x	
	c		
	d		
3S	a	x	
	b		
	c	x	
	d		x
P3			x
P4			x

posameznih foraminifer. Povečini je pirit v peščenjaku že oksidiran, kar se lepo vidi pod optičnim mikroskopom. Prav tako tudi točkovna kemična analiza na zrnih pirita ni več pokazala prisotnosti žvepla. Kljub vsemu v nekaterih predelih tako v sveži kot vgrajeni kamnini še ni prišlo do oksidacije pirita. Framboidalni pirit se najpogosteje pojavlja v velikostih od 5 do 20 µm, ki jih sestavljajo manjši kubični piritni kristali, velikosti do 1 µm. Makroskopsko so ta gnezda na površini peščenjaka vidna kot rjavi madeži, velikostnega reda okoli 1 mm. V sedimentih najdemo pirit pogosto skupaj z glavkonitom, ki je značilen za redukcijske morske pogoje (Deer et al.,1962 v Queene, 1990).

Glinenci so spremenjeni v vseh vzorcih. Opazujemo lahko raztapljanje, ki se prične po razkolnih ploskvah minerala. Pri preperevanju glinencev prihaja do nastanka sekundarnih glinenih mineralov, kot sta illit in kaolinit (Hamblin and Christiansen, 1997). Pod elektronskim mikroskopom smo opazili preperevanje glinenca v illit, z rentgensko difrakcijo pa smo ugotovili prisotnost kaolinita. Kaolinit je v prepereli kamnini prisoten v vzorcih 1aŠJ, 2cŠJ, 2 dŠJ, 3dŠJ, 4dŠJ ter 3dS, v sveži kamnini iz kamnoloma pa v obeh vzorcih (Tabela 1). Iz razmerja illit/kaolinit je možno sklepati na stopnjo degradacije kamnine. Ponavadi je v bolj sveži kamnini prisotnega več illita kot kaolinita ter *vice versa* (Gal, 2005). Preperevanje illita nadalje vodi do nastanka smektitov, ki pa imajo veliko sposobnost nabrekanja. Torej prisotnost glinencev v peščenjaku negativno vpliva na obstojnost, ker pri preperevanju prehajajo v glinene minerale. Najmanj odporen je kalcijev plagioklaz, sledi mu kalijev plagioklaz. V peščenjaku je prisotnih nekaj mas.% kaolinita. Nastali glineni minerali pa neugodno vlivajo na obstojnost kamnine, ker imajo nižje mehanske trdnosti, zmanjšujejo vezne sile (kohezijske sile) v strukturi kamnine in v svojo kristalno zgradbo vežejo molekule vode, zaradi česar nabrekajo. Dilatacija kamnine z veliko vsebnostjo glinene komponente je zato zelo velika. Razen tega glinenci hitro preperevajo zaradi mehanskih površinskih procesov kot so vodna in vetrna erozija, kristalizacija soli in abrazivne čistilne metode. Njihova izguba mase je v primerjavi z ostalimi komponentami večja (FRANKLIN, 2000). Peščenjaki kaolinitno kremenove sestave, ki so mehki in zelo porozni ter vsebujejo manj kot 2 mas.% kaolinita, preperevajo počasneje kot manj porozni peščenjaki z večjim odstotkom kaolinita (SŘAMEK, 1992, V MIRTIČ ET AL.,1999). Iz kvalitativne rentgenske analize (tabela 1) lahko sklepamo, da kaolinit vsebuje kamnina že v kamnolomu (vzorca P3 in P4). V vzorcih, vzetih iz posameznih objektov, se kaolinit v površinskem delu kamnine ne pojavlja (izjema je samo vzorec 1ŠJ). Kaolinit smo ugotovili šele od globine 2 cm naprej. Iz tega lahko povzamemo, da med degradacijske procese peščenjaka iz Sedovca spada tudi mehansko odstranjevanje drobnozrnatega kaolinita iz površinskega dela kamnine. Kaolinitna zrna so slabo povezana z matično kamnino in jih migrirajoča voda lahko odnaša iz kamnine. Pojav označujemo kot izgubo materiala. Kaolinit v kamnini torej dodatno zmanjšuje njeno obstojnost.

Glavkonita je v kamnini do 5 %, kar zadostuje, da peščenjaku daje zelenkasto barvo. Pod optičnim mikroskopom lahko opazujemo, da so nekatera zrna pričela razpadati, izgubljati železo iz kristalne strukture, saj je okoli zrna vidna limonitizacija (slika 1). Winkler ga sicer opisuje kot stabilen železov mineral (WINKLER, 1997).

Minerali, ki v peščenjaku vsebujejo železo, so večinoma limonit, goethit in hematit. Nastali so bodisi med diagenezo bodisi med preperevanjem kamnine. Navadno nastopajo kot medzrnski porni ali obrobni cement. Železo lahko izvira iz primarnih mineralov biotita, pirita ali glavkonita. Cementacija s hematitom ali limonitom je ponavadi nepopolna. Železo potuje v Fe^{2+} obliki, a v večini okolja postane netopno. Ko se železo pretvori v netopno obliko (Fe^{3+}), ki tvori cement, ostane skoraj netopno v normalnih površinskih razmerah (WINKLER, 1997, FRANKLIN, 2000). Glinena osnova je lahko delno ali v celoti nadomeščena z relativno netopnimi železovimi oksidi/hidroksidi, kar zmanjša poroznost peščenjaka. To je tudi eden izmed procesov otrdevanja površine (FRANKLIN, 2000).

Preperevanje kamnine zaradi delovanja mikroorganizmov

Različne kamnine prestavljajo ekstremno okolje za mikroorganizme, ki jih naseljujejo. S prevladujočimi fizikalno – kemijskimi dejavniki delujejo na mikroorganizme in omogočajo rast samo tistim, ki so se na to prilagodili tako na morfološkem kot tudi na fiziološkem nivoju. Zunanje kamnine predstavljajo za mikroorganizme večinoma suhe habitate, ker razen izjemoma ne zadržujejo vode, ki je pomembna za življenje vseh organizmov. Poleg tega so tudi revne s hranivi in običajno izpostavljene UV sevanju. Na njih in v njih lahko torej preživijo le oligotrofni, kserofilini, pred sevanji zaščiteni mikroorganizmi. Poleg prokariontskih mikroorganizmov (bakterij in arhej), so le redki evkariontski organizmi sposobni tovrstnih prilagoditev. Mednje vsekakor lahko prištevamo glive in lišaje, kot ene najbolj prilagodljivih evolucijskih linij živega sveta. Po drugi strani pa so stene v vlažnih stavbah ali notranja okolja večinoma kolonizirana z glivami, kadar se na njih zadržuje voda zaradi kapilarnega dviga iz podlage, slabega prezračevanja ali pa zaradi uporabe neustreznih barvil. Glive, ki naseljujejo tovrstna okolja, se razlikujejo po biodiverziteti in po fizioloških prilagoditvah od tistih, ki naselijo zunanjim dejavnikom izpostavljene kamnine. Zlasti za te glive je značilna bogata produkcija sekundarnih metabolitov, med katerimi je precej mikotoksinov.

Z metodo inkubacije drobirja na selekcijskih gojiščih za izolacijo mezofilnih in kserofilnih gliv smo v celoti izolirali 12 gliv v čisti kulturi. Identificirali smo jih kot pripadnike naslednjih rodov: *Cladosporium, Alternaria, Trichoderma sp., Penicillium, Trichotecium, Nigrospora, Coelomycetes* in pa neidentificirano glivo iz razreda *Basidiomycota.*

Preperevanje kamnine je odvisno od izmeničnega močenja in sušenja. Večina poškodb nastaja v procesih sušenja. Ko relativna vlažnost v kamnini pade pod določeno vrednost (pod prag topnosti minerala v vodi), se prične kristalizacija soli, tako v notranjosti kamnine kot tudi na površju (eflorescenca, subeflorescenca). Najbolj pogoste soli so sulfati, kloridi, nitrati in karbonati alkalijskih kovin in magnezija. Zato lahko na kamninah, kjer prihaja do tega pojava pričakujemo halotolerantne mikroorganizme.

Določeni rodovi gliv izoliranih iz vzorcev iz kapelice sv. Roka (*Cladosporium, Alternaria Coelomycetes)* so značilni za okolja, ki za večino mikroorganizmov predstavljajo precejšen stres zaradi pomanjkanja vode ali nihanja v vodni aktivnosti. Za te halotolerantne glive je značilna tudi oligotrofnost ter pa zaščita pred UV in ostalimi neugodnimi pogoji v okolju na račun melanina v celični steni. Glive rodu *Trichoderma* in pa neidentificirana bazidiomiceta, pa so verjetno sekundarnega izvora, in so bile naključno prinešene na kamnino, kjer so zaradi aktivnih procesov preperevanja tudi na račun primarnih kolonizatorjev, lahko vzkalile in doprinesle k sekundarni razgradnji.

Glive, ki so bile izolirane iz Strtenice *(Penicillium, Trichotecium roseum, Nigrospora),* pa so bolj značilne kot primarni kolonizatorji vlažnih površin, kjer se nahajajo v večji količini organske snovi.

Čeprav smo v določenih primerih z opazovanjem vzorcev z vrstičnim elektronskim mikroskopom videli sledove rasti gliv, le-teh na agarnih gojiščih nismo uspeli vzgojiti. Razlog temu je lahko uporaba neustreznih gojišč ali inokuluma ali pa kompleksnost mikrobne združbe, ki je v soodvisnosti od neidentificiranih biotskih faktorjev onemogoča uspešno gojenje v kulturi. Biotska pestrost gliv je namreč izjemno velika. Danes poznamo 100.000 vrst, ocenjujejo pa, da obstaja več kot 1.500.000 vrst, kar pomeni, da je znanih le okoli 5 % vrst gliv. Mnogih gliv še ne znamo gojiti v kulturi in zanje vemo le posredno preko izolacije DNA iz okoljskih vzorcev in prepoznave zaporedij baz, ki so indikativne za posamezne glivne taksone. Nove vrste odkrivamo v najrazličnejših okoljih, ki so prej veljala za abiotska oz. naseljena le s prokariontskimi mikroorganizmi. Glive so

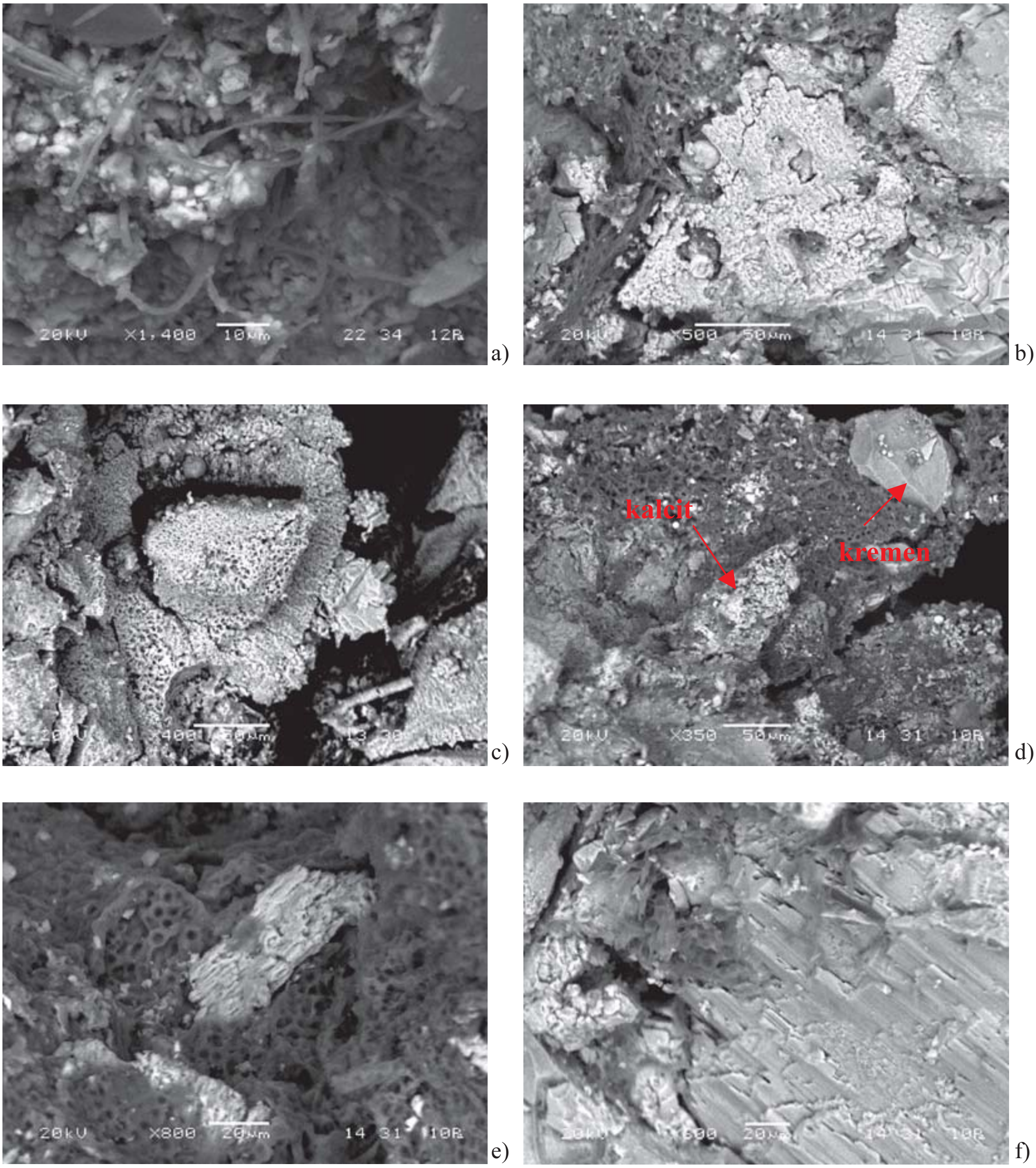

Slika 5. Kemično in fizikalno delovanje mikroorganizmov v vzorcu 4ŠJ. Hife (a) so preluknjale zrno kalcita (b), zrno glinenca se luknjičasto raztaplja (biopitting) (c). Slika d prikazuje fragmentacijo kalcita, medtem ko je kremen nespremenjen. Zrno kalcita (e) in zrno glinenca (f) se ob stiku z mikroorganizmi lamelarno raztapljata - biokorozija. SEM, SE

Figure 5. Chemical and physical influences of microorganisms in sample 4ŠJ. Hyphae (a) have penetrated calcite grain (b), biopitting of feldspar (c). Figure d shows fragmentation of calcite and quartz uneffected by microorganisms. Calcite grain (e) and feldspar grain (f) are subjected to lamelar dissolution - biocorrosion. SEM, SE

bile v zadnjih letih odkrite v kamninah, snegu in ledu Arktike in Antarktike (Gunde-Cimerman et al., 2003; Onofri et al., 2004), v globinah oceanov (Nagahama et al., 2001), v izjemno slanih vodah solin (Gunde-Cimerman et al., 2000) in jezer in celo v savnah (Matoz et al., 2002). V polarnih področjih celo predstavljajo prevladujočo obliko življenja, ki je našla zatočišče prav v tleh ali pa v globini kamnin (endolitske glive). Prodor v kamnine in njihovo naseljevanje jim omogoča mehanska moč njihovih najbolj tipičnih struktur – hif in pa produkcija številnih ekstracelularnih metabolitov, s pomočjo katerih lahko razgrajujejo kamnine (slika 5). Na življenje v in na kamnu, pa se pogosto prilagodijo tudi z melanizacijo celičnih sten, spremenjeno morfologijo in prilagojenim načinom reprodukcije (Sterflinger et al., 1999).

Pod elektronskim mikroskopom smo opazovali posledice delovanja mikroorganizmov na peščenjak oziroma posamezna mineralna zrna. Posamezna zrna se pod vplivom mikroorganizmov lamelarno (slika 5e in 5f) in luknjičasto raztapljajo (slika 5c) ter razpadajo v majhna zrna (slika 5d). Luknjice so reda velikosti približno 5 μm (micropits), ponavadi pravilnih zaobljenih oblik, so posledica delovanja posameznih hif. Večje so reda velikosti 25 μm (mesopits), in so posledica delovanja skupka hif (micelij). Lamelarno raztapljanje je prisotno tako na kalcitu kot na glinencih (slika 5e in f). Opazili pa smo, da zrna kremena ostajajo nespremenjena (slika 5d).

Pojavi razjed in lukenj pri procesih raztapljanja kalcita so posledica različnih koncentracij kislin pri različnih temperaturah. Lamelarna površina nastaja pri topljenju z močno razredčenimi kislinami, hitrost raztapljanja pa je odvisna od medsebojnega vpliva ionov v kislinah in razporeditev ionov na površini kristala. Lamelarna površina nastane zaradi prehajanja Ca^{2+} in CO_3^{2-} ionov v raztopino (Keith et al., 1960, v Golež, 1999). Z nasičenjem vodne raztopine nastopi dinamično ravnotežje, kjer se ponovno izloča kalcit. To lahko potrdimo z opazovanji pod elektronskim mikroskopom, kjer ob direktnem stiku hif s kalcitom opazimo luknjičasto (točkasto) raztapljanje, medtem pa v neposredni bližini vidimo lamelarno raztapljanje, saj so kisline, ki jih izločajo mikroorganizmi, že razredčene.

Sklepi

Procese preperevanja kamnine povzročajo različni med seboj prepletajoči dejavniki, zato je nemogoče izdelati preprost linearni model propadanja. V pričujočem primeru procesi razpadanja peščenjaka vključujejo oksidacijo pirita, raztapljanje kalcita in glinencev ter nastanek sekundarnih mineralov (kaolinita) oziroma kristalizacijo sadre, ki so lahko posledica tako anorganskih dejavnikov kot delovanja mikroorganizmov. Stopnjo delovanja procesov preperevanja in načine propadanja peščenjaka v veliki meri pogojujejo lastnosti same kamnine, kot so lastnosti posameznih mineralov in tekstura kamnine, t.j. laminacija. Najpomembnejši minerali, ki vplivajo na obstojnost peščenjaka, so kalcit, pirit in glinenci. Pri preperevanju glinencev prihaja do nastanka sekundarnih glinenih mineralov, kot sta illit in kaolinit. Prisotnost pirita je lahko škodljiva, ker pri njegovi oksidaciji pride do nastajanja sadre in pa spremembe barve peščenjaka v rjavorumeno. Kristalizacija sadre vpliva na porazdelitev velikosti por v peščenjaku, kar spremeni proces pretakanja raztopin, posledično vpliva na nadaljno kristalizacijo soli in hitrost izgube materiala.

K preperevanju v veliki meri prispevajo tudi različne sile, ki izvajajo pritisk na okolna zrna. Slednji so lahko posledica rasti organizmov ali nabrekanja hif pri ciklih močenja in sušenja, ali pa so kristalizacijski pritiski, nastali pri kristaljenju sadre ali nastanku ledu ter hidratacijski pritiski pri hidrataciji sadre in kaolinita. Nastanek sadre v porah (kristalizacijski in hidratacijski pritisk, termična ekspanzija) povzroči zadostno napetost, ki preseže tlačno trdnost obravnavanega peščenjaka, kar pripelje do zrnatega razpada in luščenja kamnine. Zaradi tega se peščenjak lušči, prihaja do delaminacije. Na te načine nastali pritiski rušijo mikrostrukuro peščenjaka in omogočajo lažji dostop vodi v notranjost peščenjaka, ki nato raztaplja minerale. Voda iz kamnine izpira tudi drobnozrnate sekundarne slabo vezane minerale in s tem zmanjšuje trdnost površinskega dela kamnine.

Vsi minerali so bolj ali manj topni že v čisti vodi. V naravi voda vsebuje še raztopljene pline in kisline, s čimer se njena destruktivna moč še poveča. V obravnavanem primeru peščenjak zrnato razpada in se lušči tudi zaradi raztapljanja kalcitnega veziva, čemur je vzrok bodisi vodna raztopina, v kateri so raztopljeni CO_2, žveplova kislina, ki nastaja pri oksidaciji pirita in pa organske kisline ali pa neposredno delovanje mikroorganizmov. Kalcit lahko ponovno precipitira v površinskem delu kamnine, zaradi česar površina otrdeva.

Pri objektih kulturne dediščine je običajno nemogoče odvzeti dovolj veliko število vzorcev in hkrati tudi zadostno količino vzorca, da bi dobili popolno sliko degradacijskih procesov. Tudi predstavljene raziskave so bile opravljene le na majhnem številu vzorcev. Vsekakor bi bilo v prihodnje smotrno opraviti petrografske analize še na kakšnem objektu, kjer je bil uporabljen peščenjak. Prav tako bo potrebno posebno pozornost posvetiti vplivu mikroorganizmov na propadanje kamnin. V Sloveniji doslej še ni potekalo nikakršno sistematsko raziskovanje mikrogliv na kamnitih podlagah, zato pričujoči članek predstavlja tudi prispevek k razvoju slovenske geomikrobiologije.

SUMMARY

Influence of mineral composition and microorganisms on sandstone degradation from Sedovec quarry

The Baroque chapels of the Way of the Cross of St. Rok's church near Šmarje pri Jelšah and the farmhouse at Strtenica which are built of Middle Miocene sandstone from Sedovec quarry have been under constant attack of combination of various environmental factors that resulted in severe damage and destruction of the monuments.

Productive stone in quarry is medium coarse siliceous calcium sandstone with transition to sandy biosparite (VESEL and SENEGAČNIK, 2002). Sandstone consists mainly of quartz, feldspars, lithic grains and muscovite are in minor proportions. On some feldspar grains sericitisation is also present. Glauconite grains

and fragments of different fossils (echinoderma, foraminifera, bivalvia, lithotamnia, briozoi) represent allochemical components of sandstone. Cements consist mainly of calcite, while pyrite is present in trace and it is already oxidized in the most of its part. Sometimes also glauconite is found like intergrain and pore - filling cement.

In fresh sandstone form quarry calcite, quartz, muscovite, plagioclases, K-feldspar, pyrite, glauconite and kaolinite have been determined by x-ray diffraction. In deteriorated sandstone then mineral composition changes with the depth of samples. In all samples calcite, quartz, muscovite, plagioclases and K-feldspars are present. Gypsum has been found in samples 1aŠJ, 2aŠJ, 2bŠJ, 2cŠJ, 4dŠJ, 1aS, 2aS, 3aS, 3bS (Table 1). Gypsum occurs in nests and pores as single flatty like crystals reach 5 - 20 μm (Figure 4a). Pyrite occurs in framboidal form (Figure 4b) or in euchedral crystals. Mono and polyframboidal pyrite appears in foraminifera chambers. Feldspars are already altered in all samples. Dissolution, which begins in cleavage planes, has been observed. The most frequent form of feldspar weathering is sericitization. This process leads to clay mineral formation, like illite and kaolinite mineral. (Hamblin and Christiansen, 1997). Kaolinite has been determined in some samples of deteriorated sandstone 1aŠJ, 2cŠJ, 2dŠJ, 3dŠJ, 4dŠJ and 3dS, as well in both samples of fresh sandstone (Table 1).

Using different techniques we have isolated diverse filamentous fungi from the sandstone. The isolated fungi are primarily terrestric xerophilic and xerotolerant species, which belong to the following genera: *Cladosporium, Alternaria, Trichoderma sp., Penicillium, Trichotecium, Nigrospora, Coelomycetes* and an unidentified fungus from the classis *Basidiomycota.* Some fungi genera isolated from one of St. Rok chapel (*Cladosporium, Alternaria Coelomycetes)* are characteristic for environments which often represent considerable stress in case of lacking or oscillating of water for great part of microorganisms. Because of presence of melanin in cell wall halotolerant fungi have another characteristics, such as oligotrophy and UV protection. Fungi of Trichoderma genera and unidentificated basidiomictaea are presumably of secondary origin. They were probably brought coincidental on sandstone surface where active weathering process and prime colonisators took place and allowed them to grow and contributed to sandstone degradation. Fungi, isolated from Strtenica *(Penicillium, Trichotecium roseum, Nigrospora),* are in opposite more characteristic like prime colonisators of moisture surfaces where in great amounts organic matter is present. Mechanical force of fungal most typical structures –hiphae enable fungi penetration and their colonization’s into stone, production of numerous extra cellular metabolites contribute to rock degradation (Figure 5). Microorganisms activity reflects in bioppiting (Figure 5c) and lamellar dissolution of minerals (Figures 5e and 5f), while hyphae (Figure 5a) disrupting stone structure and increasing porosity.

Processes of deterioration of natural building stone cause different interacting factors make out simple linear model of degradation impossible. In studied case degradation processes include oxidation, dissolution and secondary mineral crystallization as consequence of inorganic factors as well of microorganism's activity. Degree of weathering processes and weathering forms mostly depend on rock (minerals, structure and texture of stone). Main minerals influencing sandstone durability are calcite, pyrite and feldspar. Feldspar weathering leads to clay minerals formation – illite and kaolinite. The oxidation of pyrite in its final state enables the formation of gypsum which leads to granular disintegration of sandstone. Process of limonitisation also turns the original stone color to braun yellow. We consider different pressures to lead to degradation of sandstone. They can originate from microorganisms growth or hyphae swooling in dry – wetting cycle as well they can be some crystallizing (gypsum and ice formation) or hydratizing pressures (gypsum and kaolinite). Calcite cements dissolution which leads to granular desintegration and scaling of sandstone is consequence of water solution contains dissolved CO_2, H_2SO_4 and organic acids. In surface area of sandstone calcite anew precipitate responsible for stone hardening.

It is important to notice that present results have been obtained with minimal number of analysis. In cultural heritage buildings it is often impossible to provide sufficient number and quantity of samples to retrieve perfect picture of degradation processes. Therefore, it is necessary to make additional petrografical analysis on more monuments built of sandstone from Sedovec quarry. Special attempt is proposed to be made on biodegradation on building stones. In Slovenia there has not been any systematical research of microfungi colonization on stone till now. Present paper represents contribution in development of geomicrobiology in Slovenia.

REFERENCE

AMOROSO, G.G. and FASSINA, V., *Stone decay and conservation, Atmospheric pollution, cleaning, consolidation and protection. Materials science Monographs.Vol.11.* Amsterdam: Elsevier, 1983. 453 str.

ANIČIČ, B. and OBLAK, K., Budinaž v plasteh srednjemiocenskih kamnin na Kozjanskem. *Proteus*, 2005, let.67, št. 5, str. 224-225.

BENAVENTE, D., DEL CURA G., M.A., BERNABÉU, A. and ORDŐŃEZ, S., Quantification of salt weathering in porous stones using an experimental continuous partial immersion method. *Engineering Geology*, 2001, no.59, str. 313-325.

BOS, K., *Weathering and conservation of ferruginous sandstones used as building material in Northern Belgium:The degree of master.* Brussel: Faculty of Medecine and Pharmacy of the Vrije Universiteit Brussel, 1990. 220 str.

CAMERON, S., URQUHART, D., WAKEFIELD, R. and YOUNG, M., *Biological growths on sandstone buildings. Control and treatment. Technical advice note. Vol. 10.* Edinburgh: Historic Scotland, 1997. 40 str.

FRANKLIN, B., The role of petrography in the selection of sandstone for repair. *Seminar on Material evidence.Conserving historic building fabric*. Sydney: NSW Heritage office, 2000. 15 str.

GAL, G., *Influence de la microstructure de différents grčs en oevre et de carričre sur leur résistance ŕ l'altération.* Aplication aux *grčs ŕ meules de la cathédrale Notre-Dame de Strasbourg.* Travail de diplôme. Ecole polytéchnique fédérale de Lausanne. 2004. 52 str.

GOLEŽ, M., *Geološko vrednotenje kamnitih izdelkov iz miocenskih peščenjakov vzhodne Slovenije: magistrsko delo*. Ljubljana: Naravoslovnotehniška fakulteta, Oddelek za geologijo,1999. 122 str.

GOLEŽ, M., MIRTIČ, B. and MLADENOVIČ, A., Študij procesov propadanja sljudnato-kremenovega peščenjaka iz Jelšingrada. *Materiali in Tehnologije*, 2004, let.38, št.1-2, str. 67-70.

GOLEŽ, M., MIRTIČ, B., MLADENOVIČ, A. and KRAMAR, S., Reopening of an abandoned quarry of calcareus sandstone for the restoration of two cultural monuments in Slovenia. *10th Euroseminar on microscopy Applied to Building Materials*. Paisley, 2005.

GOSSELIN, C. Le ciment romain. Une source potentielle de sulfates dans la dégradation des pierres de la Cathédrale de Bourges: Travail du Master. Paris: Université Paris 7 et Laboratoire de Recherche des Monuments Historiques, 2005. 81 str.

GUNDE-CIMERMAN, N., ZALAR, P., HOOG, S. and PLEMENITAŠ, A., Hypersaline waters in salterns : natural ecological niches for halophilic black yeasts. FEMS microbiol. ecol., 2000, let. 32, št. 3, str. 235-240.

GUNDE-CIMERMAN, N., SONJAK, S., ZALAR, P., FRISVAD, J.C., DIDERICHSEN, B. and PLEMENITAŠ, A., Extremophilic fungi in arctic ice : a relationship between adaptation to low temperature and water activity. *Phys. chem. earth (2002)*, 2003, letn. 28, str. 1273-1278.

HAMBLIN, W. K. and CHRISTIANSEN, E.H., *Earth´s dinamic systems.* Provo (Utah): Brigham Young Univerity, Upper Saddle river (New Yersey). Prentice Hall, 1997. 740 str.

HUESTON, F.M., Subflorescence and deterioration of historic masonry. *Stone world,* 1997. str. 74-80.

KASTELIC, V. and KRAMAR, S., Vrednotenje vunduškega peščenjaka z vidika možnosti uporabe v restavratorske namene. *RMZ-Materials and Geoenvironment*. 2005. no.52, vol.2, str. 447-462.

KOESTLER, R.J., WARCHEID, T. and NIETO, F., Biodeterioration: Risk Factors and Their Management. V *Saving Our Architectural Heritage. The Conservation of Histoic Stone Structures.Dahlem Workshop Report.* Edited by Baer, N.S. in Snethlage, R. Berlin: Freie Universität Berlin, 1996. str. 25-36.

LORUSSO, S., MARABELLI, M. and VIVIANO, G. *Pollution de l'environnement et impact sur les biens culturels.* Université de la Tuscia. Département des sciences de l'environnement.Collection l'environnement et les biens culturels.EREC, 1999. 254 str.

MATOZ, T., DE HOOG S., DE BOER A.G., DE CROM, I. and HAASE G., High prevalence of the neurotrope *Exophiala dermatitidis* and related oligotrophic black yeasts in sauna facilities. *Mycoses* 2002, letn. 45, str. 373-377.

MIRTIČ, B., MLADENOVIČ, A., RAMOVŠ, A., SENEGAČNIK, A., VESEL, J. and VIŽINTIN, N., *Slovenski naravni kamen*. Ljubljana : GZS, ZAG, NTF, 1999. 131 str.

NAGAHAMA, T., HAMAMOTO, M., NAKASE, T., TAKAMI, H. and HORIKOSHI, K., Distribution and identification of red yeasts in deep-sea environments around the northwest Pacific Ocean. *Antonie van Leeuwenhoek*, 2001, letn. 80, str. 101-110.

ONOFRI, S., SELBMANN, L., ZUCCONI, L. and PAGANO S., Antarctic microfungi as models for exobiology, *Planetary and Space Science*, 2004, let. 52, št. 1-3, str. 229-237.

PAQUET, H. and CLAUER, N., *Soils and Sediments. Mineralogy and Geochemistry.* Heidelberg, 1997. 369 str.

PRICE, C. A., *Stone conservation. An Owerview of Current Research.* USA: The Getty Conservation Institute, 1996. 73 str.

QUENEE, B., *Transformations minéralogiques et texturales de matériaux rocheux, mortiers et bétons d'ouvrages varies. Approche de la cinétique des mécanismes et identification des facteurs responsables.* Thčse. Université de Nancy I Laboratoire de géologie des ensembles sédimentaires. Equipe de géologie appliquée. Nancy, 1990.

SAIZ-JIMENEZ, C., Biogeochemistry of Weathering processes in Monuments. *Geomicrobiology Journal*, no.16, str. 27-37.

STERFLINGER, K, DE HOOG, GS, and DE HAASE, G., Phylogeny and ecology of meristematic ascomycetes. *Stud Mycol.,* 1999, str. 43: 5-22.

VESEL, J. and SENEGAČNIK, A., *Poročilo o rezultatih predhodnega raziskovanja naravnega kamna - peščenjaka na območju opuščenega kamnoloma Sedovec pri Šmarju pri Jelšah.* Ljubljana: Geološki zavod Slovenije, 2002. 10 str., 5 pril.

VILES, H.A. and GORBUSHINA, A., Soiling and microbial colonisation on urban roadside limestone: a three year study in Oxford, England. *Building and Environment*, 2003, no.38, str. 1217-1224.

WARSCHEID, T. and BRAAMS, J., Biodeterioration of stone: a review. *International Biodeterioration* and *biodegradation*, 2000, no. 46, str. 434-368.

WINKLER, E.M., *Stone: Properties, Durability in Man's Environment*. Verlag, Berlin Heidelberg New York: Springer, 1997. 313 str.

Study of Cladding of Steels by Laboratory Hot Rolling

Študij platiranja jekel z laboratorijskim toplim valjanjem

T. Večko Pirtovšek[1], G. Borchardt[2], M. Terčelj[1] and R. Turk[1]

[1] Faculty of Natural Science and Engineering, University of Ljubljana, Aškerčeva cesta 12, 1000 Ljubljana, Slovenia; E-mail: rado.turk@ntf.uni-lj.si
[2] TU Clausthal, BR Deutschland

Received: June 15, 2006 **Accepted**: July 20, 2006

Abstract: Cladding of commercial steels (tool steel OCR12VM - AISI D2 - DIN X155CrVMo12-1 and construction steel EC100 - DIN 20MnCr5) was studied by laboratory hot rolling experiments under the same thermo-mechanical conditions at which commercial rolling of compound strips is performed, i. e. at a temperature of 1150 °C with a high degree of deformation (0 - 0.5 for OCR12VM tool steel and 0 - 0.7 for EC100 constructional steel) and a slow cooling rate. Microstructure, hardness, tensile strength and diffusion of carbon were evaluated. The relations between the thermo-mechanical conditions during hot rolling and the mechanical properties of the compound strip are discussed in terms of the properties of the interfacial layer.

Povzetek: Platiranje orodnega jekla OCR12VM - AISI D2 - DIN X155CrVMo12-1 in konstrukcijskega jekla EC100 - DIN 20MnCr5) je bilo študirano z laboratorijski toplim valjanjem pri podobnih termomehanskih pogojih kot to poteka v industrijski praksi. Ovrednoten je bil mikrotdotni profil, natezna trdnost dobljenega spoja (vmesna plast), ter difuzija ogljika. Posebna pozornost je bila namenjena povezavi med trdnostnimi lastnostmi dobljenega spoja in pogoji valjanja.

Key words: Compounding, OCR12VM, EC 100, Hot rolling
Ključne beside: Platiranje, OCR12VM, EC 100, toplo valjanje OCR12VM, EC 100

Introduction

Various phenomena arise during the hot plastic deformation of compound steel which are interesting from both a fundamental and a commercial point of view. From the fundamental point of view the influence of plastic state and diffusion on the formation of the cladding zone are important, whereas the commercial point of view is concerned more with the preparation of the contact surfaces, the welding of the compound pack and the behaviour of the interfacial layer during the cooling process to room temperature. For the purpose of commercial rolling of strips it is important that laboratory rolling also takes place continuously in the plain strain state and with similar thermo-mechanical parameters. The cladding is considered to be successful if a good quality joint is already ensured at the first pass - thus avoiding oxidation of the contact surfaces at the following deformations - and if the joint strength at room temperature equals at least that of the basic metal [1-7].

Scientific paper

EXPERIMENTS

Both steels OCR12VM tool steel and EC100 constructional steel (compositions given in Table 1) were received as hot rolled plates with a thickness of 25 mm. Wedges were made out of these plates. Their basic surfaces were ground to the desired degree of roughness. The wedges of both steels were welded together (at the outside) just before heating (Figure 1). The conditions of heating, rolling, and cooling are shown in Figure 2. The microstructures of the as received steels are shown in Figures 3 a-b.

The plain strain state was achieved with an appropriate starting geometry. As the elongation of both steels is different, the local values of the average strain and strain rate were determined separately for each layer of

Table 1: The composition of the two steels used in this investigation (see text)

	Alloying elements (composition in weight %)						
Steel	C	Si	Mn	Cr	Mo	Ni	V
EC100	0.19	0.22	1.30	1.33	0.044	0.16	0.014
OCR12VM	1.52	0.26	0.28	11.82	0.65	0.28	0.91

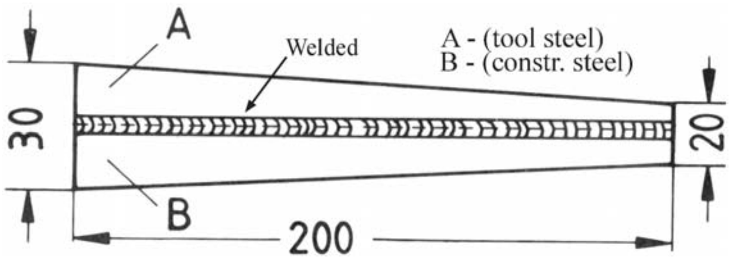

Figure 1: Geometry of the welded sample for the laboratory hot rolling experiment

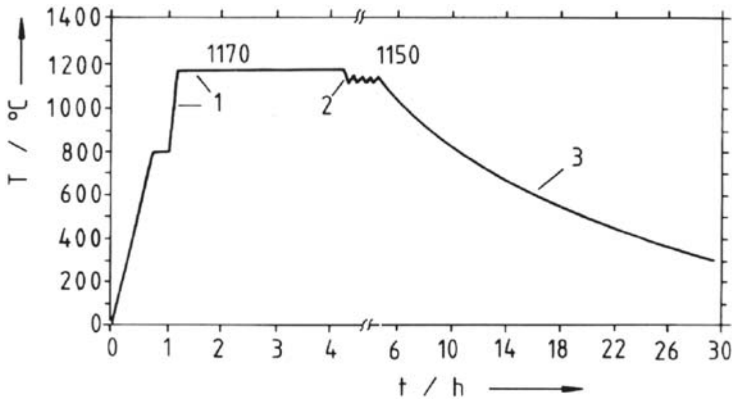

Figure 2: Temperature programme for cladding experiment: 1- heating, 2- rolling, 3- cooling

a.) 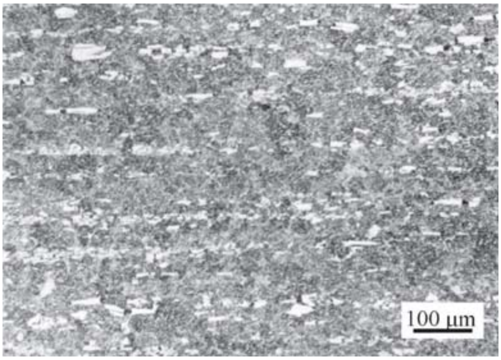

b.) 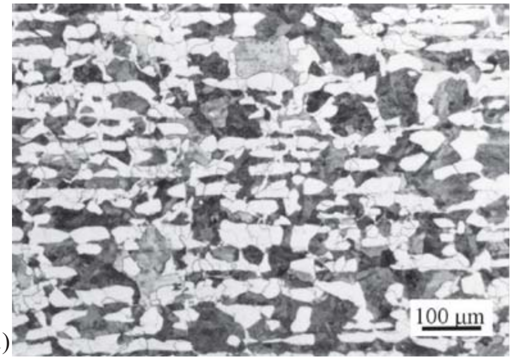

Figure 3: Initial microstructure: a.) OCR12VM, microhardness 250 HV_3, b.) EC 100, microhardness 160 HV_3

the deformed wedge. The rolled compound plates were controled cooled in the furnace. The clad layers of the wedge, dependant on the degree of reduction, were metallographically analysed with an optical microscope. The diffusion of the alloying elements was analysed using an electronic microanalyser and Auger electron spectroscopy (for carbon only). The clad strength of the compound plate was determined in a microtensile test, as shown in Figure 4.

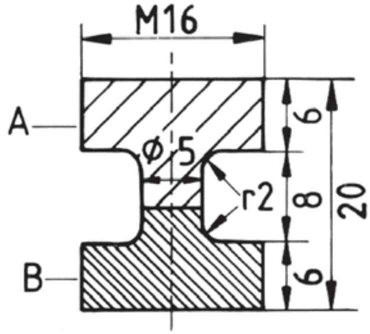

Figure 4: Geometry of the welded sample for the microtensile experiment

Results

Microstructure

The final microstructure is the result of all the three processes through which the compound passes during its production (see Figure 5).

Heating

During the heating phase diffusion of C, Cr, Mn, V and Mo occurs only in places where both steels are in direct contact and not via the gas phase. An adhesive clad of weak strength already appears in this phase. Weakness of the joint is due to the presence of surface contamination; incomplete metal contact because of the roughness of both surfaces, and growth of grains as a result of secondary recrystallisation.

Rolling

During the hot rolling process, direct contact between the surfaces is only possible in places which are free of oxides. Where the atoms of both surfaces reach an inter-atomic distance so that a metal bond appears among them, the so-called “anchor places” are formed. These are areas where the joining of both metals starts. As the deformation continues, the anchor places spread into cohesive bridges and the free surfaces on both sides gradually decrease. The process is completed when a common intermediate layer has been formed. The unjoined places are filled by atomic diffusion. The cohesive bridges between the grains have similar energy and mobility as the usual grain boundary. Voids, dislocations and other microstructural faults in anchor places and in cohesive bridges enable an intensive diffusion parallel to the surface which is more rapid than volume diffusion.

Cooling

The rolled compound samples were cooled (average cooling rate cca 42 °C/h) in a furnace to reduce thermal stresses. Diffusion also continues during the cooling process. Finally, the following microstructure is obtained at room temperature. Microstructure of EC100 steel consists from grains of lamellar perlit and grains of ferrite. Towards the OCR12VM/EC100 interface the amount of lamellar perlit increases (Figure 5, zone I). Very close to the mentioned OCR12VM/EC100 interface (still in EC100 constructional steel) the ferrite cone (Figure 5, zone III) of thickness of cca 80 - 100 μm with very finely precipitated carbides is visible. The microstructure of tool steel consists of spheroidal and dispersed perlit and carbides (Figure 5, zone II), further very close to OCR12VM/EC100 interface the tool steel microstructure (Figure 5, zone IV) is carburized and increased amount of carbides is visible. The thickness of the decarburized layer in the construction steel and the thickness of the carburized layer in the tool steel is independent of the degree of deformation. That is why both layers are considered to be formed during the cooling phase.

Microhardness

The microhardness of the cross section of the compound sample is in accordance with the structural changes in the intermediate layer Figure 6.

Concentration profile

The overall concentration profiles for Cr, Mo, V, Mn (Figure 7a), and C (Figure 7b) agree with the microstructure (Figure 5) and the microhardness (Figure 6), respectively.

Tensile strength

The tensile strength of the compound increases slightly during deformation from 620 N/mm^2 to 680 N/mm^2. Micro-tensile test samples broke down outside the contact surface namely in the ferrite layer, which was formed by the diffusion of carbon from construction steel to tool steel during the cooling process.

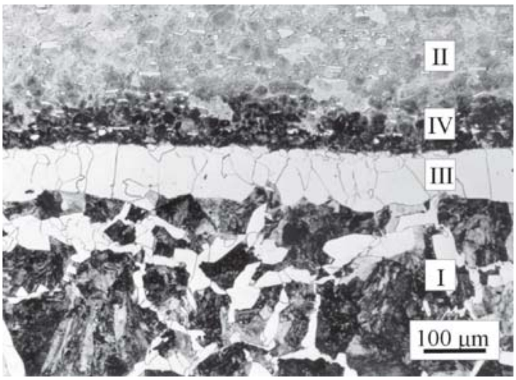

Figure 5: Microstructure of the interfacial layer of the compound OCR12VM/EC 100

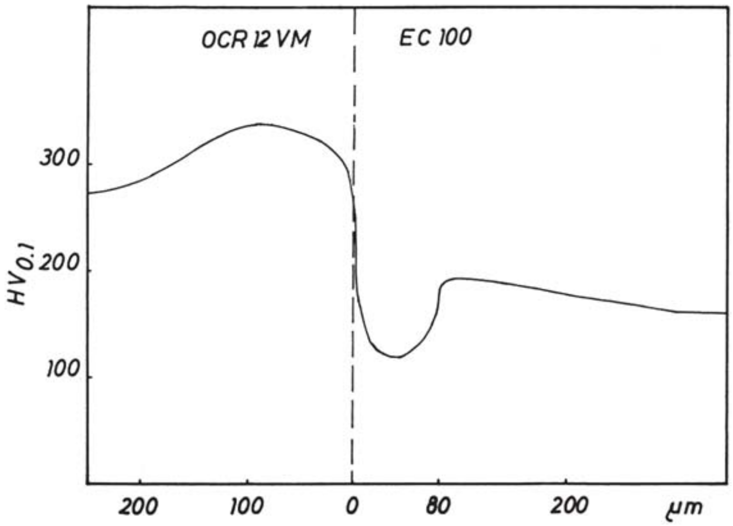

Figure 6: Microhardness profile in the contact zone

Diffusion of carbon

Microstructures in the intermediate layer are the result of the diffusion of carbon and alloying elements. Carbon diffuses at 1170 °C from tool steel to construction steel. During the cooling process the direction of the diffusion of carbon is changed at a certain temperature. Different degrees of carburisation of construction steel and different thicknesses of decarburized layers directly on the contact surface are obtained depending on the time of heating at 1170 °C and the cooling rate. In the literature [8] the expression "up hill" diffusion is found for this kind of diffusion. The activity of carbon changes because of alloying elements. The carbide-forming elements which reduce the activity of carbon in the range where the carbides precipitate, cause carbon to start diffusing in the opposite direction to the concentration gradient.

Decarburization of the construction steel and carburization of the tool steel probably occur in the temperature range between transformation points A_3 and A_1 of the construction steel (800 - 680 °C).

This possibility allows the following consideration: An eutectoid change (820 - 700 °C) occurs in tool steel in this temperature range. The average thickness of the diffusion layer of carbon (decarburized and carburized layer) is in our case 160 µm. The sample was in this temperature range for about two hours. From literature [8] values for the diffusiability of carbon it was estimated that diffusion occurred at 750 °C.

The boundaries of ferrite grains in the decarburized layer are perpendicular to the contact surface that is in the direction of diffusion. It is one of the pieces of evidence showing that decarburization occurs in the temperature range between transformation points A_{r3} and A_{r1} of the construction steel. The direction of the diffusion of carbon at a given temperature can be determined if the activity of carbon in both steels is known.

Diffusion of carbon at 1170 °C

The state before diffusion is shown in Figure 8a. Let us assume that a one-phase (gamma solid solution) binary (Fe - C) range is used for the construction steel EC100 and that a two-phase (gamma + one carbide phase) ternary (Fe - C - M) range is used for OCR12VM steel. This steel contains another carbide-forming element M. On the left of the figure a precisely determined concentration of carbon N_C corresponds to the activity of carbon a_C, on the right a concentration range appears which corresponds to the width of the two-phase range.

The activity of carbon can be approximately calculated in both steels. This activity is greater in OCR12VM than in EC100 steel.

According to the phase role there is another degree of freedom on the ternary side in addition to the temperature (p = const.). The activity of carbon can be changed.

The decrease in activity of the carbon causes the increase in activity of the element M. When the gamma and carbide phases are in a state of equilibrium, a change of activity in the gamma phase corresponds to an equal change of activity in the carbide phase. The mobility of the carbon in the carbide is much lower than in the gamma phase. This is the reason why carbon will only diffuse during the gamma phase. In EC100 steel there are, according to the phase rule, also two degrees of freedom, so the activity of carbon can be changed. The state after the completed diffusion is as follows - Figure 8b.

The diffusion of carbon in the cooling process in the temperature range between transformation points A_3 and A_1 of EC steel

In EC100 steel the transformation gamma to alpha occurs, the gamma and alpha phases being in equilibrium. In OCR12VM an eutectoid change occurs, the alpha, gamma and carbide phases being in equilibrium. In both steels the concentration of carbon moves in the ranges which correspond to the widths of the two-phase and three-phase ranges (Figure 9a). The activity of carbon in OCR12VM steel decreases because of the precipitation of the carbide phase. In the first approximation it is assumed that only one carbide phase is precipitated (Cr_7C_3). All three phases - alpha, gamma and carbide – are in equilibrium. A decrease in the activity of carbon in the carbide phase corresponds to an equal decrease in the activity in the other two phases. The activity of carbon in OCR12VM is because of the carbide precipitation much lower than in EC100 steel. Carbon diffuses in the opposite direction to the decrease in concentration. OCR12VM steel has only one degree of freedom (temperature) and therefore the activity can not be changed. The same applies to EC100 steel. Because of the diffusion of carbon, it accumulates in the intermediate layer on the side of OCR12VM so long, that when one of the two phases decomposed on the account of the other, a two-phase range would appear and as a result two degrees of freedom. On the side of EC100 steel close to the contact surface a one-phase range appears due to the outward diffusion of the carbon (Figures 9b and Figure 10).

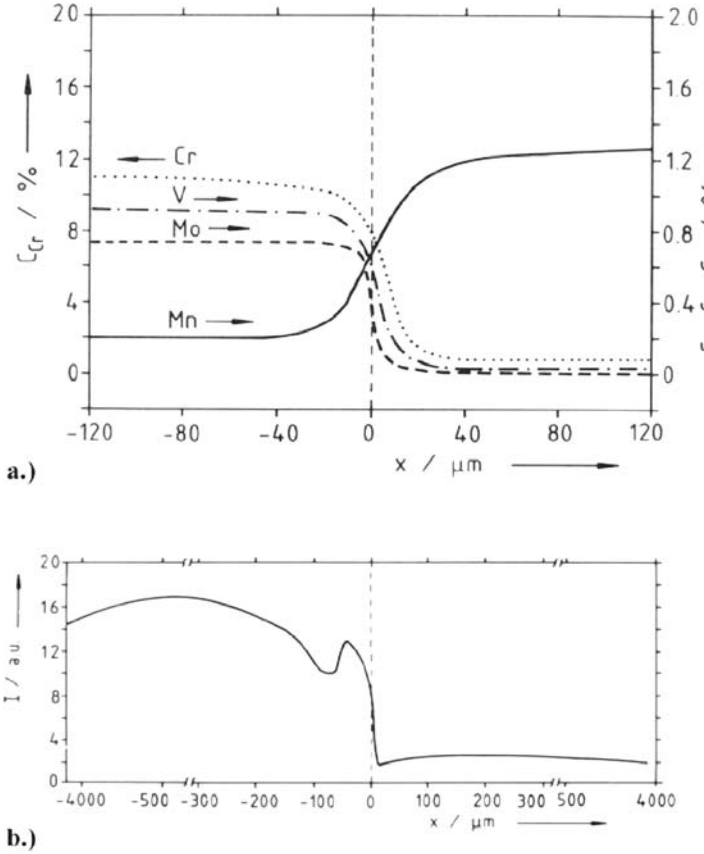

Figure 7: Concentration profiles after the cladding experiment: a.) Cr, Mn, Mo and V (WDS); b.) C (AUGER microscope)

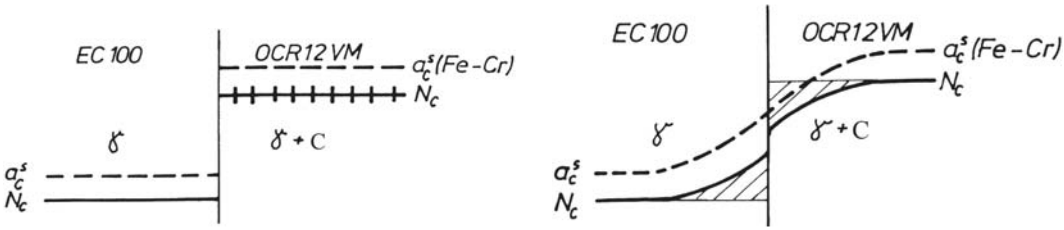

a.) b.)

Figure 8: Diffusion of carbon on temperature 1170 °C (theoretical explanation): a.) state before diffusion process, b.) state after diffusion process, N_c=concentration of carbon, a5C= activity of carbon, C=carbides

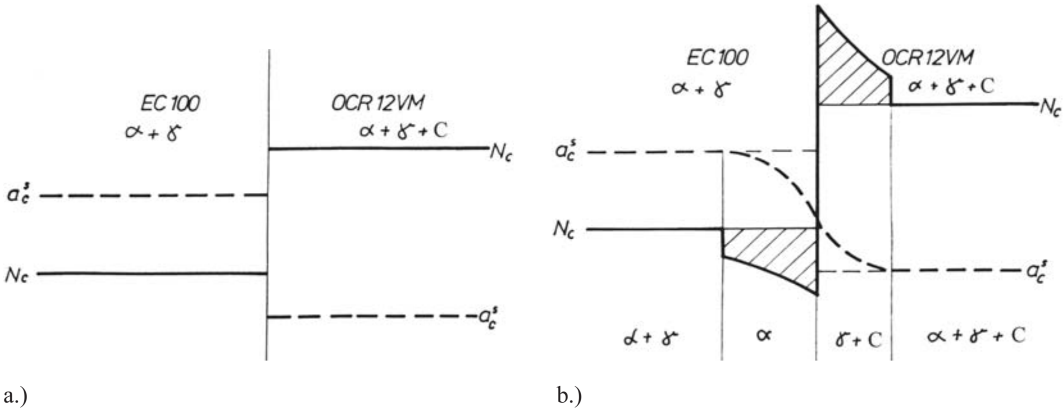

Figure 9: Diffusion of carbon in EC100 steel at cooling in temperature range between A_3 and A_1 transformation point (theoretical explanation): a.) state before diffusion process, b.) state after diffusion process, N_c=concentration of carbon, a5C= activity of carbon, C=carbides

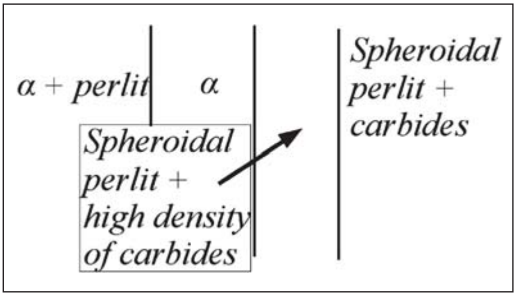

Figure 10: Microstructure of transition layer composed from clearly separated areas of particular phase after diffusion process

CONCLUSIONS

The experiments that simulate cladding of the two steels (OCR12VM/EC100) has been carried out. On the side of EC100 steel close to the contact surface a one-phase range appears due to the outward diffusion of the carbon that results in formation of pure ferrite layer. The thickness of the decarburized layer in the construction steel and the thickness of the carburized layer in the tool steel is independent of the degree of deformation. The moderate tensile strength of the compound material is due to mentioned pure ferrite layer in the contact zone. In further cooperative investigations we shall try to optimise the cooling conditions in order to avoid excessive uphill diffusion of carbon.

References

[1] A. Knauscher, Plattierte werkstoffe, Freiberger Forschungshefte, B 170, 1973.

[2] W. Hartweck, Die metallische Adhäsion und ihre Einflussgrössen, Stahl und Eisen 97 (1977) 13.

[3] S. Pimpasakdi, F.G. Albermani, S. Kitipornchai, Journal of constructional steel research, 60(2004) 1409-1423.

[4] R. Kacar, M. Acarer, Mikrostructure-property relationship in explosively welded duplex stainless steel-steel, Materials Science and Engineering A363 (2003) 290-296.

[5] H. Brandis, H. Preisendanz, P. Schüler, Über die Wirkung einiger carbidbildener Elemente auf den Verlauf der Aktivität des Kohlenstoffes in Fe-X-C-Legierungen im Temperaturbereich von 900 bis 1100 °C, HTM 36/3 (1981) 121 - 127.

[6] H. Schenck, H. Kaiser, Untersuchungen über die Aktivität des Kohlenstoffs in kristallisierten binären und ternären Eisen - Kohlenstoff - Legierungen. Arch. Eisenhüttenwesen, 4 (1960) 227 - 235.

[7] H. Zitter, G. Veitl, Zum Transport des Kohlenstoffes in plattierten Werkstoffen. Arch. Eisenhüttenwessen 48 (1977)1.

[8] W. Seith: Diffusion in Metallen. Berlin: Springer Verlag, 1955.

Experimental Study of Hot Deformability Of 1.2690 Tool Steel - Preeliminary Results

Experimentalna študija tople preoblikovalnosti 1.2690 orodnega jekla - preliminarni rezultati

T. Večko Pirtovšek[1], G. Kugler[1], M. Godec[2], R.Turk[1] and M. Terčelj[1]

[1] Faculty of Natural Sciences and Engineering University of Ljubljana, Ljubljana, Slovenia
[2] Institute of Metals and Technology, Ljubljana, Slovenia;
E-mail: milan.tercelj@ntf.uni-lj.si

Received: June 15, 2006 **Accepted**: July 20, 2006

Abstract: 1.2690 is a high alloyed cold work tool steel with about 1.1 % C, 0.3 % Si, 0.3 % Mn, 11 % Cr, 1.5 % V, 2.3 % W and 1.3 % Mo. As such it has a lot of ledeburitic carbides in microstructure, thus its hot plasticity should be investigated. For this purpose hot compression tests of cylindrical specimens, taken from annealed forged billet square 95 mm, were carried out on thermo-mechanical simulator Gleeble 1500D in order to establish suitable parameters for hot working of mentioned tool steel. The temperature range was 850 °C to 1200 °C and the strain rates varied from 0.001 s^{-1} to 6 s^{-1}. Special attention was paid to mechanisms, which are responsible for poor plasticity at upper and lower border of temperature range of hot working. Hot deformation behaviours of steel CRV3 have been studied also by using Prasad's processing (efficiency of power dissipation) and instability maps developed on the basis of dynamic materials model. 1.2690 tool steel exhibits flow instability at lower strain rates and temperatures.

Povzetek: 1.2690 je visokolegirano orodno jeklo za delo v hladnem s približno 1,1 % C, 0,3 % Si, 0,3 % Mn, 11 % Cr, 1,5 % V, 2,3 % W and 1,3 % Mo. V mikrostrukturi je prisotno veliko ledeburitnih carbidov kar zmanjšuje njegove toplo plastičnost. Za njeno raziskavo smo na Gleeble 1500D termomehanskem simulatorju izvedli tople stiskalne preizkuse s cilindričnimi vzorci izrezanih iz kvadratne gredice (95 mm x 95 mm). Na ta način smo dobli primerne parametre za toplo preoblikovanje omenjenega jekla. Testi so bili izvedeni v temperaturnem območju 850 °C to 1200 °C in hitrostih deformacije v območju 0,001 s^{-1} to 6 s^{-1}. Posebna pozornost je bila namenjena mehanizmom, ki so odgovorni za slabo plastičnost na zgornji in spodnji meji varnega toplega preoblikovanja. Toplo stiskanje je bilo študirano tudi s pomočjo Prasadovih procesnih map ter mapami nestabilnosti. Te nam razkrijejo nestabilna področja preoblikovanja pri nižjih teperaturah in nižjih hitrostih deformacije.

Keywords: 1.2690 tool steel; hot compression; flow curves; processing maps
Ključne besede: 1,2690 orodno jeklo; toplo stiskanje; krivulje tečenja; procesne mape

INTRODUCTION

High alloyed tool steels cause a lot of production problems due to their narrow hot working temperature range and low hot ductility and as such they usually belong to a low deformable steel. Due to the already mentioned problems, the economy of production and quality of products should be further improved also by means of a better knowledge of behavior (processes) of steel during its hot forming. There is little work published in scientific literature on hot workability of tool steel; thus, more contribution from this research area is desired [1-4]. Ledeburitic cold work tool steel CRV3 (1.2690) contains many alloying elements and ledeburitic carbides. It results in a high strength and hardness, small deformation during heat treatment, very good wear resistance, and also in poor ductility (plasticity) during its hot deformation. Its microstructure during hot deformation can be characterized as a two-phase system consisting of austenite matrix and a combination of ledeburitic carbides. The total volume fraction of carbides is in the range of about 9 - 19 %, depending on heat treatment condition [5]. The distribution, the quantity and size of carbides in ledeburitic tool steel have a large effect on its hot deformation behavior. Both the dissolution of alloying elements and the precipitation of carbides result in strengthening the tool steel during hot deformation. In order to prevent hot cracking and microstructural damage during the several deformation steps of a hot working process it is necessary to understand the interaction between the strain hardening and softening mechanisms governing the flow behavior of the matrix compound between the primary carbides.

The objective of this work is to investigate hot workability of 1.2690 tool steel, i.e. to find the optimum working conditions, to find out the upper and lower limits of parameters of hot working and to study the reasons of hot cracking. Prasad's processing map was used to reveal the instable zone of working conditions.

EXPERIMENTAL TECHNIQUES

The chemical composition of CRV 3 tool steel is given in Table 1. The cylindrical specimen dimensions ϕ 10 mm x 15 mm were machined from an annealed forged billet square 95 mm. Center lines of specimens were orthogonal to longitudinal direction of the billet. Because of some microstructural inhomogeneity across the section of a forged billet, all the compression specimens were taken from the same depth of a square billet. The initial microstructure of applied samples is given in Figure 1.

Physical simulation of hot forming process was carried out on Gleeble 1500D thermo-mechanical simulator. The following testing conditions were chosen: the temperature range 850 °C to 1200 °C, strain rates of 0.001 s^{-1} - 6 s^{-1} and true strains of 0 - 0.9 (Table 2). The tantalum follies thickness of 0.05 mm were inserted between cylindrical specimen and compression tool (anvil) to avoid inhomogeneous deformation. The nominal maximum strain for all tests was cca 0.9. After deformation, specimens were water quenched to freeze over their microstructure. The following parameters were measured during tests: compression force, temperature of cylindrical specimen, shift of active jaws (sample height). The

Table 1: Chemical composition of the 1.2690 steel in wt. %

	C	Si	Mn	Cr	V	W	Mo
1.2690	1.17	0.24	0.26	11.3	1.48	2.24	1.35

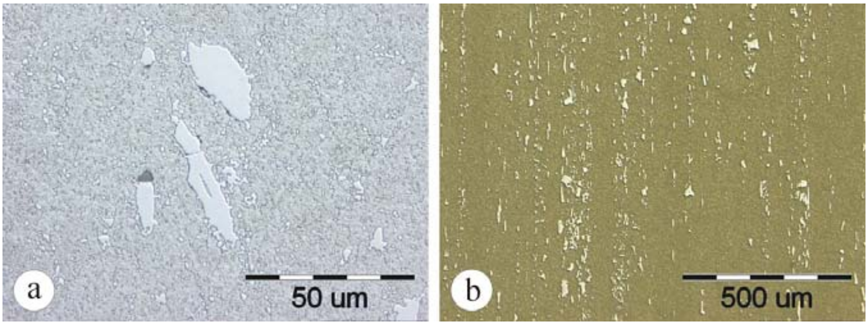

Figure 1: The initial microstructure of a forged billet square 95 mm: (a) quenched microstructure, (b) distribution of carbides

Table 2: Deformation conditions

Deformation temperature / ºC	Strain rate / s^{-1}
850, 900, 950, 1000, 1050, 1100, 1150, 1160, 1170, 1180, 1200	0.001, 0.01, 0.1, 1.0, 6.0

strain rate was programmed as a constant value. These data were the basis for calculating of the stresses and strains and for the evaluation of flow curves. The temperature of deformed samples was measured continuously with a thermocouple during the deformation, so that the deformation heating could be corrected.

Deformed samples were visually surveyed and then longitudinally cut for the preparation of matallographic samples.

Results

True stress-strain (σ–ε) curves

The typical stress-strain curves in the range of 850 °C to 1200 °C and strain rates of 0. 01 s^{-1} and 1 s^{-1} are shown in Figure 2. All flow curves at all strain rates exhibit a maximum, which is a result of dynamic softening - dynamic recovery and dynamic recrystallisation. The maximum is very clear at low temperatures, 850 - 900 °C. Lower testing temperature and lower strain rates result in more emphasized peaks and vice versa. It can be seen that the strain corresponding to the peak flow stress increases with the decrease in temperature and with the increment of strain rate. However, decreasing temperature and increasing strain rate will delay the onset of dynamic softening. The peak of flow stress is in the strain range of 0.05 - 0.3.

In order to present more clearly the relationship between deformation temperature, strain rate and maximal stress, the peak stresses are

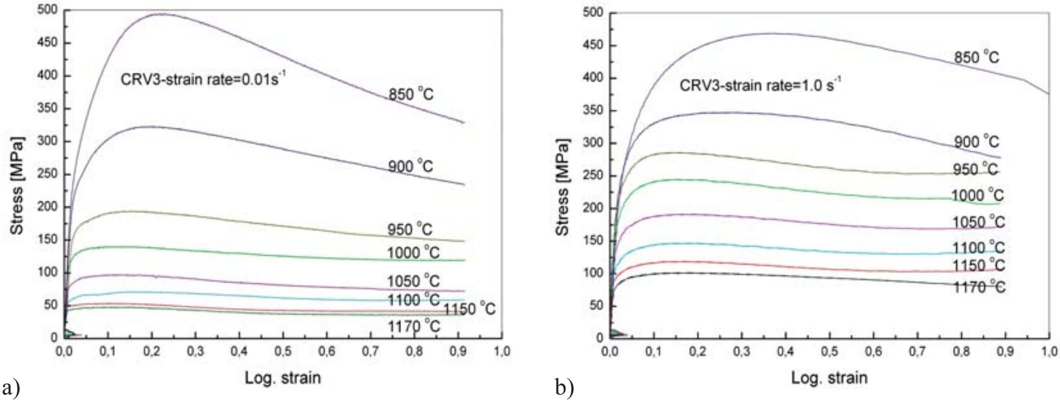

Figure 2: Stress-strain curves in the range of 850 °C to 1170 °C: (a) strain rate 0.01 s-1, (b) strain rate 1.0 s^{-1}

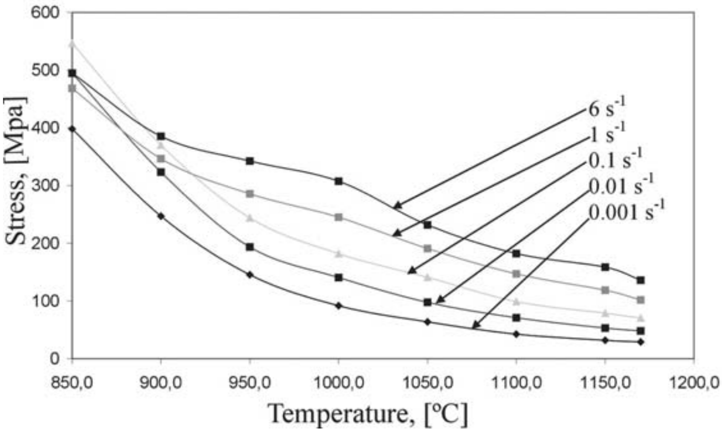

Figure 3: Dependence of the peak of flow stress on temperature for different strain rates (0.001 s^{-1} - 6 s^{-1})

plotted against the temperature for different strain rates in Figure 3. With decreasing of temperature in the temperature range 1170 - 1000 °C and with increasing of strain rate the peaks of flow stress also increase almost proportionally. This behaviour changes at temperature 1000 °C; namely the increase of peak of flow stress of strain rates 0.001 s^{-1} - 0.1 s^{-1} is much higher in comparison to strain rates 1 s^{-1} - 6 s^{-1}. Thus at 900 °C the peak value of strain rate of 0.1 s-1 exceeds the peak value of strain rate 1 s-1 and at 850 °C also the peak value of 6 s^{-1}.

Influence of test parameters on macro cracks

The sample deformed at 1200 °C and presented on Figure 4a is completely destroyed, while the sample deformed at 1180 °C shows a lot of macroscopic surface cracks occurring parallel to the direction of compression axis (Figure 4b). The samples deformed at temperatures 1160 °C, 1100 °C, 1050 °C, 1000 °C, 950 °C, 900 °C and 850 °C do not exhibit any cracks (Figure 4c), except a sample deformed at 850 °C and

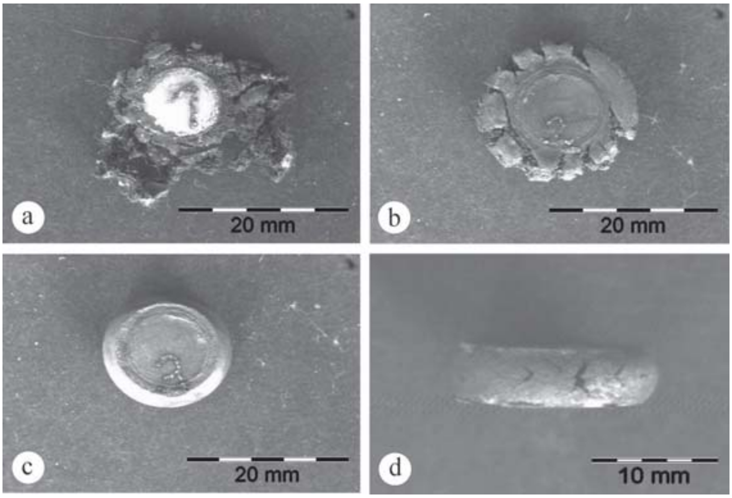

Figure 4: Macrograph of deformed samples (a) 1200 °C, strain rate 6 s^{-1}, (b) 1180 °C, strain rate 6 s^{-1} , (c) 1160 °C, strain rate 6 s^{-1}, (d) 850 °C, strain rate 0.01 s^{-1}

strain rate 0.01 s^{-1} (Figure 4d). This sample exhibits typical surface cracks occurring parallel to the direction of the main stress.

Influence of test parameters on microstructure

The microstructure of deformed and water quenched samples is austenitic with different contents of martensite and carbides. Figure 5 represents microstructures of some samples deformed at strain rates 6 s^{-1} and 0.01 s^{-1}. On deformation temperatures between 1160 °C and 1200 °C the ledeburitic carbides dissolve to a great extent (Figures 5a-b). During the deformation at temperature 1160 °C, a precipitation of a thin layer of carbides along grain boundaries occurs (Figures 5b-c), and at higher temperatures, a new eutectic appears (Figure 5a). Melting on grain boundaries causes the weakening of grain boundaries and cracking of steel. At lower deformation temperatures to about 1100 °C and at strain rate 6 s^{-1}, the microstructure is recrystallised, composed of equiaxial grains (Figure 5d). At deformation temperature 1050 °C, the crystal grains are also equiaxial, but they are arranged within the earlier deformed austenitic crystal grains (Figure 5e). The majority of carbides is arranged along the earlier deformed austenitic crystal grains. For deformation temperatures 1000 °C and lower, deformed initial austenitic crystal grains and carbide precipitation along them are typical (Figure 5f). The grain boundaries were not revealed by etching very well. At the strain rate 0.01 s^{-1}, recrystallisation is running completely at temperature 1150 °C only (Figure 5g), while at temperature 1050 °C deformed initial austenitic crystal grains with some equiaxial crystal grains within predominate (Figure 5h).

During the cooling from the austenitization temperature and under 1000 °C the precipitation of secondary carbides along austenite grain boundaries takes place. With decreasing temperature the mentioned precipitation process accelerates that causes an intensive weakening of primary grain boundaries. At temperature 1000 °C the

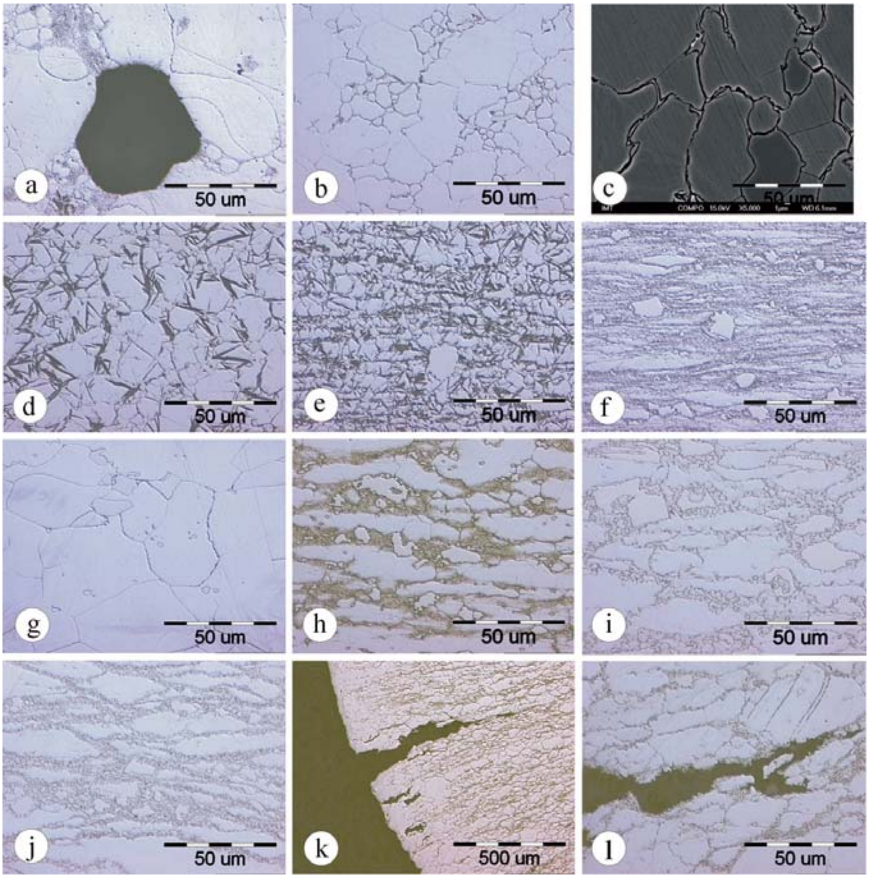

Figure 5: Microstructures of deformed samples: (a) 1200 °C, 6 s^{-1}, (b) 1160 °C, 6 s^{-1}, (c) 1160 °C, 6 s^{-1}, (d) 1100 °C, 6 s^{-1}, (e) 1050 °C, 6 s^{-1}, (f) 850 °C, 6 s^{-1}, (g) 1150 °C, 0.01 s^{-1}, (h) 1050 °C, 0.01 s^{-1}, (i) 950 °C, 0.01 s^{-1}, (j, k, l) 850 °C, 0.01 s^{-1}

precipitation of secondary carbides starts along the deformed initial austenitic crystal grains, which are getting clearer along with the deformation temperature lowering (Figure 5i); at temperature 850 °C, it causes an intensive weakening of crystal boundaries resulting in intercrystalline cracks (Figures 5j-l).

PROCESSING MAP

Processing map is developed on the basis of a dynamic material model (DMM) which has been developed and widely used by the group of Y. V. R. K. PRASAD[6, 7]. The processing map of material can be described as an explicit representation of its response to the imposed process parameters. It is a superimposition of the efficiency of power dissipation and an instability map.

Efficiency of power dissipation

The workpiece under hot deformation conditions of this model works as an essential energy dissipater. The constituent equation describes the manner in which energy (P) is converted at any instant into two forms, thermal energy (G) making temperature increase and microstructural change caused by transform of metallurgical dynamics (J), which are not recoverable. In general, most of the dissipation is due to a temperature rise and only a small amount of energy dissipates through microstructural changes. The power partitioning between G and J is controlled by the constitutive flow behavior of the material and is decided by the strain rate sensitivity (*m*) of flow stress as shown in the Equation

$$\frac{dJ}{dG}=\frac{\dot{\bar{\varepsilon}}\, d\bar{\sigma}}{\bar{\sigma}\, d\dot{\bar{\varepsilon}}}=\frac{\dot{\bar{\varepsilon}}\,\bar{\sigma}\, d\ln\bar{\sigma}}{\bar{\sigma}\,\dot{\bar{\varepsilon}}\, d\ln\dot{\bar{\varepsilon}}}\approx\frac{\Delta\log\bar{\sigma}}{\Delta\log\dot{\bar{\varepsilon}}}=m \qquad (1)$$

For an ideal dissipator it can be shown that both quantities J and G are equal in their amount, which means that $m = 1$ and $J = J_{max}$ whereas the efficiency of power dissipation η is given by:

$$\eta=\frac{J}{J_{\max}}=\frac{2m}{m+1} \qquad (2)$$

The variation of η with temperature and $\dot{\varepsilon}$ represents the relative value of energy dissipation occurring through microstructural changes. Microstructural changes can be stable, which includes a dynamic recovery and dynamic recrystallization, and instable which includes wedge cracking, void formation at hard particles, dynamic strain ageing and macrostructural cracking. As new surfaces will form during instable changes, more energy is required, while stable changes always take place by grain boundary migration.

Flow instability

The instability map is defined by a stability criterion for a dynamic material, where the differential quotient of its dissipative function has to satisfy an inequality condition, given by Equation 10, to allow a stable flow.

$$\xi\left(\dot{\bar{\varepsilon}}\right)=\frac{\partial\ln(m/(m+1))}{\partial\ln\dot{\bar{\varepsilon}}}+m>0 \qquad (3)$$

Figures 6a-b represents processing and instability contour map for temperature range from 850 °C to 1160 °C and strain rates 0.001 s^{-1} to 6 s^{-1} at strains 0.2 and 0.6. The maps are relatively similar at various strains, but at all strains the instable zone with $\xi < 0$ appears in the temperature range between 850 °C and 970 °C at strain rates about 0.1 s^{-1} - 0.01 s^{-1}. This also proves the Figure 4d and Figures 5k-l (brittle cracking on grain boundary due to precipitation of secondary phases). At lower strains the instable zone moves towards lower strain rates and temperatures and at higher strains towards higher strain rates and higher temperatures.

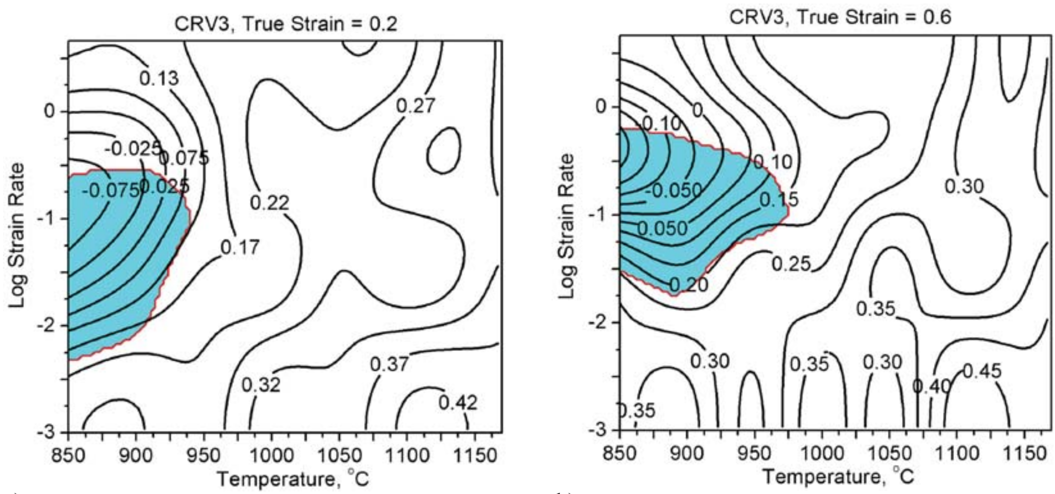

a) b)

Figure 6: Superimposition of power dissipation map and instability map for temperature range from 850 °C to 1160 °C, strain rates 0.001 s^{-1} to 6.0 s^{-1} and at strains 0.2 (a) and 0.6 (b).

DISCUSSION

The optimal deformation conditions for steel 1.2690 are at temperatures between 1000 °C and 1150 °C at strain rates 1.0 - 6.0 s^{-1}. Deformation at higher temperatures may cause incipient melting at grain boundaries and a dramatical drop of hot ductility. The result of deformation at temperatures between 1160 and 1100 °C is a recrystallized microstructure. At lower deformation temperatures, recrystallization is not completed.

During the cooling from the austenitization temperature and under 1000 °C the precipitation of secondary carbides along austenite grain boundaries takes place. Especially this process took place at lower strain rates that resulted in higher peaks stress of flow curves.

Lower strain rates and lower deformation temperatures result in an accelerated precipitation of secondary carbides on grain boundaries and consequently, in increased flow curves. Thus at lower temperature and strain rates higher flow stresses than those at higher strain rates were obtained.

The precipitation of secondary carbides causes also a weakness of grain boundaries and cracking along them. Processing maps ware made for temperature range from 850 °C to 1160 °C and for strain rates between 0.001 s^{-1} and 6.0 s^{-1}. The high temperature region with appearance of incipient melting at grain boundaries was not included in a processing and instability maps. Processing maps at strains 0.2, 0.4 and 0.6 show the some result as the investigation of microstructures of deformed samples. The instable zone appears at strain rates 0.1 s^{-1} - 0.01 s^{-1} and deformation temperatures between 850 and 970 °C, where an intensive precipitation of secondary carbides at grain boundaries occurs.

Conclusion

The optimum deformation conditions for steel 1.2690 are at temperatures between 1000 °C and 1150 °C at strain rates 1.0 - 6.0 s^{-1}. Deformation at higher temperatures may cause incipient melting at grain boundaries and a dramatical drop of hot ductility. During deformation at temperatures below 1000 °C and lower strain rate an intensive precipitation of secondary carbides at grain boundaries occurs and causes a strong work hardening and weakness of grain boundaries. The formerly mentioned secondary precipitation also results in a higher flow stress at lower strain rates in comparison to flow stress at higher strain rates. The experimental results also confirm the predictions of processing maps about the position of the instable zone.

References

[1] C. A. C. Imbert, G. J. McQueen, Hot Ductility of tool Steels, Canadian Metallurgical Quarterly, 40/2 (2001) 235 – 244.

[2] Gao Shan, Liu Xianghua, Wang Guodong, Study on Hot Deformation Cracks of Steel D2 Using Processing Map, J. Iron & Steel Res., Int., 4/2 (1997) 44 - 49.

[3] C. Rodenburg, M. Krzyzanowski, J. H. Beynon, W. M. Rainforth, Hot workability of spray-formed AISI M3:2 high-speed steel, Materials Science and Engineering A, 386 (2004) 420 - 427.

[4] C. Imbert, N. D. Ryan, H. J. McQueen, Hot Workability of Three Grades of Tool Steel, Metallurgical Transactions A, 15A (1984) 1855 - 1864.

[5] Catalogue of Steel Properties of Metal Ravne Company.

[6] Y. V. R. K. Prasad, S. Sasidhara, Hot Working Guide, Compendium of Processing Maps, ASM - International, pp. 1 - 24, OH, USA, 1997.

[7] S. V. S. Narayana Murty, B. Nageswara Rao, B. P. Kashyap, Instability criteria for hot deformation of materials, International Materials Reviews, 45/1(2000) 15 - 26.

Long-term deformation processes in the wider area of the closed Idrija Mercury Mine

Dolgotrajni deformacijski proces v širšem območju Rudnika živega srebra Idrija

Jakob Likar[1], Marko Cigale [2], Bojan Režun [2]

[1]University of Ljubljana, Faculty of Natural Sciences and Engineering, Aškerčeva 12, 1000 Ljubljana, Slovenia; E-mail: jakob.likar@ntf.uni-lj.si
[2]Idrija Mercury Mine, Arkova 43, 5280 Idrija, Slovenia; E-mail: bojan.rzs.idrija@s5.net

Received: April 10, 2006 **Accepted**: July 20, 2006

Abstract: The past five centuries of the Idrija Mercury Mine's operation have had consequences on the environment, which have directly influenced the deformations developing in the wider exploration area. In order to guarantee safe and technically progressive ore mining, permanent pumping of mine water and the constant modernization of technology and other working fields, including ore processing and heating, increased ore production, the spread of mine works into greater depths, and difficult rock conditions have in the past demanded the effective cooperation of different branches of technical and natural sciences. During the many years of mercury ore excavation, the cross-stope mining method with backfilling from down to up in low-bearing rocks was used. Mine shutdown works, which include grouting and hardening destroyed areas, as well as filling parts of the mine and backfilling empty spaces (i.e. mine roadways), are now in the final stage. The efficiency of mine shutdown works is constantly being verified by means of geotechnical and other measurements and observations, while considering the local rock conditions. The paper presents some results of the measurements and observations performed, as well as the changes in the wider area of the Idrija Mercury Mine during shutdown works and an estimation of surface deformation changes in future.

Povzetek: Dolga doba obratovanja Rudnika živega srebra v Idriji (SLO) v preteklih petih stoletjih je za sabo pustila posledice, ki se kažejo na okolju in posredno še vedno vplivajo na deformacijska dogajanja na širšem raziskovalnem območju.Postopno večanje proizvodnje rude, širjenje rudarskih del v večje globine in zahtevne hribinske razmere odkopavanja, so v preteklosti zahtevali učinkovito sodelovanje različnih strok. Dolgotrajno odkopavanje živosrebrne rude, ki je potekalo z uporabo t.i. prečne odkopne metode za zasipavanjem odkopnih prostorov od spodaj navzgor v relativno zahtevnih hribinskih pogojih.. Zapiralna dela, ki vključujejo tudi injektiranje in utrjevanje porušenih območij ter starih zasipov, kakor tudi zasipavanje praznih prostorov, so v zaključni fazi. Uspešnost teh del se stalno preverja z geotehničnimi meritvami in drugimi opazovanji, ob upoštevanju lokalnih hribinskih pogojev. Nekateri rezultati teh opazovanj in meritev so podani v prispevku v okviru interpretacij dogajanj na območju Rudnika živega srebra med zapiralnimi deli z oceno možnih deformacijskih sprememb v prihodnosti.

Key words: Mercury mine, rock structure, sublevel mining method, reinforced backfill, stress measurement in rocks, surface displacement, analyses of the time dependant processes; old fill grouting

Ključne besede: Rudnik živega srebra, struktura kamnin, podetžna odkopna metoda, meritve napetosti v kamninah, pomiki površine, analize časovno odvisnih procesov; utrjevanje starih zasipov

Scientific paper

INTRODUCTON

Sinking terrain and other deformations are an integral part of the occurrences in the wider area of the closed Idrija Mercury Mine. The mine closure works are progressing in accordance with the approved program, which includes various observations and measurements in the mine and on the surface above the mine. To ensure the stabilization of broader rock areas over the long term, the filling and injection of areas with the highest deformation intensity is of great significance.

The time-dependant deformation processes currently in progress in the wider area of the Idrija Mercury Mine were monitored by surveying and other measurements and geological-geotechnical observations. The measurements were conducted in the prescribed time intervals twice a year in order to ensure the time-dependant monitoring of deformation processes. The results of measurements and observations give a realistic insight into the actual occurrences, which also enables verification of the effects of reinforcement works and other activities in the mine and on the surface. Although mining works were stopped more than ten years ago, the sinking and subsidence of time-dependant areas in the pit and on the surface have not yet stabilized completely. Long-term time-dependant processes, which are closely linked to the methods and extent of ore mining in the past, and in particular to the natural geological conditions, primary stress states and other influences, are still present particularly in areas built of Permian-Carboniferous layers and other low-bearing-capacity rocks. The sublevel mining method with reinforced backfilling from the top downwards[1], introduced in the last years of the mine's operation, had a significant impact on the reduced intensity of deformation processes in the mine, and consequently on the surface above the mining fields.

The final stabilization of the area therefore depends on a gradually stabilized deformation field, which will indirectly have a favorable impact on eventual construction projects in the area concerned.

Figure 1. Layout of the town Idrija with Mercury Mine
Slika 1. Lokacija mesta Idrija z Rudnikom živega srebra

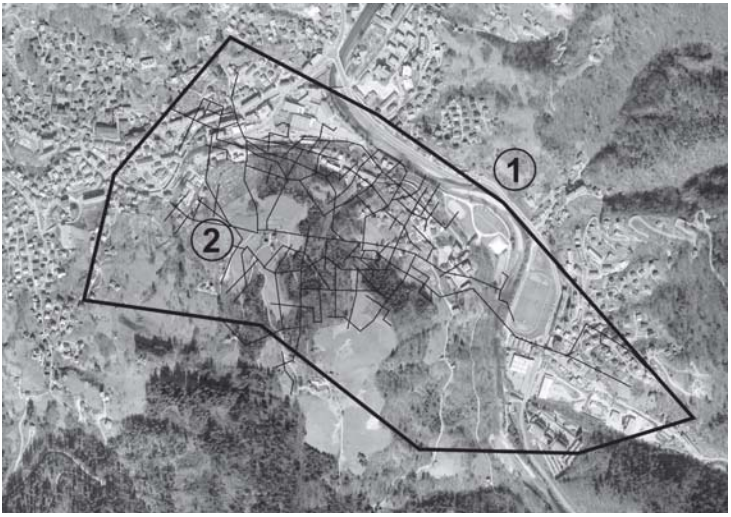

Figure 2. Layout of the Idrija Mercury Mine
Slika 2. Območje Rudnika živega srebra Idrija

Geological and hydrogeological interpretation of the wider mercury mine area

The Idrija mercury ore deposit is located directly below the town of Idrija between the Idrijca River and its tributary, the Nikova stream. The ore deposit extends in the directions north-west and south-east. It is 1500 m long and 300-600 m wide. The depth of the ore-bearing zone is about 450 m. The deposit is open and has vertical shafts. The deepest shaft reached a depth of 420 m and linked all 15 levels, the lowest of which extended 36 m below sea level. The distance between levels varies from 15 to 30 m. Over a period of five hundred years, miners have dug out more than 700 kilometers of road-ways and shafts. Today, only about 20 km of roadways are still open.

Geology

The hydrothermal mercury deposit in Idrija is a geological natural treasure of global significance, and is ranked among the most complex ore deposits in the world.

The Idrija ore deposit is classified as a monometal as well as a monomineral deposit. It has the second largest concentration of mercury in the world, second only to Almaden in Spain. Most of the mercury appears in the form of cinnabar (HgS, ~70%), and the remainder in the form of native mercury (Hg, ~30%). Pyrite, marcasite, dolomite, calcite, kaolinite, epsomite and idrialin (named after Idrija) represent the main gangue or waste rocks.

The Idrija ore deposit was formed during two phases: in the lower part of Middle Triassic (Anisian), and in the second, Ladinian phase during a period of intense volcanic activity in Slovenian geological history. Middle Triassic tectonics led to the upwelling of hydrothermal solutions, which expelled their deposits onto the sea bed through a thick layer of Upper Palaeozoic, Permian, Scythian and

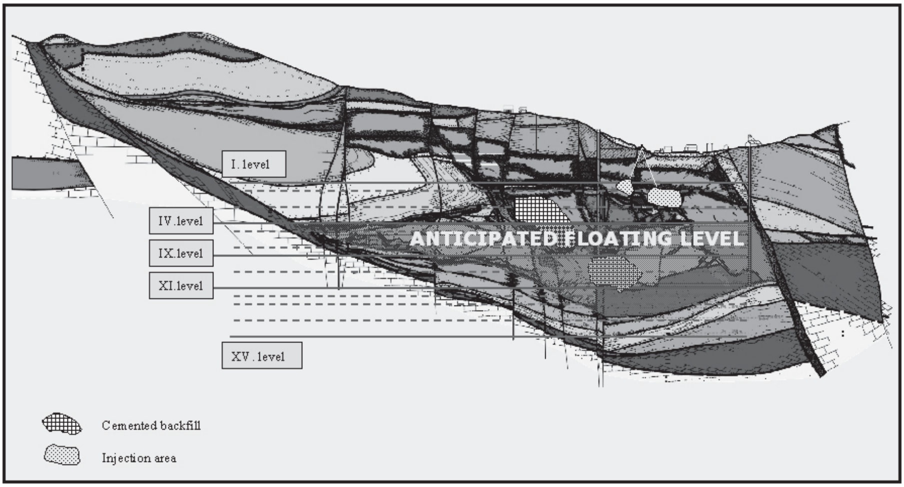

Figure 3. Geological cross section through the Idrija Mercury Mine
Slika 3. Geološki prerez Rudnika živega srebra Idrija

Anisian clastic and carbonate rocks. Due to gradually declining temperatures, part of the mercury condensed and was released as pure mercury in the form of drops. Hydrothermal underwater springs deposited the mercury in littoral swamps forming the synsedimentary ore beds and lenses in the black Skonca shales and tuffs of the Ladinian age.

The geological structure of the Idrija ore deposit is fairly complicated as the result of tectonic activity. The ore deposit was cut into blocks by napping and thrusting. In the final phase of alpine orogenesis, ore bodies were disintegrated and moved along the faults. The Idrija ore deposit has 158 known orebodies, 17 with native mercury are in carboniferous shale, while the remaining 141 are in clastic and carbonate rocks. These ore bodies have extremely different forms and sizes, and are irregularly distributed throughout the entire ore deposit.

Hydrogeology of the ore deposit

The ore deposit and its surroundings are comprised of several hydrogeological blocks and impermeable hydrogeological barriers. The hydrogeological block of the Idrija ore deposit is highly specific. It is also characterized by the presence of backfills (40 % porosity) and unfilled shafts on lower levels of the ore deposit.

The impermeable barriers enclosing the old part of the Idrija ore deposit are built of Carboniferous shale below the deposit, thrust sheets along the southern edge, and a Carboniferous layer above the deposit. On the north side, the deposit is closed in by an impermeable, clayey zone of the Idrija fault. In all aquifers, the level of ground water is above the level of mine infrastructure. The pit waters do not supply water to any of the aquifers in the vicinity, but precisely the opposite – the waters of neighboring aquifers flow into the pit. The main inflows of water into the ore deposit occur through shafts, galleries, drilled hydrological barriers or barriers partly demolished due to excavation works.

The flooding of the ore deposit up to the IVth level (+192 m) will keep pit waters within the limits of the abandoned ore deposit, and the only possible source of pollution with pumped pit water will be at the discharge into the above-ground water course – the Idrijca River (+331 m). At present, the pit is flooded up to the IXth level (+115 m)

Due to the geological structure of the Idrija ore deposit, water inflows into the pit facilities are relatively small (avarage 25 l/s). Approximately half of the water comes from the carbonate cover above the ore deposit, while the remainder comes from indirect sources in the periphery of the pit structure.

Mercury ore mining methods used during the mine's operation

The mercury ore mining technologies employed in the five centuries of the mine's history were adapted to the state of development of mining science and the existing natural mining conditions. On the basis of historical sources, we have assessed that the most frequently used was the mining method with backfilling from down to up, where ore was released through jack pits to lower levels and then exported to the surface for further processing. It should be emphasized that throughout the mine's operation, wood was the principal material used to make supports in mining areas, as well as at the main and auxiliary gates on various levels. These gates were developed between levels in the areas of individual ore bodies.

Particularities of the cross-stope mining method

Ore mining using the cross-stope mining method required a good knowledge of the behavior of strata in relatively tectonic and mechanically damaged rocks embodied in the hanging wall, mineralized and footwall layers of the ore deposit. It should be noted that the inflows of underground water were relatively low in view of the size of open ore bodies, which on the one side had a favorable effect on the development of mining works. Strata water frequently appeared in the lower levels of the mine and, in exceptional cases, on higher levels, e.g. the IVth level of the mine.

Ore extraction using the above-mentioned method was conducted in several phases, depending on the geometric and geotechnical characteristics of the ore body and surrounding layers. In order to develop an individual level, it was initially necessary to carry out preparations of the main gate on the main level and install a separate ventilation system so that mining works could be started at individual excavation areas. These were made from a preparatory gate at a 45^0 or 90^0 angle with respect to the main axis. The dimensions of the cross-sections in the preparatory gate and in individual excavation areas were within the limits of 2.0 m to 4.0 m in width, 1.8 m to 3.0 m in height, and a variety of lengths ranging from a few meters to about 50 m to 80 m in some cases. The horizontal and

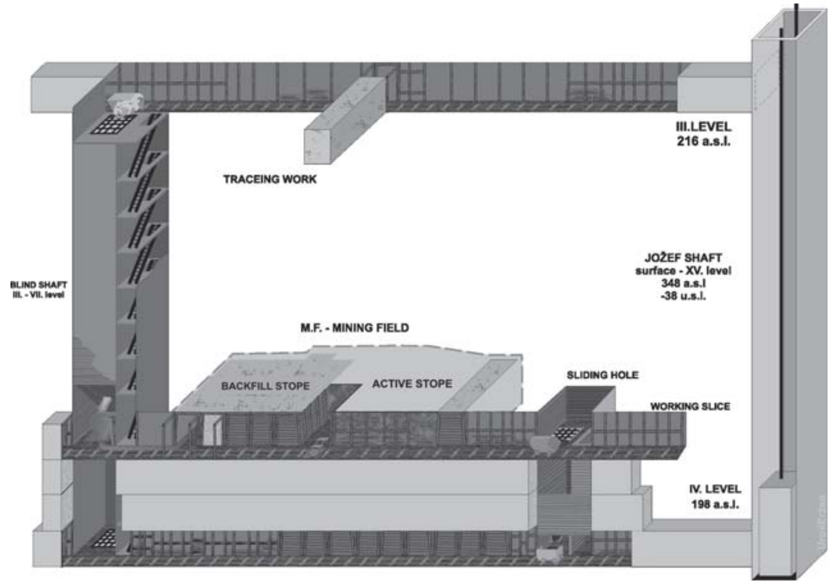

Figure 4. Cross stopping with backfill
Slika 4. Odkopavanje rude s prečno odkopno metodo z zasipom

slightly inclined mine areas were lined with wood supporting. Wood support was also installed in back mines, jack pits and chutes connecting individual levels and intermediate levels where ore was mined.

Ore was transported on various levels and roadways used small and medium-sized mine carts (volume from 0.3 to 0.8 m^3) on wooden and steel rails. After the mine's modernization in the 20th century, mine locomotives were used to transport extracted ore and reproductive materials to various levels, while on working levels the ore was mostly transported manually to blinded shaft or chutes.

Geotechnical evaluation of mining method from down to up

Changes in primary stress-strain states as the consequence of ore extraction works occurred in surrounding rocks and ore bodies, and gradually increased with the increasing volume of extracted ore and gangue in areas where the existing natural conditions called for the excavation of individual masses of no mineralized rock. Although excavation areas were backfilled regularly, the filling material was quite compressible and deformable, resulting in minor stress-strain concentrations in backfilled spaces and indirectly in increased deformations, which were transferred to the wood supporting and particularly to the surrounding rocks.

The preparation and mining of higher lying levels, as shown in Figure 4, was conducted successively after the lower level was backfilled and works were begun on a higher level. The height of each level was approx. 2.5 m to 3.0 m, allowing miners to manually perform such works as drilling, blasting, loading and transporting of extracted ore, as well as installing wood supporting and, finally, backfilling excavated mining areas. The relatively complex geological-geotechnical conditions, part of which is presented in the geological description of the ore deposit, additionally contributed to the worsening mining conditions in higher-lying levels. In practice, this was evident in the increasingly more damaged rock masses and additional stresses on the wood supporting which, considering its subsidence and collapsibility, survived the increased pressure of the rock mass relatively well. In some cases, e.g. when ore was extracted from Carboniferous shale, the additional stresses in the rocks on the first level were so intense that mining from down to up was practically impossible.

In addition to the above-mentioned, the time-dependant phenomena were so intensive that reprofiling had to be performed already during ore extraction on the first level. The above-described occurrences of gradually sliding rocks and backfills have not stabilized to this day.

Mining method with consolidated back filling from the top downwards

The complex geological and geotechnical conditions accompanying mining works in Carboniferous ore bodies, as well as increased environmental requirements and special concern for the health and safety of miners at work, called for radical changes in the ore extraction method. In the 1970's and

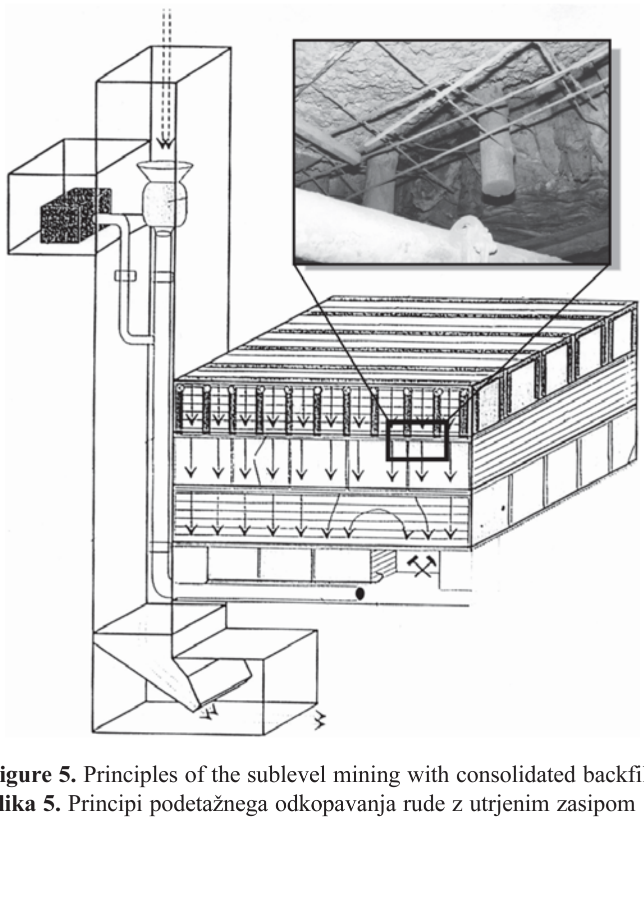

Figure 5. Principles of the sublevel mining with consolidated backfilling
Slika 5. Principi podetažnega odkopavanja rude z utrjenim zasipom

1980's, Prof. U. BAJŽELJ[1] introduced a new mining method from the top downwards, which involved highly different mining and backfilling technologies than had previously been used.

Particularities of mining from the top downwards

The new system of mining from the top downwards represented a significant turning point in the history of the mercury mine, as it completely changed individual technological procedures, particularly those designed to protect miners against caving and collapses of the ceiling and partly also the side walls. The use of reinforced backfill with a minimum required strength and minimum subsidence contributed to the substantial improvement of mining conditions. Figure 5 shows the mining method from the top downwards using reinforced backfill with a compressive strength of 6.5 MPa, which was still sufficient to ensure the prescribed stability conditions during mining works in lower levels. The final requirement for normal mine operation, backfill with compressive strength 4 MPa was sufficient.

Since the established mining method had not changed significantly for more than a century, the introductory procedures were carefully planned and gradually implemented in the so-called trial mining area in Carboniferous shale on the IVth level (Figure 5) at a depth of 150 m.

An analysis of the results of trial mining works showed encouraging results and the possibility of introducing the proposed sublevel mining method with reinforced backfilling also in the excavation of other ore bodies.

Geotechnical evaluation of mining from the top downwards

From the geotechnical aspect, the transfer of secondary stress deformation states to surrounding rock strata and consolidated backfilling also represents a considerable reduction of shifts occurring with this mining method. The small deformability of backfilling material and the minimal compressive strength compensate for the additional stresses in the backfill itself. It should be emphasized that the strength characteristics of surrounding rocks – particularly Carboniferous shale – are lower than those of the consolidated backfill, which means that technical conditions of mining works improve with the increasing size of mining areas, and indirectly with the changed material of higher strength. This was also proven by calculations used the Finite Element Method, taking into account the nonlinear relations between stresses and strains by means of simulations of mining works and successive injections of reinforced backfill into each mining area separately[2].

The calculated deformations amounted to maximally 10 cm, which is substantially lower than the deformations that would have developed in the old mining method from down to up, i.e. the so-called cross-stope method.

In addition to the above-mentioned, mining from the top downwards also has positive effects on the reduction of losses during the mining of mercury ore and native mercury present in Carboniferous shale.

Determination of shutdown works and their execution

Several reasons influenced the abandonment of mercury ore excavation, initially in the 1970's and finally in the late 1980's. On the one side, an intensive international campaign had been launched against mercury, whose harmful effects were researched in various fields. Another reason was the very low selling price of this metal, which in some cases fell below USD 100 per flask (34.5 kg of mercury). Several years passed before the state administration adopted a decision on the gradual shutdown of the mine and the long-term abandonment of mercury production. In addition to the above-mentioned factors, particular emphasis was laid on the long-term effects of the mine on the sinking surface, i.e. the town of Idrija, which stands directly above the mining facilities, the potential instability of the natural and artificial slopes above the mine, and the pollution of the environment with mercury in the town of Idrija itself and far downstream along the Idrijca River and the Soča River, including the Gulf of Trieste.

The principal tasks were to select and justify the technology required for shutdown works, with the clear goal of attaining the long-term stability of the vibrant surface area above the mine, reducing to the greatest possible extent any possible damage to buildings caused by mining activities, regulating the hydrological and hydrogeological environments, establishing supervision over harmful concentrations of mercury in various forms or aggregate states, and constantly controlling the effects of mercury on miners and other inhabitants of the town of Idrija and the broader affected region.

Estimation of geological and geotechnical conditions prior to determining the mine shutdown procedure

Surveying and geometric observations of surface shifts in the broader affected area of the mine from the beginning of the 20th century onwards, as well as the excellent geological and hydrogeological studies and interpretations of the origin of the ore deposit and subsequent tectonic and other occurrences, have enabled engineers to evaluate various parameters serving as a basis for the formation of a strategy of gradual shutdown of the mine and mining facilities, including the rehabilitation of ore residue deposits. On the basis of a well argument analysis of planned shutdown works, the legislative body of the government passed a law ensuring the allocation of funds for the execution of planned works, accompanied by regular controls and measurements of the effects of such works on set goals. For this purpose, extensive simulations and analyses of the impact of reinforcement processes on the rock structure and old mining works using the finite element method were performed. A specific question was raised in connection with the estimated consequences of possible flooding of the pit up to different height levels, as the considerable worsening of geotechnical conditions was expected in areas where pit water came into contact with rocks and old backfills, which are sensitive to water. In situ investigations in the mine confirmed the fear that increased shifts would develop in the event of uncontrolled flooding of the mine. For this reason, a plan foreseeing the gradual reinforcement and backfilling of empty spaces as well as flooding of the mine in several phases was adopted. These procedures would be accompanied by regular controls of deformation changes in the mine and on the surface in the broader affected area of the mine. The proposed measures were approved by the state authorities, which passed a relevant law and allocated funds for financing shutdown works and research activities.

Methods of execution of shutdown works

The gradual shutdown of the mine and the rehabilitation of the area of the mine's operation on the surface is progressing according to project solutions and the adopted shutdown strategy, and in line with the long-term rehabilitation of degraded areas. Special attention has been devoted in past years to the improvement of reinforcement and backfilling technologies, as most of the vertical and horizontal mine areas below the IVth level have been filled with reinforced backfill. For the purpose of injection and backfilling of pit areas, a special injection device was erected on the surface above the mine. The device is used to pump backfilling materials into lower lying mine areas through an open shaft and drill holes.

The pumping capacity is around 10,000 m^3 per year, which in view of the selected technology is the optimal capacity. Problems have arisen due to our unfamiliarity with the exact position and size of abandoned underground areas, which has rendered the planning of quantities and volume of required backfilling materials difficult.

The shutdown works in those sections of the pit where backfilling was not necessary due to the solid rock structure generally comprised the removal of steel, wooden and other parts in order to reduce their potential effects on mine water.

In my estimate, the shutdown works will be completed by the year 2010.

MEASUREMENTS OF GEOTECHNICAL AND HYDROGEOLOGICAL PARAMETERS

Geodetic measurements on the surface

Geodetic measurements were begun in the initial years of the 20th century, while extensive geometric observations aimed at monitoring the stabilization of the mine were not performed until 1990. Measurement was carried out in profiles net installed on the disturbed surface above the mine. Measurements were also performed on important infrastructural buildings and facilities too. Before the commencement of shutdown works, the horizontal and vertical movements of terrain above the mine were up to 25 mm/year and up to 14 mm/year, respectively.

Displacement measurements in the mine

The wide mine surveying mesh included measuring points placed on different mine levels connected to main points near the main shafts "Delo" and "Borba". Each measuring point is stabilized on the bottom or in the roof of mine roadways to allow for the measurement of vertical movements and, in some cases, horizontal movements as well. Each measuring cycle was performed twice per year if any extreme displacements occurred as the result of closure works or during flooding of the deeper part of the mine.

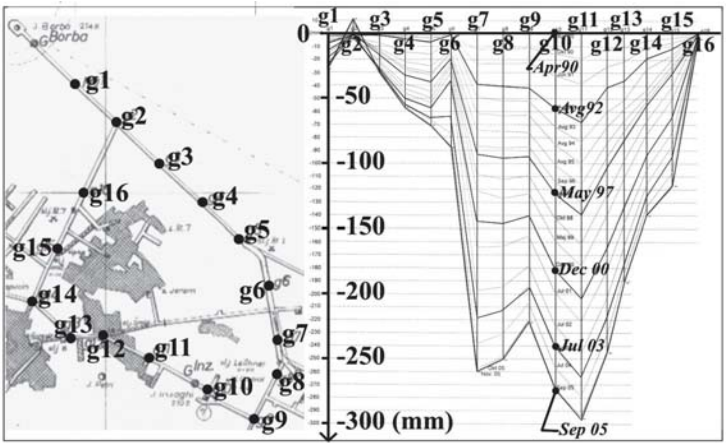

Figure 6. Measured settlements at the III[th] level
Slika 6. Izmerjeni posedki na III. obzorju

A trend of vertical displacement similar to that on the surface was also found in the mine. The measurements executed on levels I to XI showed a displacement syncline near the Inzaghi shaft, where a maximum subsidence was found. The measured movements gradually decreased and, in the past year, horizontal movements declined to an average 8 mm and vertical displacements to 4 mm. The typical result of vertical movements is shown in Figure 6.

Measurements of horizontal displacement in vertical inclinometers

Measurements of inclinometric boreholes have been conducted since 1989. The boreholes are located in areas with the most intensive shifts. In the period from 1989 to 1996, 17 inclionometric boreholes were activated. In that year the horizontal shifts, measured twice a year, attained values of up to 21 mm/year and vertical shifts of up to

Figure 7. Results of the inclinometer measurement G9
Slika 7. Rezultati inklinometrskih meritev merskega mesta G9

10 mm/year. However, measurements of inclinometric borehole deformations conducted in the period from 1996 to 2001 have shown that the shifting of terrain above the pit is continuing, but with a decreasing tendency, which is undoubtedly the consequence of the abandonment of excavation works and the conduction of consolidation-fortifying works in the pit. In the last four years (2001 – 2005), we measured some local increasing deformations in an area with geotechnical unstable rocks (Carboniferous shale), but these are still in the process of stabilizing and do not present any major hazard.

The results of several years of measurements and observations have shown that not only are different slides forming above the pit, but a large sinking crater is also forming with its centre around the Inzaghi shaft, where most of the excavation works took place.

Measurements of stress changes using measurement cells

In addition to other measurements and observations, probes were initially incorporated at various locations to monitor stress deformation changes in rocks and backfills during shutdown works and partial flooding of the mine. The measurements described below have served to illuminate the deformation processes in progress. Our principal intention, however, was to determine the impacts of flooding of part of the pit on the rock structure of the mine.

Measurements of secondary stress deformation changes at the XIVth and XVth levels

For the purpose of monitoring stress deformation changes in rocks and backfills in the deepest parts of the pit during flooding up to the XIth level, measurement probes, i.e. cells equipped with "strain gauges" in different directions, were incorporated into boreholes and injected with cement grouting material.

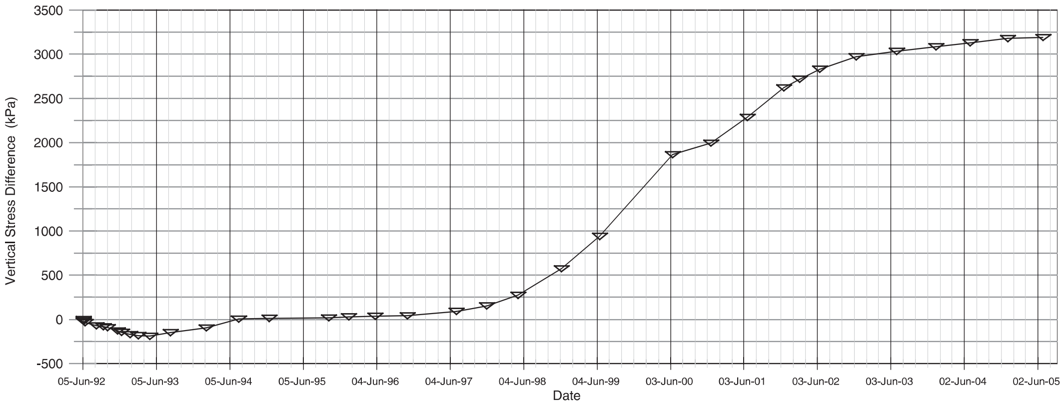

Figure 8. Results of the additional vertical stress measurement in the shale on the XVth level
Slika 8. Rezultati meritev dodatnih vertikalnih napetosti v skrilavcu na XV. obzorju

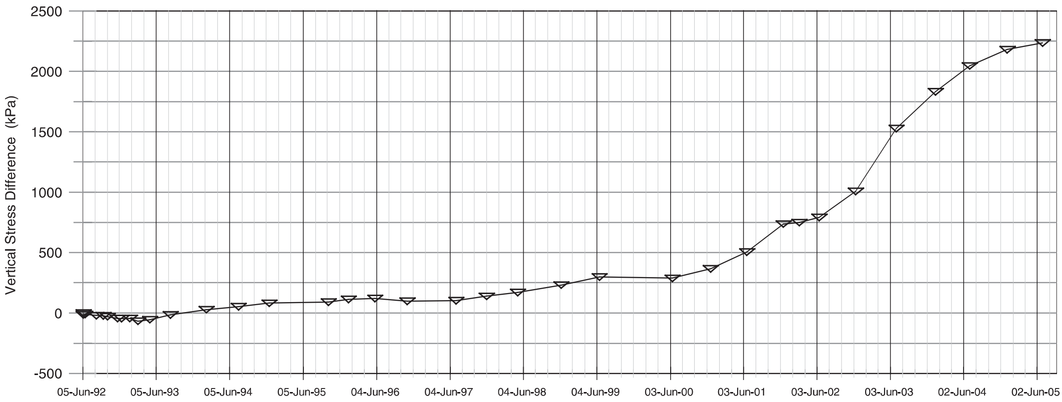

Figure 9. Results of the additional vertical stress measurement in the dolomite on the XIVth level
Slika 9. Rezultati meritev dodatnih vertikalnih napetosti v dolomitu na XIV. obzorju

Since the incorporation of measurement probes at the XIVth and XVth levels in the middle of 1992, i.e. in the past 13 years, measurements of specific deformations in backfill (XIVth level, elevation – 6.45), dolomite (XIVth level, elevation. – 6.45) and shale (XVth level, elevation – 32) have been performed twice yearly.

It is evident from the results of measurements shown in Figure 8 in the form of diagram that the course of time-dependant deformations changed in 1995 and partly in 1996, when shifts or changes in stresses and deformations in the rock structure occurred as the consequence of mine flooding up to the XIth level. Rapid changes in deformations stopped occurring later on. The results of measurements in the past year indicate that the deformation processes are still in progress, but the trends do not point to any major stress changes in surrounding rocks. All measuring points still indicate changes in increasing vertical stresses. This is more pronounced in dolomite and, to a smaller extent, in shale, which may be explained by the greater rigidity of dolomite.

It is highly probably that the changes found are linked to the sinking of areas above mine extraction works and the effects of time-dependant occurrences around the Idrija fault. In the past four years, stress changes (shifts) have been more intensive in dolomite on the XIVth level, while those in shale on the XVth level are rapidly decreasing.

Measurements of secondary stress states on the IVth, VIth and VIIth levels

Triaxial cells for the measurement of stress changes were installed on the IVth level in the beginning of 1996, on the VIIth level in December 1996, and on the VIth level in July 2004. In the most recent period, measurements have been performed twice a year in order to determine whether there are any stress changes in consolidated backfills in the broader area, where extensive mining works were performed in the past.

The results of measurements shown in Figure 10 indicate that the time-dependant changes occurring in the past year are considerably more extensive than in approximately the same time intervals in previous years. The substantially increased stress in cells on the IVth and VIIth levels is explained by the fact that the rigidity of old reinforced backfills in the broader areas is incomparably higher than in other backfills, which were not additionally injected or grouted.

a)

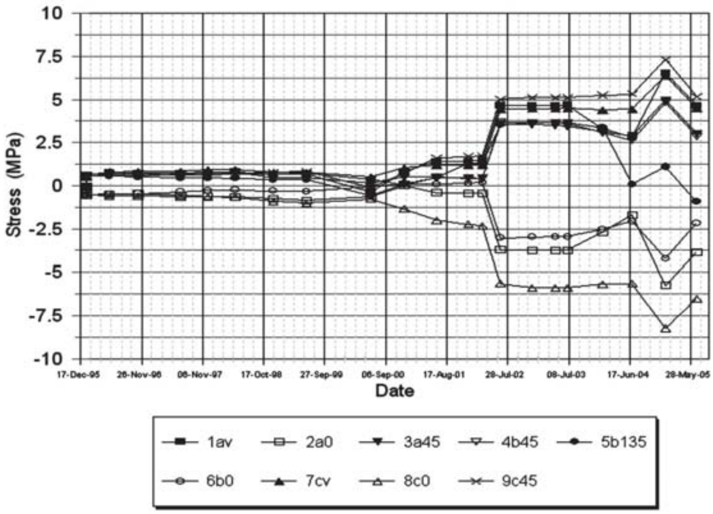

b)

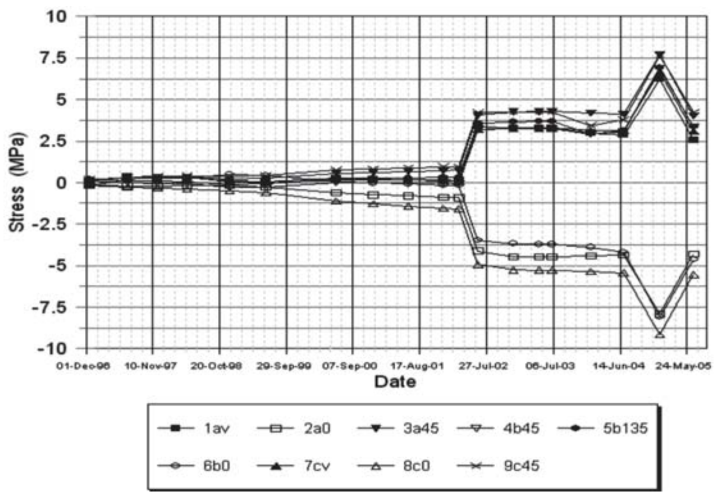

Figure 10. Stress changes versus time in the consolidated backfill on the **a)** IVth level **b)** VIIth level measured by triaxial cell
Slika 10. Časovno odvisne spremembe napetostnih stanj v utrjenem zasipu izmerjene s triosnimi celicami **a)** na IV. obzorju, **b)** na VII. obzorju

Evaluation of adequacy of executed consolidated works

Although the success of reinforcement and backfilling works cannot be evaluated at present, a number of indicators point to the adequacy of planned and executed procedures. It cannot be denied that five centuries of the mine's operation below the town of Idrija have caused various changes in the mine, rock structure in the vicinity of the mine, and on the surface. Although mining works were continuously accompanied by backfilling of dug out areas during the mine's entire operation, the backfills were so deformable that they were unable to prevent the sinking of the surface, and their rheological characteristics were not such as to reduce sinking without additional reinforcement measures.

Visual assessment of adequacy of shutdown works

Frequent visual inspections of various facilities on the surface have shown that the intensity of time-dependant shifts is gradually decreasing, and that damage in the form of cracks and shear shifts has also decreased considerably. In some cases when cracks were more open in a specific period, but closed after a number of years. It may therefore be concluded that the sinking of the surface was not uniform and that reinforcement measures indirectly influenced the gradual reduction of damage on the surface.

Supporting walls and other structures which underwent time-dependant shifts are only cracked and damaged to the extent of requiring rehabilitation, but only when the

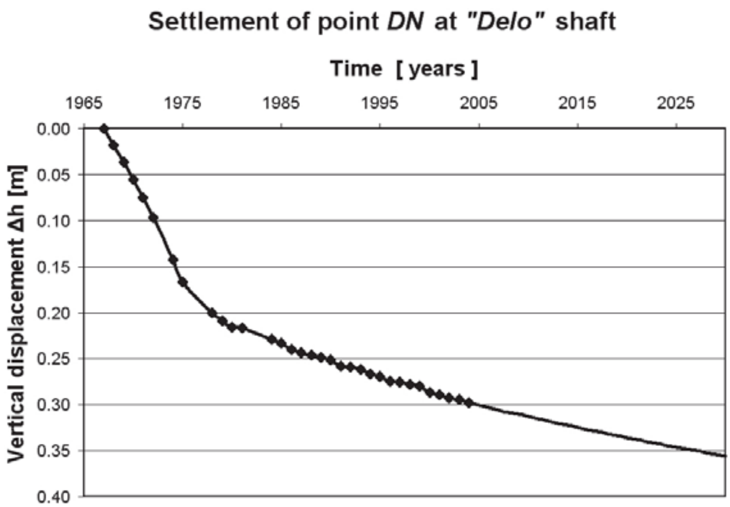

Figure 11. Estimation of the time dependant deformation point DN on the surface above mine
Slika 11. Ocena poteka časovno odvisne deformacije točke DN na površini nad jamo

time gradient of deformations is sufficiently small, or when a sinking rate criterion of less than 1cm/year is attained, which, from the aspect of time prognosis, is still acceptable. Newly constructed structures and rehabilitated facilities will need to be adapted to primary ground shifts.

Prognosis of the development of deformation processes in the long term

The estimation of time-dependant deformations on the surface above the mine has allowed us to prepare a prognosis of the development of the deformation field in the next ten or twenty years. According to the simple logarithmic approximation shown in Figure 11, the sinking of ground in a specific area can be expected to continue for at least 10 years, and therefore the set deformation reduction rate criterion of 1cm/year will be attained after this period.

It should be emphasized that the time frame of shifts in Permian-Carboniferous rocks is more pronounced in comparison with other rocks found in the broader area of the mine. A second threat that is indirectly linked to the sinking of ground is the increased lability of natural and artificial slopes in the southern hinterland of the town of Idrija. Although no major collapses have occurred so far, there have been some occasional minor slides which have had an unfavorable effect on the well-maintained natural surroundings.

CONCLUSIONS

a) The complex geological composition of rocks in the area of the town of Idrija and the mercury mine, major tectonic occurrences in the broader area, and other geological changes are the principal factors which, alongside mining works, continue to influence the development of deformation fields in the mine and on the surface.

b) More than five centuries of mining activity in the area of the town of Idrija have caused major changes in the stress deformation states of rocks and backfills in the affected areas of the mercury mine. It has indirectly called for the implementation of measures for improvement of the rock structure and backfills incorporated in the period of intensive mercury ore extraction.

c) Twenty years ago, extensive numerical models were used to determine the grouted measures to be used within the scope of shutdown works, and laboratory and in situ investigations were conducted in order to determine the geotechnical characteristics of relevant rock strata and artificial backfills.

d) Observation systems for measuring movements in the mine and on the surface were set up. These included inclinometric and piezometric measurements as well as measurements of stress changes using measurement cells, which are still used today and will continue to be used to a certain extent after the completion of shutdown works.

e) Time-dependant occurrences of sliding rocks and artificial backfills are still present, yet the intensity of time-dependant movements is considerably reduced and indirectly depends on the speed of filling empty spaces with grout materials.

f) An evaluation of the adequacy of grouting and backfilling works in the shutdown of the mine has shown that the selected procedures are appropriate for the given geological, geotechnical and mining conditions, and that the long-term stabilization of the broader area will be attained.

Povzetek

Dolgotrajni deformacijski proces v širšem območju Rudnika živega srebra Idrija

V pričujočem prispevku so podane nekatere posebnosti o izbiri, načrtovanju in načinu izvajanja zapiralnih del v Rudniku živega srebra Idrija. Ker je več faktorjev, ki vplivajo na časovni razvoj deformacijskega polja, so bile pred potrditvijo programa zapiralnih del narejene obsežne študije in strokovne utemeljitve, kar se je kasneje pokazalo kot upravičeno. Predstavljeno in dokazano je bilo, da je zahtevna geološka sestava hribin, ki gradijo območje mesta Idrije skupaj z Rudnikom živega srebra ter izrazita tektonska dogajanja na širšem prostoru in druge geološke spremembe v geološki zgodovini, pomembni vplivni faktorji, ki poleg več stoletij trajajočih rudarskih pridobivalnih del, še danes vplivajo na časovni razvoj deformacijskih polj v jami in na površini. Tako lahko zagotovo trdimo, da so več kot petstoletne rudarske aktivnosti na območju mesta Idrija pustile za sabo velike spremembe v napetostno deformacijskih odnosih v kamninah in zasipih v vplivnem območju delovanja Rudnika živega srebra ter da je takšno stanje s tem posredno botrovalo utrjevalnim ukrepom hribinskega ogrodja ter zasipov, ki so bili vgrajeni v odkopne prostore v času intenzivnega pridobivanja živosrebrne rude. Z obsežnimi numeričnimi modeli so bili pred dvajsetimi leti utemeljeni utrjevalni ukrepi v okviru zapiralnih del ter narejene laboratorijske in in situ raziskave za potrebe ugotavljanja geotehničnih lastnosti nastopajočih hribin in umetnih zasipov. Za potrebe sprotnega preverjanja časovno odvisnih dogajanj, so bili vzpostavljeni opazovalni sistemi za merjenje pomikov v jami in na površini vključno z inklinometrskimi in piezometrskimi meritvami ter meritvami sprememb napetosti s tlačnimi merskimi celicami. Te meritve se izvajajo še danes in se bodo v dopolnjenem obsegu tudi po končanih zapiralnih delih, saj so časovno odvisni pojavi lezenja kamnin in umetnih zasipov so še vedno prisotni, čeprav je intenzivnost časovno odvisnih pomikov precej manjša ter je posredno odvisna od hitrosti zapolnjevanja praznih prostorov z utrjevalnimi materiali.

Preverjanje uspešnosti utrjevalnih in zapolnjevalnih del pri zapiranju rudnika je pokazalo, da so bili izbrani postopki ustrezni danim geološko geotehničnim in rudarsko tehničnim razmeram, ter da bo dosežena dolgoročna stabilizacija širšega območja.

REFERENCES

[1] BAJŽELJ,U. 1984. Underhand Cut -and –Fill Stoping Experiments In Carboniferrous Schists at the Idrija Mine ,Symposium AIME, *Society of Mining Engineers of the American Institute of Mining, Metallurgical and Petroleum Engineers ,Inc. New York* :163-183

[2] BAJŽELJ, U. & LIKAR, J. 1991.Analysis of the stress-deformational state in the wider area of stopes at the Idrija Mine. *Bolletino della Associazione Mineraria Subalpina, XXVIII,n.4:* 699- 712, *Torino, 29-30 aprile 1991.*

[3] CIGALE, M. 1988. Dolgoročni program postopnega, popolnega in trajnega zapiranja Rudnika živega srebra Idrija. Idrija1988.

[4] REŽUN, B. & DIZDAREVIČ, T.1997. The Influence of Surface Waters and Mine Waters on the Closing Down of the Idrija Mercury Mine . *6th IMWA Congress,* Vol.(1): 85-94

[5] Archive documents, reports and studies in the Idrija Mercury Mine.

Review of the Previously Considered Mining Solutions for the Ore Body „Borska Reka"

Dragan Štrbac[1], Živorad Milićević[2]

[1] RTB Bor Group, Copper Institute Bor, Zeleni bulevar 35, 19210 Bor, Serbia;
E-mail: strbac@ibb-bor.co.yu
[2] University of Belgrade, Technical Faculty V.J. 12, 19210 Bor, Serbia;
E-mail: zmilicevic@tf.bor.ac.yu

Received: July 5, 2006 **Accepted**: July 20, 2006

Abstract: The ore body „Borska reka" is the biggest one discavered in the metalogenetic Zone of Bor. On the contrary of the others, previously discovered and mined highly grade ore bodies, „Borska Reka" is the ore body with low grade ore and it's the deepest one in the Zone. Therefore, only underground mining could be applied to mine this ore body. But there were some difficulties about the possibilities for the mining because on the surface above of the ore body exist a few very important facilities as well as in previous years the copper price was too low. Therefore from the time when the ore body had been discovered, during the years, many possibilities and opportunities for profitable mining of the ore body were considered by many experts from almost all Researching Institutions and Consultants in Serbia. In this paper work the review of those researching is shown, focused on the considered mining methods.

Key words: Ore body, mining depth, profitable mining, the methods

Introduction

The ore body „Borska Reka" is shown on the figure no.1 and it is a massive mineralisation shape. The lenghtway direction is the northwest-southeast, and it is dumped to the west-suothwest direction with general angle of 45°-55°. The maximum lenght of the ore body had been estimated on the K -400 level and it is reached 1410 m distance. On the same level had been estimated the maximum width of 360 m as well. The above data are valid for the cut – off – grade of 0.3 % Cu. For that cut-off-grade, the average high from the top to the bottom of the pre body is approximately 620 m[1].

Taking account the location of the ore body as well as the existing facilities on the surface above of the ore body, the question tag is about the opportunities for its profitable mining. On the other point of view, discovering a possibility for economic sustainable mining would be extended the working life of the currnet active underground site „Bor".

During the researching about the mining method selection, two group of methods habe been considered: backfilling group of methods and caving group of methods[2]. But the most important issue about the method selection is relocation of the facilities on the surface above the ore body and the costs for their relocation[3, 4]. The relocation cost are

Scientific paper

related with the caving methods and therefore a backfill group of methods had been considered for the porposes to avoid relocation of the facililties and too high relocation costs.

Researchings about the profitable mining of the ore body „Borska Reka" have been going on for more then twenty years in the Copper Institute, Technical Faculty at Bor and The Faculty of Mining and Geology in Belgrade. These researchings could be split in three stages:

The first stage with duration of about 10 - 12 years the theoretical works had been done with the some researchings in the laboratories and a small level of the in situ researchings. These researchings didn't show some especial results. In this stage, a certain number of different mining methods were considered for mining of the „Borska Reka" ore body.

Several different caving methods had been designed and performing appropriate reserachings on the demonstration models of the designs in the laboratories. Because of the caving methods effects on the surface, the facilities on the surface had been detailed recorded and the estimation fo their values was done.

Also, a few methods without the effects on the surface had been designed. These method belong to a backfilling group of mining methods with hydraulic backfill as well as the room – and pillars methods.

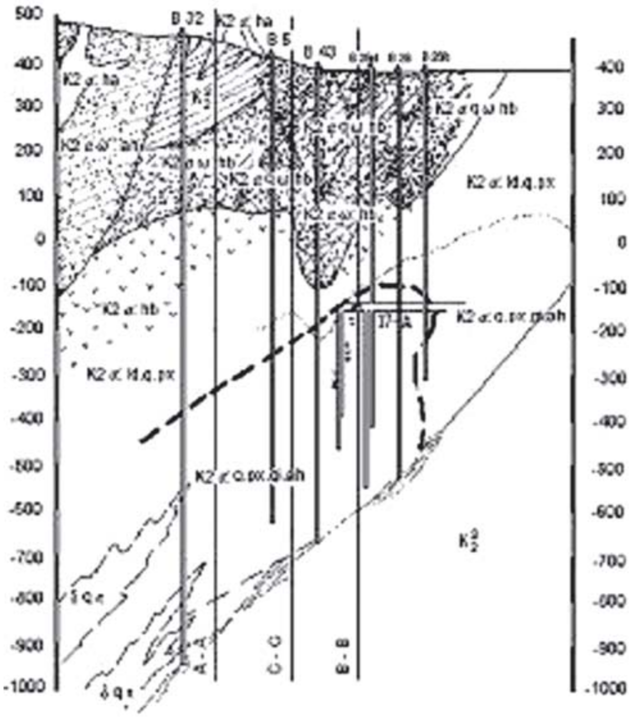

Figure 1. Transversal geological sectionplane 2-2 fo the ore body „Borska Reka"

In the second stage some other variants had been considered, but the works were focused to the cutting the costs. More attention was considered about the application of different types of mining equipment for bogging, loading, haulage transport, crushing and hoisting. Previouosly considered solutions included LHD diesel boggars. In the second stage the same method were designing like in the first stage but with application of the electrical power equipment, due to high ventilation costs in the case of diesel equipment application.

Some new variants of sublevel caving methods were proposed, with higher distance between the levels. During the designing of those methods the application of the vibrofeeder for bogging and ankle – conveyors for haulage transport. Some of those solutions were original ones[3, 8].

One of the most important outcome from the performed researching was about the possibility to take a higher distance between the levels and this result focused further reserachings in that way. As a result of those efforts „The Level Caving” methods were designed and on the basis of those one, finally two variants of „Semi-Level Caving” methods were proposed[3, 12].

To keep surface of collapsing due to mining activities only one method was considered. It was Open Stope method with backfilling, with some modifications and improvement in mining layout pattern.

The third researching stage has being performed during the last ten years related with the start use of mining software „Gemcom” and statr work of the new Rock and Soil Mechanics laboratory in the Copper Instiute Bor. Then were analysed all previously considered methods and the Room and Pillar methods were excluded for further considerations becouse of the following reasons:

- too low level of ore recovery (32 % ¸ 40 %) and
- impossibility to keep persistant the open stops without backfilling, but bacfilling would be significantly increasing the operating costs.

Finnaly, the caving methods were accepted as the best solution, taking account technical and economical aspects of the mining operations. In this researching stage some variants of Block –Level Caving and Sublevel Caving methods were considered.

Because the decision about the most appropriate mining method has not done yet, it’s obiously that the researching will continuing in the fiture as well. The authors af this paper, because of the reasons mentioned above, decided to show a review of all researchings related with the mining method selection for the ore body „Borska Reka” with analyses of the outcomes from past researchings, with the aim to show to future researchers the issue which should be focused. In some considerations even Block Caving methods have been taken account, althought Block Caving was not been considered in the past researhings, but as an possible option was proposed for the mining of the remained ore reserves in some other ore bodies (Veliki Krivelj and Južni Revir – Majdanpek)[22].

The Researched Mining Methods

The Ist Researching Stage

The first considerations about the possibilities for ore bodu „Borska Reka" mining were done in 1983. Then was made in „Copper Institute Bor" a project „Researching, Exploiatation and Processing of the Base Metals" and as a part of that project a „Study of Longterm Development and Mining the Copper Ore Bodies in Basin Bor"[5]. In that study, in the chapter related with underground mining in RTB Bor, in a few words was mentioned that in north-western part of the ore deposit Bor a geological exploration was going on. It was noticed that the current proved ore reserves were more than 250 million tonnes with average copper grade of 0.7 % and that the explorations would be continued according to the official programme. Also, in the study was noticed that theore body, later named „Borska Reka" is a future of mining activities in Bor Mine. About the mining methods it was just mentioned that the prospective method had to provide high level ore recovery, minimum ore dilution, to be low costs and maximum take care about safety aspect of work. In the continuation of the above mention project, „The Study of Ore Body »Borska Reka« Mining Applying Sublevel Caving" was done[6]. Considering possible mining methods, a broadly selection was made and the following methods were emphasized:

1. The Longhole Block Mining Method with the Compensation Room,
2. The Longhole Block Mining Method with Srinkage Mining without Pillars,

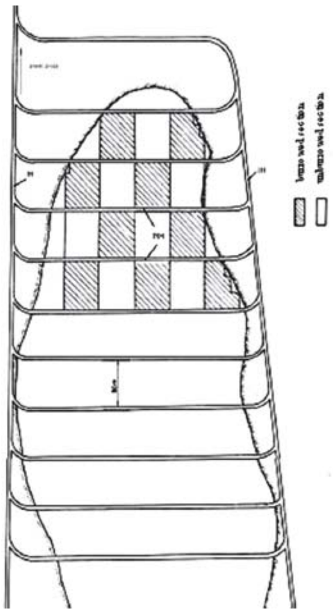
a)

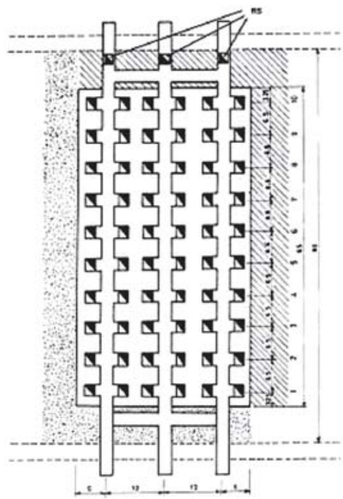
b)

Figure 2.: a) The mining layout scheme for cross-disposeed mining blocks and mining development drives on a level, b)The scheme of a mining block on the loading level

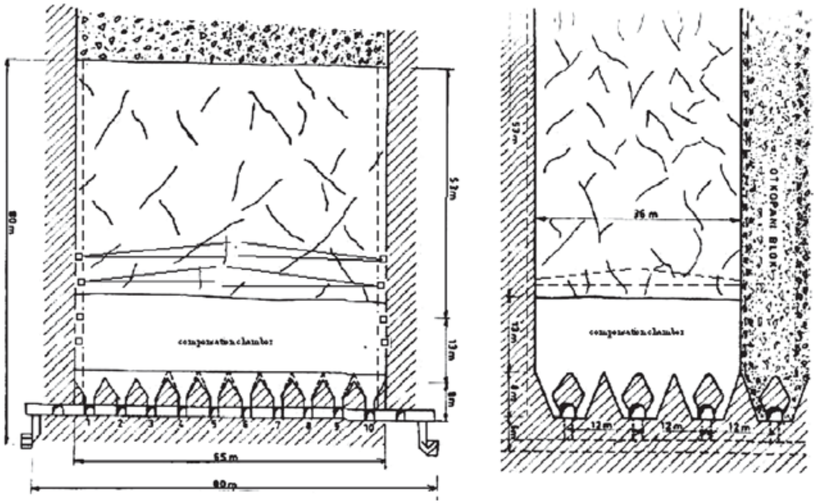

Figure 3. The shema of the mining method in the vertical sectionplanes[6]

3. The Longhole Block Mining with Shrinkage Mining and Post-Mining of the Remained Pillars,
4. Sublevel Caving – the Swedish Variant,
5. Sublevel Caving in Compressed Environment with Shrinkage Mining,
6. The Frontal Sublevel Caving Method.

After above review, authors of this study decided to consider the first three methods [6].

1. The Longhole Block Method with the Compensation Room

The mining layout for this method is consist of mining blocks with rectangle shape and dimensions of 65 x 36 m, as it shown at the figure 2. High distance between the levels is 80 m, and the mining blocks are disposed on the lenghtway of the ore body. The main haulage and loading levels are connected by ore passes.

The loading and cutting level where is a compensation room, are connected by funnel – shaped ore passes. The distance between the ore passes is 6.5 m. The ore mining is going on by drilling and blasting works with horizontal drill holes. The compensation room is extended across the all block area due to set down the volumetric surplus of ore, as it shown at the Figure 3.

2. The Longhole Block Mining Method with Srinkage Mining without Pillars

The mining blocks here are disposed cross over the lenghtway of the ore body. The width of the blocks is 15 m and the height 80 m as wells as the height between the levels.

Mining development on each level is consist of the number of parallel loading ore drives with 15 m distance between each of them, as can be seen on Figure 4. 20 and 50 m Above of the loading ore drives are the drilling ore drives of the first and the second drill level respectively. The mining activity at each block beginning with boring a slot ore raise in the middle of a block, and then to extend a ore raise to reach a width of a block and that extended ore raise should be used as a vertical compensation room (the start free space).The drill holes are bored

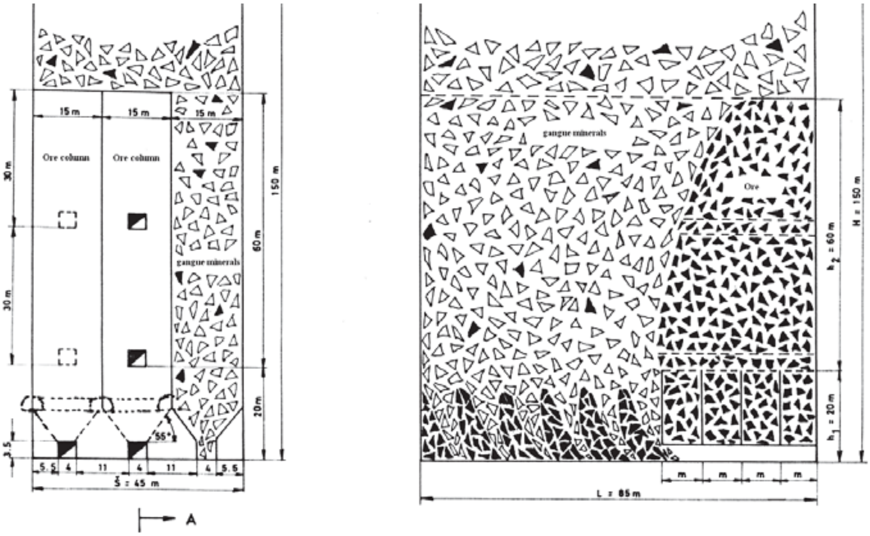

Figure 4. Scheme of The Sublevel Caving Method with Temporarily Shrinkage Mining[6]

from the both sublevel ore drives and simultaneously are blasted rings from the upper and lower drilling ore drives. From the loading ore drives are bored shorter rings due to cut off the blocks and to provide access for bogging the ore.Blasted ore is loaded by boggars from the loading ore drives, Becouse of the too much hight of the blocks due to achieve a good caving process of ore, the ore is bogged from an extended ore belt (on the figure is marked as „m"). As an effect of that activity there is a certain amount of ore loss in the lower part of the block , as is shown on the figure. This is one disadvantage of the method , because when the blocks are too hight there is higher level of ore dilution.

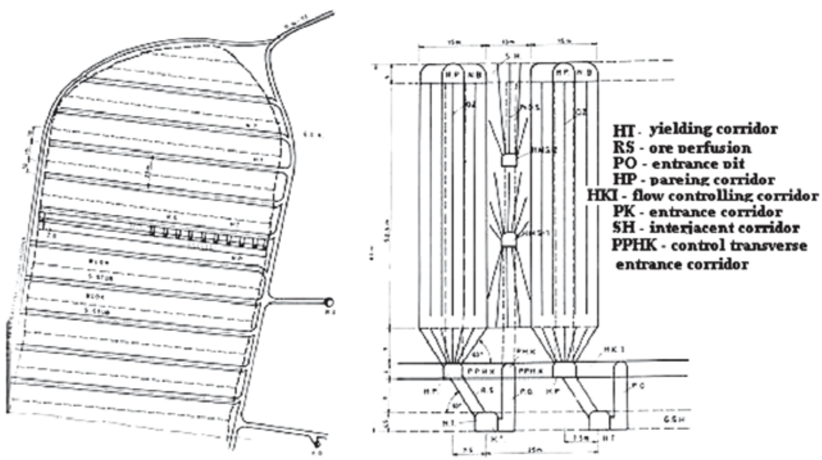

a) b)

Figure 5.: a) Disposition of the mining blocks and loading ore drives on a level;
b) Vertical sectionplane of the method[6]

Also, this construction of the method with the sublevel drilling ore drives is related with higher level of development works.

3. The Longhole Block Mining with Shrinkage Mining and Post-Mining of the Remained Pillars

In this method the mining is consist of two stages , the primary and the secondary mining stage. The primary mining stage is going on in the blocks 15 m width using paralle long hole drilling and blasting pattern. Between the blocks (rooms) the pillars 10 m width are left, those pillars would be drilled nad blasted later, in the second stage, and the ore would be caved from the drawpoints of the primary stage. The location and the shape of the mining methods and the vertical sectionplane of the method are shown in the Figure 5. As can be seen, the mining layout on the each level is consist of loading ore drives and cutting ore drives , and ore is caved from the cutting ore drives. Due to control of the caving process, would be done the control ore drives with the transverse ore drives to the each drawpoint.

In the first mining stage ore is mined by parallel drill longholes which are drilled from the cutting drives below of the roof on the upper level. After mining and bogging the ore from the blocks are finished, then start mining of the remained pillars, this is the second stage, using the drill holes blasting which are drilled from two sublevel ore drives in the middle of the pillars. The mined ore is bogging from the same drawpoints as the ore from the first stage.

At the end of t „The Study of Ore Body »Borska Reka« Mining Applying Sublevel Caving” it was emphasized that the correct selection of the mining method of the ore body „Borska Reka” could be achieved taking account the following conditions:

- a study for ore body „Borska Reka” mining without collapsing of the surface should be done;
- in the proposed study the mining should be performed in two stages as well;
- according to the supposed results of the both studies should be done a technical and economic analyses as the basic issues for a mining optimization- the selection of the most appropriate mining method for the ore body „Borska Reka”.

According to the above mention conclusion „The Study of the Ore Body »Borska Reka« Mining with Keeping the Surface” [7], and in the study two the new ones method were considered to avoid potentially collapsing the surface. These methods are:

1. Room and Pillar Method with Backfill Mining and
2. Sublevel Stoping Method.

Room and Pillar Method with Backfill Mining

This method belongs in the group of mining methods which are keep the solid the reock massive around the ore body and do not cause collapsing of the surface above the ore body and the facilities on the surface[7].

Mining layout for this method is consist of the 15 x 80 x 59 m blocks. Mining perations is going by blasting of longhole drill holes with diameter of 165 mm. Mined ore is coming down into the cutting level and then throught ore passes is loading into the suitable mine loading eqipment in the loading ore dirves. The distance between ore passes is 7 m, oriented toward ore body lenghtway.

For mine haulage it's proposed application of the trucks with 30 t capacity which are should be loaded direct form the ore passes. Oversize materials would be broken by secondary blasting or mechanical crushing.

Between the mining blocks 10 m width pillars would be left. The length of the pillars is the same as the length of the mining blocks. The height of the pillars is 69.5 m plus 10.5 m is the width of the roof plate pillar disposed above the blocks. On the Figure 6 is shown this mining method.

Development mining works are consist of the haulage drive on the level and tunneling the ore drives from the haulage drive, oriented rectangle of the ore body lenghtway. 10 m above of the loading level the cutting ore drives are tunneled. From the cutting ore drives , the blocks is cut of by the 7 m height bored tranches 59 m Above of the cutting level, in the middle of the blocks, are located the drilling ore drives. They are extended up to the edges of the blocks and then from the drilling ore dives start boring longohole drill holes down to the cutting level.

In the roofwall part of the ore body, from the drilling level is located the bacfill ore drives which are connect the drilling ore drives. The porposes of these ore drives is ventilation and the supplying of the backfill materials up to the stopes. The loading, cutting, caving control and drilling levels are connected by an incline with 20 % inclination which one should be used for vetilation and servis issues.

Sublevel Stoping Method

Subelev stoping method was considered just ones. The reality of the application of this methods is doubtfull, because it is not expect that the pillars are able to persist the stress for a long time. The existence of the faults and shears in the ore body could be affected the pillars and certainly soon or later some sort of backfilling would have to be provided to fullfil the remained stopes. One of the solution could be backfilling with the tailing waste, expecially taking account the problems in the surface about the tailing waste disposal.

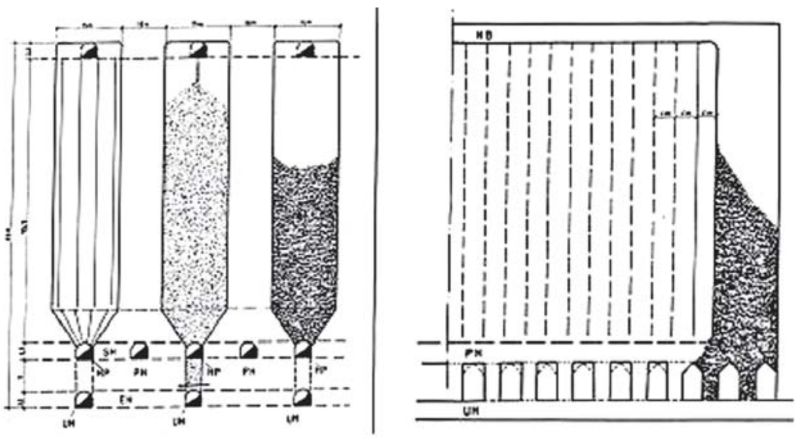

Figure 6. Room and Pillar Method with Backfill Mining[7]

The proposed method is consist of simply solutions for develolpment and mining works. Development works are consist of the ore drives at the bottom and the top of the rooms. The longhole parallel drill holes are bored from the top ore drives, and the bottom drives are used for bogging. Because the boggars should be bogging the row materials into the unsupported area, they should be remote controlled. On the Figure 7. is shown the layout of the method which is very similar with previous described method.

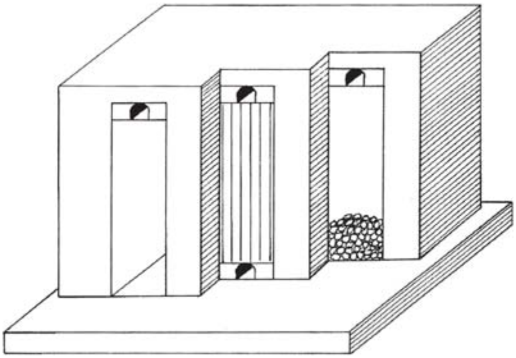

Figure 7. Sublevel Stoping Method

The IInd Researching Stage

In the second researching stage some other opportunities were considered , priority focused to find out the possibilities for cut the operation cost and provide the economical and profitable exploatation of the ore body „Borska Reka”. In this stage all previously described methods of the first stage were considered but this time with the electrical powered equipment. This is because previously researchings determinated that for the high capacities (e.g. 4-10 million tones per year) ventilation costs would be too high as well as some technical problems related with intakeing the fresh air throught the existing mining infrastructure could be occure. These researchings have shown the opportunities for cutting off the ventilation costs as well as the necessity to take account variable solutions and opportunities for the furher researchings. Except already above desribed methods, some other methods were designed, as would be shown.

Sublevel Caving in Compressed Environment with Shrinkage Mining

Sublevel Caving methods had not been seriously considered previously because the longyears of experience with sublevel caving in Bor Mine. Althought some researching have shown some opportunities to change some parameters of the method related with the following issues:

- to increase the distance between the levels which would decrease the amount of development works per tonne of ore,
- to find out the possibilities to decrease the ore dilution by applying the ore mining in the wider ore belts.

These suppositions were considered in a few paper works [8]. The basic for researching was a designed Sublevel Caving method as it is shown at the Figure 8. This is a proposed method with some combinations of Sublevel Caving and some variants of ore bogging. In odd ore blocks the ore is mined in a wider ore belts(15 - 20 m) and bogging from the lateral ore drives tunneled from the subsequent coupled ore blocks. In these blocks ore is mined in the shorter ore belts (3 - 4 m) and boged from the drawpoint in the pre drivea to the haulage drive.

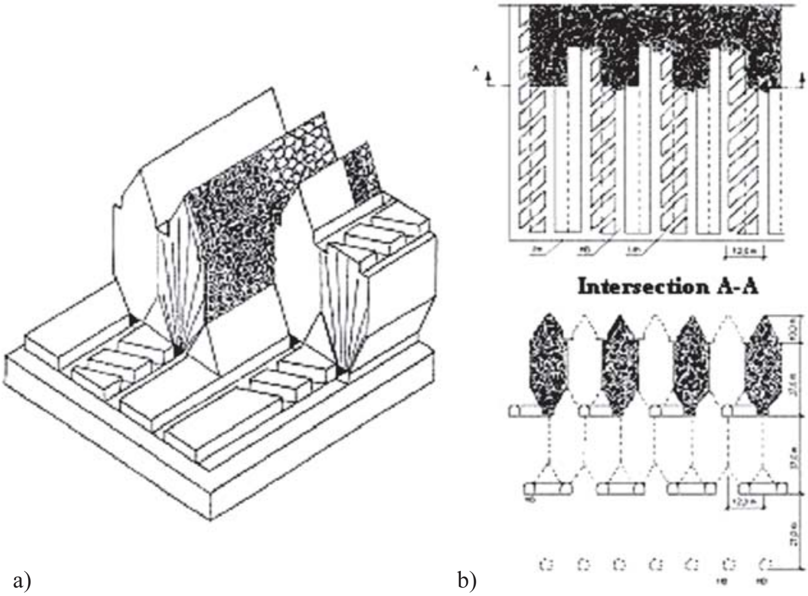

a) b)

Figure 8. Sublevel Caving in Compressed Environment with Shrinkage Mining: a) aksonometric Plan; b) horizontal and vertical sectionplanes oh the method[8]

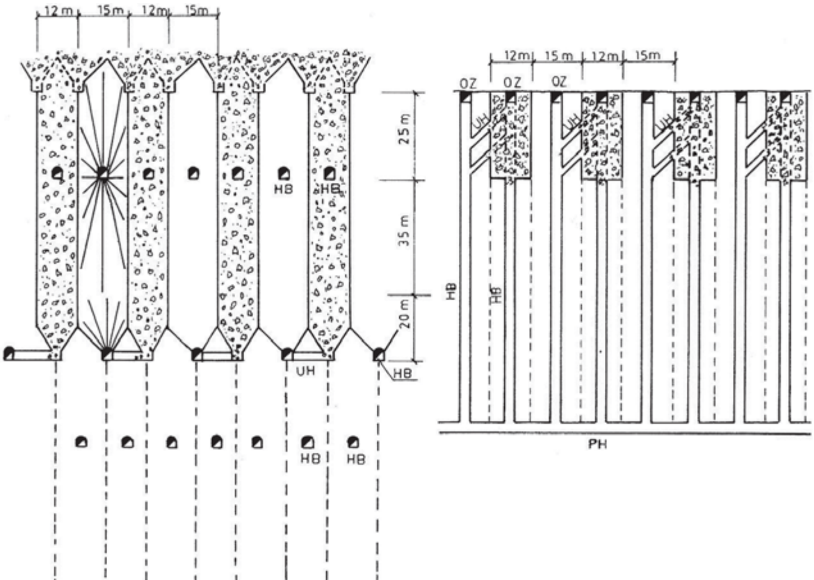

Figure 9. The proposed method of longhole block mining coming form the method shown in the Figure 8.

As can be seen , in the researchings the start distance between the levels was 27 m althought during the some Lab. analyses that the hight of the levels can be increased. Demonstration model was done for the distance up to the 50 m between the levels, and the caving process shown that there are possibilities for further increasing the distance which was done in some furthermore proposed solutions. One of them is shown on the Figure 9.

In this method the mining layout consist of the blocks 80 m height and 12 – 15 m width. The mining blocks are oriented with rect angle to the ore body lenghtway. Development works are located on the basic level and in the sublevel where are located the ore drives.

There is a combination of mining works. In one block the ore is mined in the wider belt and the bogging is going from the sides, and in the next block the ore is mined in the shorter belt and bogging is going from the face. The researchings which are done to prove applicability of this method have shown that better results could be achived with mining in the wider ore belts. In this case could be expected better ore granulation as well, what is expected for blasting in the compressed environment.

The last one mining method has a significant advantages compare with the previous considered methods. These are the following advantages:

- less development works;
- better blasted ore granulation;
- less consumption of explosive and rock supporting materials;
- increasing the ore recovery;
- decreasing the ore dilution;
- improvement of the work safety;
- better efficiency and mining capacity;
- less mining costs.

From the furthermore researhings come some new proposed variants for longhole block mining:

- the block longhole mining methods with ore blasting in the compressed environment;
- the semilevel caving methods with the lateral ore bogging from one side;
- the semilevel caving methods with the lateral ore bogging from two sided.

The block longhole mining method with ore blasting in the compressed environment

The mining layout and designed solutions of previously described mining method had not provided appropriate solutions for effectively the ore body Borska Reka mining. The designed blocks bottoms could not been able to provide effective ore loading. It was expected that the ore should be bogged by LHD, then dump into the ore passes to the lower haulage level. However some researching [23] have shown that proposed solution is not economical. Therefore some other solution were proposed, with the block – bottoms level just above of the haulage level, as can be seen on Figure 10.

This method belongs of longhole groups of method, with a excessive blasting works in the wider ore belts and the proposed design should provide a high capacity of the method, and as a result reduction of the operating costs, which is very important due to relatively low ore grade in the considered ore body.

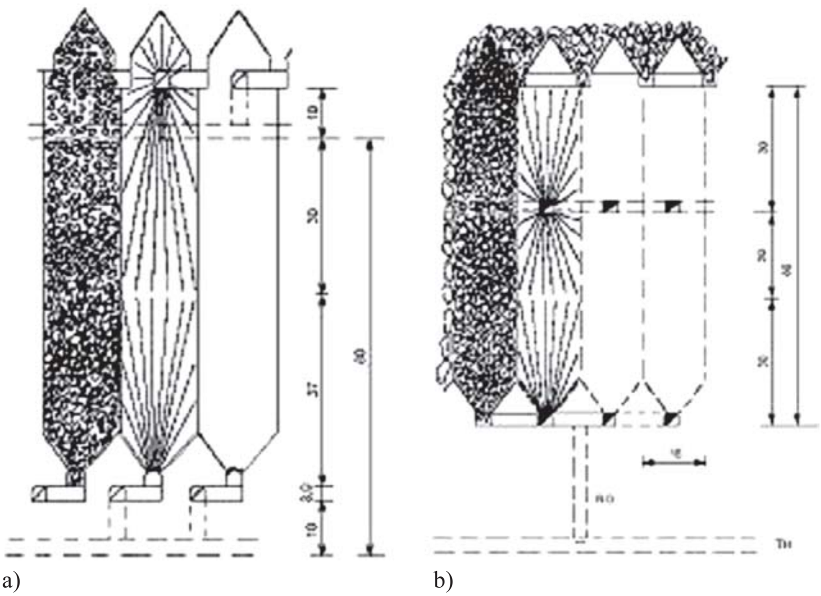

Figure 10. Two variants of the longhole block mining in the compressed environment

As a results of researchings on the demonstration models outcome the following geometrical pattern:

- the width of the mining blocks: 12 m;
- the height of the mining blocks: 80 m;
- the length of the mining blocks: 100 ÷ 120 m.

On the Figure 10 two variants of the proposed method are shown. The difference is related with the orientation of the ore drives. From these ore drives would be bored longholes. Also, it is different disposition of the blocks and haulage drive. In the first case a block is 10 m above of the haulage drive and the ore is blasted from the upper prodiction level. In the second case drilling and blasting works are going from the ore drives on the same level as the haulage drive, 30 m below of the blocks.

The Semi-Level Caving Method with One and Duble Side Lateral Bogging

In Time, the variouos researchings led to the chose of the loghhole groups of methods, and that was a focuse to find out the appropriate method and layout design. That issue leads to the Semi-Level Caving Methods proposal, which ones were the greatest modification compare with previously conidesred grops of mining methods. Two variants were been considered:

- The Semi-Level Caving Method with One Side Lateral Bogging (Figure 11);
- The Semi-Level Caving Method with Duble Side Lateral Bogging (Figure 12).

The methods have the specific position of the mining blocks, becouse the neigburing blocks are relocated for the half – level distance, up to the middle of the block height. That mining layout should be ensure a lower ore dillution.

In the both variants the ore should be blasted in the mining blocks 80 m height, and the width of the blocks is 12 m in the first variant and 24 m in the second one. The ore would be mined in the belts at least 10 – 16 m width and the height equail with the distance between the levels (80 m)[11, 12]. By manyfold ore mining and preiviosly bogging a certain amount of ore, the ore could be mined in the even wider belts and the bogging could be done from a lot of drawpoins.

On the basis of the researchings on the demonstration models the following parameters of the mining method were suggested:

- the level
  H = 80 m;
- the semi – level height
  h = 40 m;
- the maximal drilling height
  H_b = 40 m;
- the distance between the bogging and drilling ore drives
  S = 12 m;
- the ore drives width
  b = 4 m;
- the ore drives height
  h = 3.5 m;
- the cros section area
  P_{OH} = 12.7 m^2;
- the ore burden
  W = 2 m;
- the length of the mining belt (6 x W)
  $l_{p.m.}$ = 12 m.

These methods is because of the double – function of the ore drives. E.g. the ore drives used for bogging from the neighboring blocks later would be used for drilling upper level of the block. In the lower level of the block drilling and blasting works are going on from the tranches ore drives and at the same time that mine the development of the lower block level by tranch shaped excavations.

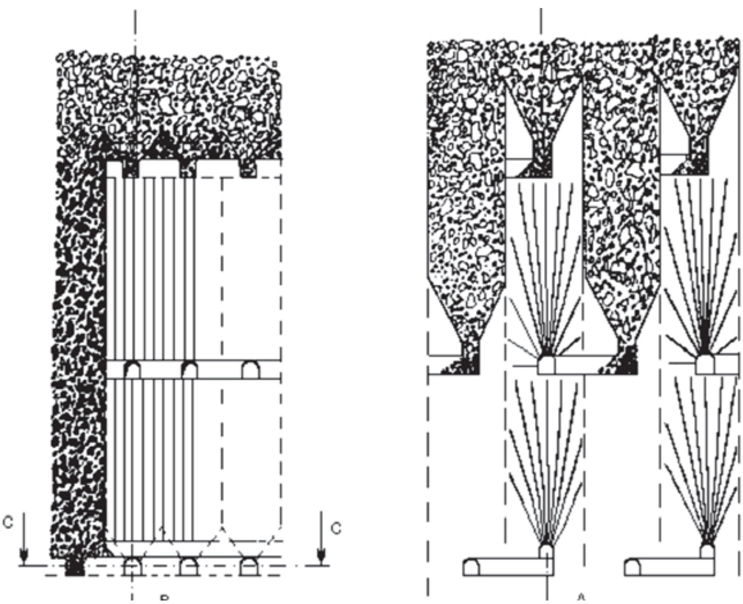

Figure 11. The Semi-Level Caving Method with One Side Lateral Bogging

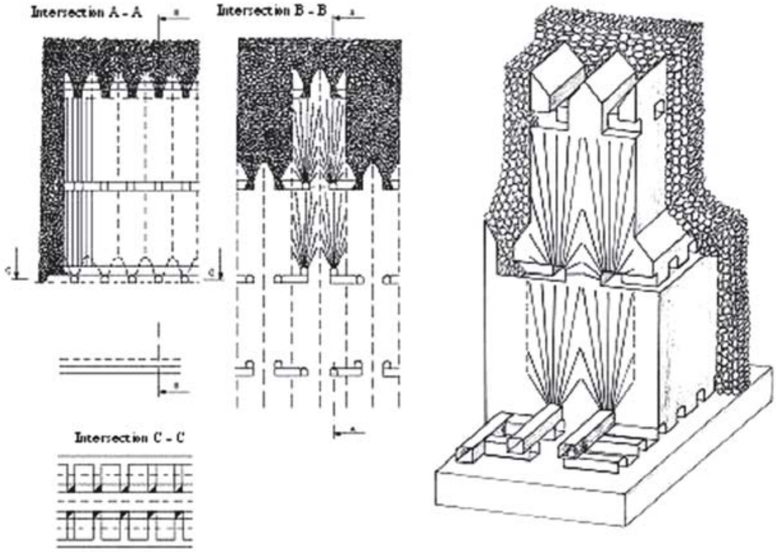

Figure 12. The Semi-Level Caving Method with Duble Side Lateral Bogging

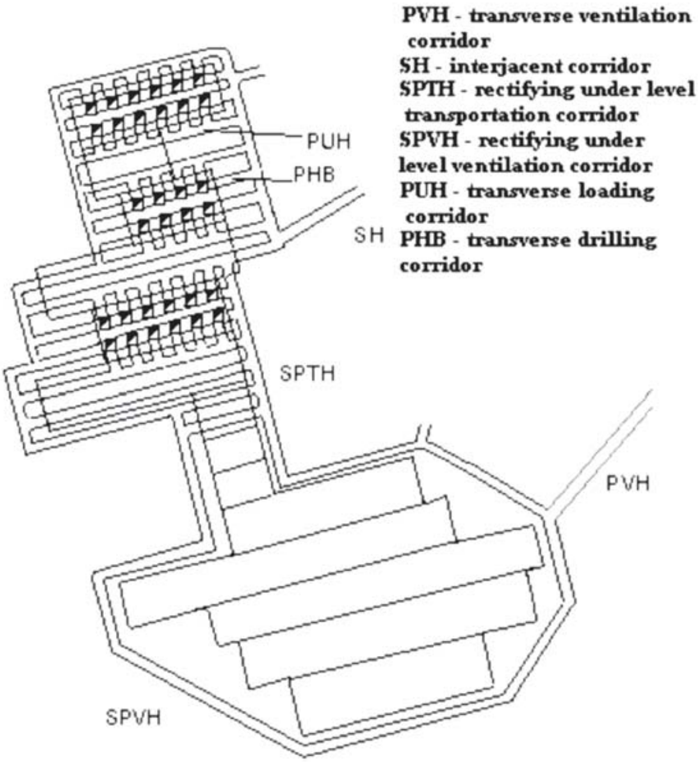

Figure 13. The mining layout at the haulage level

Ore drives are located on the basic level of mining blocks. On the sides of the ore drives are located the excavations which are used for bogging. The distance between the excavations is 10 – 12 m. In the first variant the excavations are located in just one ore drive, and in the second variant in two ore drives. Simultaneously bogging from the several excavations (drawpoints) should provide lower ore dilution level and better ore recovery.

The mining development layout is consist of the some other excavations as well: connecting ore drives, ventilation drives, slot ore rises, haulage drives, ore passes etc. The mining block are located transverse to the ore body, as can be seen on the Figure 13. Figure 13 is shown development layout for the highest part of the ore body where is relatively small the width of the ore body. Also, it is proposed that the ore should be loaded up to the ore passes, then should be dump into the ore passes and from there direct to mobile crushers as a primary crushers. After primary crushing the ore would be haulage further by belt conveyors.

Room and Pillar, VCR and Backfilling Mining Methods

This researching stage was related to find out an appropriate method which should be keep the surface of collapsing. The layout for these methods are the similar with the previous ones, but the development works are a bit different. The rooms are located transverse to the ore body and the rooms and pillars width were taken using rules of thumb (the rooms width 15 m and the pillars width 10 m). But the width of the rooms are a bit biger in the higher levels compere with the roms width in the lower levels.And on the other side , the pillars width is biger in the lower levels then in the upper ones. This is related to the underground stress and necessity of the disposal of the pillars because they should be strict located ones above of the others. The proposed rooms disposition is shown on the Figure 14. The length of the rooms is limited to the 80 – 100 m maximum.

The Rooms have tranches at the bottoms located 20 m above of the haulage level. That kind of layout provides a certain number of

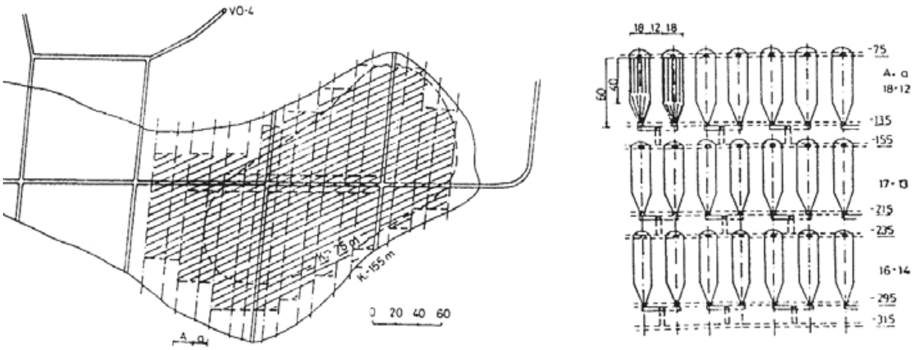

Figure 14. The mining layout in the ore body , horizontal and vertical sectionplane (K -155)

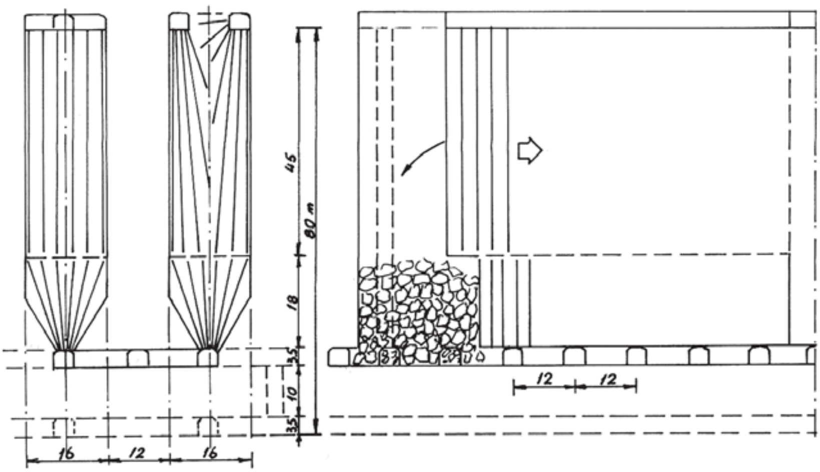

Figure 15. The sublevel stoping longhole mining in the vertical belts (here are shown two different drilling patterns)

ore passes with enough volumetric space to stockpile the ore and at the same time this part of mining block remained unmined serving as a roof pillar for the next downward level. That means that the ore from a lower level rooms would be mined from an upper level ore drives.

The ore recovery depands of the ration between rooms width and pillars width but usually is no more than 30 – 35 % (exceptionally up to the 40 %).

The mining pricip in the rooms can be different, so there are proposed three different variants of the mining method:

- the sublevel stoping longhole mining in the vertical belts (Figure 15.);
- the VCR mining in the horizontal belts(Figure 16.);
- room and pillar mining with simultaneoulsy mining on two levels, where the ore from the upper caming down on the previously mined lower level.

For the porposes of the designing this method it had been chosen the previoulsy conidered 80 m height levels, but the height of the blocks bottom is shorten to 13.5 m (it is distance between haulage and cutting ore drives).

Tecnical and economical analyses shown that the third one variant had the best performance, but the preliminary geomechanical researchings shown that could be a problem with the pillars stability due to the their height and big underground stress deeper in the ore body[15]. Due to fulfill the requirements for the rooms height decreasing, in the paper work [15] had been performed the third variant of the lognhole methods as a part of preliminary researchings. It was proposed the two – stage room and pillar mining method as it shown on the Figure 17.

The Method is specific because of a horizontal pillar in the middle of the rooms with the ore passes for the porposes of ore caving

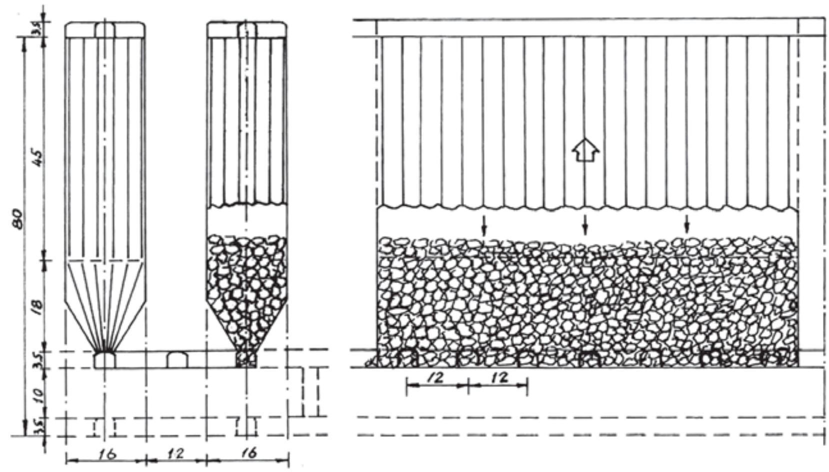

Figure 16. VCR mining method

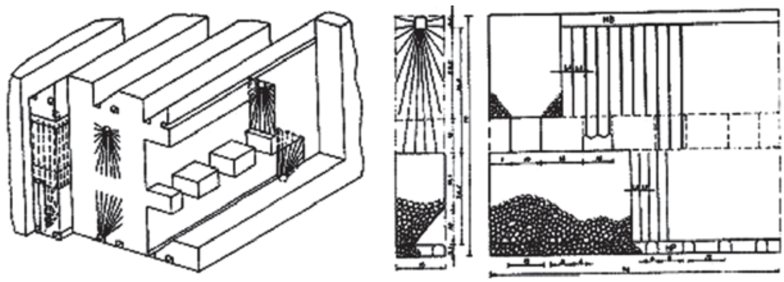

Figure 17. The plan of the two – stage room and pillar method with the basic parametars of the method[15]

from the upper to the lower part of the room. Drilling and blasting works are going on simultaneously in the both part of the room taking account the mining front is 10 – 15 m in advance in the lower level compare with the upper level front. Development pattern of the bottom of the lower level consist of two paralle ore drives: a trench one (for the ore drilling porposes) and an ore drive for bogging. The detailed design of the method outcame the following parameters:

- the room and pillar width 16 + 16 m;
- the room legth 96 m;
- the upper and lower room height 30 m;
- the intensity of the ore body mining 71.3 t/m^2.

The proposed mining methods have not been excepted due to the following reasons:

- low level of ore recovery (30 % ¸ 40 %);
- impossibility to keep stabile the open spaces (rooms) higher then 30 m without backfilling and consequently.

The IIIrd Researching Stage

The third researching stage has been going on during the last few years, since mining software Gemcom had been supplied and since the starting work of the new Laboratory for Rock and Soil Mechanic at the Copper Institute Bor.

Once again were analyzed all prevously considered methods but this time using mining software Gemcom. Finnely, the Caving group of methods were acepted as the better solutions compare with others groups of mining methods. The researchings was focused to the following method:

Sublevel Caving – Swedish Variant[16]

At the first production stage it was suggested „Super Scale Sublevel Caving". By this method is proposed to be mined the upper level of the ore body (downward by the level K -295)[16].To Determine the mining layout and the basic parameters of the method the most important issue is to determine the height between the levels which is related to the drill equipment performances. Also very important issue is the width of the ore drives and the distance between them due to achived as more as possible parallel ring drill holes pattern .The distance between the ore drives is related with the width of the drawpoints . The mining layout would be consist of ore drives and haulage drives. The distance between the ore drives woould be 18 m, and they would be located in the alternate – "Chess" pattern. The distance between the levels is 30 m. Ored rives are fully arch shaped 6 m width and 4 m height, and haulage drives fully arch shaped as well but 5m width and 3.5 m height.

The Super Scale Sublevel Caving method has the following parameters:

- $H = 40$ m - the drilling height;
- $h_p = 30$ m - the level height;
- $B = 18$ m - the distance between the axles fo the ore drives;
- $b = 6$ m - the ore drive width;
- $h = 4$ m - the ore drive height;
- $W = 4$ m - the burden.

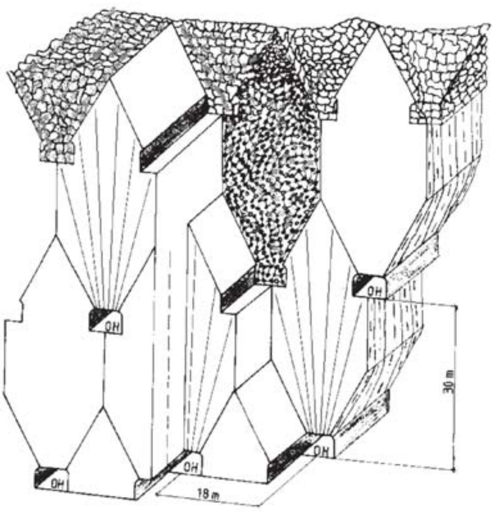

Figure 18. Sublevel caving, mining layout

Results

The Ist Researching Stage

For all three caving methods as well as to – keep – surface method of the first researching stage some model researchings have been done due to gain some parameters about of ore dilution and recovery. The reselts are shown in the Table 1. as well as the develop-ment works coefficient.

Table 1. The Mining Methods Parameters from the I Researching Stage

	Parameters of the Methods	Mining Methods			
		The Longhole Block Method with the Compensation Room	The Longhole Block Mining Method with Srinkage Mining without Pillars	The Longhole Block Mining with Shrinkage Mining and Post-Mining of the Remained Pillars	Room and Pillar Method with Backfill Mining
1.	Ore Recovery (%)	92.4	67	73	62.5
2.	Ore Dillution (%)	6	15	6	0
3.	Development Works Coefficient (mm/t)	3.75	1.48	1.5	2.44

The IInd Researching Stage

Like in the previous researching stage, in the second stage researchings were done by some demonstration models. The parameters related to the ore recovery and ore dilution as well as the developent works coefficient are shown in the Table 2.

Table 2. The Mining Methods Parameters from the II Researching Stage

	Parameters of the Methods	Mining Methods			
		Sublevel Caving in Compressed Environment with Shrinkage Mining	The block longhole mining method with ore blasting in the compressed environment	The Semi-Level Caving Method with One and Duble Side Lateral Bogging	Room and Pillar Method with Backfill Mining
1.	Ore Recovery (%)	80	84.89	88	39.24
2.	Ore Dillution (%)	15	10	12	0
3.	Development Works Coefficient (mm/t)	1.94	1.37	1.312	2.36

The IIIrd Researching Stage

The parameters related to the ore recovery and ore dilution as well as the developent works coefficient from the third researching stage are shown in the Table 3.

Table 3. The Mining Methods Parameters from the III Researching Stage

	Parameters of the Methods	Mining Methods
		Sublevel Caving – Swedish Variant
1.	Ore Recovery (%)	80.2
2.	Ore Dillution (%)	10.5
3.	Development Works Coefficient (mm/t)	1.24

DISCUSSION

The Ist Researching Stage

Analysing the achieved results from the first researching stage it is concluded that the best solution is to select The Longhole Block Mining with Shrinkage Mining and Post-Mining of the Remained Pillars. By this method couold be reached 77 % of the primary ore recovery. After the second exploatatio stage, after the stage of post – mining of the remained pillars, total ore recovery would be 73 %, and ore dilution 6 %. Furthermore, this method can ensure good Safety apsects of mining works, good ground conditions control especially related with the pillars stability, and effective secondary blasting of over – sized materials.

„The Study of Techno – Economical Feasibilty for the Ore baody »Borska Reka« Mining by Caving Methods"[19] has proved that this method is the best and the most applicabile compare with therest two methods, with the best economical effects.

Further, in the Copper Insitute Bor was done „The Study for Ore Body »Borska Reka« Mining by Keep – The Surface Methods - The Economy of Investment-"[20]. In this stady were considered the economical point of view for the methods without collapsing the surface, like Room and Pillar method etc. for the mining ore body „Borska Reka". To compare with the previously considered caving methods, in the study had been taken account the same parameters for economical assessment. From the Study outcame the investment level and costs, and expected economical effects (profit) for the exploitation for each method in the first and second exploitation stage.

ON the basis of the achieved results, the Study concluded that under that time available circumstancies the profitable mining was impossible and that therefore future researchigs should be focused on the cost reduction of the mining.

The II and III Researching Stage

The second Researching stage was focused of the cost reduction analyses to find out the posiblities and solutions for profitable mining of the ore body „Borska Reka”. The ways for cost reduction were based on the change the power supply of the mining equipment e.g. from diesel change into the electrical powered loaders,furthermore applying vibro – feeders and belt conveyers.

These attempts did not gave appropriate results due to the decreasing trend of the copper price in the world market at the time. The decreasing copper price trendline was conitinuing during the III researching stage as well. In the third stage only caving group of methods were analysed. Due to the base and precious metals prices downward trendlines, it was selected the Sublevel Caving – Swedish Variant for ore body „Borska Reka” mining. Then The Main Mining Project was designed but only for the upper part of the ore body so – called „The Hat” of the ore body. According to the Main Mining Project the profitable mining was ensure but in the case without collapsing of the surface and facilities above of the ore body. But some later researchings shown that by applying the Sublevel Caving or any other caving method, it is sure that the surface and facilities would be collapsed, and The Main Mining Project has been droped out.

Conclusions

As can be seen above, the final decision about the ore body „Borska Reka” mining have not done jet. To make a final decision would be necessary furthermore technical and technological researching works and the market researching as well which should provide more trusty data for a future investment programme.

But should be emphasized one good think. Last a few years the copper price has a upward trend. Current price is such that is certainly stimulative to continue further researching. Therefore in the work [13] a researching was done to find out applicability of the Caving group of methods in the ore body „Borska Reka” taking account current opward trends in the copper market place. It was considered a profitable applicability for the two mining methods already aready designed during the previous researching stages:

1. the possibilities for the profitable ore body „Borska Reka” mining applying The Super Scale Sublevel Caving in the first exploitation stage, but taking account the investment costs to relocate the facilities which would be affected by mining works, these costs have not been considered in the previously so – called GRP Mining Project;
2. the possibilities for the profitable ore body „Borska Reka” mining applying The Semilevel Caving method.

The both method can ensure profitable mining and good economic results. Those results shown that further researching should be focused to the Caving group of method, and related to this statement should be mentioned that currently they are thinking about applicability of Block Caving method.

References

[1] Institut za bakar Bor (1999): *Glavni rudarski projekat eksploatacije rude bakra u Jami Bor do K -315 – I faza eksploatacije, knjiga 1.1. Opšti deo – Geologija ležišta–*. Bor.

[2] Milićević, Ž. (1988): Eksploatacija rudnih ležišta na većim dubinama. *XX Oktobarsko savetovanje rudara i metalurga*, Bor, str. 1-9.

[3] Milićević, Ž. (1988): Modifikacija metode podetažnog zarušavanja rude u cilju povećanja moćnosti pojasa iz koga se istovremeno istače minirana ruda. *XX Oktobarsko savetovanje rudara i metalurga*, Bor, str. 11-17.

[4] Milićević, Ž. (1995): Degradacija površine terena kao posledica eksploatacije ležišta mineralnih sirovina. *„Naša ekološka istina", I-3*, Borsko Jezero, str. 49-53.

[5] Institut za bakar Bor (1984): *„Istraživanje, dobijanje i prerada obojenih metala; Studija dugoročnog razvoja i eksploatacije ruda bakra u basenu Bor"*. Bor.

[6] Institut za bakar Bor (1985): *„Istraživanje, dobijanje i prerada obojenih metala; Studija otkopavanja rudnog tela »Borska Reka« sa metodama zarušavanja"*. Bor.

[7] Institut za bakar Bor (1986): *„Studija otkopavanja rude u rudnom telu „Borska Reka" sa očuvanjem površine"*. Bor.

[8] Kojdić, R. (1991): *Prilog određivanju najpovoljnijih parametara otkopne metode, sa tehno-ekonomskog aspekta, u uslovima eksploatacije bakarnog ležišta Bor na velikim dubinama*. Doktorska disertacija, Bor: Tehnički fakultet 1991.

[9] Kojdić, R., Milićević, Ž., Cokić, Lj. (1992): Izbor metode otkopavanja za rudno telo »Borska Reka«. *XXIV Oktobarsko savetovanje rudara i metalurga*, Donji Milanovac, str. 110-113.

[10] Šćekić, V., Milićević, Ž. (1994): Određivanje dužine otkopnih blokova za metodu blokovskog podetažnog zarušavanja u rudnom telu »Borska Reka«". *Drugo naučno savetovanje iz oblasti podzemne eksploatacije ležišta čvrstih mineralnih sirovina*, Beograd, str. 75-85.

[11] Milić V., Milićević Ž. (1996): Istraživanje novih metoda blokovskog zarušavanja rude na modelima. XXVIII Oktobarsko savetovanje, D. Milanovac, 1996, str. 121-126.

[12] Milić, V. (1996): *Istraživanje osnovnih parametara novih metoda poluetažnog prinudnog zarušavanja za otkopavanje dubokih delova borskog ležišta*. Doktorska disertacija, Bor: Tehnički fakultet 1996.

[13] Štrbac, D. (2005): *Istraživanje primenljivosti metoda otkopavanja sa zarušavanjem u rudnom telu »Borska Reka«*. Magistarska teza, Bor: Tehnički fakultet 2005.

[14] Milićević, Ž., Nenadić, D., Mihajlović, B. (1997): Razmatranje rešenja otkopavanja vrha rudnog tela »Borska Reka« sa očuvanjem površine terena. *V naučno-stručni skup „Naša ekološka istina"*, Donji Milanovac, str. 22-27.

[15] Milićević, Ž., Nenadić, D., Mihajlović, B. (1998): Novi koncept otkopavanja rudnog tela »Borska Reka« sa očuvanjem površine". *XXX Oktobarsko savetovanje*, Donji Milanovac, str. 93-99.

[16] Institut za bakar Bor (1999): *Glavni rudarski projekat eksploatacije rude bakra u Jami Bor do K-315 – I faza eksploatacije, knjiga 2.4.*, Bor.

[17] Milićević, Ž. (1980): *„Prilog utvrđivanju uticaja bušačko-minerskih radova kod metode podetažnog zarušavanja na kvalitet minirane rude i veličinu gubitaka i osiromašenja"*. Doktorska disertacija, Bor: Tehnički fakultet 1980.

[18] Aksić, N. (1991): *Modelska ispitivanja parametara metode podetažnog zarušavanja sa većom visinom podetaža*. Diplomski rad, Bor: Tehnički fakultet 1991.

[19] Rudarsko – geološki fakultet (1985): *„Studija tehničko – ekonomske opravdanosti otkopavanja rudnog tela »Borska Reka« u Jami Bor metodama zarušavanja površine"*. Beograd.

[20] Institut za bakar Bor (1987): *„Studija otkopavanja rudnog ležišta »Borska Reka« sa očuvanjem površine – ekonomika investicija"*. Bor.

[21] Institut za bakar Bor (1992): *„Dugoročni program proizvodnje bakra u RTB – Bor; Tehno-ekonomsko sagledavanje mogućnosti ekonomičnog podzemnog otkopavanja u Borskom ležištu ispod XIII horizonta"*. Bor.

[22] Mihajlović, B. (2003): *Istraživanje mogućnosti ekonomične podzemne eksploatacije postojećih rezervi ruda bakra*. Doktorska disertacija, Bor: Tehnički fakultet 2003.

[23] Milić, V. (1993): *Određivanje optimalne visine koncentracionih horizonata pri otvaranju rudnog tela „Borska Reka"*. Magistarska teza, Bor: Tehnički fakultet 1993.

Pregled dosedanjih raziskovalnih spoznanj v ekspoataciji rudnega telesa "Borska reka", Bor

Rudno telo "Borska reka" je največje najdeno v metalogenetski coni Bor. V nasprotju z drugimi, prej odkritimi bogatimi rudnimi telesi, je "Borska reka" manj bogata in je najglobja v regiji. Zato bo možna samo jamska eksloatacija, ker so v krovnini le siromašne zmogljivosti, ki so bile ustavljene v obdobju nizke cene bakra. Od odkritja rudnega telesa pa so bile opravljene raziskave mnogih strokovnjakov iz različnih institucij v Srbiji, ki sedaj omogočajo razmislek o ekonomsko upravičenem izkoriščanju ležišča. V tem prispevku je podan pregled raziskav, ki obravnavajo možne jamske metode. (vsebinski prevod, J.Pezdič)

Autor's Index, Vol. 53, No. 1

(NEW) INSTRUCTIONS TO AUTHORS (from Sep. 2003)

RMZ-MATERIALS & GEOENVIRONMENT (RMZ- Materiali in geookolje) is a periodical publication with four issues per year (established 1952 and renamed to RMZ-M&G in 1998). The main topics of contents are Mining and Geotechnology, Metallurgy and Materials, Geology and Geoenvironment.
RMZ-M&G publishes original Scientific articles, Review papers, Technical and Expert contributions (also as short papers or letters) **in English**. In addition, evaluations of other publications (books, monographs, …), short letters and comments are welcome. A short summary of the contents in Slovene will be included at the end of each paper. It can be included by the author(s) or will be provided by the referee or the Editorial Office.
***Additional information and remarks for Slovenian authors:**
English version with extended "Povzetek", and additional roles (in Template for Slovenian authors) ***can*** *be written. Only exceptionally the articles in the Slovenian language with summary in English will be published. The contributions in English will be considered with priority over those in the Slovenian language in the review process.*

Authorship and originality of the contributions. Authors are responsible for originality of presented data, ideas and conclusions as well as for correct citation of data adopted from other sources. The publication in RMZ-M&G obligate authors that the article will not be published anywhere else in the same form.

Specification of Contributions

Optimal number of pages of full papers is 7 to 15, longer articles should be discussed with Editor, but 20 pages is limit.
Scientific papers represent unpublished results of original research.
Review papers summarize previously published scientific, research and/or expertise articles on the new scientific level and can contain also other cited sources, which are not mainly result of author(s).
Technical and Expert papers are the result of technological research achievements, application research results and information about achievements in practice and industry.
Short papers (Letters) are the contributions that contain mostly very new short reports of advanced investigation. They should be approximately 2 pages long but should not exceed 4 pages.
Evaluations or critics contain author's opinion on new published books, monographs, textbooks, exhibitions …(up to 2 pages, figure of cover page is expected).
In memoriam (up to 2 pages, a photo is expected).
Professional remarks (Comments) cannot exceed 1 page, and only professional disagreements can be discussed. Normally the source author(s) reply the remarks in the same issue.

Supervision and review of manuscripts. All manuscripts will be supervised. The referees evaluate manuscripts and can ask authors to change particular segments, and propose to the Editor the acceptability of submitted articles. Authors can suggest the referee but Editor has a right to choose another. **The name of the referee remains anonymous**. The technical corrections will be done too and authors can be asked to correct missing items. The final decision whether the manuscript will be published is made by the Editor in Chief.

The Form of the Manuscript

The manuscript should be submitted as a complete hard copy including figures and tables. The figures should also be enclosed separately, both charts and photos in the original version. In addition, all material should also be provided in electronic form on a diskette or a CD. The necessary information can conveniently also be delivered by E-mail.

Composition of manuscript is defined in the attached Template

The original file of Template is temporarily available on E-mail addresses:
joze.pezdic@ntfgeo.uni-lj.si, joze.pezdic@guest.arnes.si
barbara.bohar@ntfgeo.uni-lj.si

References – can be arranged in two ways:
- first possibility: alphabetic arrangement of first authors – in text: (Borgne, 1955),
or
- second possibility: [1] numerated in the same order as cited in the text: example[1]

Format of papers in journals:

Le Borgne, E. (1955): Susceptibilite magnetic anomale du sol superficiel. *Annales de Geophysique*, 11, pp. 399-419.

Format of books:

Roberts, J. L. (1989): Geological structures, *MacMillan, London*, 250 p.

Text on the hard print copy can be prepared with any text-processor. The electronic version on the diskette, CD or E-mail transfer should be in MS Word or ASCII format.
Captions of figures and tables should be enclosed separately. **Figures (graphs and photos)** and tables should be original and sent separately in addition to text. They can be prepared on paper or computer designed (MSExcel, Corel, Acad)
Format. Electronic figures are recommended to be in CDR, AI, EPS, TIF or JPG formats. Resolution of bitmap graphics (TIF, JPG) should be at least 300 dpi. Text in vector graphics (CDR, AI, EPS) must be in MSWord Times typography or converted in curves.
Color prints. Authors will be charged for color prints of figures and photos.
Labeling of the additionally provided material for the manuscript should be very clear and must contain at least the lead author's name, address, the beginning of the title and the date of delivery of the manuscript. In case of an E-mail transfer the exact message with above asked data must accompany the attachment with the file containing the manuscript.
Information about RMZ-M&G:
Editor in Chief prof. dr. Jože Pezdič (tel. ++386 1 4704-633) or
Secretary Barbara Bohar Bobnar, un. dipl. ing. geol. (++386 1 4704-630),
Aškerčeva 12, Ljubljana, Slovenia

or at E-mail addresses:
joze.pezdic@ntfgeo.uni-lj.si, joze.pezdic@guest.arnes.si
barbara.bohar@ntfgeo.uni-lj.si

Sending of manuscripts. Manuscripts can be sent by mail to the **Editorial Office** address:

- RMZ-Materials & Geoenvironment
  Aškerčeva 12,
  1001 Ljubljana, Slovenia

or delivered to:

- **Reception** of the Faculty of Natural Sciences and Engineering (for RMZ-M&G)
  Aškerčeva 12, Ljubljana
- E-mail – addresses of Editor and Secretary
- You can also contact them on their phone numbers.

These instructions are valid from September 2003

TEMPLATE

The title of the manuscript should be written in bold letters (Times New Roman, 14, Center)

Name Surname[1], …. , & Name Surname[X] (Times New Roman, 12, Center)

[x]Faculty of ... , University of ... , Address…, Country, e-mail: ... (Times New Roman, 12, Center)

THE LENGTH OF FULL PAPER SHOULD NOT EXCEED TWENTY (20, INCLUDING FIGURES AND TABLES) PAGES (OPTIMAL 7 TO 15), SHORT PAPER FOUR (4) AND OTHER TWO (2) WITHOUT TEXT FLOWING BY GRAPHICS AND TABLES.

Abstract(Times New Roman, Bold/Normal, 11): The text of the abstract is placed here. The abstract should be concise and should present the aim of the work, essential results and conclusion. It should be typed in font size 11, single-spaced. Except for the first line, the text should be indented from the left margin by 10 mm. The length should not exceed fifteen (15) lines (10 are recommended).

Key words: a list of up to 5 key words (3 to 5) that will be useful for indexing or searching. Use the same styling as for abstract.

Introduction (Times New Roman, Bold, 12)

Two lines below the keywords begin the introduction. Use Times New Roman, font size 12, Justify alignment.

There are two (2) admissible methods of citing references:

1. by stating the first author and the year of publication of the reference in the parenthesis at the appropriate place in the text and arranging the reference list in the alphabetic order of first authors; e.g.:
   "Detailed information about geohistorical development of this zone can be found in: Antonijević (1957), Grubić (1962), ..."
   "… the method was described previously (Hoefs, 1996)"
2. by consecutive Arabic numerals in square brackets, superscripted at the appropriate place in the text and arranging the reference list at the end of the text in the like manner; e.g.:
   "... while the portal was made in Zope[3] environment."

Results and discussion (Times New Roman, Bold, 12)

Tables, figures, pictures, and schemes should be incorporated (inserted, not pasted) in the text at the appropriate place and should fit on one page. Break larger schemes and tables into smaller parts to prevent extending over more than one page.

Conclusions (Times New Roman, Bold, 12)

This paragraph summarizes the results and draws conclusions.

Acknowledgements (Times New Roman, Bold, 12, Center - optional)

This work was supported by the ****.

References (Times New Roman, Bold, 12)

Regardless of the method used, in the reference list, the styling, punctuation and capitalization should conform to the following:

FIRST OPTION – in alphabetical order

Casati, P., Jadoul, F., Nicora, A., Marinelli, M., Fantini-Sestini, N. & Fois, E. (1981): Geologia della Valle del'Anisici e dei gruppi M. Popera – Tre Cime di Lavaredo (Dolomiti Orientali). *Riv. Ital. Paleont.*; Vol. 87, No. 3, pp. 391-400, Milano.

Folk, R. L. (1959): Practical petrographic classification of limestones. *Amer. Ass. Petrol. Geol. Bull.;* Vol. 43, No. 1, pp. 1-38, Tulsa.

SECOND OPTION – in numerical order

[1] Trček, B. (2001): *Solute transport monitoring in the unsaturated zone of the karst aquifer by natural tracers.* Ph.D. Thesis. Ljubljana: University of Ljubljana 2001; 125 p.

[2] Higashitani, K., Iseri, H., Okuhara, K., Hatade, S. (1995): Magnetic Effects on Zeta Potential and Diffusivity of Nonmagnetic Particles. *Journal of Colloid and Interface Science 172*, pp. 383-388.

Citing the Internet site:

CASREACT-Chemical reactions database [online]. Chemical Abstracts Service, 2000, updated 2.2.2000 [cited 3.2.2000]. Accessible on Internet:<http://www.cas.org/CASFILES/casreact.html>.

Povzetek (Times New Roman, 12)

A short summary of the contents in Slovene (up to 400 characters) can be written by the author(s) or will be provided by the referee or by the Editorial Board.

TEMPLATE for Slovenian Authors

The title of the manuscript should be written in bold letters (Times New Roman, 14, Center)

Naslov članka (Times New Roman, 14, Center)

NAME SURNAME[1], …. , & NAME SURNAME[X] (TIMES NEW ROMAN, 12, CENTER)
IME PRIIMEK[1], …, IME PRIIMEK[X] (TIMES NEW ROMAN, 12, CENTER)

[x]Faculty of ... , University of ... , Address…, Country; e-mail: ... (Times New Roman, 12, Center)
[X]Fakulteta…, Univerza…, Naslov…, Država; e-mail: … (Times New Roman, 12, Center)

THE LENGTH OF ORIGINAL SCIENTIFIC PAPER SHOULD NOT EXCEED TWENTY (20, INCLUDING FIGURES AND TABLES) PAGES (OPTIMAL 7 TO 15), SHORT PAPER FOUR (4) AND OTHER TWO (2) WITHOUT TEXT FLOWING BY GRAPHICS AND TABLES.
DOLŽINA IZVIRNEGA ZNANSTVENEGA ČLANKA NE SME PRESEGATI DVAJSET (20, VKLJUČNO S SLIKAMI IN TABELAMI), STROKOVNEGA ČLANKA ŠTIRI (4) IN OSTALIH PRISPEVKOV DVE (2) STRANI.

Abstract(Times New Roman, Bold/Normal, 11): The text of the abstract is placed here. The abstract should be concise and should present the aim of the work, essential results and conclusion. It should be typed in font size 11, single-spaced. Except for the first line, the text should be indented from the left margin by 10 mm. The length should not exceed fifteen (15) lines (10 are recommended).
Izvleček(TNR, B/N, 11): Kratek izvleček namena članka ter ključnih rezultatov in ugotovitev. Razen prve vrstice naj bo tekst zamaknjen z levega roba za 10 mm. Dolžina naj ne presega petnajst (15) vrstic (10 je priporočeno).

Key words: a list of up to 5 key words (3 to 5) that will be useful for indexing or searching. Use the same styling as for abstract.
Ključne besede: seznam največ 5 ključnih besed (3-5) za pomoč pri indeksiranju ali iskanju. Uporabite enako obliko kot za izvleček.

INTRODUCTION – UVOD (TIMES NEW ROMAN, BOLD, 12)

Two lines below the keywords begin the introduction. Use Times New Roman, font size 12, Justify alignment. All captions of text and tables as well as the text in graphics must be prepared in English and Slovenian language.

Dve vrstici pod ključnimi besedami se začne Uvod. Uporabite pisavo Times New Roman, velikost črk 12, z obojestransko poravnavo. Naslovi slik in tabel (vključno z besedilom v slikah) morajo biti pripravljeni v slovenskem in angleškem jeziku.

There are two (2) admissible methods of citing references – obstajata dve sprejemljivi metodi navajanja referenc:

1. by stating the first author and the year of publication of the reference in the parenthesis at the appropriate place in the text and arranging the reference list in the alphabetic order of first authors; e.g.:
1. z navedbo prvega avtorja in letnice objave reference v oklepaju na ustreznem mestu v tekstu in z ureditvijo seznama referenc po abecednem zaporedju prvih avtorjev; npr.:
   "Detailed information about geohistorical development of this zone can be found in: Antonijević (1957), Grubić (1962), ..."
   "… the method was described previously (Hoefs, 1996)"
2. by consecutive Arabic numerals in square brackets, superscripted at the appropriate place in the text and arranging the reference list at the end of the text in the like manner; e.g.:
2. z zaporednimi arabskimi številkami v oglatih oklepajih na ustreznem mestu v tekstu in z ureditvijo seznama referenc v številčnem zaporedju navajanja; npr.;
   "... while the portal was made in Zope[3] environment."

Results and discussion – Rezultati in razprava (Times New Roman, Bold, 12)

Tables, figures, pictures, and schemes should be incorporated (inserted, not pasted) in the text at the appropriate place and should fit on one page. Break larger schemes and tables into smaller parts to prevent extending over more than one page.

Tabele, sheme in slike je potrebno vnesti (z ukazom Insert, ne Paste) v tekst na ustreznem mestu. Večje sheme in tabele je potrebno ločiti na manjše dele, da ne presegajo ene strani.

Conclusions – Sklepi (Times New Roman, Bold, 12)

This paragraph summarizes the results and draws conclusions.
Povzetek rezultatov in zaključki.

Acknowledgements – Zahvale (Times New Roman, Bold, 12, Center - optional)

This work was supported by the ****.

References - Viri (Times New Roman, Bold, 12)

Regardless of the method used, in the reference list, the styling, punctuation and capitalization should conform to the following:
Ne glede na uporabljeno metodo pri seznamu citiranih referenc upoštevajte naslednjo obliko:

FIRST OPTION – in alphabetical order (v abecednem zaporedju)

Casati, P., Jadoul, F., Nicora, A., Marinelli, M., Fantini-Sestini, N. & Fois, E. (1981): Geologia della Valle del'Anisici e dei gruppi M. Popera – Tre Cime di Lavaredo (Dolomiti Orientali). *Riv. Ital. Paleont.*; Vol. 87, No. 3, pp. 391-400, Milano.

Folk, R. L. (1959): Practical petrographic classification of limestones. *Amer. Ass. Petrol. Geol. Bull.;* Vol. 43, No. 1, pp. 1-38, Tulsa.

SECOND OPTION – in numerical order (v numeričnem zaporedju)

[1] Trček, B. (2001): *Solute transport monitoring in the unsaturated zone of the karst aquifer by natural tracers.* Ph.D. Thesis. Ljubljana: University of Ljubljana 2001; 125 p.

[2] Higashitani, K., Iseri, H., Okuhara, K., Hatade, S. (1995): Magnetic Effects on Zeta Potential and Diffusivity of Nonmagnetic Particles. *Journal of Colloid and Interface Science 172*, pp. 383-388.

Citing the Internet site:

CASREACT-Chemical reactions database [online]. Chemical Abstracts Service, 2000, updated 2.2.2000 [cited 3.2.2000]. Accessible on Internet:<http://www.cas.org/CASFILES/casreact.html>.

Citiranje internetne strani:

CASREACT-Chemical reactions database [online]. Chemical Abstracts Service, 2000, obnovljeno 2.2.2000 [citirano 3.2.2000]. Dostopno na svetovnem spletu: <http://www.cas.org/CASFILES/casreact.html>.

Povzetek – Summary (Times New Roman, 12)

An extended summary of the contents in Slovene (from one page to approximately 1/3 of the original article length).
Razširjeni povzetek vsebine prispevka v Angleščini (od ene strani do približno 1/3 dolžine izvirnega članka).

Number of SCI search (število SCI citatov) 185

Number of paper indexing in different bases
(Število indeksiranih člankov v posameznih bazah)

CA SEARCH – Chemical Abstracts (1967 – present) 375

METADEX: Metal Science 135

GeoRef 125

Inside Conferences 76

PASCAL 30

Energy Science and Technology 27

Aluminium Industry Abstracts 18

Ei Compendex 13

EngineeredMaterials Abstracts 3

Analytical Abstracts 1

FLUIDEX (Fluid Engineering Abstracts) 1

TULSA™ (Petroleum Abstracts) 1

Indexing also in (number of indexing not yet available)
(Indeksiran tudi v (števila vpisov še nimamo)

Alloys Index, Bibliography and Index of Geology, Chemical Titles, IMM Abstracts and Index (Institution of Minimg and Metallurgy), INIS Atomindex, Metals abstracts Index, Nonferrous Metals Alert, Polimers, Ceramics, Composites Alert, Steel Alerty

RMZ - Materials and Geoenvironment

RMZ-M&G, Vol. 53, No. 1 pp. 1-153 (2006)

Contents